

Indole Compounds in Oncology: Therapeutic Potential and Mechanistic Insights

Sara M. Hassan¹, Alyaa Farid¹, Siva S. Panda^{2,3,*}, Mohamed S. Bekheit⁴, Holden Dinkins², Walid Fayad⁵ and Adel S. Girgis^{4,*}

¹ *Biotechnology Department, Faculty of Science, Cairo University, Giza 12613, Egypt*

² *Department of Chemistry and Biochemistry, Augusta University, Augusta, GA 30912, USA*

³ *Department of Biochemistry and Molecular Biology, Augusta University, Augusta, GA 30912, USA*

⁴ *Department of Pesticide Chemistry, National Research Centre, Dokki, Giza 12622, Egypt; m_bekheit@yahoo.com*

⁵ *Drug Bioassay-Cell Culture Laboratory, Pharmacognosy Department, National Research Centre, Dokki, Giza, 12622. Egypt*

* Correspondence: sipanda@augusta.edu or sspanda12@gmail.com (S.S. Panda); girgisas10@yahoo.com or as.girgis@nrc.sci.eg (A.S.G.)

Supplementary material

Figure captions

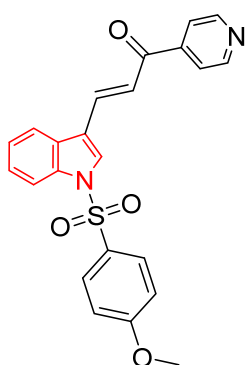
- Fig. S1.** Antiproliferation properties ($\mu\text{M} \pm \text{SD}$) and carbonic anhydrase inhibitory activity (μM) of the prepared chalcones **50** and standard references (Doxorubicin and AZM)..... 6
- Fig. S2.** Antiproliferation properties ($\mu\text{M} \pm \text{SD}$) of the synthesized agents **54**, **55**, Camptothecin and Harmine..... 8
- Fig. S3.** Antiproliferation properties (μM) and binding affinity with ER- α (nM) of the synthesized indole-benzimidazole conjugates **58**..... 12
- Fig. S4.** Antiproliferation properties of the synthesized indolyl sulfonhydrazones **66** and Doxorubicin..... 14

| | |
|---|----|
| Fig. S5. Antiproliferation and tubulin polymerization inhibitory properties ($\mu\text{M} \pm \text{SD}$) of the synthesized thiazolyl hydrazones linked to indolyl scaffold 71 , Colchicine and CA-4 (control drugs)..... | 16 |
| Fig. S6. Antiproliferation ($\mu\text{M} \pm \text{SD}$) and % inhibitory properties of tubulin polymerization at 10 μM of the synthesized 3-amidoindoles 80 and CA-4 (control drug)..... | 21 |
| Fig. S7. Antiproliferation and tubulin polymerization inhibitory properties ($\mu\text{M} \pm \text{SD}$) of the synthesized 3-arylthio-1 <i>H</i> -indoles 83 , 3-aryl-1 <i>H</i> -indoles 85 and standard drugs (CA-4 and Colchicine)..... | 26 |
| Fig. S8. Antiproliferation ($\text{nM} \pm \text{SD}$) and tubulin polymerization inhibitory ($\mu\text{M} \pm \text{SD}$) properties of 6-aryl-3-aryllindoles 89 and CA-4 (standard reference)..... | 29 |
| Fig. S9. Antiproliferation properties ($\mu\text{M} \pm \text{SD}$) of the synthesized indolyl-arylaminopropenone conjugates 93 and reference drug (Doxorubicin)..... | 31 |
| Fig. S10. Antiproliferation properties ($\mu\text{M} \pm \text{SD}$) of the synthesized 3-pyrrolylisatin-triazole conjugates 104 and Tamoxifen citrate "reference drug" (ND = not determined)..... | 34 |
| Fig. S11. Antiproliferation properties ($\mu\text{M} \pm \text{SD}$) of spirochromenocarbazols linked to 1,2,3-triazole 106 , and standard references (Paclitaxel and Doxorubicin)..... | 37 |
| Fig. S12. Antiproliferation properties (μM) of tetrahydro- <i>b</i> -carboline and isatin scaffolds connected by 1 <i>H</i> -1,2,3-triazolyl heterocycle 109 and reference standards (Plumbagin, Peganumine A and Tamoxifen)..... | 41 |
| Fig. S13. Antiproliferation properties (μM) of the synthesized ospemifene-isatins 116 and ospemifene-spiroisatins 117 conjugates and reference standards (Ospemifene, Tamoxifen and Plumbagin) against MCF-7 and MDA-MB-231.... | 45 |
| Fig. S14. Antiproliferation properties of spiroxindoles bearing 2-furanyl heterocycle 121 and Staurosporine..... | 49 |
| Fig. S15. Antiproliferation properties (μM) against MDA-MB-231 and inhibitory properties ($\mu\text{M} \pm \text{SD}$) against EGFR of spiroxindoles 124 and standard references (Doxorubicin (Adriamycin) and Erlotinib..... | 51 |
| Fig. S16. Antiproliferation properties ($\mu\text{M} \pm \text{SD}$) and EF- α inhibitory properties | |

| | |
|--|----|
| (nM \pm SD) of the synthesized <i>N</i> -(1 <i>H</i> -indole-6-yl) benzamides 127 and their benzene sulfonamide analogs 128 | 53 |
| Fig. S17. Antiproliferation properties (μ M) of [1,3]thiazino[3,2- <i>a</i>]indol-4-ones 131 | 54 |
| Fig. S18. Antiproliferation properties (μ M \pm SD) of the synthesized indole-podophyllotoxin conjugates 133 , and standards (Colchicine, Podophyllotoxin and Nocodazole) against HepG-2, HL-7702 (liver), HeLa, H8 (cervical), A549, MRC-5 (lung), MCF-7, and HMEC (breast) cancer cell lines..... | 55 |
| Fig. S19. Antiproliferation properties (μ M \pm SD) of the synthesized indolylthiosemicarbazones 139 and standards (Etoposide and Colchicine)..... | 57 |
| Fig. S20. Antiproliferation properties (μ M) and % inhibition of microtubule polymerization at 10 μ M of the respective ligand of the synthesized bis(indolyl)hydrazide-hydrazones 142 and Colchicine..... | 60 |
| Fig. S21. Antiproliferation properties of indole-based tambjamine analogs 144 and Cisplatin..... | 61 |
| Fig. S22. Antiproliferation properties (μ M \pm SD) of indirubin 145 , indirubin-piperidine conjugates 146-148 and Bortezomib..... | 62 |
| Fig. S23. Antiproliferation properties (μ M) of the synthesized piperlongumine pharmacophore conjugated with indolyl scaffold 152 . and its precursor piperlongumine 149 | 63 |
| Fig. S24. Kinase inhibitory (% control at 1.0 μ M) and antiproliferation (μ M \pm SD) properties of the synthesized indole-containing compounds linked to urea function 156 and Dasatinib (reference standard)..... | 64 |
| Fig. S25. enzymatic inhibitory properties of synthesized agents 160 , 161 and Gefitinib against EGFR[L858R]..... | 69 |
| Fig. S26. Antiproliferation properties (μ M \pm SD) of the synthesized coumarin-indole conjugates 168 , Cisplatin and Colchicine..... | 73 |
| Fig. S27. Antiroliferation properties (μ M \pm SD) of thiochromeno[4,3- <i>c</i>]pyrazole-indole conjugates 173 , Etoposide and Cisplatin (standard references)..... | 75 |
| Fig. S28. Antiproliferation properties of the synthesized indolylhydrazine-1-carboximidamide 175 | 77 |

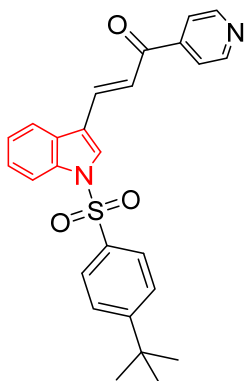
| | |
|---|-----|
| Fig. S29. Antiproliferation properties of the synthesized 2-oxo-3-indolylidene-2-indolecarbohydrazones 179 and Sunitinib..... | 78 |
| Fig. S30. Antiproliferation and carbonic anhydrase inhibitory properties of 1-(indole-2-carbonyl)thiosemicarbazides incorporating sulfonamide group 182 and standard references (Doxorubicin and Acetazolamide "AAZ")..... | 81 |
| Fig. S31. Antiproliferation properties of thiazolidinone-indoles 184 and Podophyllotoxin..... | 84 |
| Fig. S32. Antiproliferation properties of spiro[indoline-3,3'-pyrrolizin]-2-ones 186 and cisplatin against HCT-116, HepG2, PC-3 (cancer) and VERO-B (normal) cell lines..... | 89 |
| Fig. S33. Antiproliferation properties of spiroindoles 187 and Cisplatin against HCT-116, HepG2, PC-3 (cancer) and VERO-B (normal) cell lines..... | 91 |
| Fig. S34. Antiproliferation (IC_{50} , $\mu M \pm SEM$ against the tested cell lines), and % inhibitory properties against EGFR and VEGFR-2 utilizing IC_{50} observed against MCF7 for the tested spiroindoles 192 and standard drugs (5-Fluorouracil and Sunitinib)..... | 93 |
| Fig. S35. Antiproliferation (IC_{50} , $\mu M \pm SE$ "standard error") and enzymatic inhibitory properties (IC_{50} , $\mu M \pm SD$) of 3-alkenyl-2-oxindoles 196 , 200 and Sunitinib..... | 96 |
| Fig. S36. Antiproliferation properties ($\mu M \pm SEM$) of indole linked to imidazo[2,1- <i>b</i>][1,3,4]thiadiazoles 203 | 98 |
| Fig. S37. Antiproliferation ($\mu M \pm SE$) and enzymatic inhibitory properties against EGFR of 5-(morpholinosulfonyl)-2-indolinones 206 , 3-ylidene-2-indolinones 208 and standard references (Doxorubicin and Lapatinib)..... | 99 |
| Fig. S38. Antiproliferation properties ($\mu M \pm SD$) of the synthesized sophoridine-indole conjugates 210 , Sophoridine 209 and Camptothecin (standard reference).... | 100 |
| Fig. S39. Antiproliferation properties of spirooxindoles 213 and Tanshinon IIA (TSA)..... | 105 |
| Fig. S40. Antiproliferation and enzymation inhibitory properties of indole-triazole conjugates 216 , Etoposide, Indomethacin, Celecoxib, and Norihydroguaiaretic acid (ND = not done)..... | 107 |

| | |
|--|-----|
| Fig. S41. Antiproliferation and enzymation inhibitory properties of indole-triazole conjugates 218 , Etoposide, Indomethacin, Celecoxib, and Norhihydroguaiaretic acid (ND = not done)..... | 111 |
| Fig. S42. Antiproliferation properties ($\mu\text{M} \pm \text{SD}$) of 3-[(indeno[1,2- <i>c</i>]pyrazole-3-yl)methylene]indolin-2-ones 221 and Combretastatin A-4 (CA-4)..... | 116 |
| Fig. S43. Antiproliferation and tubulin polymerization inhibitory properties of the synthesized nicotinoyl/isonicotinyl pyrazolines featuring indolyl heterocycle 223 and Combretastatin A-4 (CA-4)..... | 119 |
| Fig. S44. Antiproliferation properties ($\mu\text{M} \pm \text{SD}$) of the synthesized indoles 225 , pyranoindole 226 and Vinblastine..... | 122 |
| Fig. S45. Antiproliferation and inhibitory properties of HDAC and BRD4 of the synthesized indole-isoxazole conjugates 235 , Vorinostat and JQ1..... | 123 |
| Fig. S46. Antiproliferation properties of 3,6-disubstituted-2-carboxyindoles 241 | 127 |



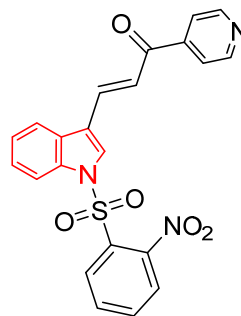
50a

$IC_{50} = 65.8 \pm 1.35$,
 $26.0 \pm 2.47 \mu M$
 against MCF7 and
 HepG2, respectively;
 $IC_{50} = 26.15$, $29.35 \mu M$
 against hCA IX, hCA II,
 respectively.



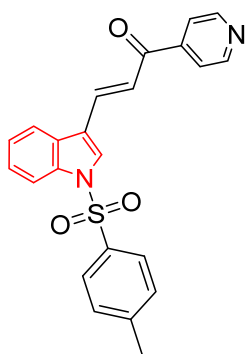
50b

$IC_{50} = 24.0 \pm 1.16$,
 $27 \pm 1.67 \mu M$
 against MCF7 and
 HepG2, respectively;
 $IC_{50} = 0.15$, $12.10 \mu M$
 against hCA IX, hCA II,
 respectively.



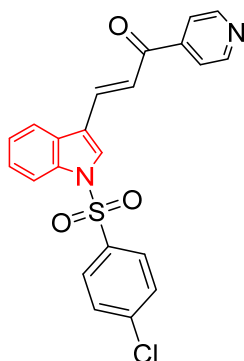
50c

$IC_{50} = 36.9 \pm 0.79$,
 $31.7 \pm 1.10 \mu M$
 against MCF7 and
 HepG2, respectively;
 $IC_{50} = 57.31$, $36.21 \mu M$
 against hCA IX, hCA II,
 respectively.



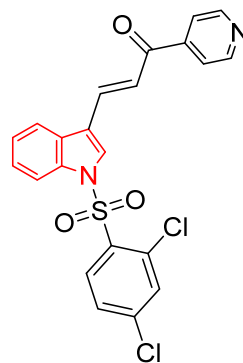
50d

$IC_{50} = 48.9 \pm 1.19$,
 $44.8 \pm 1.35 \mu M$
 against MCF7 and
 HepG2, respectively;
 $IC_{50} = 29.9$, $38.40 \mu M$
 against hCA IX, hCA II,
 respectively.



50e

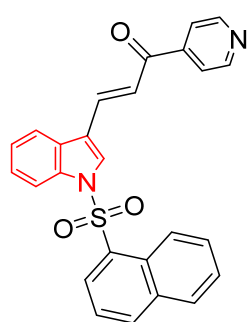
$IC_{50} = 37.5 \pm 1.34$,
 $35.1 \pm 1.47 \mu M$
 against MCF7 and
 HepG2, respectively;
 $IC_{50} = 14.41$, $13.50 \mu M$
 against hCA IX, hCA II,
 respectively.



50f

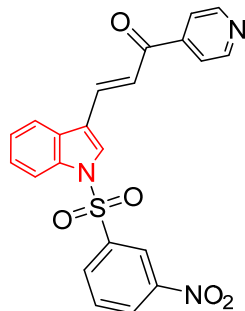
$IC_{50} = 12.2 \pm 1.02$,
 $14.8 \pm 1.28 \mu M$
 against MCF7 and
 HepG2, respectively;
 $IC_{50} = 0.13$, $9.10 \mu M$
 against hCA IX, hCA II,
 respectively.

Fig. S1. Antiproliferation properties ($\mu M \pm SD$) and carbonic anhydrase inhibitory activity (μM) of the prepared chalcones **50** and standard references (Doxorubicin and AZM).



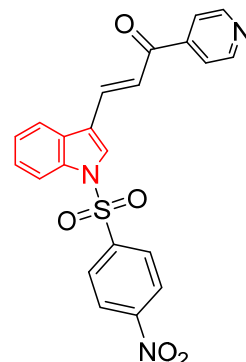
50g

$IC_{50} = 58.0 \pm 2.18$,
 $62.9 \pm 1.34 \mu M$
 against MCF7 and
 HepG2, respectively;
 $IC_{50} = 44.08$, $65.22 \mu M$
 against hCA IX, hCA II,
 respectively.



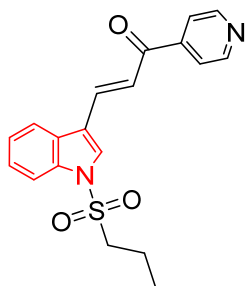
50h

$IC_{50} = 36.3 \pm 1.16$,
 $42.6 \pm 1.41 \mu M$
 against MCF7 and
 HepG2, respectively;
 $IC_{50} = 37.56$, $24.32 \mu M$
 against hCA IX, hCA II,
 respectively.



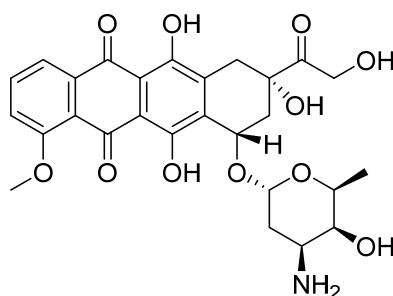
50i

$IC_{50} = 14.5 \pm 1.15$,
 $18.3 \pm 1.44 \mu M$
 against MCF7 and
 HepG2, respectively;
 $IC_{50} = 0.15$, $14.10 \mu M$
 against hCA IX, hCA II,
 respectively.



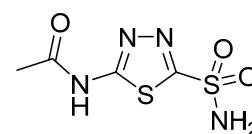
50j

$IC_{50} = 52.4 \pm 1.22$,
 $46.2 \pm 1.14 \mu M$
 against MCF7 and
 HepG2, respectively;
 $IC_{50} = 44.52$, $>100.00 \mu M$
 against hCA IX, hCA II,
 respectively.



Doxorubicin

$IC_{50} = 20.2 \pm 1.70$,
 18.7 ± 1.37 , $142.8 \pm 1.62 \mu M$
 against MCF7,
 HepG2, and HEK-293
 respectively.



Acetazolamide (AZM)

$IC_{50} = 0.027$, $0.013 \mu M$
 against hCA IX, hCA II,
 respectively.

Fig. S1 (continued). Antiproliferation properties ($\mu M \pm SD$) and carbonic anhydrase inhibitory activity (μM) of the prepared chalcones **50** and standard references (Doxorubicin and AZM).

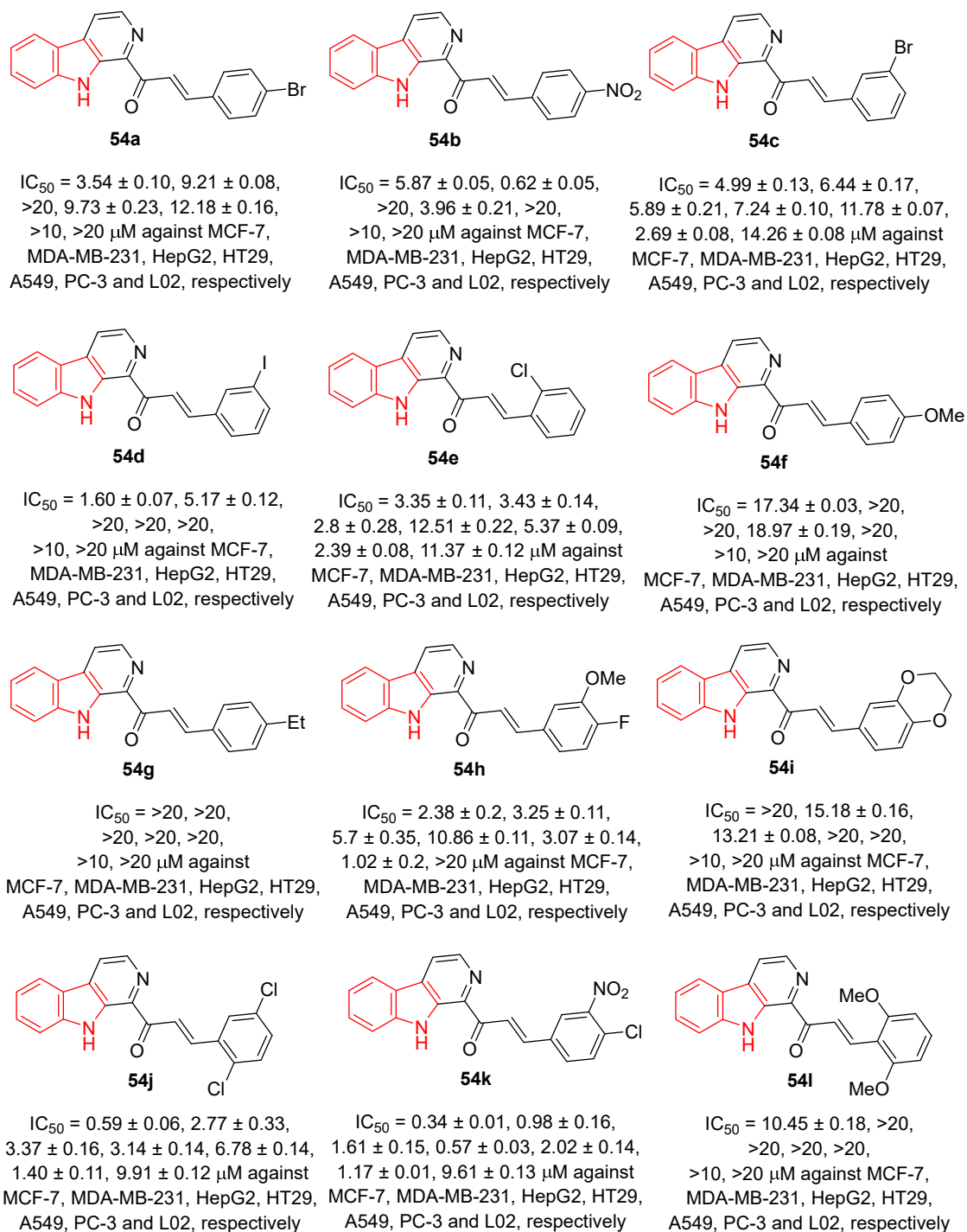


Fig. S2. Antiproliferation properties (μM ± SD) of the synthesized agents **54**, **55**, Camptothecin and Harmine.

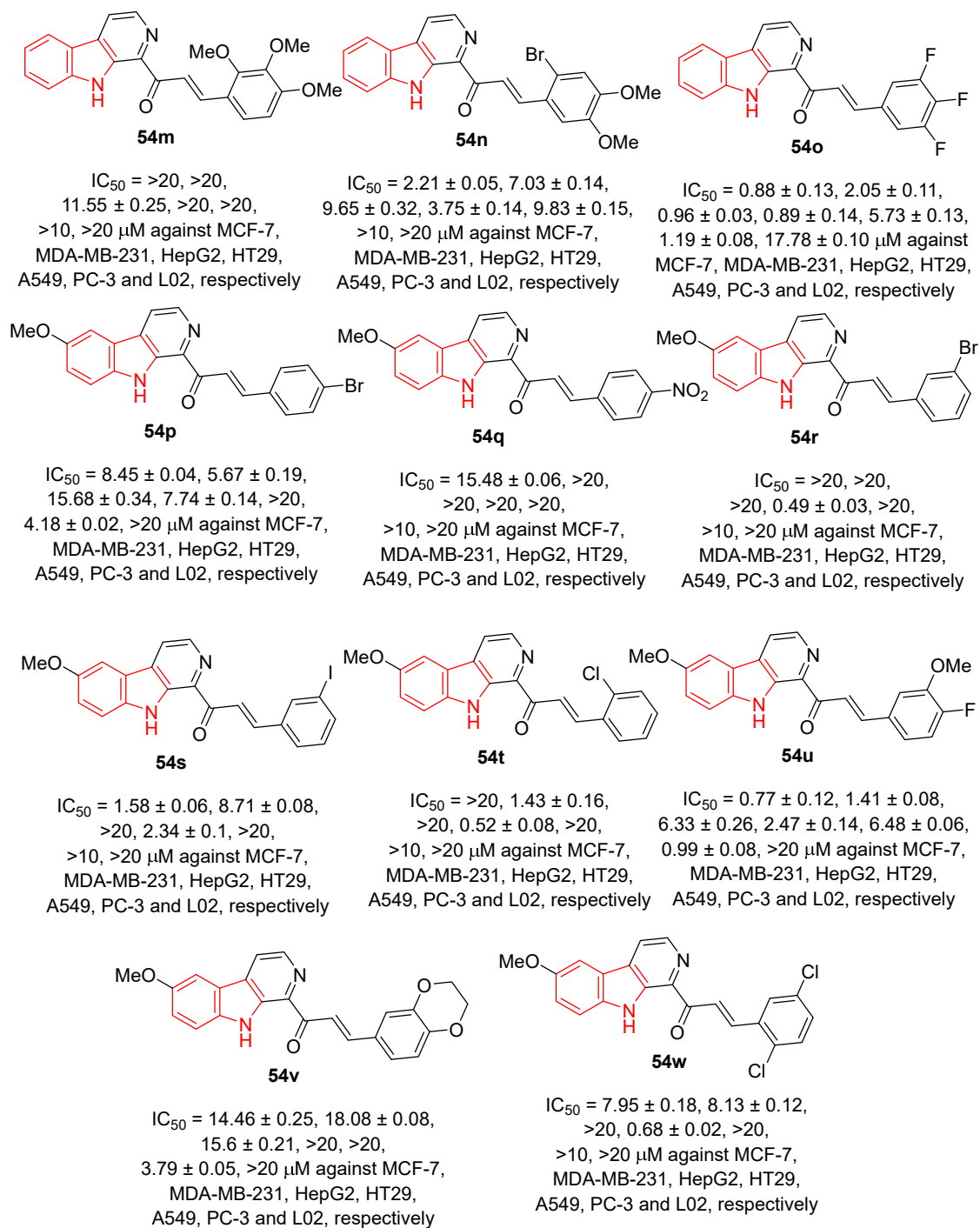
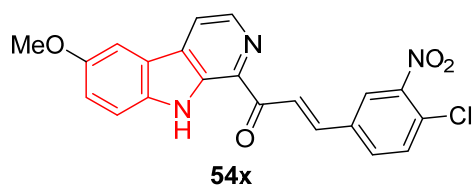
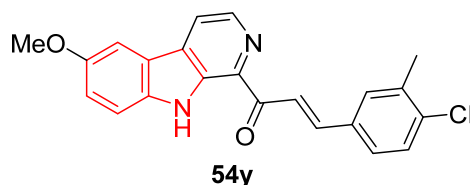


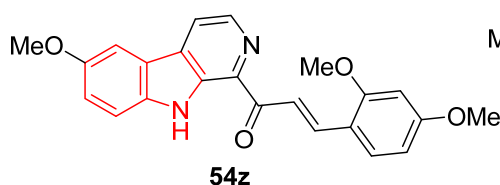
Fig. S2 (continued). Antiproliferation properties (μM ± SD) of the synthesized agents **54**, **55**, Camptothecin and Harmine.



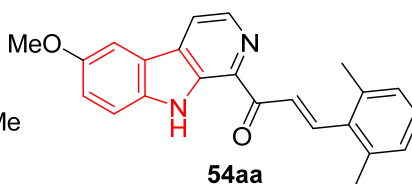
IC₅₀ = >20, 2.99 ± 0.28,
7.72 ± 0.16, >20, 5.72 ± 0.21,
>10, >20 μM against MCF-7,
MDA-MB-231, HepG2, HT29,
A549, PC-3 and L02, respectively



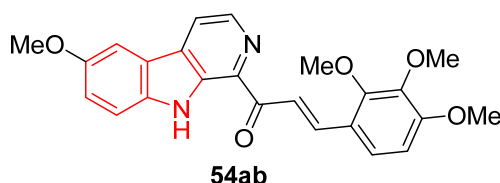
IC₅₀ = 4.38 ± 0.2, 6.45 ± 0.11,
2.74 ± 0.17, 1.89 ± 0.21, 7.49 ± 0.10,
>10, >20 μM against MCF-7,
MDA-MB-231, HepG2, HT29,
A549, PC-3 and L02, respectively



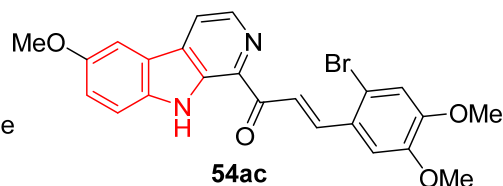
IC₅₀ = 5.71 ± 0.08, 11.98 ± 0.27,
7.13 ± 0.26, 13.59 ± 0.21, 15.3 ± 0.13,
>10, >20 μM against MCF-7,
MDA-MB-231, HepG2, HT29,
A549, PC-3 and L02, respectively



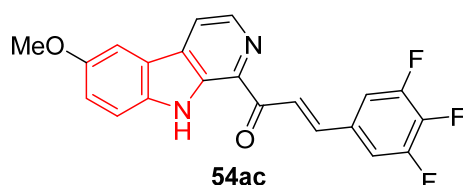
IC₅₀ = 10.14 ± 0.18, >20,
>20, >20, >20,
>10, >20 μM against MCF-7,
MDA-MB-231, HepG2, HT29,
A549, PC-3 and L02, respectively



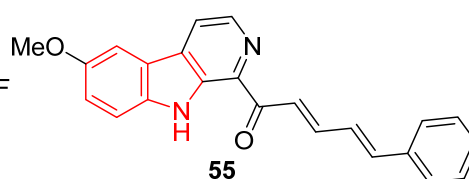
IC₅₀ = 6.1 ± 0.14, >20,
>20, 6.08 ± 0.20, 7.1 ± 0.16,
>10, >20 μM against MCF-7,
MDA-MB-231, HepG2, HT29,
A549, PC-3 and L02, respectively



IC₅₀ = 8.05 ± 0.25, >20,
>20, 11.34 ± 0.17, 4.51 ± 0.13,
>10, >20 μM against MCF-7,
MDA-MB-231, HepG2, HT29,
A549, PC-3 and L02, respectively

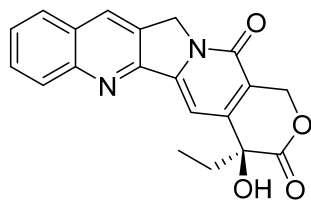


IC₅₀ = 4.23 ± 0.09, 6.52 ± 0.23,
15.94 ± 0.31, 2.72 ± 0.04, >20,
>10, >20 μM against MCF-7,
MDA-MB-231, HepG2, HT29,
A549, PC-3 and L02, respectively



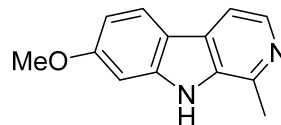
IC₅₀ = 17.53 ± 0.02, >20,
18.93 ± 0.23, >20, >20,
>10, >20 μM against MCF-7,
MDA-MB-231, HepG2, HT29,
A549, PC-3 and L02, respectively

Fig. S2 (continued). Antiproliferation properties (μM ± SD) of the synthesized agents **54**, **55**, Camptothecin and Harmine.



Camptothecin

$IC_{50} = 6.85 \pm 0.11, 0.62 \pm 0.27, 1.80 \pm 0.14, 1.87 \pm 0.09, 7.80 \pm 0.14, 6.60 \pm 0.29, 0.59 \pm 0.08 \mu\text{M}$ against MCF-7, MDA-MB-231, HepG2, HT29, A549, PC-3 and L02, respectively



Harmine

$IC_{50} = 13.37 \pm 0.05, 13.21 \pm 0.08, 19.23 \pm 0.19, 12.15 \pm 0.18, 17.3 \pm 0.04, 15.57 \pm 0.10, 9.49 \pm 0.11 \mu\text{M}$ against MCF-7, MDA-MB-231, HepG2, HT29, A549, PC-3 and L02, respectively

Fig. S2 (continued). Antiproliferation properties ($\mu\text{M} \pm \text{SD}$) of the synthesized agents **54**, **55**, Camptothecin and Harmine.

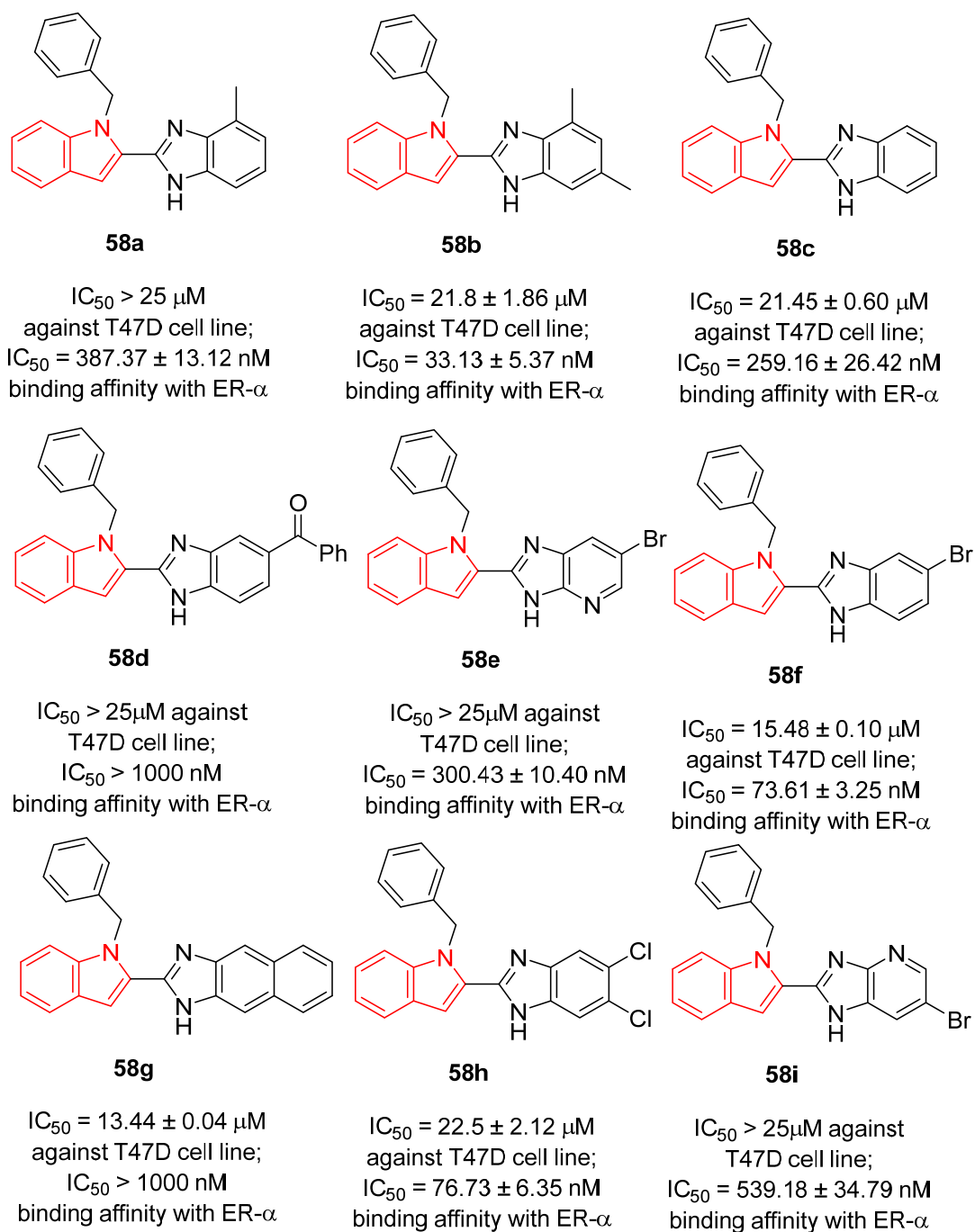


Fig. S3. Antiproliferation properties (μM) and binding affinity with ER-α (nM) of the synthesized indole-benzimidazole conjugates **58**.

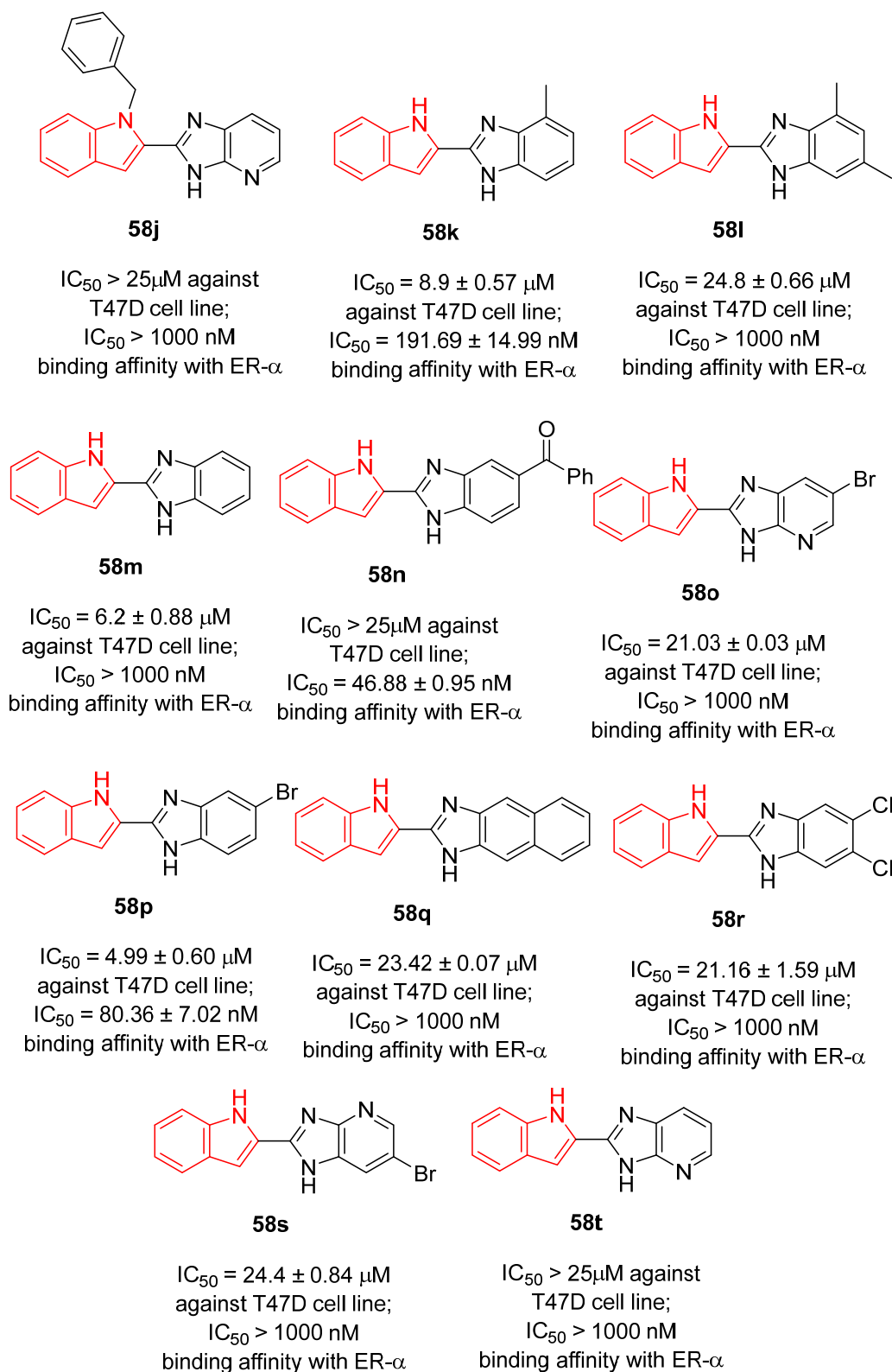
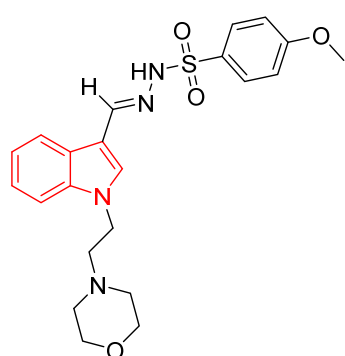
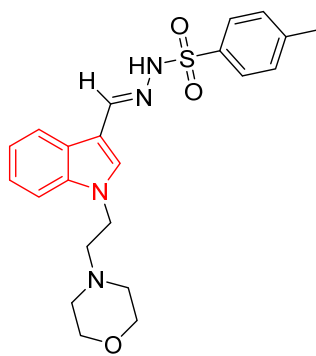


Fig. S3 (continued). Antiproliferation properties (μM) and binding affinity with ER- α (nM) of the synthesized indole-benzimidazole conjugates **58**.



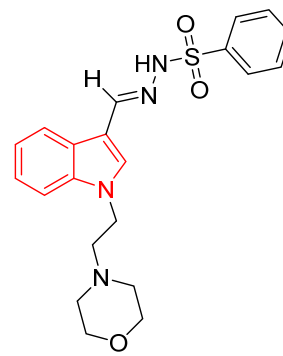
66a

IC_{50} = 62.75, 43.32 μ M against MCF7 and MDA-MB468, respectively



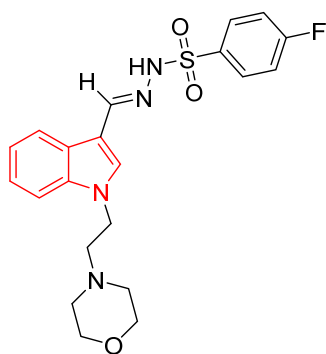
66b

IC_{50} = 61.14, 40.81 μ M against MCF7 and MDA-MB468, respectively



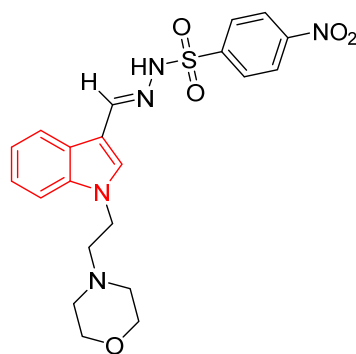
66c

IC_{50} = 73.15, 47.02 μ M against MCF7 and MDA-MB468, respectively



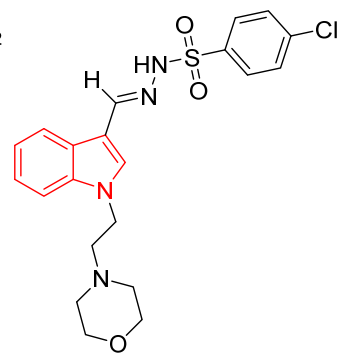
66d

IC_{50} = 32.59, 15.00 μ M against MCF7 and MDA-MB468, respectively



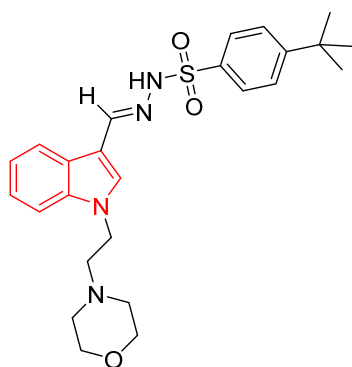
66e

IC_{50} = 82.03, 37.07 μ M against MCF7 and MDA-MB468, respectively



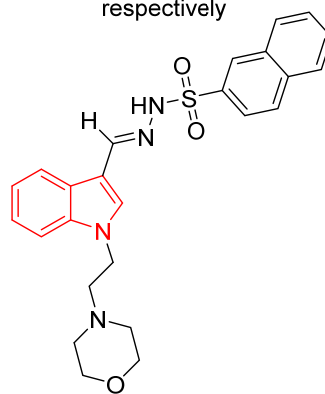
66f

IC_{50} = 13.2, 8.2 μ M against MCF7 and MDA-MB468, respectively



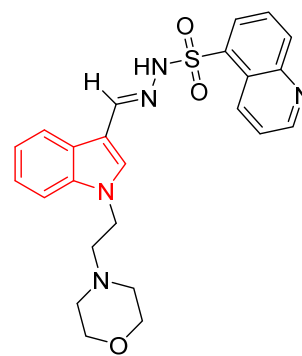
66g

IC_{50} = 67.84, 29.63 μ M against MCF7 and MDA-MB468, respectively



66h

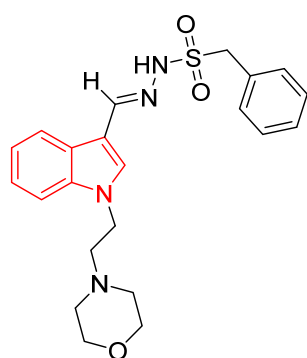
IC_{50} = 29.93, 53.38 μ M against MCF7 and MDA-MB468, respectively



66i

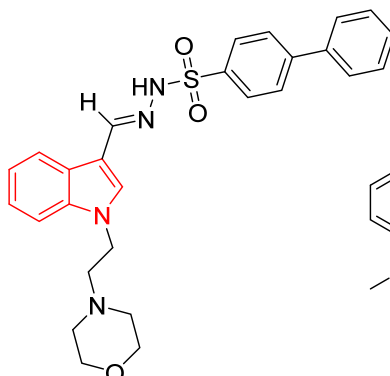
IC_{50} = 79.13, 32.20 μ M against MCF7 and MDA-MB468, respectively

Fig. S4. Antiproliferation properties of the synthesized indolyl sulfonylhydrazones **66** and Doxorubicin.



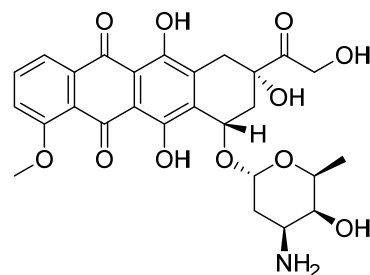
66j

IC_{50} = 62.53, 50.63 μ M against
MCF7 and MDA-MB468,
respectively



66k

IC_{50} = 17.30, 31.98 μ M against
MCF7 and MDA-MB468,
respectively



Doxorubicin

IC_{50} = 0.06, 0.08 μ M against
MCF7 and MDA-MB468,
respectively

Fig. S4 (continued). Antiproliferation properties of the synthesized indolyl sulfonohydrazones **66** and Doxorubicin.

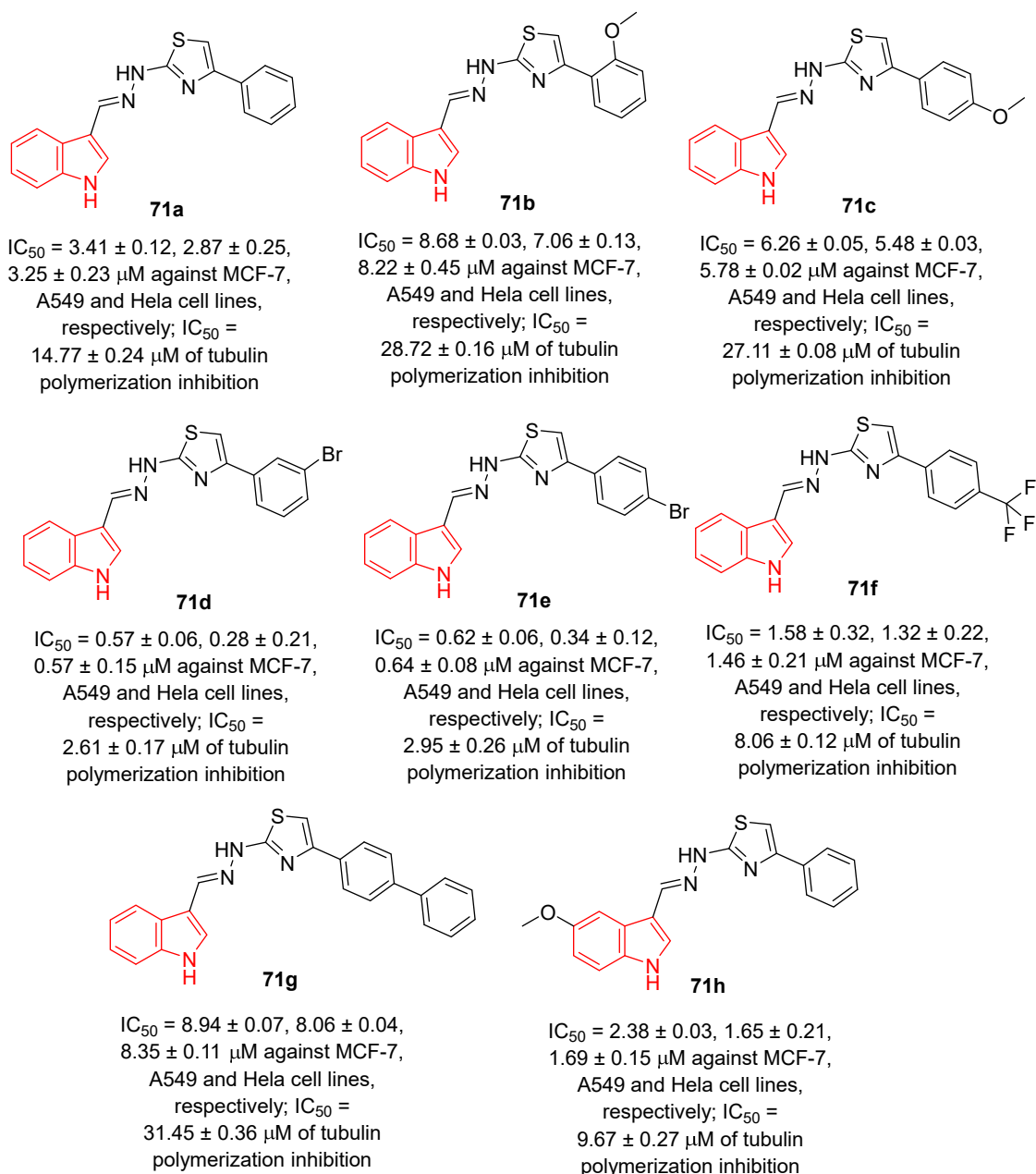
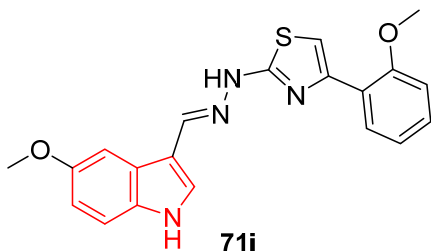
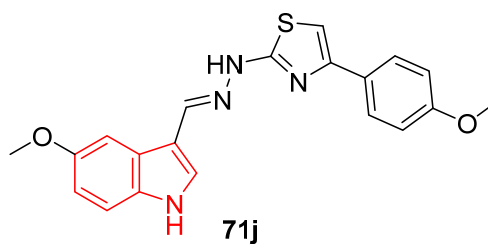


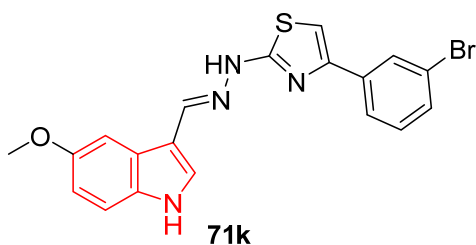
Fig. S5. Antiproliferation and tubulin polymerization inhibitory properties (μM ± SD) of the synthesized thiazolyl hydrazones linked to indolyl scaffold **71**, Colchicine and CA-4 (control drugs).



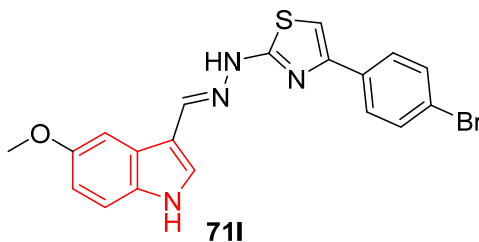
$IC_{50} = 5.82 \pm 0.08, 5.09 \pm 0.04, 5.52 \pm 0.18 \mu\text{M}$ against MCF-7, A549 and Hela cell lines, respectively; $IC_{50} = 24.62 \pm 0.19 \mu\text{M}$ of tubulin polymerization inhibition



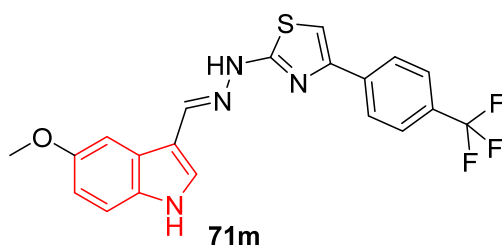
$IC_{50} = 5.29 \pm 0.11, 4.86 \pm 0.07, 5.08 \pm 0.25 \mu\text{M}$ against MCF-7, A549 and Hela cell lines, respectively; $IC_{50} = 24.13 \pm 0.02 \mu\text{M}$ of tubulin polymerization inhibition



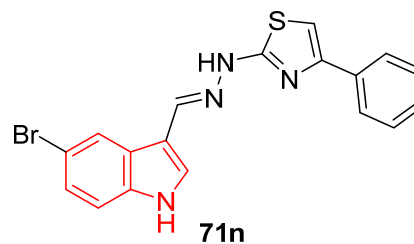
$IC_{50} = 0.46 \pm 0.13, 0.21 \pm 0.02, 0.32 \pm 0.26 \mu\text{M}$ against MCF-7, A549 and Hela cell lines, respectively; $IC_{50} = 1.68 \pm 0.07 \mu\text{M}$ of tubulin polymerization inhibition



$IC_{50} = 0.50 \pm 0.04, 0.23 \pm 0.42, 0.45 \pm 0.04 \mu\text{M}$ against MCF-7, A549 and Hela cell lines, respectively; $IC_{50} = 1.96 \pm 0.04 \mu\text{M}$ of tubulin polymerization inhibition

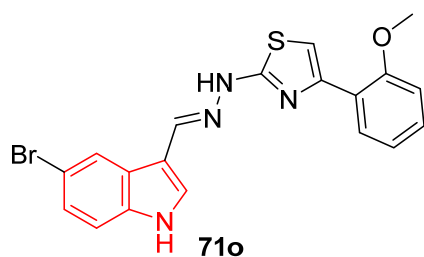


$IC_{50} = 1.23 \pm 0.35, 0.94 \pm 0.15, 1.17 \pm 0.11 \mu\text{M}$ against MCF-7, A549 and Hela cell lines, respectively; $IC_{50} = 6.42 \pm 0.32 \mu\text{M}$ of tubulin polymerization inhibition

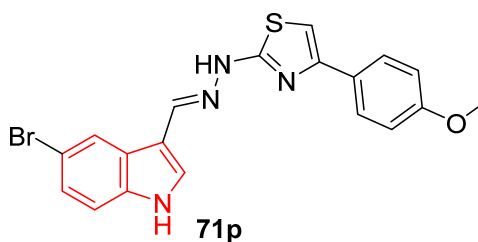


$IC_{50} = 5.09 \pm 0.07, 4.72 \pm 0.12, 4.94 \pm 0.09 \mu\text{M}$ against MCF-7, A549 and Hela cell lines, respectively; $IC_{50} = 22.35 \pm 0.15 \mu\text{M}$ of tubulin polymerization inhibition

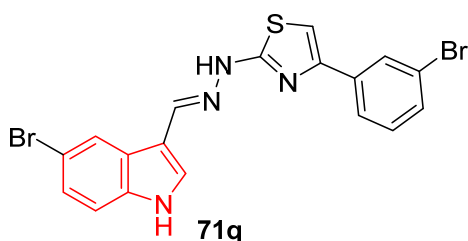
Fig. S5 (continued). Antiproliferation and tubulin polymerization inhibitory properties ($\mu\text{M} \pm \text{SD}$) of the synthesized thiazolyl hydrazones linked to indolyl scaffold **71**, Colchicine and CA-4 (control drugs).



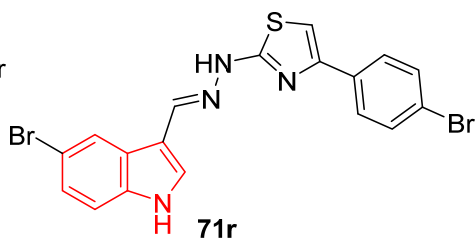
$IC_{50} = 11.32 \pm 0.26, 9.45 \pm 0.05, 10.33 \pm 0.12 \mu\text{M}$ against MCF-7, A549 and Hela cell lines, respectively; $IC_{50} = 38.40 \pm 0.06 \mu\text{M}$ of tubulin polymerization inhibition



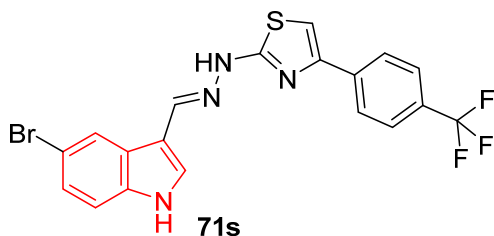
$IC_{50} = 9.23 \pm 0.07, 8.44 \pm 0.07, 8.81 \pm 0.06 \mu\text{M}$ against MCF-7, A549 and Hela cell lines, respectively; $IC_{50} = 35.26 \pm 0.27 \mu\text{M}$ of tubulin polymerization inhibition



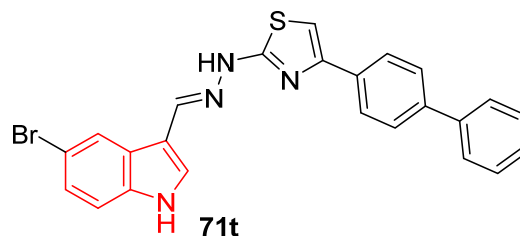
$IC_{50} = 0.77 \pm 0.03, 0.72 \pm 0.15, 0.75 \pm 0.08 \mu\text{M}$ against MCF-7, A549 and Hela cell lines, respectively; $IC_{50} = 4.66 \pm 0.04 \mu\text{M}$ of tubulin polymerization inhibition



$IC_{50} = 0.84 \pm 0.26, 0.79 \pm 0.34, 0.82 \pm 0.13 \mu\text{M}$ against MCF-7, A549 and Hela cell lines, respectively; $IC_{50} = 5.77 \pm 0.23 \mu\text{M}$ of tubulin polymerization inhibition

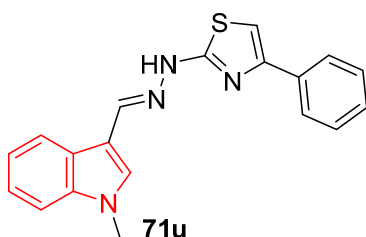


$IC_{50} = 4.86 \pm 0.08, 3.75 \pm 0.12, 4.39 \pm 0.21 \mu\text{M}$ against MCF-7, A549 and Hela cell lines, respectively; $IC_{50} = 21.32 \pm 0.08 \mu\text{M}$ of tubulin polymerization inhibition

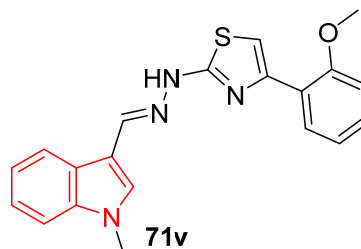


$IC_{50} = 14.24 \pm 0.13, 10.42 \pm 0.37, 11.44 \pm 0.18 \mu\text{M}$ against MCF-7, A549 and Hela cell lines, respectively; $IC_{50} = 41.33 \pm 0.11 \mu\text{M}$ of tubulin polymerization inhibition

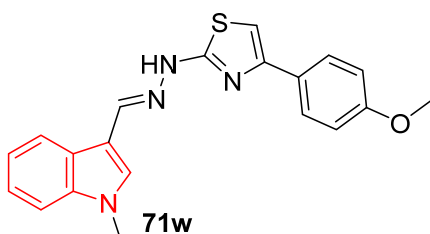
Fig. S5 (continued). Antiproliferation and tubulin polymerization inhibitory properties ($\mu\text{M} \pm \text{SD}$) of the synthesized thiazolyl hydrazones linked to indolyl scaffold **71**, Colchicine and CA-4 (control drugs).



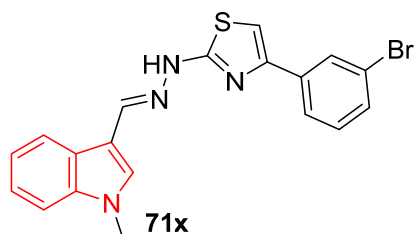
$IC_{50} = 4.67 \pm 0.08, 3.30 \pm 0.05, 3.42 \pm 0.09 \mu\text{M}$ against MCF-7, A549 and Hela cell lines, respectively; $IC_{50} = 17.21 \pm 0.03 \mu\text{M}$ of tubulin polymerization inhibition



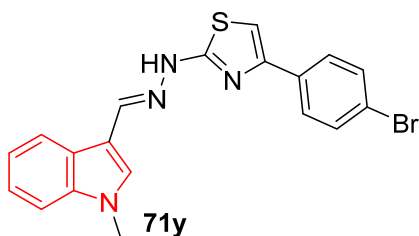
$IC_{50} = 9.86 \pm 0.15, 8.56 \pm 0.33, 8.83 \pm 0.22 \mu\text{M}$ against MCF-7, A549 and Hela cell lines, respectively; $IC_{50} = 36.18 \pm 0.09 \mu\text{M}$ of tubulin polymerization inhibition



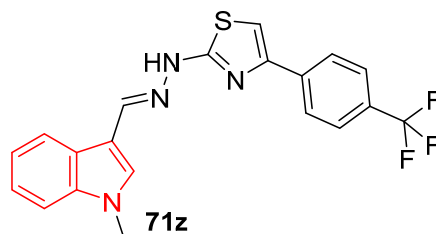
$IC_{50} = 7.08 \pm 0.16, 5.78 \pm 0.08, 5.86 \pm 0.14 \mu\text{M}$ against MCF-7, A549 and Hela cell lines, respectively; $IC_{50} = 28.16 \pm 0.22 \mu\text{M}$ of tubulin polymerization inhibition



$IC_{50} = 0.69 \pm 0.26, 0.61 \pm 0.19, 0.68 \pm 0.15 \mu\text{M}$ against MCF-7, A549 and Hela cell lines, respectively; $IC_{50} = 3.12 \pm 0.42 \mu\text{M}$ of tubulin polymerization inhibition

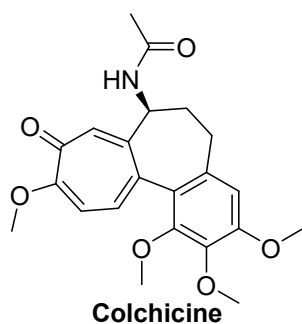


$IC_{50} = 0.78 \pm 0.25, 0.76 \pm 0.22, 0.76 \pm 0.13 \mu\text{M}$ against MCF-7, A549 and Hela cell lines, respectively; $IC_{50} = 4.86 \pm 0.31 \mu\text{M}$ of tubulin polymerization inhibition

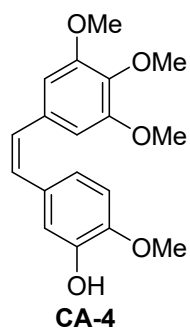


$IC_{50} = 2.84 \pm 0.09, 1.85 \pm 0.04, 1.93 \pm 0.23 \mu\text{M}$ against MCF-7, A549 and Hela cell lines, respectively; $IC_{50} = 11.43 \pm 0.15 \mu\text{M}$ of tubulin polymerization inhibition

Fig. S5 (continued). Antiproliferation and tubulin polymerization inhibitory properties ($\mu\text{M} \pm \text{SD}$) of the synthesized thiazolyl hydrazones linked to indolyl scaffold **71**, Colchicine and CA-4 (control drugs).



$IC_{50} = 0.75 \pm 0.08, 0.68 \pm 0.12, 0.72 \pm 0.16 \mu\text{M}$ against MCF-7, A549 and Hela cell lines, respectively; $IC_{50} = 3.28 \pm 0.25 \mu\text{M}$ of tubulin polymerization inhibition



$IC_{50} = 0.52 \pm 0.04, 0.24 \pm 0.21, 0.48 \pm 0.24 \mu\text{M}$ against MCF-7, A549 and Hela cell lines, respectively; $IC_{50} = 2.12 \pm 0.07 \mu\text{M}$ of tubulin polymerization inhibition

Fig. S5 (continued). Antiproliferation and tubulin polymerization inhibitory properties ($\mu\text{M} \pm \text{SD}$) of the synthesized thiazolyl hydrazones linked to indolyl scaffold **71**, Colchicine and CA-4 (control drugs).

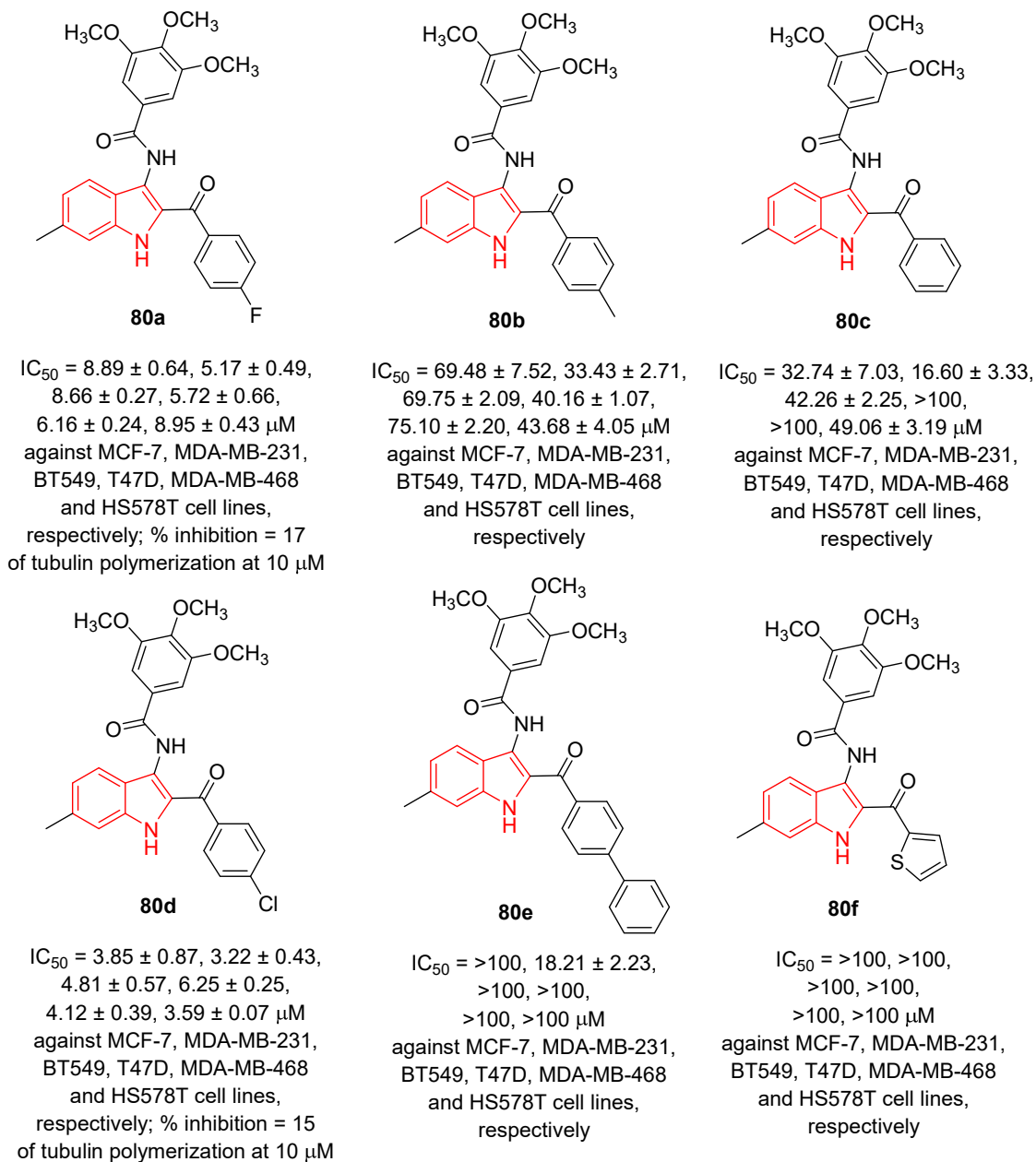
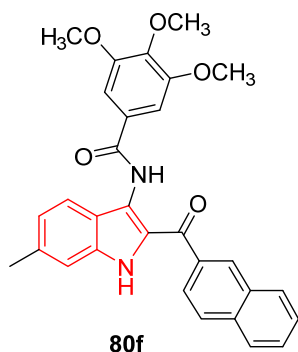
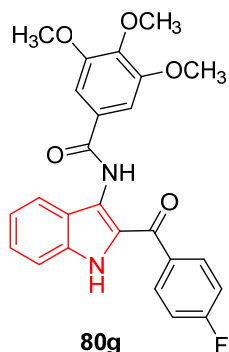


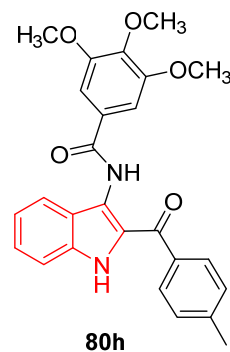
Fig. S6. Antiproliferation (μM ± SD) and % inhibitory properties of tubulin polymerization at 10 μM of the synthesized 3-amidoindoles **80** and CA-4 (control drug).



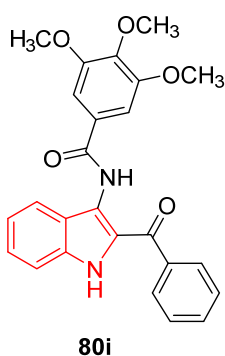
IC₅₀ = >100, >100,
39.75 ± 3.36, >100,
>100, 53.32 ± 6.62 μM
against MCF-7, MDA-MB-231,
BT549, T47D, MDA-MB-468
and HS578T cell lines,
respectively



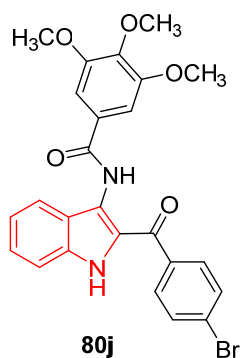
IC₅₀ = 77.92 ± 10.01, 50.76 ± 3.86,
42.58 ± 2.97, 60.86 ± 3.32,
>100, >100 μM
against MCF-7, MDA-MB-231,
BT549, T47D, MDA-MB-468
and HS578T cell lines,
respectively



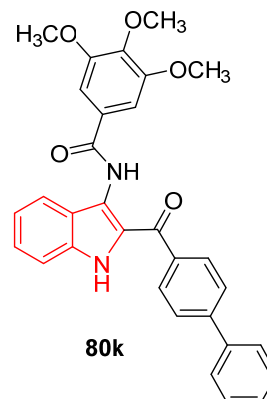
IC₅₀ = 50.00 ± 14.35, 12.61 ± 1.78,
17.07 ± 0.87, 20.06 ± 2.04,
14.52 ± 0.99, 50.49 ± 2.26 μM
against MCF-7, MDA-MB-231,
BT549, T47D, MDA-MB-468
and HS578T cell lines,
respectively



IC₅₀ = >100, 17.22 ± 2.04,
>100, >100,
>100, >100 μM
against MCF-7, MDA-MB-231,
BT549, T47D, MDA-MB-468
and HS578T cell lines,
respectively

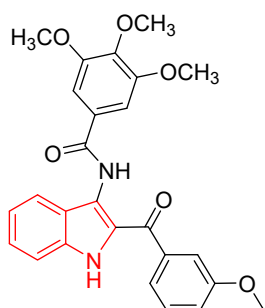


IC₅₀ = 7.14 ± 1.15, 6.47 ± 0.95,
10.31 ± 1.42, 9.55 ± 0.31,
7.87 ± 0.55, 7.52 ± 0.61 μM
against MCF-7, MDA-MB-231,
BT549, T47D, MDA-MB-468
and HS578T cell lines,
respectively, % inhibition = 37
of tubulin polymerization at 10 μM



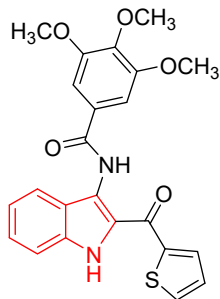
IC₅₀ = >100, >100,
>100, >100,
>100, 22.24 ± 1.42 μM
against MCF-7, MDA-MB-231,
BT549, T47D, MDA-MB-468
and HS578T cell lines,
respectively

Fig. S6 (continued). Antiproliferation (μM ± SD) and % inhibitory properties of tubulin polymerization at 10 μM of the synthesized 3-amidoindoles **80** and CA-4 (control drug).



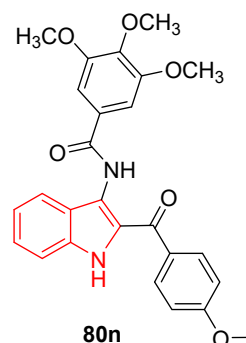
80l

IC_{50} = >100, >100,
65.53 \pm 7.13, 53.39 \pm 3.25,
>100, 9.06 \pm 4.22 μ M
against MCF-7, MDA-MB-231,
BT549, T47D, MDA-MB-468
and HS578T cell lines,
respectively



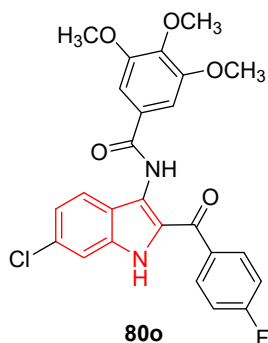
80m

IC_{50} = >100, >100,
>100, >100,
>100, 29.57 \pm 1.13 μ M
against MCF-7, MDA-MB-231,
BT549, T47D, MDA-MB-468
and HS578T cell lines,
respectively



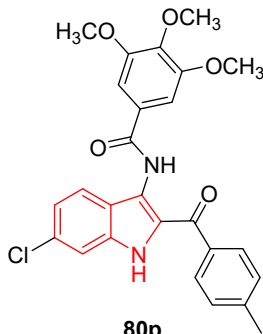
80n

IC_{50} = 10.70 \pm 0.77, 34.96 \pm 2.92,
10.37 \pm 0.23, 5.56 \pm 0.37,
7.09 \pm 0.78, >100 μ M
against MCF-7, MDA-MB-231,
BT549, T47D, MDA-MB-468
and HS578T cell lines,
respectively, % inhibition = 20
of tubulin polymerization at 10 μ M



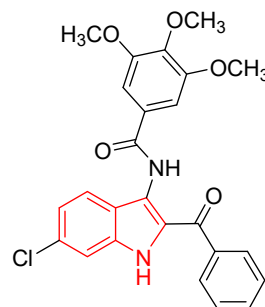
80o

IC_{50} = 61.08 \pm 17.61, 46.65 \pm 7.47,
35.54 \pm 3.13, 76.17 \pm 2.93,
>100, >100 μ M
against MCF-7, MDA-MB-231,
BT549, T47D, MDA-MB-468
and HS578T cell lines,
respectively



80p

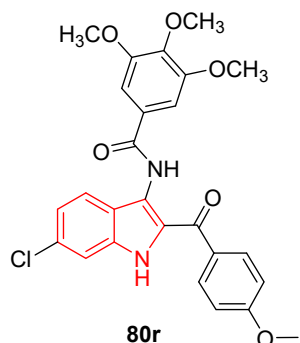
IC_{50} = 34.33 \pm 2.98, 33.65 \pm 0.61,
25.05 \pm 2.09, 16.65 \pm 0.34,
5.79 \pm 0.09, 14.19 \pm 0.54 μ M
against MCF-7, MDA-MB-231,
BT549, T47D, MDA-MB-468
and HS578T cell lines,
respectively, % inhibition = 36
of tubulin polymerization at 10 μ M



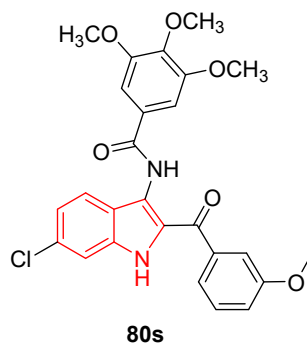
80q

IC_{50} = 51.78 \pm 5.84, 32.66 \pm 5.27,
26.89 \pm 1.78, 45.51 \pm 2.69,
11.04 \pm 0.19, >100 μ M
against MCF-7, MDA-MB-231,
BT549, T47D, MDA-MB-468
and HS578T cell lines,
respectively, % inhibition = 41
of tubulin polymerization at 10 μ M

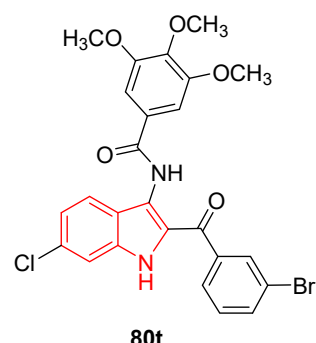
Fig. S6 (continued). Antiproliferation (μ M \pm SD) and % inhibitory properties of tubulin polymerization at 10 μ M of the synthesized 3-amidoindoles **80** and CA-4 (control drug).



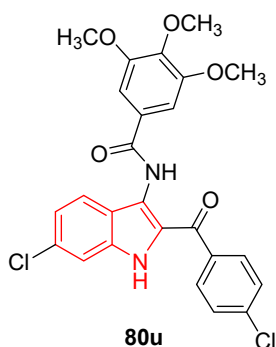
$IC_{50} = 17.62 \pm 0.40, 9.17 \pm 1.01, 11.14 \pm 0.43, 11.09 \pm 1.31, 8.61 \pm 0.51, 15.93 \pm 1.27 \mu M$ against MCF-7, MDA-MB-231, BT549, T47D, MDA-MB-468 and HS578T cell lines, respectively, % inhibition = 47 of tubulin polymerization at $10 \mu M$



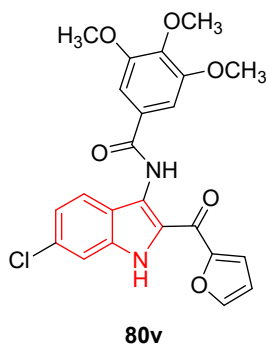
$IC_{50} = >100, >100, >100, 52.41 \pm 1.06, >100, >100 \mu M$ against MCF-7, MDA-MB-231, BT549, T47D, MDA-MB-468 and HS578T cell lines, respectively



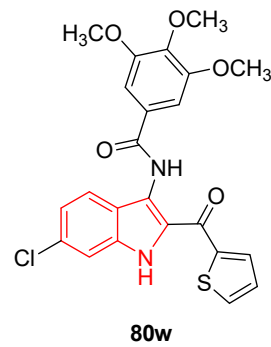
$IC_{50} = 23.02 \pm 2.47, 26.75 \pm 1.12, 8.42 \pm 1.06, 14.07 \pm 0.61, 20.79 \pm 0.34, 4.10 \pm 0.27 \mu M$ against MCF-7, MDA-MB-231, BT549, T47D, MDA-MB-468 and HS578T cell lines, respectively, % inhibition = 25 of tubulin polymerization at $10 \mu M$



$IC_{50} = 10.87 \pm 0.87, 6.43 \pm 1.12, 3.17 \pm 0.46, 0.04 \pm 0.06, 7.92 \pm 1.36, >100 \mu M$ against MCF-7, MDA-MB-231, BT549, T47D, MDA-MB-468 and HS578T cell lines, respectively, % inhibition = 59 of tubulin polymerization at $10 \mu M$

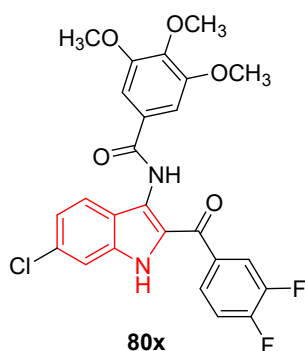


$IC_{50} = >100, >100, >100, >100, >100, >100 \mu M$ against MCF-7, MDA-MB-231, BT549, T47D, MDA-MB-468 and HS578T cell lines, respectively

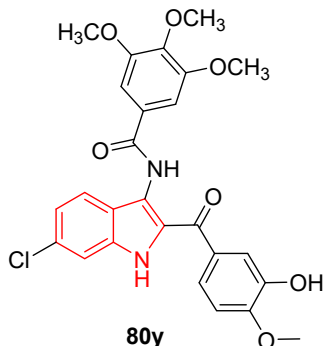


$IC_{50} = 47.46 \pm 3.29, >100, 37.51 \pm 7.14, 31.45 \pm 1.87, 15.33 \pm 3.11, 49.23 \pm 4.6 \mu M$ against MCF-7, MDA-MB-231, BT549, T47D, MDA-MB-468 and HS578T cell lines, respectively

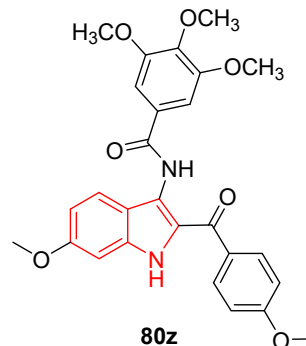
Fig. S6 (continued). Antiproliferation ($\mu M \pm SD$) and % inhibitory properties of tubulin polymerization at $10 \mu M$ of the synthesized 3-amidoindoles **80** and CA-4 (control drug).



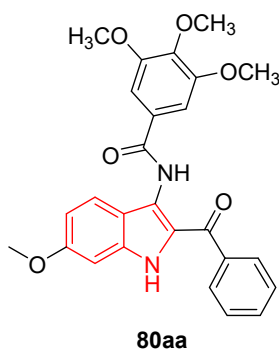
$IC_{50} = 10.14 \pm 1.16$, >100 ,
 10.14 ± 1.16 , >100 ,
 >100 , $64.57 \pm 5.73 \mu M$
 against MCF-7, MDA-MB-231,
 BT549, T47D, MDA-MB-468
 and HS578T cell lines,
 respectively



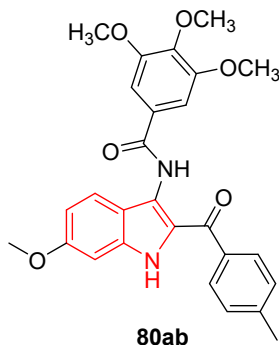
$IC_{50} = 32.60 \pm 0.68$, 22.18 ± 1.38 ,
 7.48 ± 0.19 , 9.28 ± 0.13 ,
 23.21 ± 2.08 , $4.35 \pm 0.14 \mu M$
 against MCF-7, MDA-MB-231,
 BT549, T47D, MDA-MB-468
 and HS578T cell lines,
 respectively, % inhibition = 30
 of tubulin polymerization at $10 \mu M$



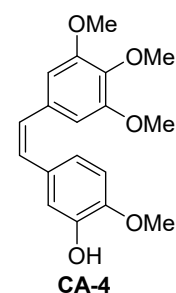
$IC_{50} = 79.27 \pm 3.05$, 48.84 ± 2.76 ,
 18.20 ± 0.13 , 6.30 ± 0.52 ,
 26.38 ± 1.36 , $10.44 \pm 0.66 \mu M$
 against MCF-7, MDA-MB-231,
 BT549, T47D, MDA-MB-468
 and HS578T cell lines,
 respectively, % inhibition = 25
 of tubulin polymerization at $10 \mu M$



$IC_{50} = >100$, >100 ,
 >100 , >100 ,
 >100 , $>100 \mu M$
 against MCF-7, MDA-MB-231,
 BT549, T47D, MDA-MB-468
 and HS578T cell lines,
 respectively

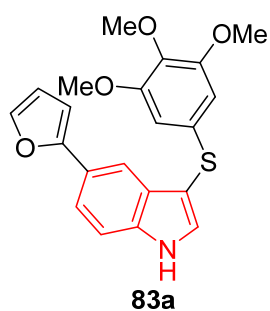


$IC_{50} = >100$, >100 ,
 >100 , >100 ,
 >100 , $>100 \mu M$
 against MCF-7, MDA-MB-231,
 BT549, T47D, MDA-MB-468
 and HS578T cell lines,
 respectively

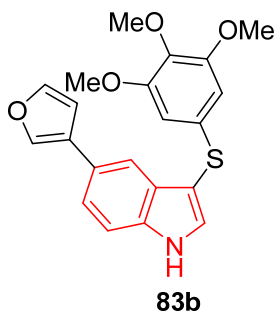


$IC_{50} = 3.00 \pm 0.65$, 3.17 ± 0.57 ,
 1.71 ± 0.44 , 1.89 ± 0.34 ,
 1.55 ± 0.18 , $1.36 \pm 0.23 \mu M$
 against MCF-7, MDA-MB-231,
 BT549, T47D, MDA-MB-468
 and HS578T cell lines,
 respectively, % inhibition = 80
 of tubulin polymerization at $10 \mu M$

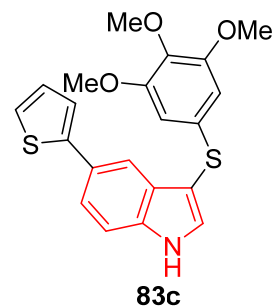
Fig. S6 (continued). Antiproliferation ($\mu M \pm SD$) and % inhibitory properties of tubulin polymerization at $10 \mu M$ of the synthesized 3-amidoindoles **80** and CA-4 (control drug).



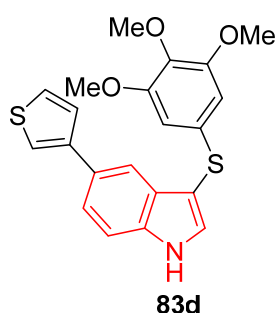
$IC_{50} = 70 \pm 10 \mu M$ against
MCF-7, $IC_{50} = 0.87 \pm 0.1$
 μM tubulin polymerization
inhibition



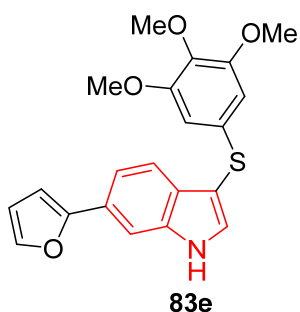
$IC_{50} = 200 \pm 100 \mu M$ against
MCF-7, $IC_{50} = 1.8 \pm 0.1$
 μM tubulin polymerization
inhibition



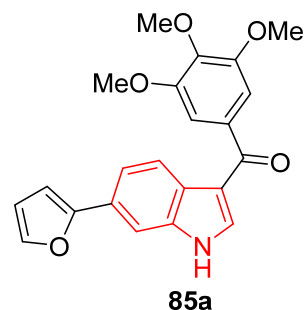
$IC_{50} = 150 \pm 70 \mu M$ against
MCF-7, $IC_{50} = 1.3 \pm 0.09$
 μM tubulin polymerization
inhibition



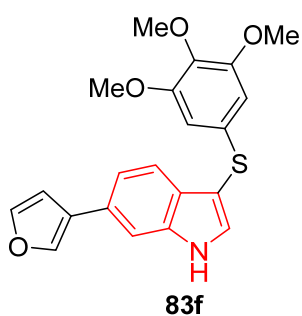
$IC_{50} = 200 \pm 0 \mu M$ against
MCF-7, $IC_{50} = 1.7 \pm 0.03$
 μM tubulin polymerization
inhibition



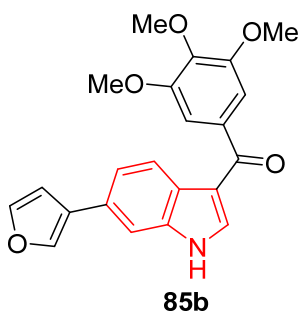
$IC_{50} = 10 \pm 3 \mu M$ against
MCF-7, $IC_{50} = 0.59 \pm 1$
 μM tubulin polymerization
inhibition



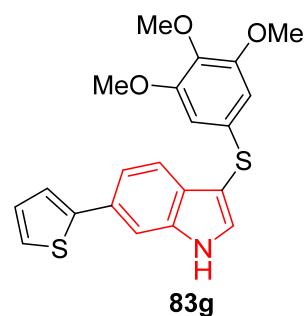
$IC_{50} = 4.7 \pm 0.6 \mu M$ against
MCF-7, $IC_{50} = 0.76 \pm 0.04$
 μM tubulin polymerization
inhibition



$IC_{50} = 10 \pm 0 \mu M$ against
MCF-7, $IC_{50} = 2.3 \pm 0.04$
 μM tubulin polymerization
inhibition



$IC_{50} = 4.3 \pm 0.6 \mu M$ against
MCF-7, $IC_{50} = 0.61 \pm 0.06$
 μM tubulin polymerization
inhibition



$IC_{50} = 6.0 \pm 1 \mu M$ against
MCF-7, $IC_{50} = 0.47 \pm 0.05$
 μM tubulin polymerization
inhibition

Fig. S7. Antiproliferation and tubulin polymerization inhibitory properties ($\mu M \pm SD$) of the synthesized 3-arylthio-1*H*-indoles **83**, 3-aroyl-1*H*-indoles **85** and standard drugs (CA-4 and Colchicine).

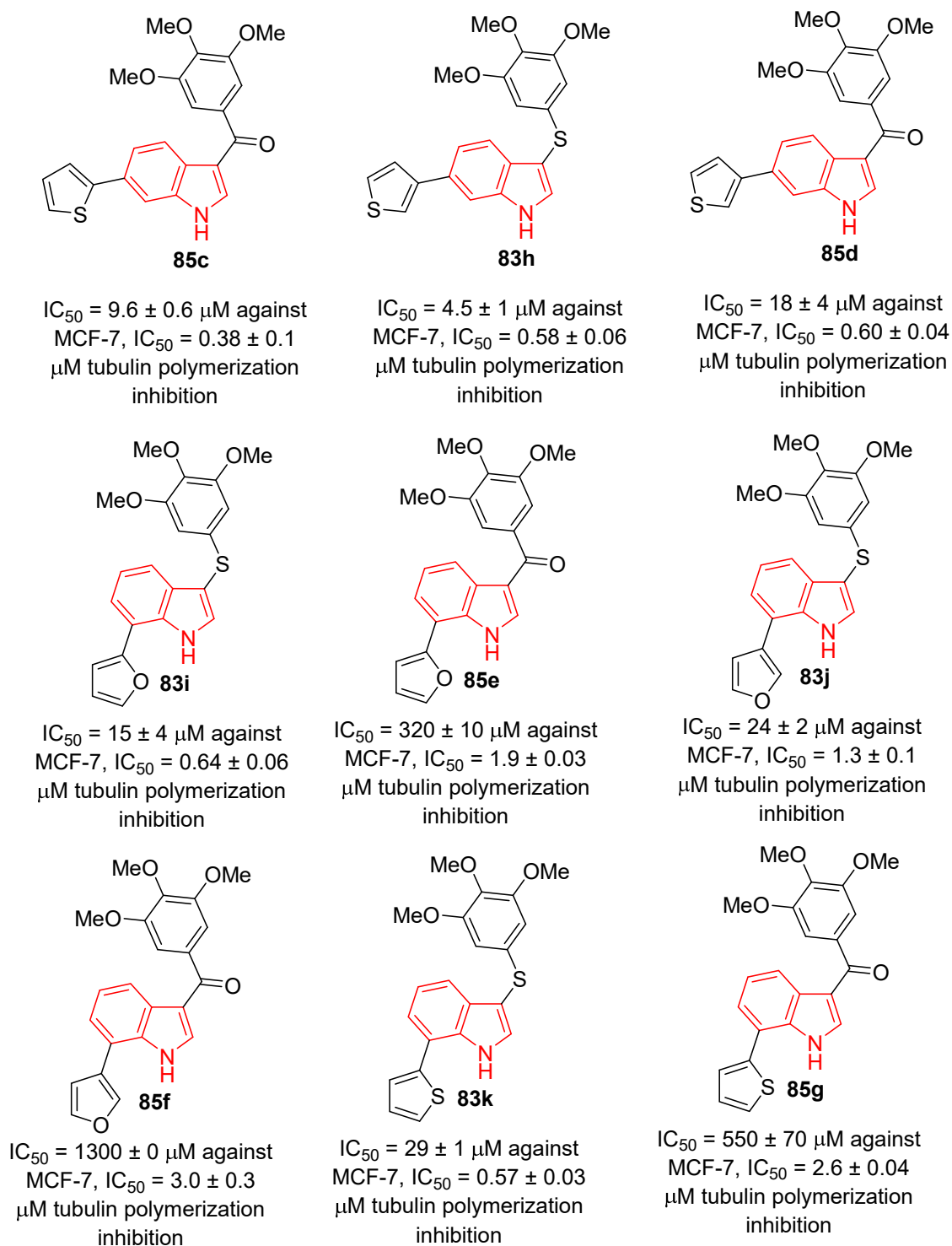


Fig. S7 (continued). Antiproliferation and tubulin polymerization inhibitory properties ($\mu M \pm SD$) of the synthesized 3-arylthio-1*H*-indoles **83**, 3-aryl-1*H*-indoles **85** and standard drugs (CA-4 and Colchicine).

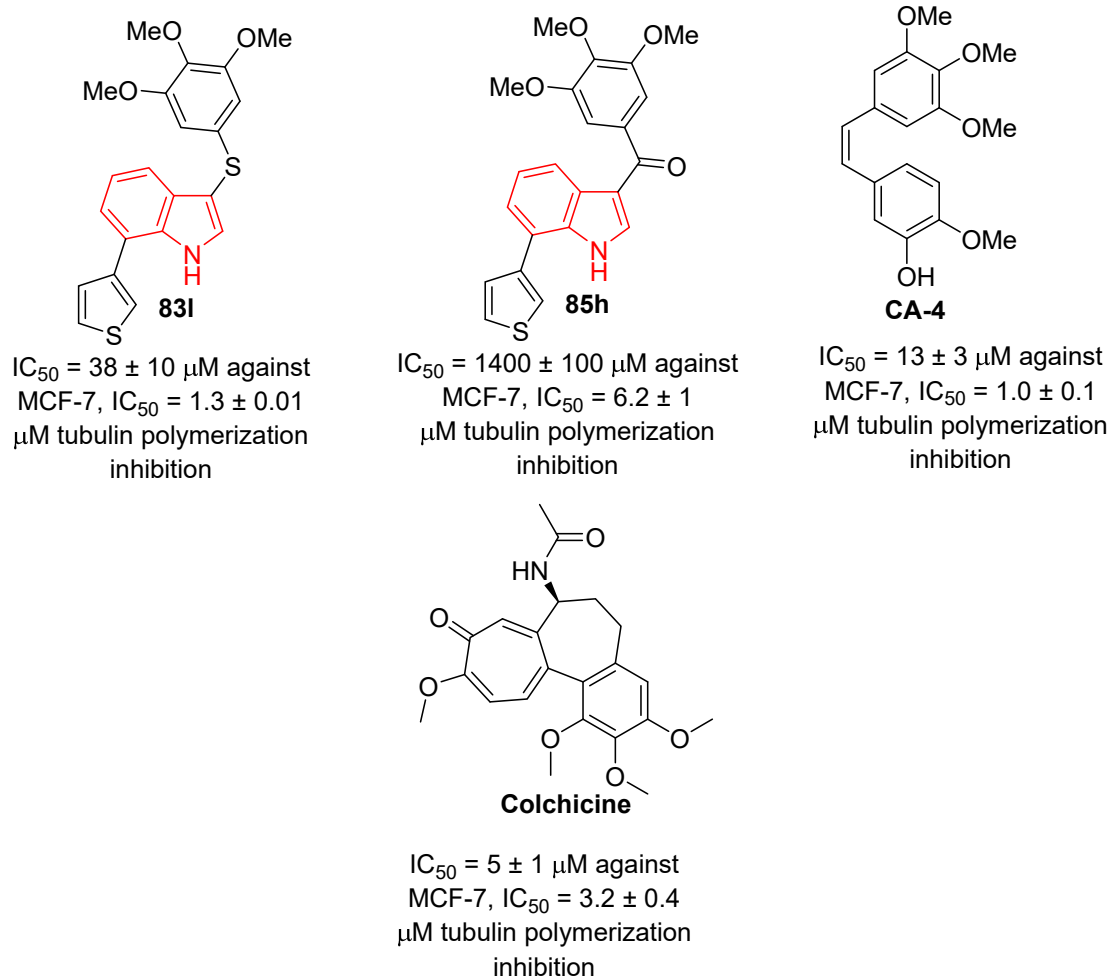
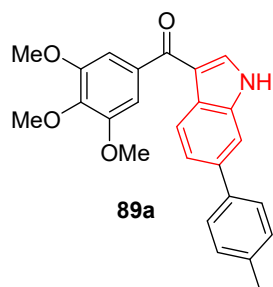
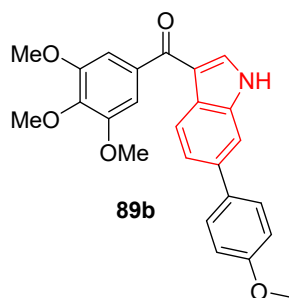


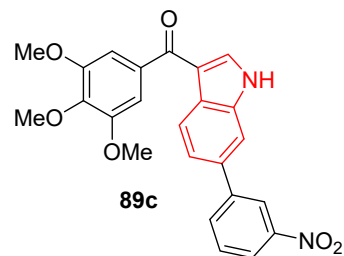
Fig. S7 (continued). Antiproliferation and tubulin polymerization inhibitory properties ($\mu M \pm SD$) of the synthesized 3-arylthio-1*H*-indoles **83**, 3-aryl-1*H*-indoles **85** and standard drugs (CA-4 and Colchicine).



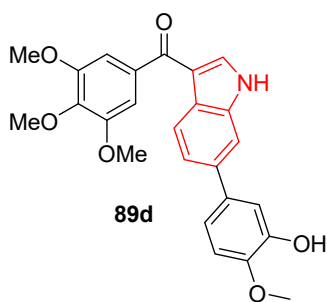
$GI_{50} = 560 \pm 60, 2010 \pm 433$
(nM) against MCF-7,
MDA-MB-231, respectively;
 $IC_{50} = 1.7 \pm 0.08 \mu M$ of
tubulin polymerization inhibition



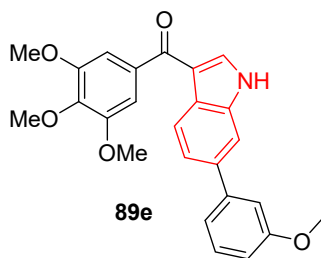
$GI_{50} = 98 \pm 30, 1860 \pm 285$
(nM) against MCF-7,
MDA-MB-231, respectively;
 $IC_{50} = 2.5 \pm 0.06 \mu M$ of
tubulin polymerization inhibition



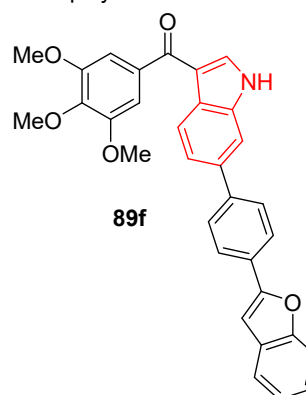
$GI_{50} = 28 \pm 10, 110 \pm 15$
(nM) against MCF-7,
MDA-MB-231, respectively;
 $IC_{50} = 0.65 \pm 0.06 \mu M$ of
tubulin polymerization inhibition



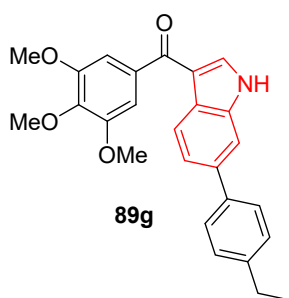
$GI_{50} = 1500 \pm 100, 828 \pm 155$
(nM) against MCF-7,
MDA-MB-231, respectively;
 $IC_{50} = >20 \mu M$ of
tubulin polymerization inhibition



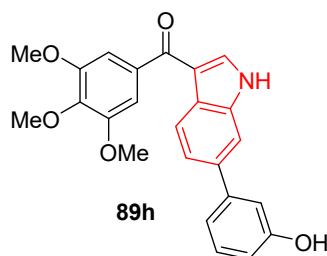
$GI_{50} = 23 \pm 7, 36 \pm 4$
(nM) against MCF-7,
MDA-MB-231, respectively;
 $IC_{50} = 0.37 \pm 0.04 \mu M$ of
tubulin polymerization inhibition



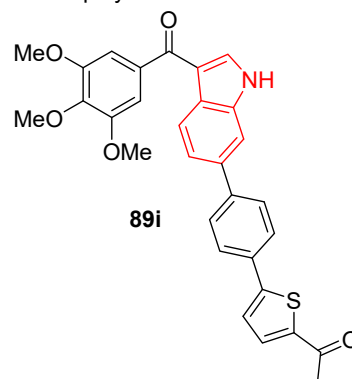
$GI_{50} = 950 \pm 200, 2066 \pm 302$
(nM) against MCF-7,
MDA-MB-231, respectively;
 $IC_{50} = >20 \mu M$ of
tubulin polymerization inhibition



$GI_{50} = 1800 \pm 500, 2220 \pm 180$
(nM) against MCF-7,
MDA-MB-231, respectively;
 $IC_{50} = >20 \mu M$ of
tubulin polymerization inhibition

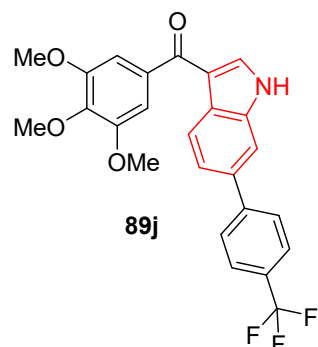


$GI_{50} = 320 \pm 20, 102 \pm 14$
(nM) against MCF-7,
MDA-MB-231, respectively;
 $IC_{50} = 0.57 \pm 0.02 \mu M$ of
tubulin polymerization inhibition

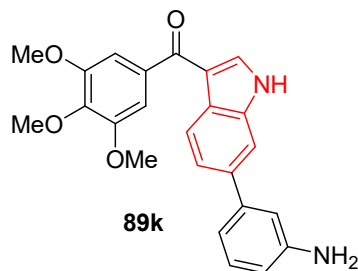


$GI_{50} = 73 \pm 4, 3231 \pm 482$
(nM) against MCF-7,
MDA-MB-231, respectively;
 $IC_{50} = >20 \mu M$ of
tubulin polymerization inhibition

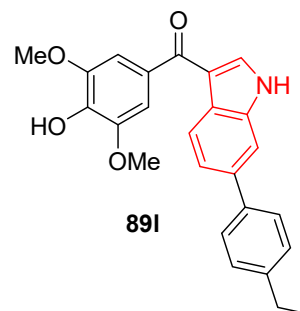
Fig. S8. Antiprolifeation (nM \pm SD) and tubulin polymerization inhibitory (μM \pm SD) properties of 6-ary-3-aryllindoles **89** and CA-4 (standard reference).



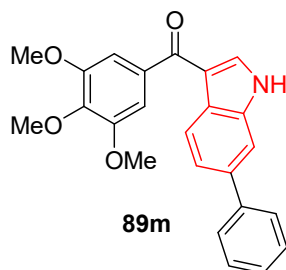
$GI_{50} = 1400 \pm 100, 4062 \pm 822$
(nM) against MCF-7,
MDA-MB-231, respectively;
 $IC_{50} = >20 \mu M$ of
tubulin polymerization inhibition



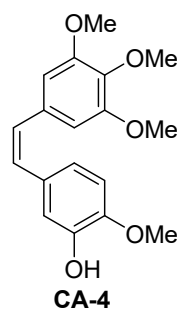
$GI_{50} = 65 \pm 7, 25 \pm 5$
(nM) against MCF-7,
MDA-MB-231, respectively;
 $IC_{50} = 0.42 \pm 0.08 \mu M$ of
tubulin polymerization inhibition



$GI_{50} = >5000, >5000$
(nM) against MCF-7,
MDA-MB-231, respectively;
 $IC_{50} = >20 \mu M$ of
tubulin polymerization inhibition



$GI_{50} = 73 \pm 10, 156 \pm 20$
(nM) against MCF-7,
MDA-MB-231, respectively;
 $IC_{50} = 0.28 \pm 0.04 \mu M$ of
tubulin polymerization inhibition



$GI_{50} = 9.0 \pm 2, 3.5 \pm 0.4$
(nM) against MCF-7,
MDA-MB-231, respectively;
 $IC_{50} = 0.75 \pm 0.06 \mu M$ of
tubulin polymerization inhibition

Fig. S8 (continued). Antiprolifeation (nM \pm SD) and tubulin polymerization inhibitory ($\mu M \pm$ SD) properties of 6-ary-3-arylindoles **89** and CA-4 (standard reference).

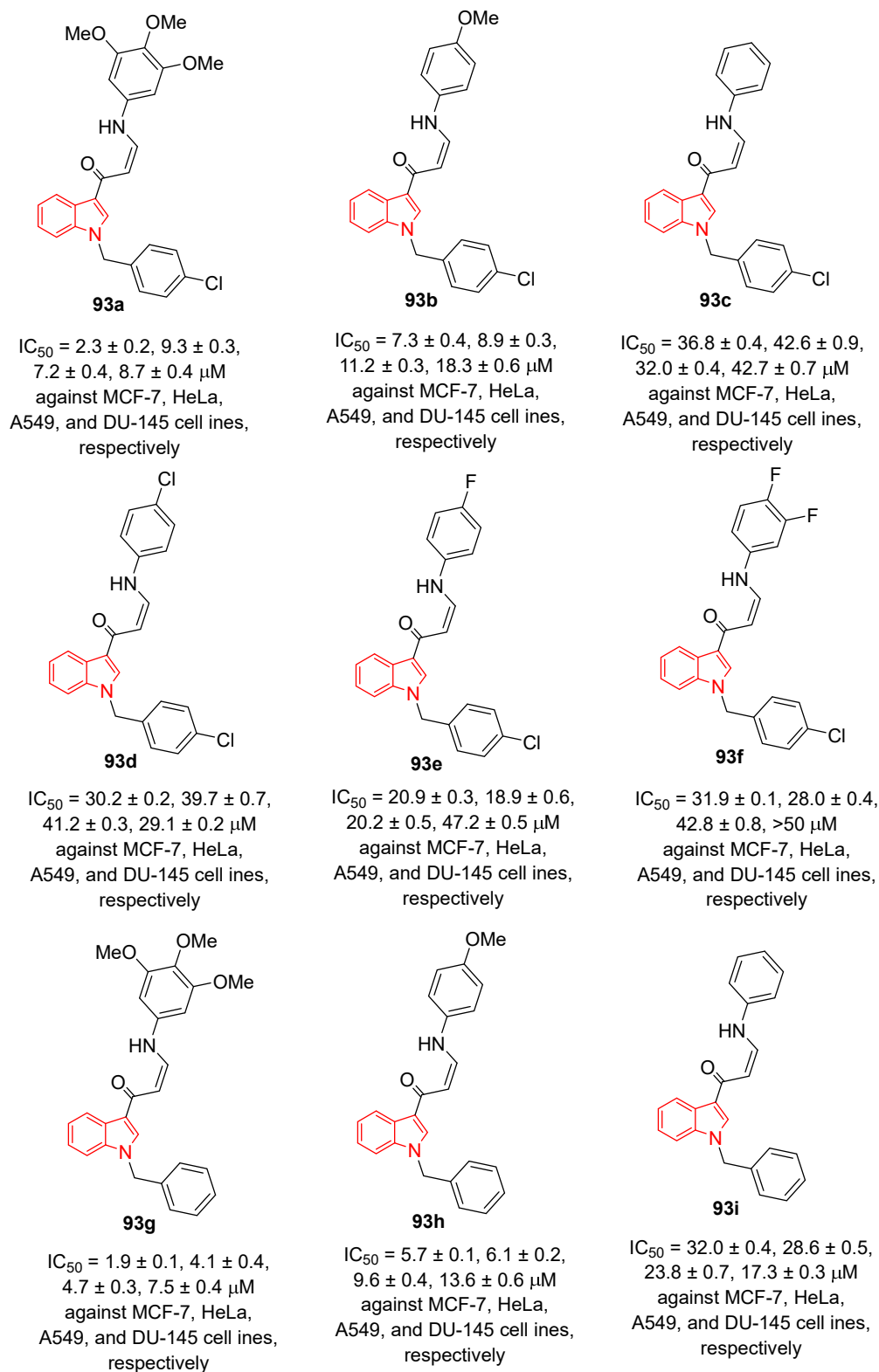


Fig. S9. Antiproliferation properties (μM ± SD) of the synthesized indolyl-arylaminopropenone conjugates **93** and reference drug (Doxorubicin).

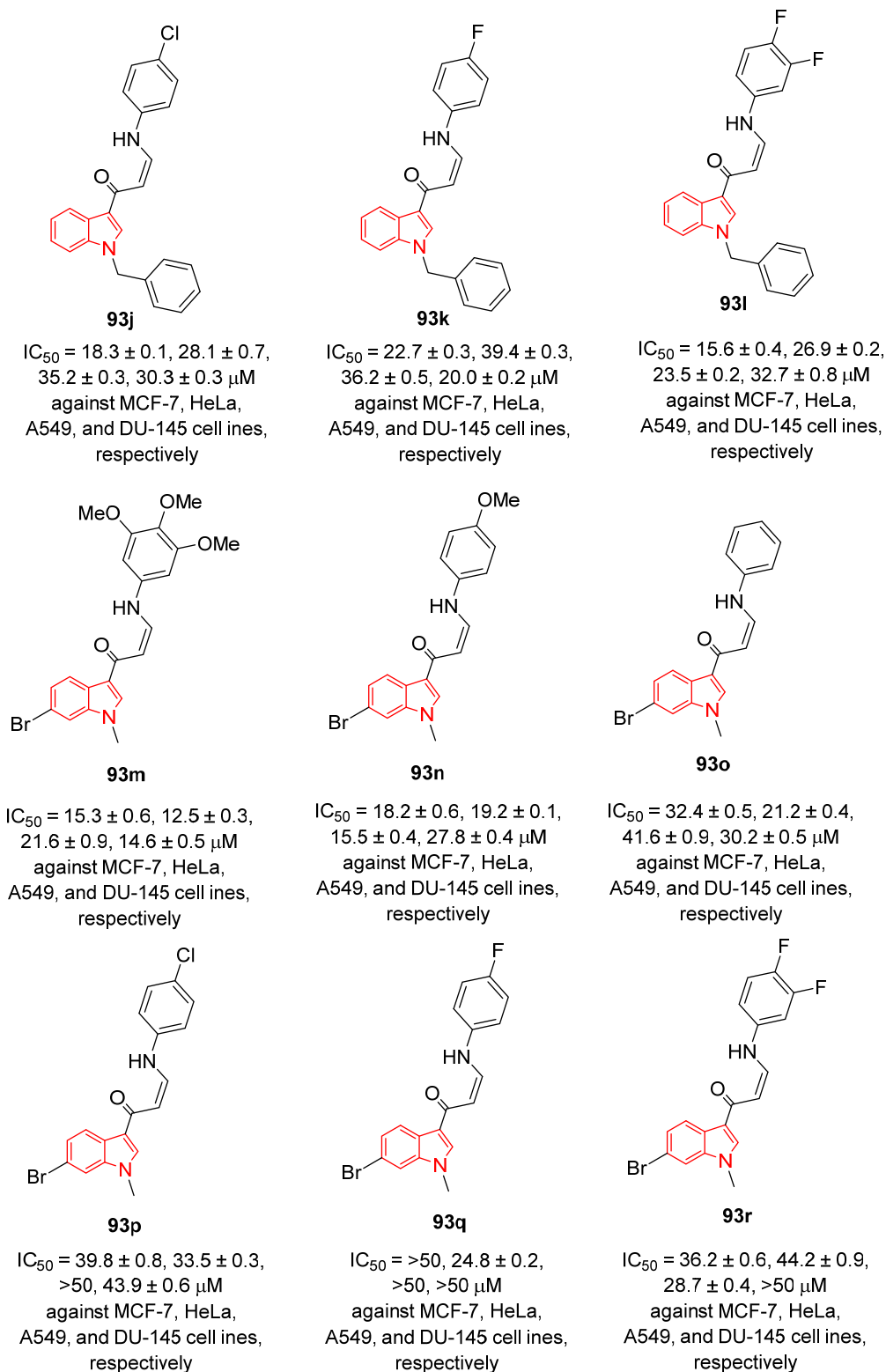
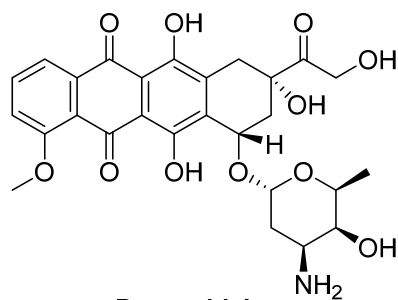


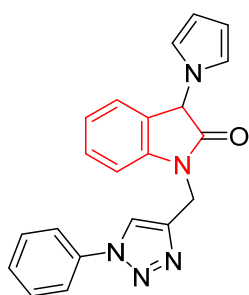
Fig. S9 (continued). Antiproliferation properties (μM ± SD) of the synthesized indolyl-arylaminopropenone conjugates **93** and reference drug (Doxorubicin).



Doxorubicin

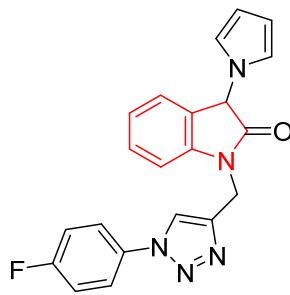
IC₅₀ = 0.8 ± 0.2, 1.6 ± 0.1,
 2.0 ± 0.1, 0.9 ± 0.1 μM
 against MCF-7, HeLa,
 A549, and DU-145 cell lines,
 respectively

Fig. S9 (continued). Antiproliferation properties (μM ± SD) of the synthesized indolyl-arylaminopropenone conjugates **93** and reference drug (Doxorubicin).



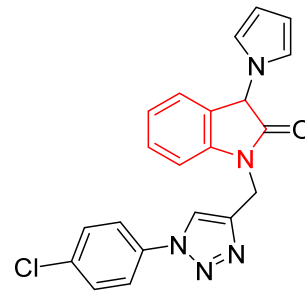
104a

IC₅₀ = >50, >50, ND
μM against MCF-7,
MDA-MB-231 and HEK-293
cell lines, respectively



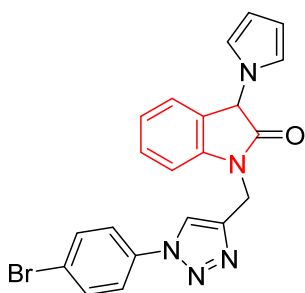
104b

IC₅₀ = >50, >50, ND
μM against MCF-7,
MDA-MB-231 and HEK-293
cell lines, respectively



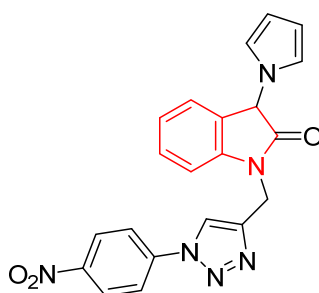
104c

IC₅₀ = >50, >50, ND
μM against MCF-7,
MDA-MB-231 and HEK-293
cell lines, respectively



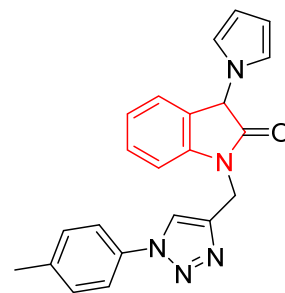
104d

IC₅₀ = >50, 18.9 ± 0.01, ND
μM against MCF-7,
MDA-MB-231 and HEK-293
cell lines, respectively



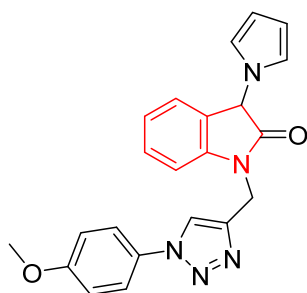
104e

IC₅₀ = >50, >50, ND
μM against MCF-7,
MDA-MB-231 and HEK-293
cell lines, respectively



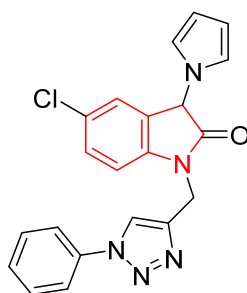
104f

IC₅₀ = >50, >50, ND
μM against MCF-7,
MDA-MB-231 and HEK-293
cell lines, respectively



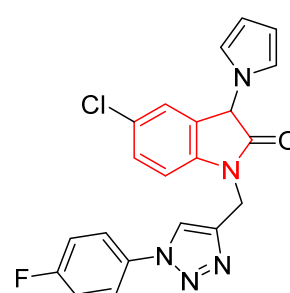
104g

IC₅₀ = >50, >50, ND
μM against MCF-7,
MDA-MB-231 and HEK-293
cell lines, respectively



104h

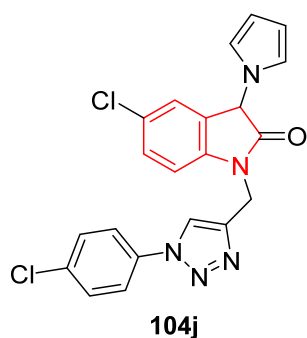
IC₅₀ = >50, 6.8 ± 0.01, >50
μM against MCF-7,
MDA-MB-231 and HEK-293
cell lines, respectively



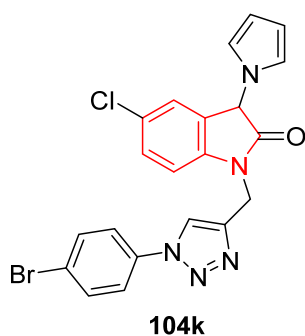
104i

IC₅₀ = >50, 35 ± 0.04, ND
μM against MCF-7,
MDA-MB-231 and HEK-293
cell lines, respectively

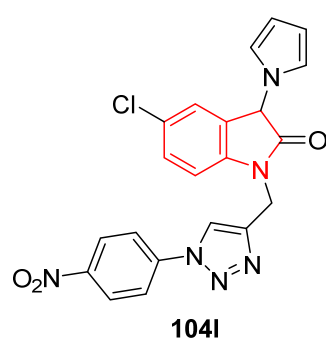
Fig. S10. Antiproliferation properties (μM ± SD) of the synthesized 3-pyrrolisatin-triazole conjugates **104** and Tamoxifen citrate "reference drug" (ND = not determined).



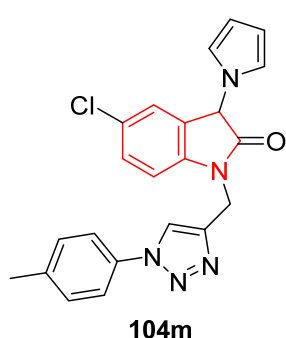
$IC_{50} = >50, >50, ND$
 μM against MCF-7,
 MDA-MB-231 and HEK-293
 cell lines, respectively



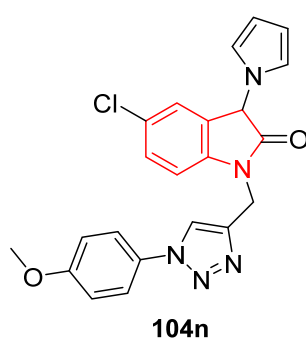
$IC_{50} = >50, >50, ND$
 μM against MCF-7,
 MDA-MB-231 and HEK-293
 cell lines, respectively



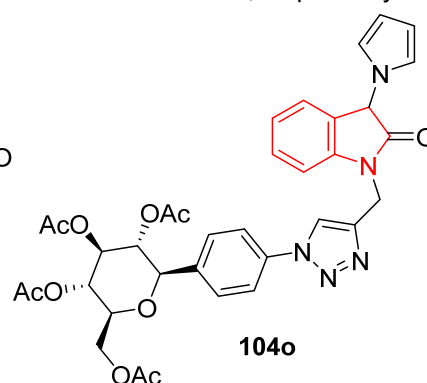
$IC_{50} = 30.1 \pm 0.02, 17.7 \pm 0.01,$
 $ND \mu M$ against MCF-7,
 MDA-MB-231 and HEK-293
 cell lines, respectively



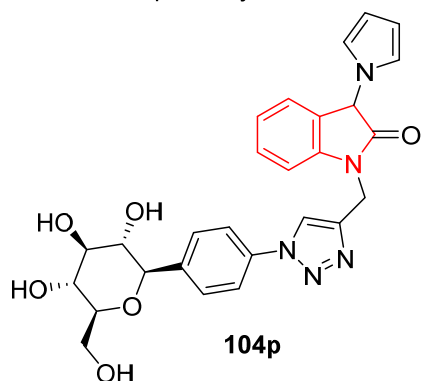
$IC_{50} = >50, 20 \pm 0.04, ND$
 μM against MCF-7,
 MDA-MB-231 and HEK-293
 cell lines, respectively



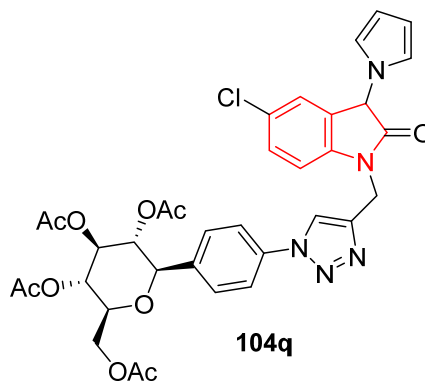
$IC_{50} = >50, >50, ND$
 μM against MCF-7,
 MDA-MB-231 and HEK-293
 cell lines, respectively



$IC_{50} = >50, >50, ND$
 μM against MCF-7,
 MDA-MB-231 and HEK-293
 cell lines, respectively

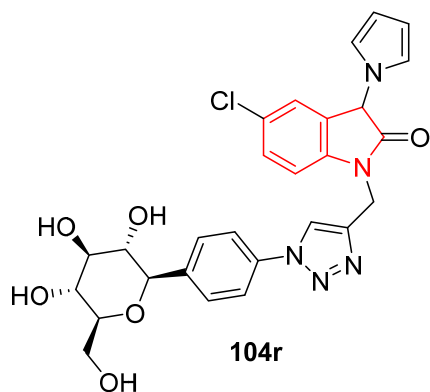


$IC_{50} = >50, >50, ND$
 μM against MCF-7,
 MDA-MB-231 and HEK-293
 cell lines, respectively

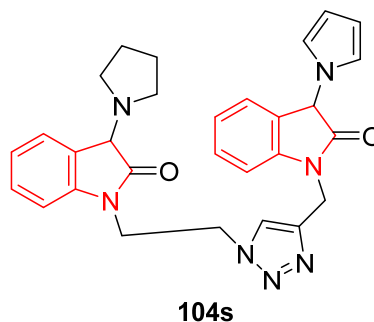


$IC_{50} = >50, 6 \pm 0.04, >50$
 μM against MCF-7,
 MDA-MB-231 and HEK-293
 cell lines, respectively

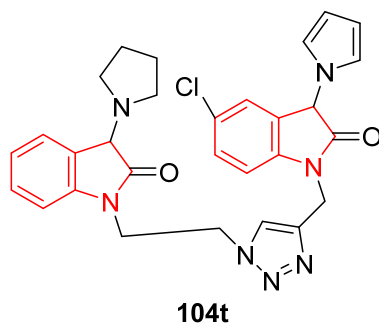
Fig. S10 (continued). Antiproliferation properties ($\mu M \pm SD$) of the synthesized 3-pyrrolylisatin-triazole conjugates **104** and Tamoxifen citrate "reference drug" (ND = not determined).



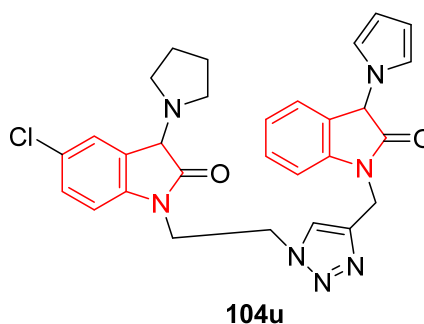
$IC_{50} = >50, 5.9 \pm 0.02, >50$
 μM against MCF-7,
 MDA-MB-231 and HEK-293
 cell lines, respectively



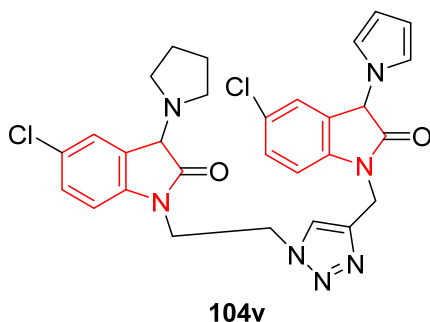
$IC_{50} = >50, 7.5 \pm 0.02, >50$
 μM against MCF-7,
 MDA-MB-231 and HEK-293
 cell lines, respectively



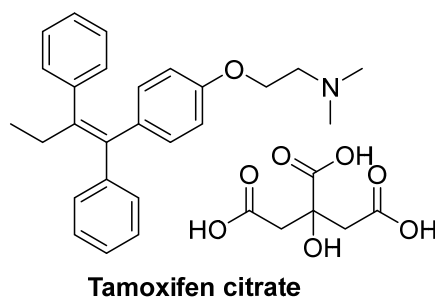
$IC_{50} = >50, 25 \pm 0.5, ND$
 μM against MCF-7,
 MDA-MB-231 and HEK-293
 cell lines, respectively



$IC_{50} = 44.3 \pm 0.03, 6.5 \pm 0.02,$
 $>50 \mu M$ against MCF-7,
 MDA-MB-231 and HEK-293
 cell lines, respectively

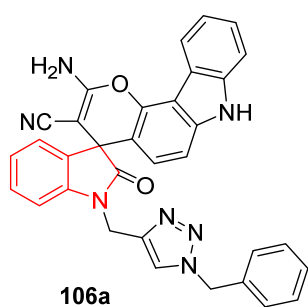


$IC_{50} = >50, 6.2 \pm 0.01,$
 $>50 \mu M$ against MCF-7,
 MDA-MB-231 and HEK-293
 cell lines, respectively

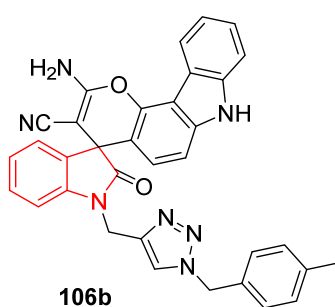


$IC_{50} = 12 \pm 0.02, 18.9 \pm 0.01,$
 $24 \pm 0.03 \mu M$ against MCF-7,
 MDA-MB-231 and HEK-293
 cell lines, respectively

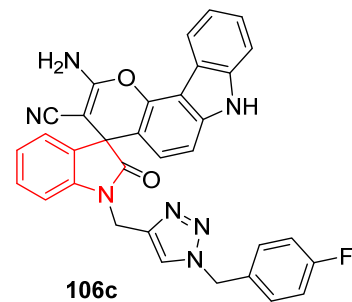
Fig. S10 (continued). Antiproliferation properties ($\mu M \pm SD$) of the synthesized 3-pyrrolylisatin-triazole conjugates **104** and Tamoxifen citrate "reference drug" (ND = not determined).



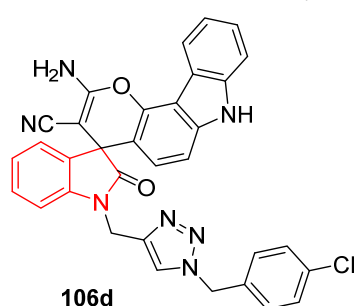
$IC_{50} = 7.02 \pm 0.93, 17.25 \pm 0.08, 12.35 \pm 0.17, >100 \mu M$ against MCF-7, MDA-MB-231, HeLa and HUVEC cell lines, respectively



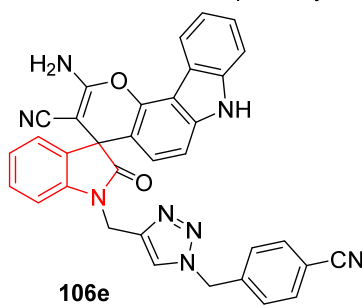
$IC_{50} = 25.56 \pm 2.12, 12.74 \pm 2.32, 4.05 \pm 0.69, >100 \mu M$ against MCF-7, MDA-MB-231, HeLa and HUVEC cell lines, respectively



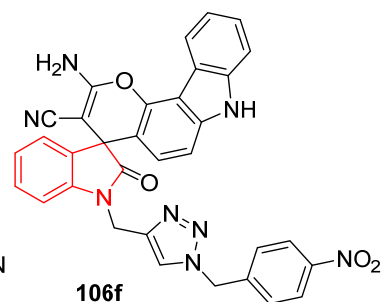
$IC_{50} = 14.37 \pm 0.95, 13.33 \pm 0.48, >100, >100 \mu M$ against MCF-7, MDA-MB-231, HeLa and HUVEC cell lines, respectively



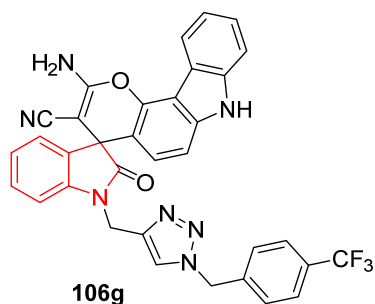
$IC_{50} = >100, >100, >100, >100 \mu M$ against MCF-7, MDA-MB-231, HeLa and HUVEC cell lines, respectively



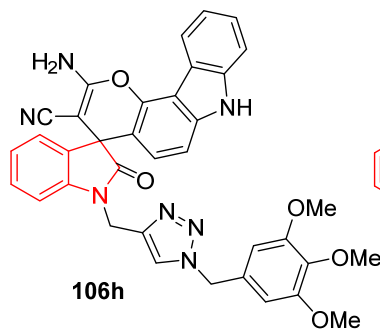
$IC_{50} = 25.51 \pm 0.32, 37.66 \pm 0.55, >100, >100 \mu M$ against MCF-7, MDA-MB-231, HeLa and HUVEC cell lines, respectively



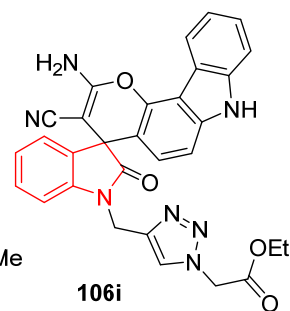
$IC_{50} = 2.13 \pm 0.16, 24.89 \pm 0.74, >100 \pm 1.6, >100 \mu M$ against MCF-7, MDA-MB-231, HeLa and HUVEC cell lines, respectively



$IC_{50} = 6.31 \pm 0.63, 14.86 \pm 0.12, 3.54 \pm 1.24, >100 \mu M$ against MCF-7, MDA-MB-231, HeLa and HUVEC cell lines, respectively

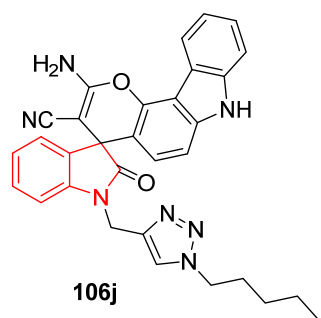


$IC_{50} = 6.97 \pm 0.83, 23.66 \pm 1.02, 15.88 \pm 1.12, >100 \mu M$ against MCF-7, MDA-MB-231, HeLa and HUVEC cell lines, respectively

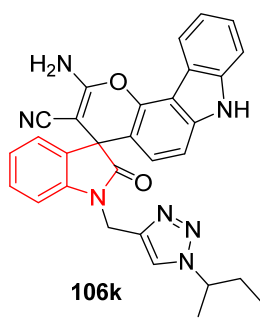


$IC_{50} = 18.00 \pm 0.32, 41.64 \pm 0.04, 10.83 \pm 0.6, >100 \mu M$ against MCF-7, MDA-MB-231, HeLa and HUVEC cell lines, respectively

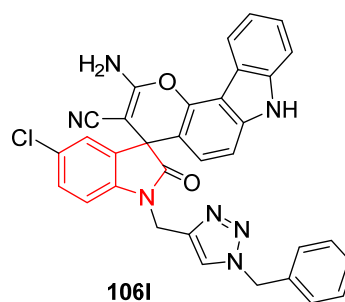
Fig. S11. Antiproliferation properties ($\mu M \pm SD$) of spirochromenocarbazols linked to 1,2,3-triazole **106**, and standard references (Paclitaxel and Doxorubicin).



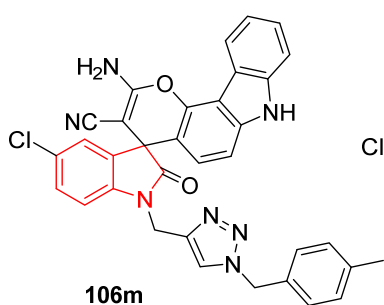
$IC_{50} = 4.80 \pm 0.25, 8.39 \pm 1.84, 9.21 \pm 0.34, >100 \mu\text{M}$ against MCF-7, MDA-MB-231, HeLa and HUVEC cell lines, respectively



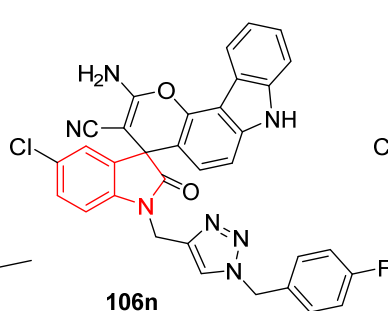
$IC_{50} = 51.16 \pm 0.53, 3.78 \pm 0.74, 61.89 \pm 2.53, >100 \mu\text{M}$ against MCF-7, MDA-MB-231, HeLa and HUVEC cell lines, respectively



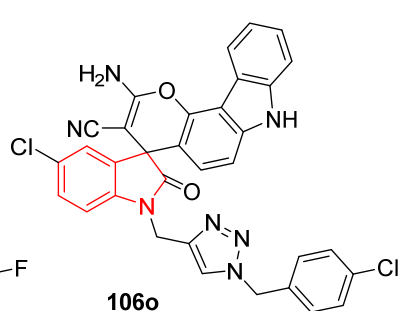
$IC_{50} = >100, >100, >100, >100 \mu\text{M}$ against MCF-7, MDA-MB-231, HeLa and HUVEC cell lines, respectively



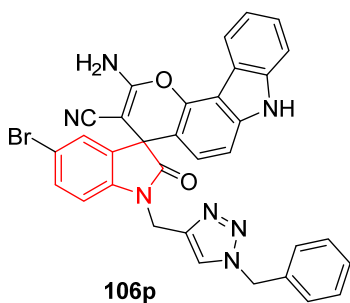
$IC_{50} = >100, >100, >100, >100 \mu\text{M}$ against MCF-7, MDA-MB-231, HeLa and HUVEC cell lines, respectively



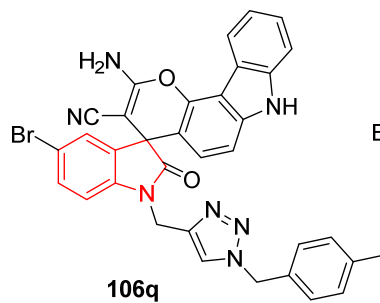
$IC_{50} = 62.74 \pm 0.17, 71.26 \pm 1.18, 75.81 \pm 0.61, >100 \mu\text{M}$ against MCF-7, MDA-MB-231, HeLa and HUVEC cell lines, respectively



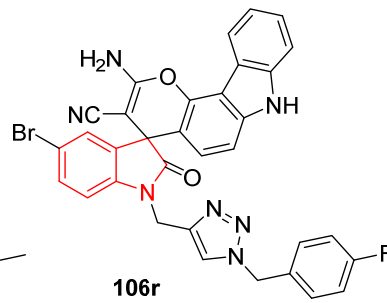
$IC_{50} = 42.50 \pm 0.67, 60.82 \pm 0.38, 13.25 \pm 0.37, >100 \mu\text{M}$ against MCF-7, MDA-MB-231, HeLa and HUVEC cell lines, respectively



$IC_{50} = 9.40 \pm 0.36, 42.37 \pm 0.55, 32.49 \pm 0.15, >100 \mu\text{M}$ against MCF-7, MDA-MB-231, HeLa and HUVEC cell lines, respectively



$IC_{50} = 7.06 \pm 0.35, 30.33 \pm 3.8, 61.29 \pm 1.67, >100 \mu\text{M}$ against MCF-7, MDA-MB-231, HeLa and HUVEC cell lines, respectively



$IC_{50} = 6.57 \pm 0.26, 25.38 \pm 0.69, 42.77 \pm 0.22, >100 \mu\text{M}$ against MCF-7, MDA-MB-231, HeLa and HUVEC cell lines, respectively

Fig. S11 (continued). Antiproliferation properties ($\mu\text{M} \pm \text{SD}$) of spirochromenocarbazols linked to 1,2,3-triazole **106**, and standard references (Paclitaxel and Doxorubicin).

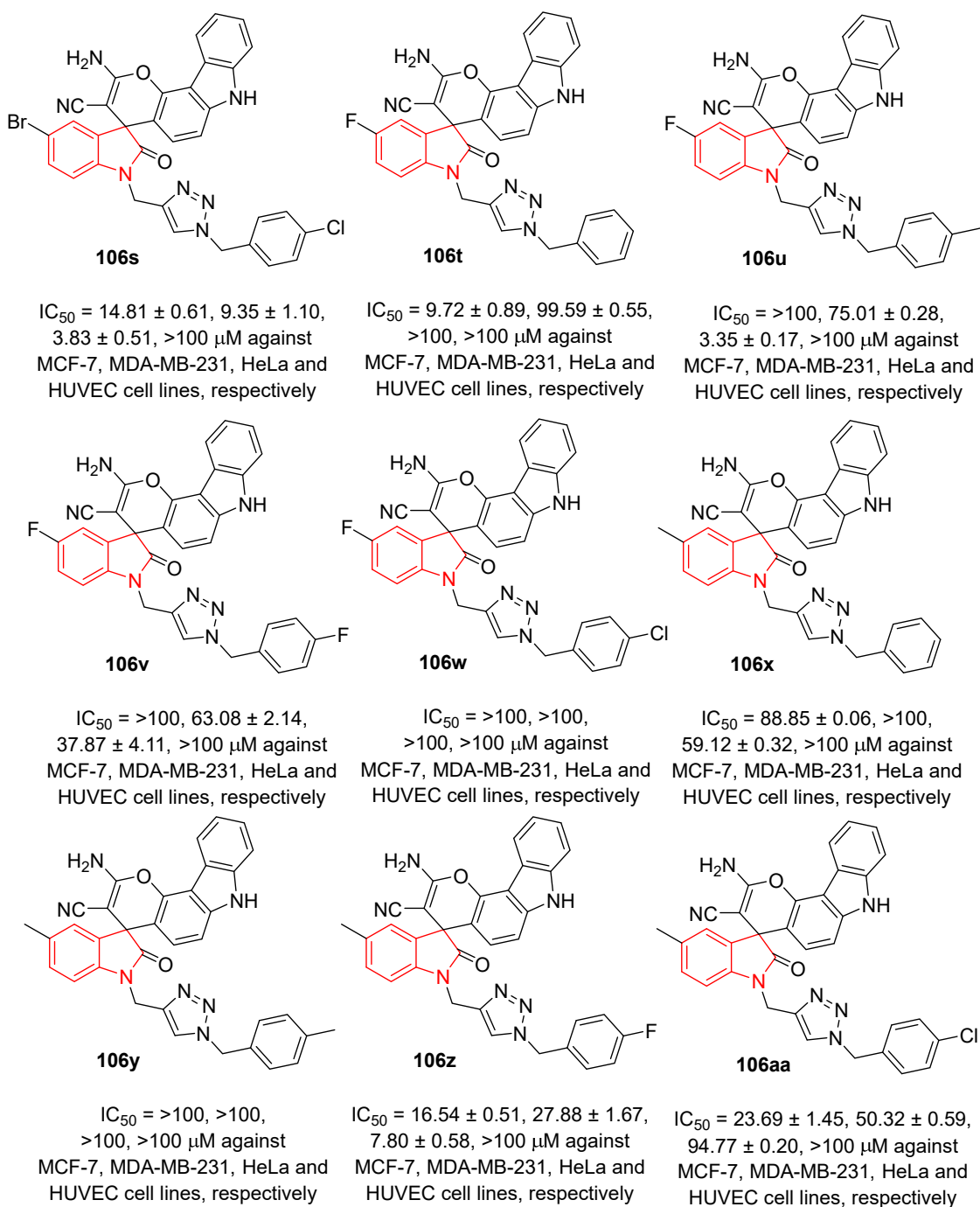
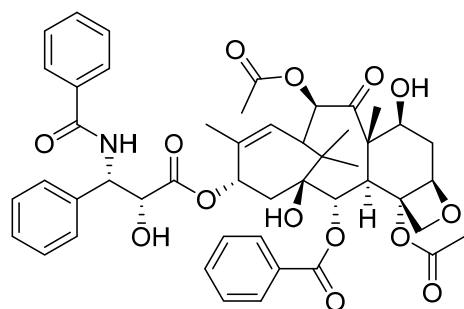
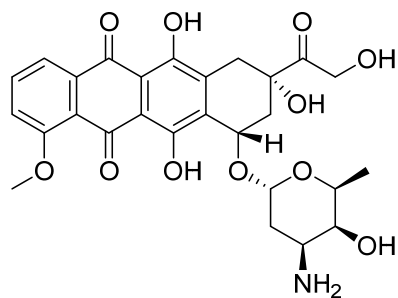


Fig. S11 (continued). Antiproliferation properties (μM ± SD) of spirochromenocarbazoles linked to 1,2,3-triazole **106**, and standard references (Paclitaxel and Doxorubicin).



Paclitaxel

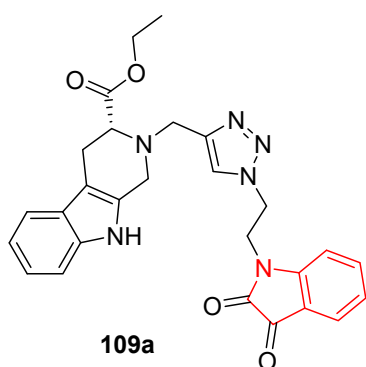
$IC_{50} = 0.0026 \pm 0.00, 0.1 \pm 0.07, 0.0061 \pm 0.00, >10 \mu M$ against MCF-7, MDA-MB-231, HeLa and HUVEC cell lines, respectively



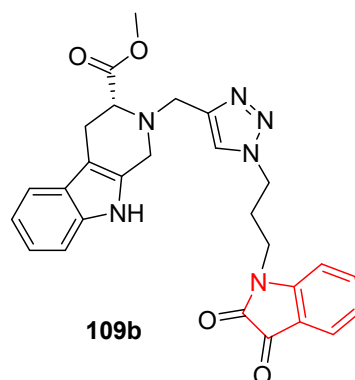
Doxorubicin

$IC_{50} = 4.63 \pm 0.41, 0.55 \pm 0.01, 2.66 \pm 0.32, >10 \mu M$ against MCF-7, MDA-MB-231, HeLa and HUVEC cell lines, respectively

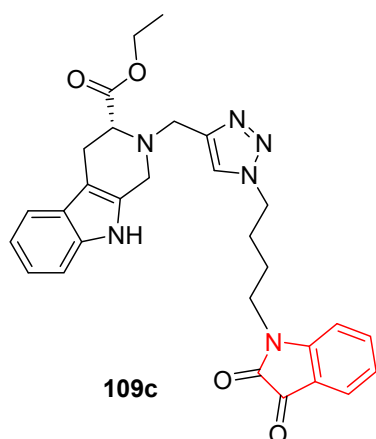
Fig. S11 (continued). Antiproliferation properties ($\mu M \pm SD$) of spirochromenocarbazols linked to 1,2,3-triazole **106**, and standard references (Paclitaxel and Doxorubicin).



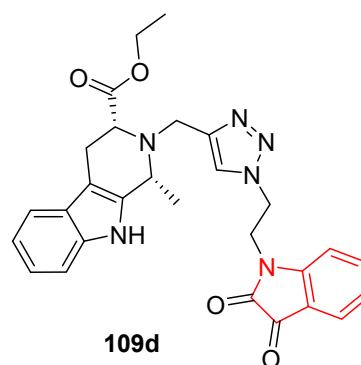
$IC_{50} = >100, >100 \mu M$ against MCF-7 and MDA-MB231, respectively



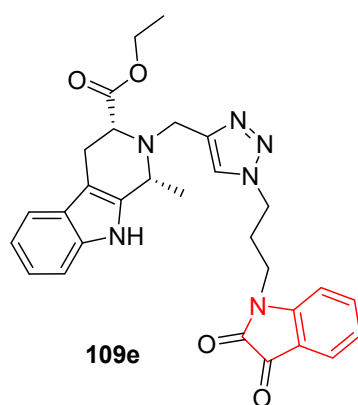
$IC_{50} = 37.42, >100 \mu M$ against MCF-7 and MDA-MB231, respectively



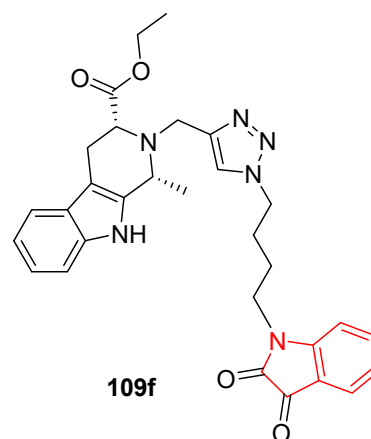
$IC_{50} = >100, >100 \mu M$ against MCF-7 and MDA-MB231, respectively



$IC_{50} = 45.3, >100 \mu M$ against MCF-7 and MDA-MB231, respectively

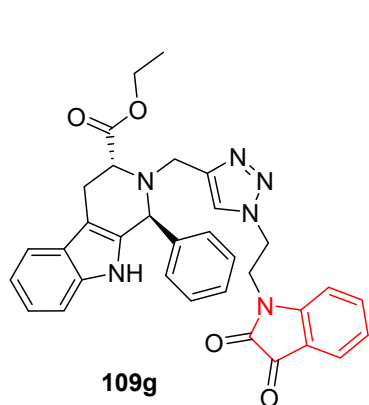


$IC_{50} = 50, >100 \mu M$ against MCF-7 and MDA-MB231, respectively

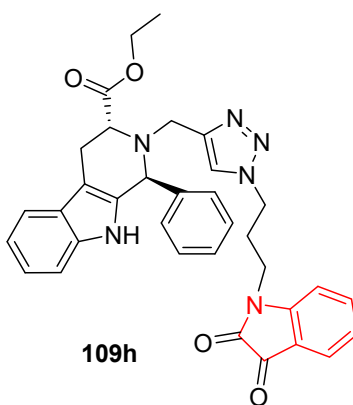


$IC_{50} = >100, >100 \mu M$ against MCF-7 and MDA-MB231, respectively

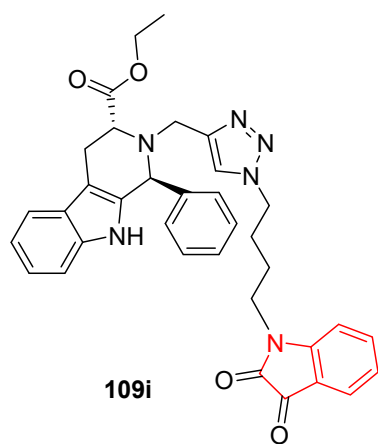
Fig. S12. Antiproliferation properties (μM) of tetrahydro- β -carboline and isatin scaffolds connected by 1*H*-1,2,3-triazolyl heterocycle **109** and reference standards (Plumbagin, Peganumine A and Tamoxifen).



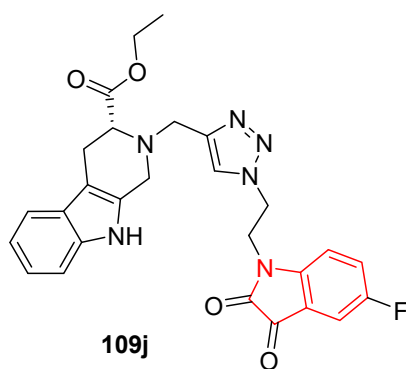
$IC_{50} = >100, >100 \mu M$ against MCF-7 and MDA-MB231, respectively



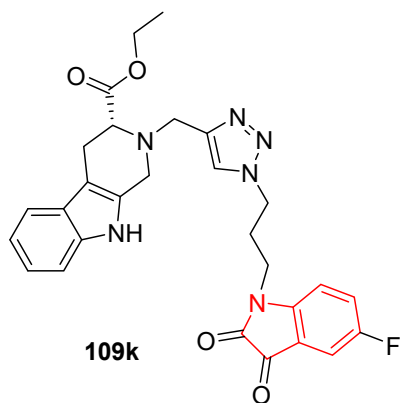
$IC_{50} = >100, >100 \mu M$ against MCF-7 and MDA-MB231, respectively



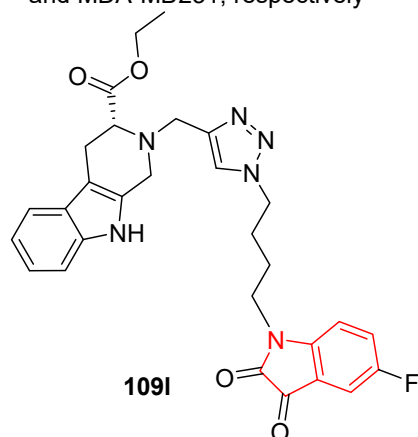
$IC_{50} = >100, >100 \mu M$ against MCF-7 and MDA-MB231, respectively



$IC_{50} = >100, >100 \mu M$ against MCF-7 and MDA-MB231, respectively

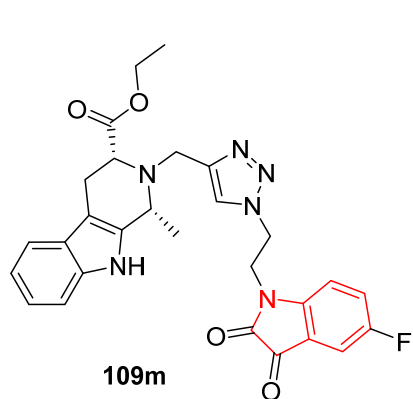


$IC_{50} = >100, >100 \mu M$ against MCF-7 and MDA-MB231, respectively

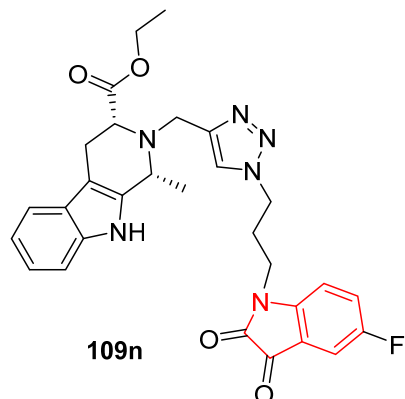


$IC_{50} = >100, >100 \mu M$ against MCF-7 and MDA-MB231, respectively

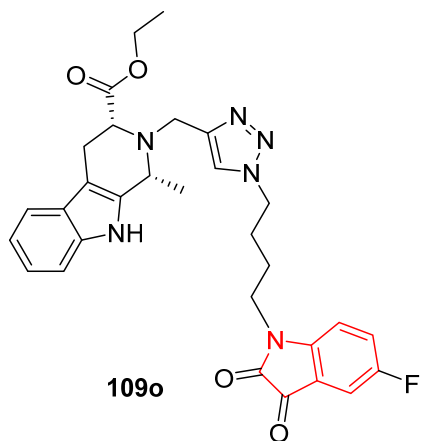
Fig. S12 (continued). Antiproliferation properties (μM) of tetrahydro- β -carboline and isatin scaffolds connected by 1*H*-1,2,3-triazolyl heterocycle **109** and reference standards (Plumbagin, Peganumine A and Tamoxifen).



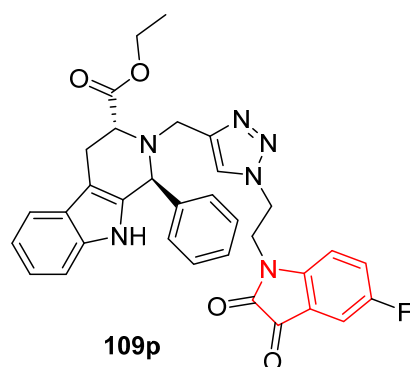
$IC_{50} = >100, >100 \mu M$ against MCF-7 and MDA-MB231, respectively



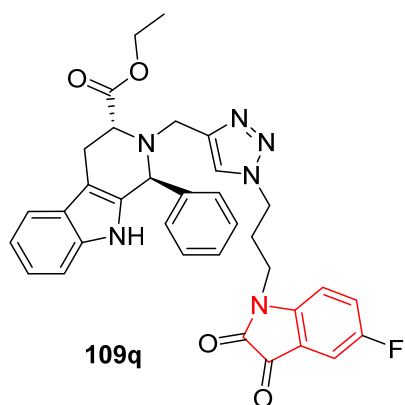
$IC_{50} = >100, >100 \mu M$ against MCF-7 and MDA-MB231, respectively



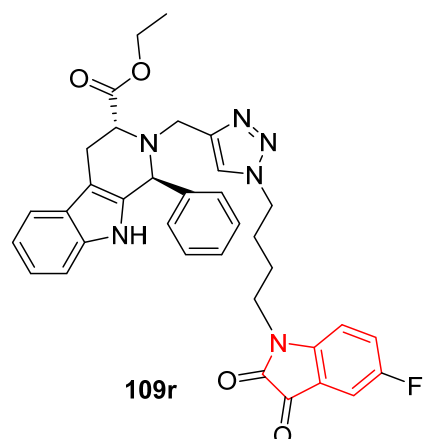
$IC_{50} = >100, >100 \mu M$ against MCF-7 and MDA-MB231, respectively



$IC_{50} = >100, >100 \mu M$ against MCF-7 and MDA-MB231, respectively

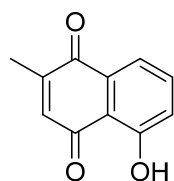


$IC_{50} = >100, >100 \mu M$ against MCF-7 and MDA-MB231, respectively



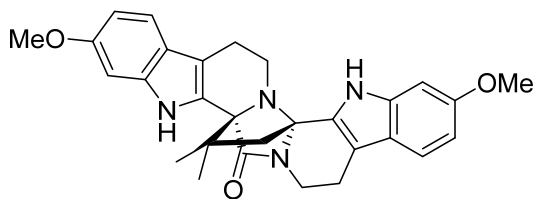
$IC_{50} = 42.11, >100 \mu M$ against MCF-7 and MDA-MB231, respectively

Fig. S12 (continued). Antiproliferation properties (μM) of tetrahydro- β -carboline and isatin scaffolds connected by 1*H*-1,2,3-triazolyl heterocycle **109** and reference standards (Plumbagin, Peganumine A and Tamoxifen).



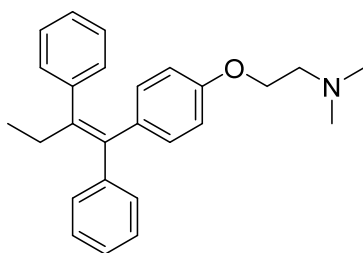
Plumbagin

IC₅₀ = 3.5, 4.4 μ M
against MCF-7
and MDA-MB231,
respectively



Peganumine A

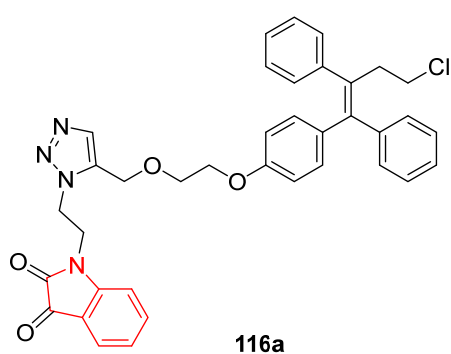
IC₅₀ = 38.5 μ M against MCF-7



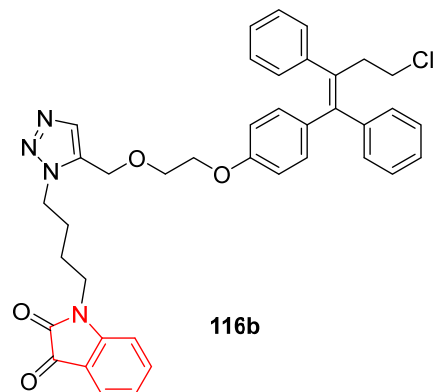
Tamoxifen

IC₅₀ = 50, 75 μ M against MCF-7
and MDA-MB231, respectively

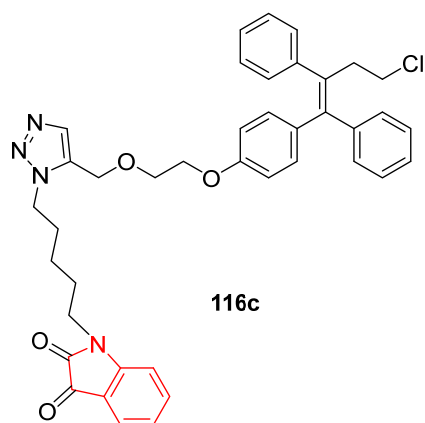
Fig. S12 (continued). Antiproliferation properties (μ M) of tetrahydro- β -carboline and isatin scaffolds connected by 1*H*-1,2,3-triazolyl heterocycle **109** and reference standards (Plumbagin, Peganumine A and Tamoxifen).



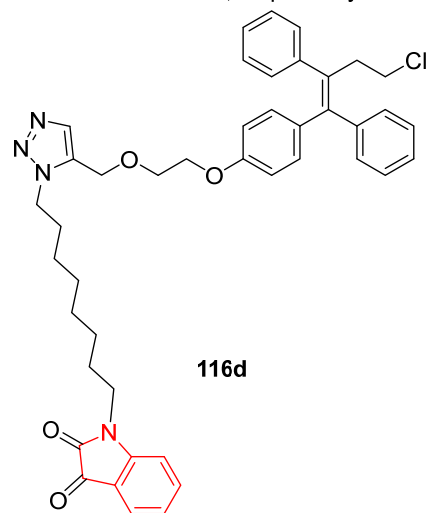
IC_{50} = 53.10, >100 μ M against MCF-7 and MDA-MB-231, respectively



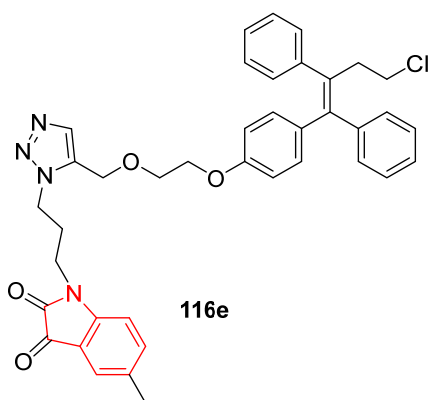
IC_{50} = >100, >100 μ M against MCF-7 and MDA-MB-231, respectively



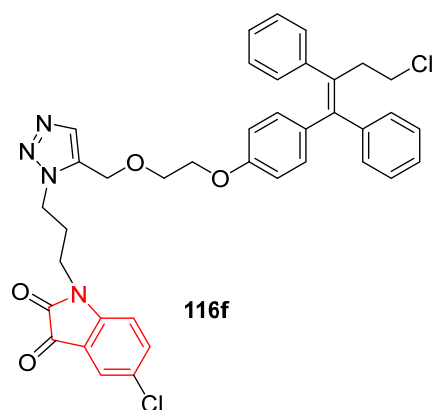
IC_{50} = >100, >100 μ M against MCF-7 and MDA-MB-231, respectively



IC_{50} = >100, >100 μ M against MCF-7 and MDA-MB-231, respectively



IC_{50} = 70.71, >100 μ M against MCF-7 and MDA-MB-231, respectively



IC_{50} = >100, >100 μ M against MCF-7 and MDA-MB-231, respectively

Fig. S13. Antiproliferation properties (μ M) of the synthesized ospemifene-isatins **116** and ospemifene-spiroisatins **117** conjugates and reference standards (Ospemifene, Tamoxifen and Plumbagin) against MCF-7 and MDA-MB-231.

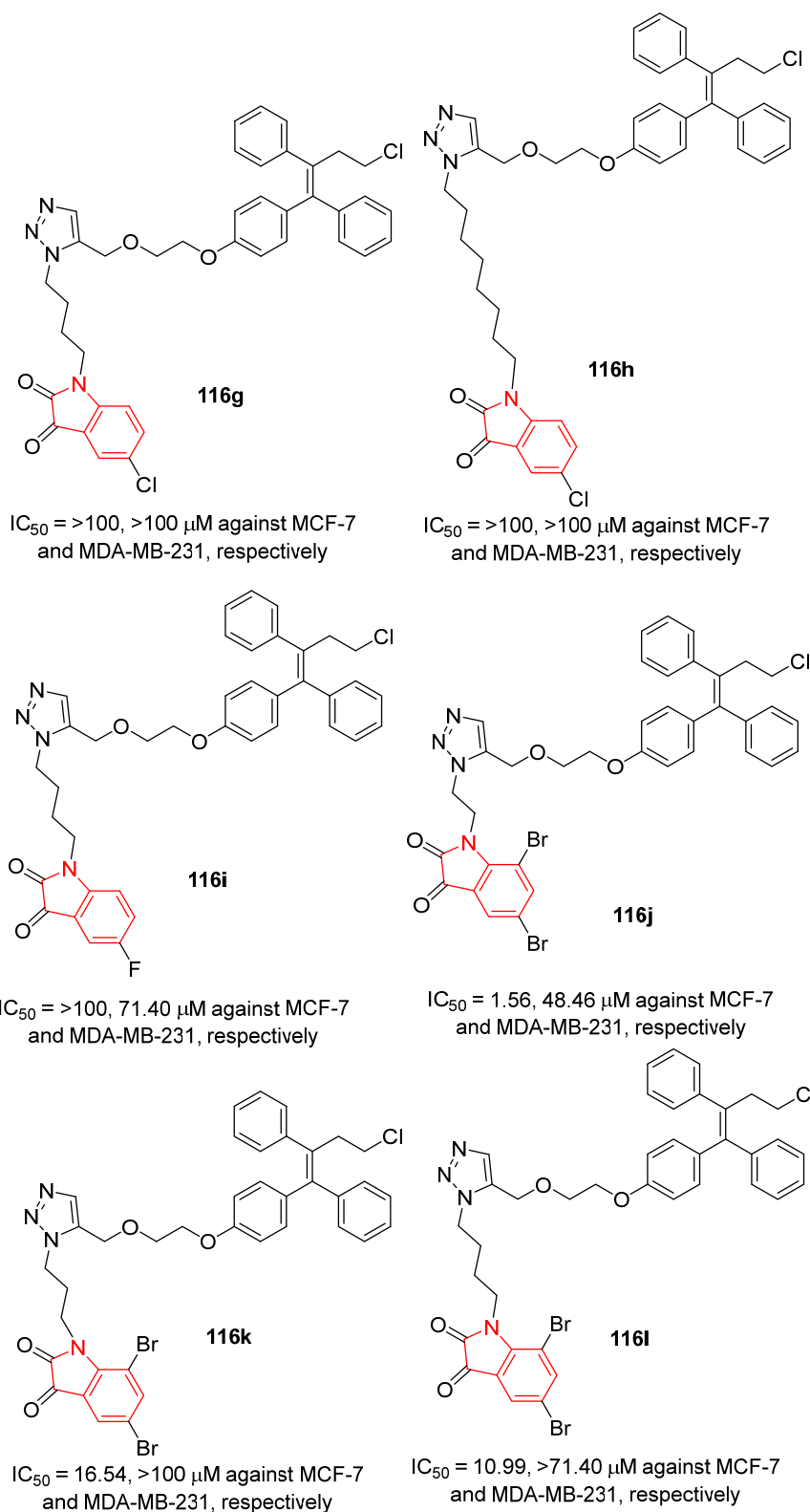


Fig. S13 (continued). Antiproliferation properties (μM) of the synthesized ospemifene-isatins **116** and ospemifene-spiroisatins **117** conjugates and reference standards (Ospemifene, Tamoxifen and Plumbagin) against MCF-7 and MDA-MB-231.

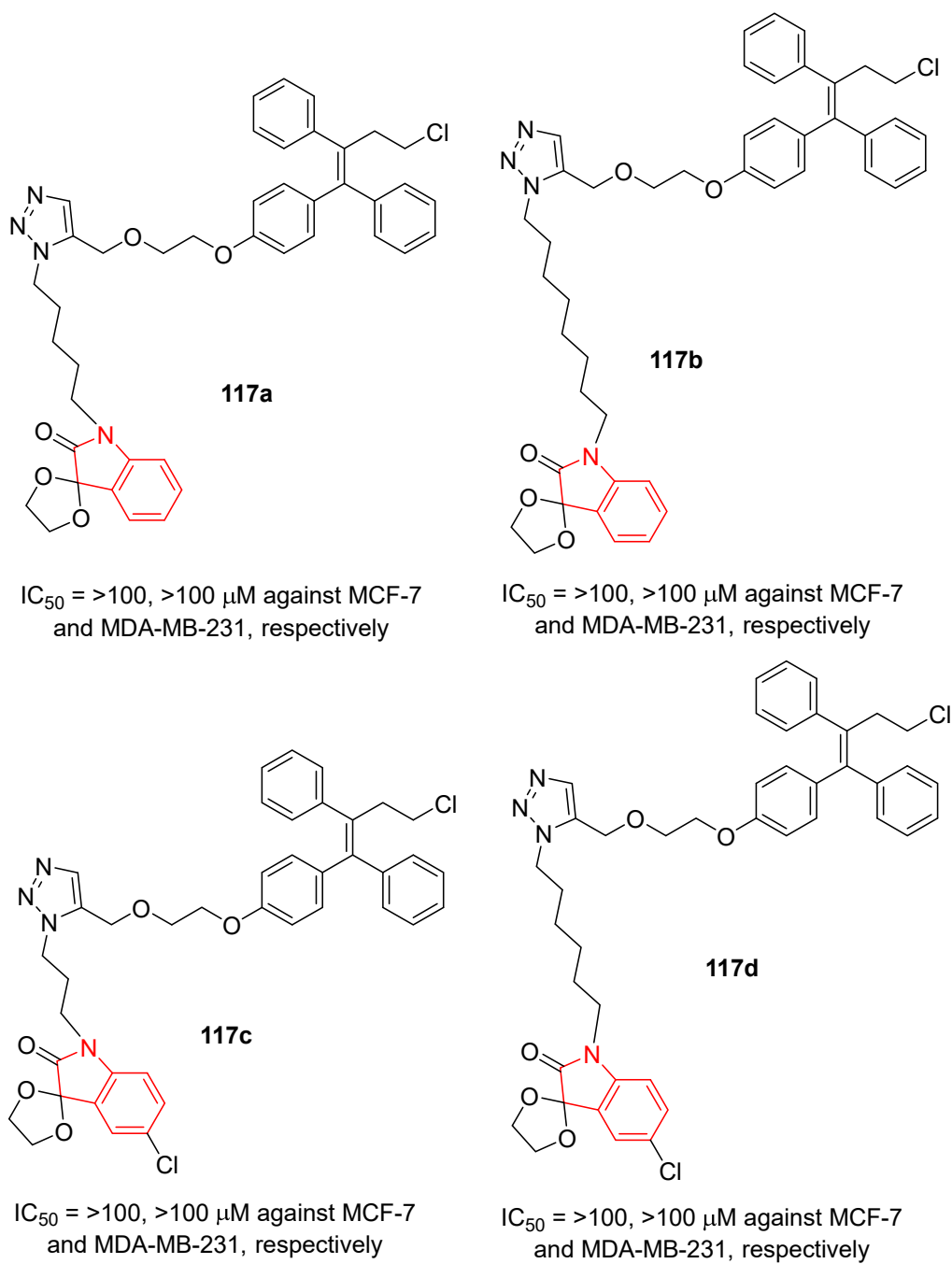
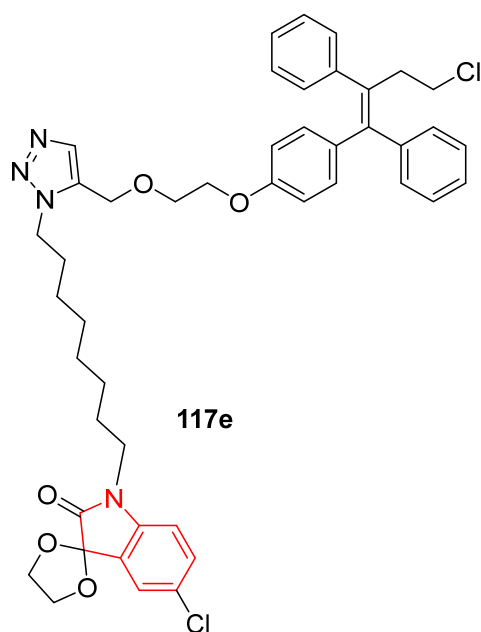
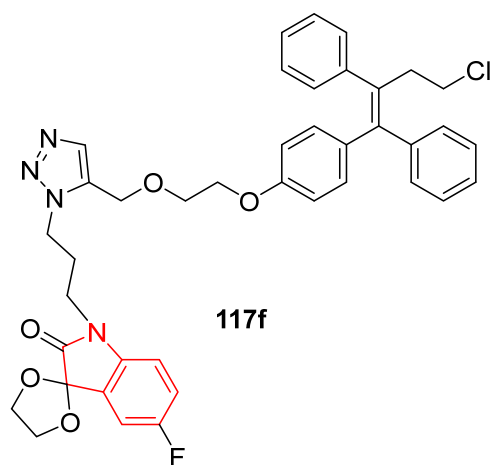


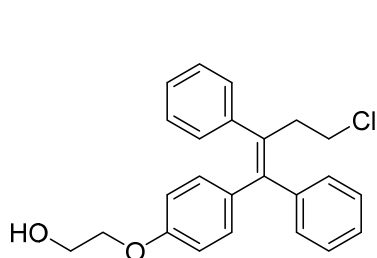
Fig. S13 (continued). Antiproliferation properties (μM) of the synthesized ospemifene-isatins **116** and ospemifene-spiroisatins **117** conjugates and reference standards (Ospemifene, Tamoxifen and Plumbagin) against MCF-7 and MDA-MB-231.



$IC_{50} = >100, >100 \mu M$ against MCF-7 and MDA-MB-231, respectively

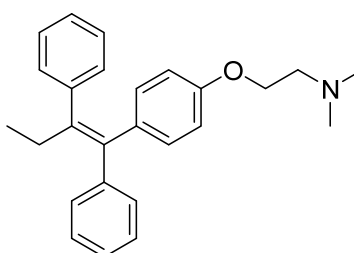


$IC_{50} = >100, 38.35 \mu M$ against MCF-7 and MDA-MB-231, respectively



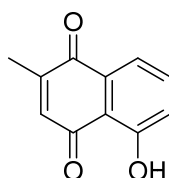
Ospemifene

$IC_{50} = 55, >100 \mu M$ against MCF-7 and MDA-MB-231, respectively



Tamoxifen

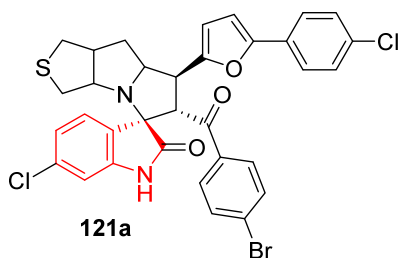
$IC_{50} = 50, 75 \mu M$ against MCF-7 and MDA-MB-231, respectively



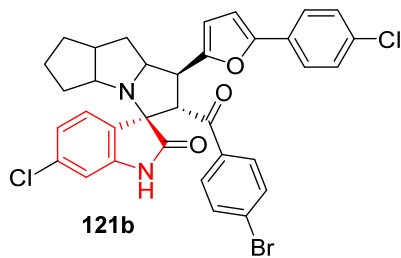
Plumbagin

$IC_{50} = 3.5, 4.4 \mu M$ against MCF-7 and MDA-MB-231, respectively

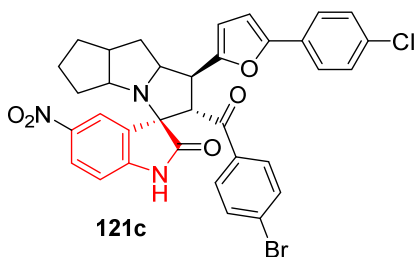
Fig. S13 (continued). Antiproliferation properties (μM) of the synthesized ospemifene-isatins **116** and ospemifene-spiroisatins **117** conjugates and reference standards (Ospemifene, Tamoxifen and Plumbagin) against MCF-7 and MDA-MB-231.



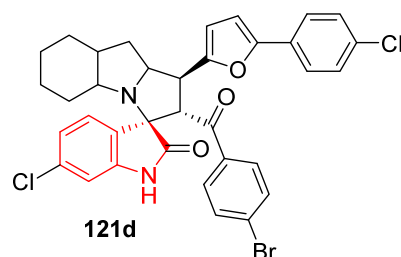
$IC_{50} = 63.1 \pm 2.45, 91.4 \pm 2.86 \mu\text{M/mL}$
against MCF-7 and HepG2 cell lines,
respectively



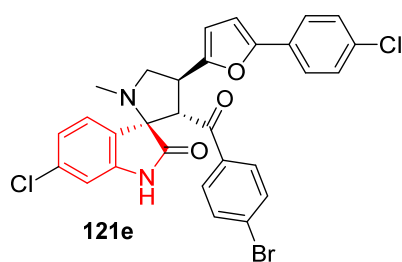
$IC_{50} = 18.2 \pm 0.69, 27.6 \pm 0.84 \mu\text{M/mL}$
against MCF-7 and HepG2 cell lines,
respectively



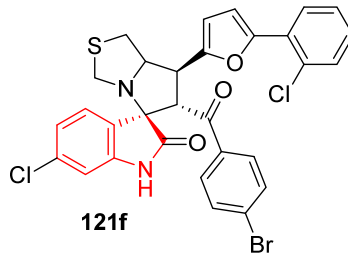
$IC_{50} = 36.7 \pm 1.41, 45.0 \pm 1.39 \mu\text{M/mL}$
against MCF-7 and HepG2 cell lines,
respectively



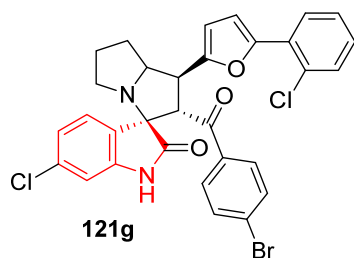
$IC_{50} = 4.3 \pm 0.18, 6.9 \pm 0.23 \mu\text{M/mL}$
against MCF-7 and HepG2 cell lines,
respectively



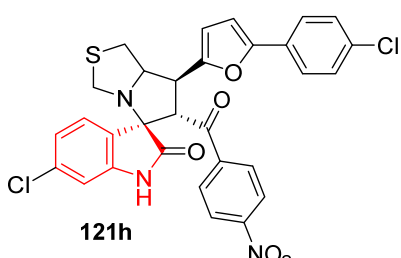
$IC_{50} = 41.2 \pm 1.49, 25.4 \pm 0.74 \mu\text{M/mL}$
against MCF-7 and HepG2 cell lines,
respectively



$IC_{50} = 10.33 \pm 0.40, 3.5 \pm 0.11 \mu\text{M/mL}$
against MCF-7 and HepG2 cell lines,
respectively

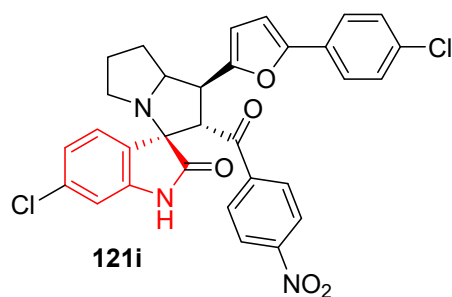


$IC_{50} = 60.5 \pm 2.28, 36.1 \pm 1.10 \mu\text{M/mL}$
against MCF-7 and HepG2 cell lines,
respectively

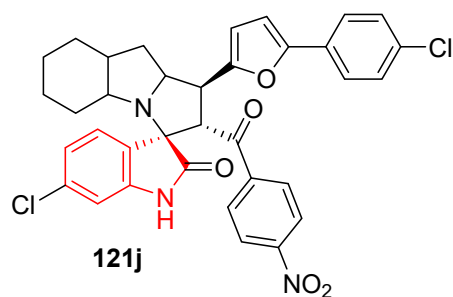


$IC_{50} = 174.3 \pm 6.41, 54.6 \pm 1.62 \mu\text{M/mL}$
against MCF-7 and HepG2 cell lines,
respectively

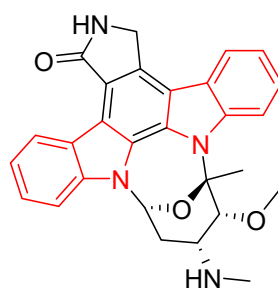
Fig. S14. Antiproliferation properties of spiroindoles bearing 2-furanyl heterocycle **121** and Staurosporine.



$IC_{50} = 10.7 \pm 0.38, 19.6 \pm 0.56 \mu\text{M/mL}$
against MCF-7 and HepG2 cell lines,
respectively



$IC_{50} = 4.7 \pm 0.18, 11.8 \pm 0.37 \mu\text{M/mL}$
against MCF-7 and HepG2 cell lines,
respectively



Staurosporine

$IC_{50} = 17.8 \pm 0.50, 10.3 \pm 0.23 \mu\text{M/mL}$
against MCF-7 and HepG2 cell lines,
respectively

Fig. S14 (continued). Antiproliferation properties of spiroindoles bearing 2-furanyl heterocycle **121** and Staurosporine.

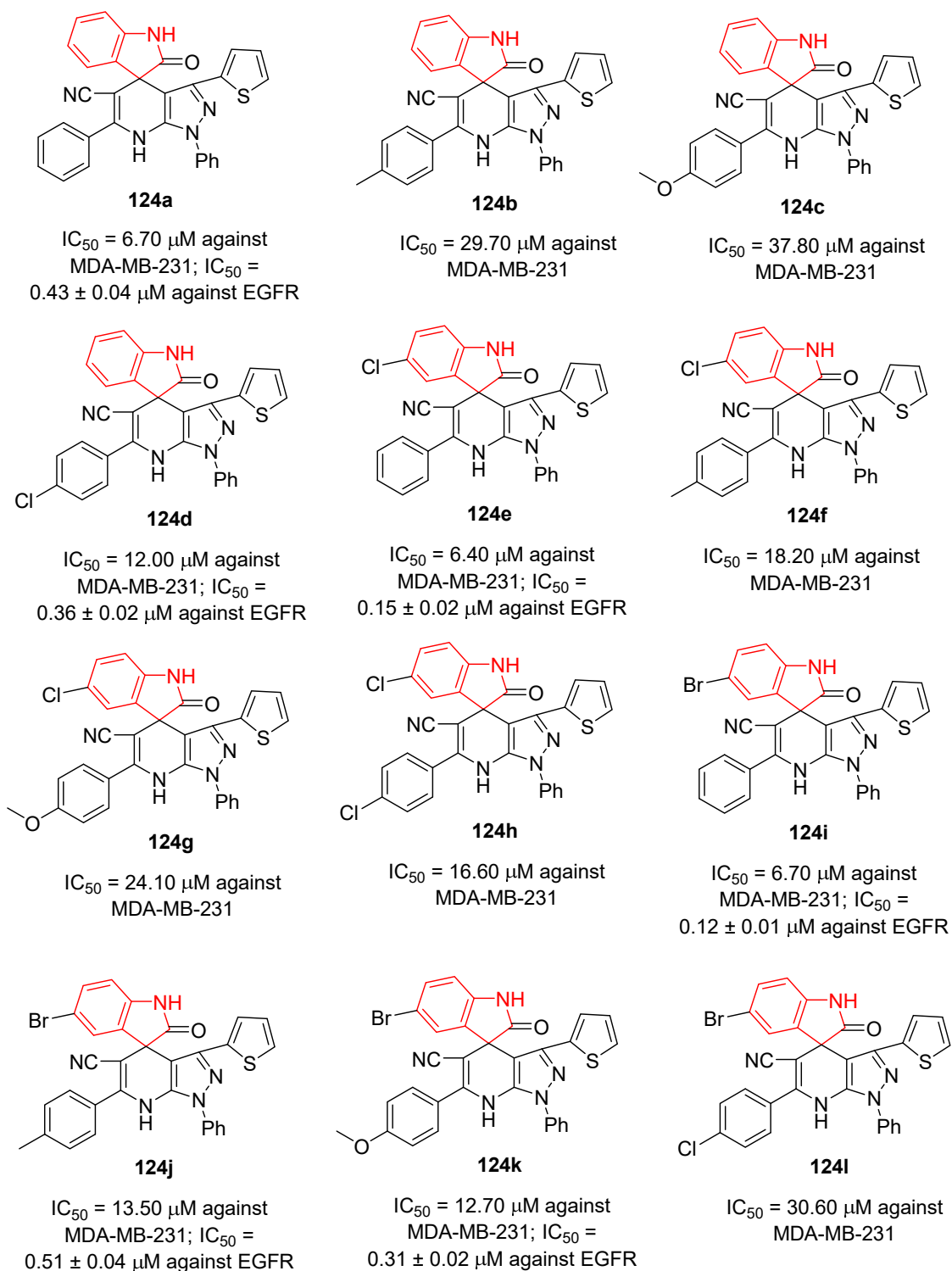


Fig. S15. Antiproliferation properties (μM) against MDA-MB-231 and inhibitory properties (μM ± SD) against EGFR of spiroindoles **124** and standard references [Doxorubicin (Adriamycin) and Erlotinib].

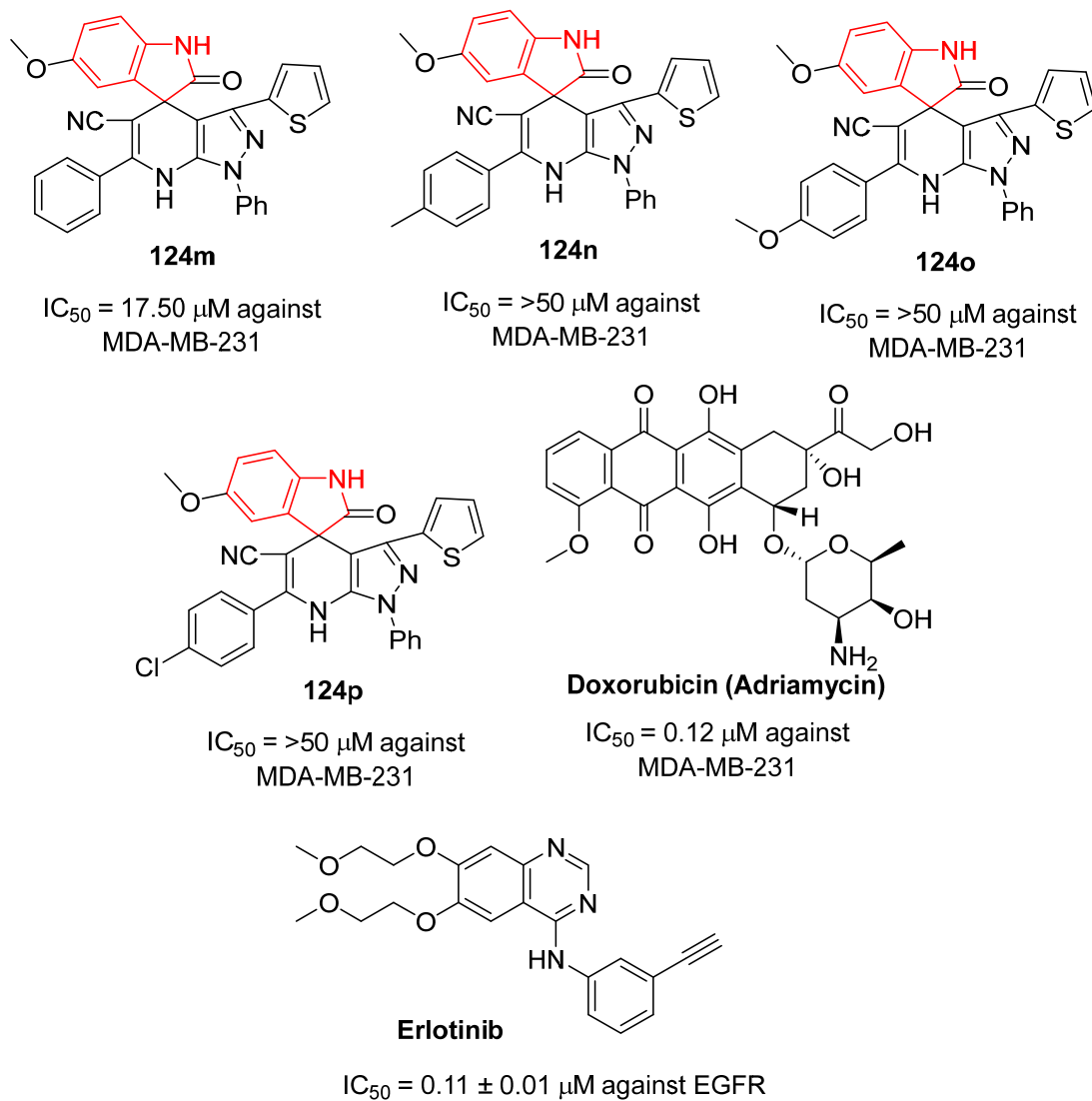


Fig. S15 (continued). Antiproliferation properties (μM) against MDA-MB-231 and inhibitory properties ($\mu M \pm SD$) against EGFR of spiroindoles **124** and standard references [Doxorubicin (Adriamycin) and Erlotinib].

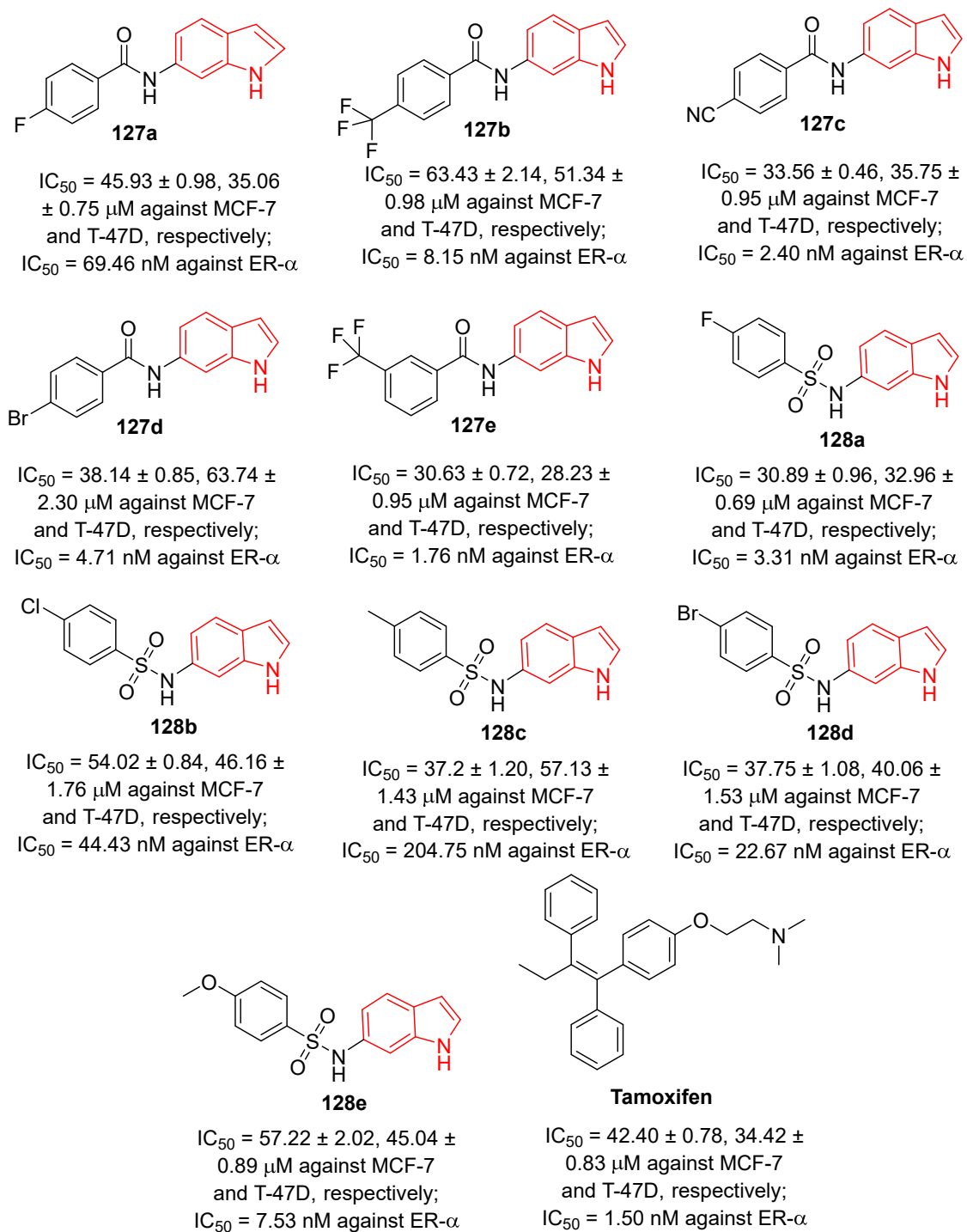


Fig. S16. Antiproliferation properties ($\mu M \pm SD$) and EF- α inhibitory properties ($nM \pm SD$) of the synthesized *N*-(1*H*-indole-6-yl) benzamides **127** and their benzene sulfonamide analogs **128**.

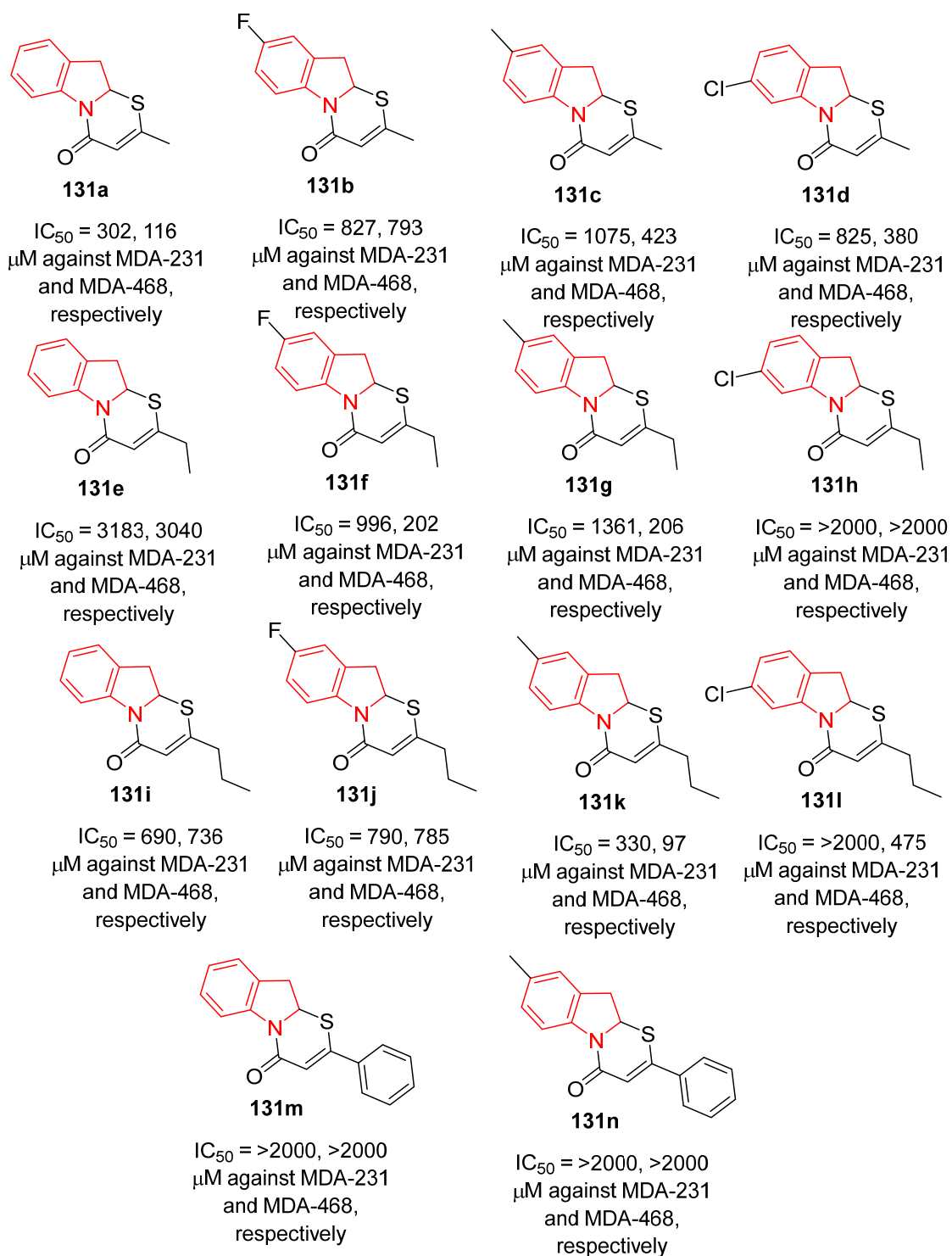
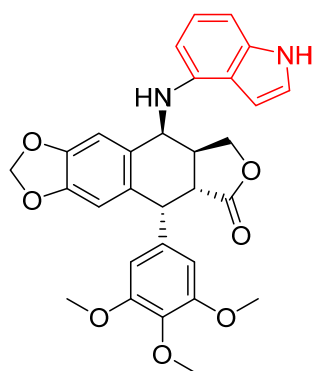
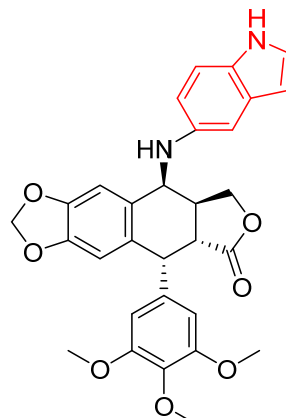


Fig. S17. Antiproliferation properties (μM) of [1,3]thiazino[3,2-a]indol-4-ones **131**.



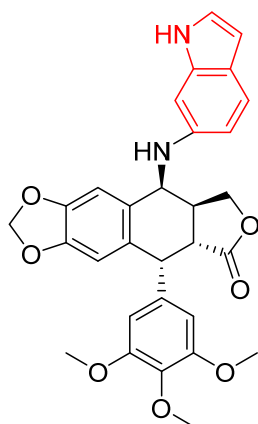
133a

$IC_{50} = 1.8 \pm 0.2, 33.6 \pm 1.5,$
 $2.1 \pm 0.3, 29.2 \pm 3.5,$
 $2.4 \pm 0.2, 32.4 \pm 2.9,$
 $1.3 \pm 0.2, 64.2 \pm 2.4 \mu M$
 against HepG-2, HL-7702,
 HeLa, H8, A549, MRC-5,
 MCF-7, and HMEC, respectively



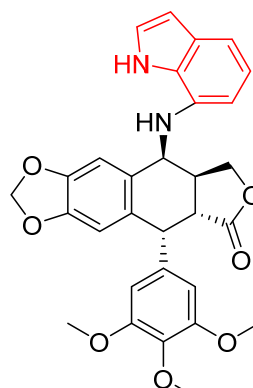
133b

$IC_{50} = 0.9 \pm 0.1, 43.3 \pm 2.8,$
 $0.9 \pm 0.01, 29.2 \pm 3.5,$
 $0.5 \pm 0.01, 51.3 \pm 3.1,$
 $0.4 \pm 0.01, 55.2 \pm 5.3 \mu M$
 against HepG-2, HL-7702,
 HeLa, H8, A549, MRC-5,
 MCF-7, and HMEC, respectively



133c

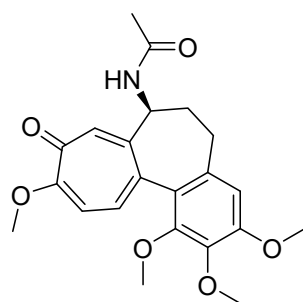
$IC_{50} = 0.1 \pm 0.01, 94.6 \pm 3.2,$
 $0.08 \pm 0.0, 84.5 \pm 2.9,$
 $0.08 \pm 0.0, 69.1 \pm 2.9,$
 $0.07 \pm 0.0, 61.6 \pm 2.3 \mu M$
 against HepG-2, HL-7702,
 HeLa, H8, A549, MRC-5,
 MCF-7, and HMEC, respectively



133d

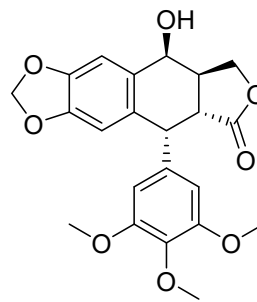
$IC_{50} = 2.5 \pm 0.6, 30.5 \pm 2.7,$
 $3.8 \pm 0.2, 19.4 \pm 1.7,$
 $2.2 \pm 0.9, 38.5 \pm 0.9,$
 $4.8 \pm 0.9, 45.5 \pm 3.5 \mu M$
 against HepG-2, HL-7702,
 HeLa, H8, A549, MRC-5,
 MCF-7, and HMEC, respectively

Fig. S18. Antiproliferation properties ($\mu M \pm SD$) of the synthesized indole-podophyllotoxin conjugates **133**, and standards (Colchicine, Podophyllotoxin and Nocodazole) against HepG-2, HL-7702 (liver), HeLa, H8 (cervical), A549, MRC-5 (lung), MCF-7, and HMEC (breast) cancer cell lines.



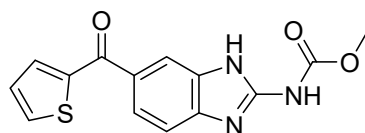
Colchicine

IC₅₀ = 5.8 ± 0.1, 9.2 ± 0.3,
10.2 ± 0.4, 6.1 ± 0.4,
9.7 ± 0.2, 6.2 ± 0.7,
14.3 ± 0.5, 8.1 ± 0.2 μM
against HepG-2, HL-7702,
HeLa, H8, A549, MRC-5,
MCF-7, and HMEC, respectively



Podophyllotoxin

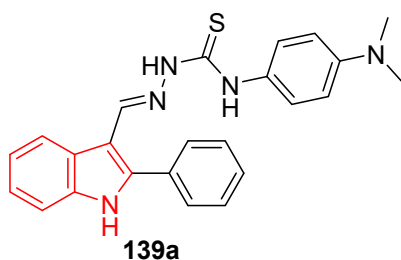
IC₅₀ = 2.4 ± 0.1, 5.0 ± 0.6,
6.9 ± 0.1, 8.4 ± 0.5,
2.6 ± 0.1, 10.6 ± 1.2,
2.4 ± 0.3, 5.6 ± 0.1 μM
against HepG-2, HL-7702,
HeLa, H8, A549, MRC-5,
MCF-7, and HMEC, respectively



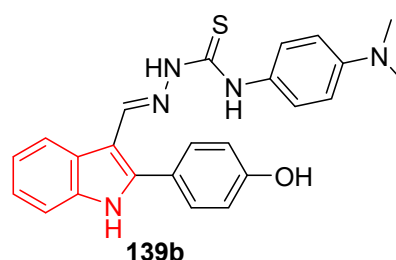
Nocodazole

IC₅₀ = 0.4 ± 0.2, 13.5 ± 1.5,
0.3 ± 0.1, 18.0 ± 2.6,
0.2 ± 0.05, 15.3 ± 1.9,
0.2 ± 0.1, 11.5 ± 2.2 μM
against HepG-2, HL-7702,
HeLa, H8, A549, MRC-5,
MCF-7, and HMEC, respectively

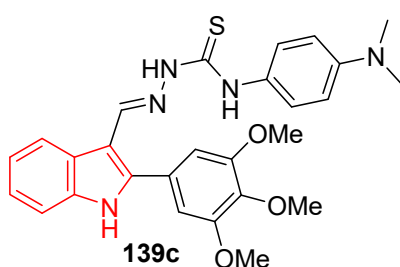
Fig. S18 (continued). Antiproliferation properties (μM ± SD) of the synthesized indole-podophyllotoxin conjugates **133**, and standards (Colchicine, Podophyllotoxin and Nocodazole) against HepG-2, HL-7702 (liver), HeLa, H8 (cervical), A549, MRC-5 (lung), MCF-7, and HMEC (breast) cancer cell lines.



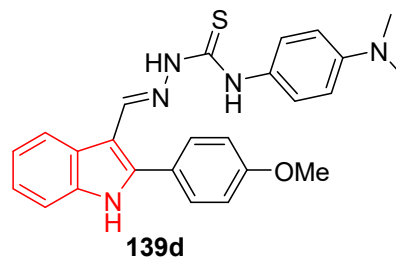
$IC_{50} = >100, >100, >100 \mu M$ against MCF-7, A-549 and HepG-2, respectively



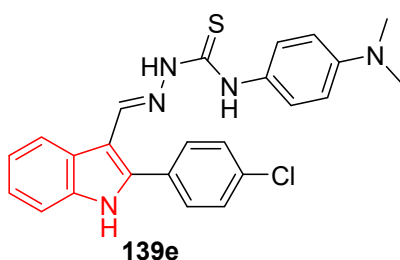
$IC_{50} = 31.38 \pm 4.96, >100, >100 \mu M$ against MCF-7, A-549 and HepG-2, respectively



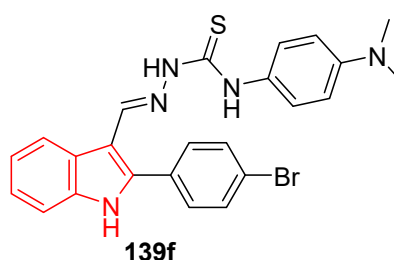
$IC_{50} = 35.78 \pm 6.89, >100, >100 \mu M$ against MCF-7, A-549 and HepG-2, respectively



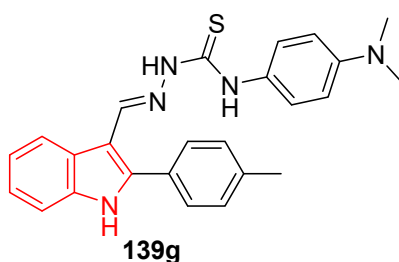
$IC_{50} = >100, >100, 36.43 \pm 4.73 \mu M$ against MCF-7, A-549 and HepG-2, respectively



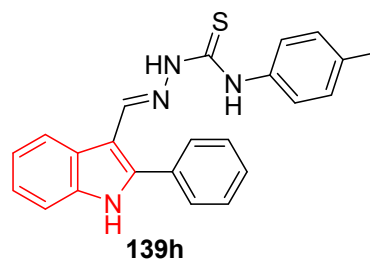
$IC_{50} = >100, >100, 72.68 \pm 6.45 \mu M$ against MCF-7, A-549 and HepG-2, respectively



$IC_{50} = >100, >100, >100 \mu M$ against MCF-7, A-549 and HepG-2, respectively

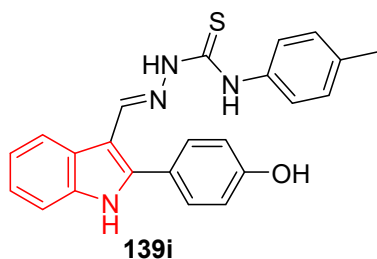


$IC_{50} = 23.39 \pm 5.47, 80.84 \pm 7.5, 24.46 \pm 1.05 \mu M$ against MCF-7, A-549 and HepG-2, respectively

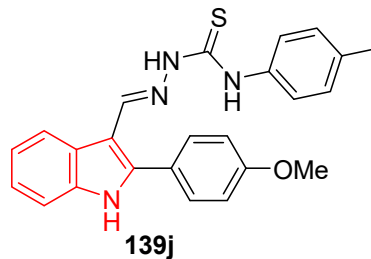


$IC_{50} = >100, >100, 42.83 \pm 5.54 \mu M$ against MCF-7, A-549 and HepG-2, respectively

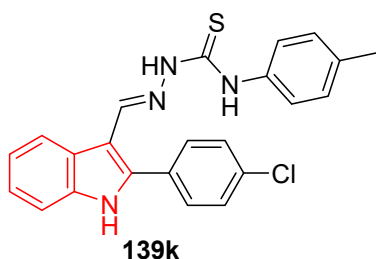
Fig. S19. Antiproliferation properties ($\mu M \pm SD$) of the synthesized indolylthiosemicarbazones **139** and standards (Etoposide and Colchicine).



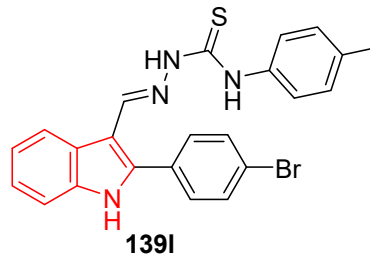
$IC_{50} = 24.97 \pm 5.32, >100, >100 \mu M$ against MCF-7, A-549 and HepG-2, respectively



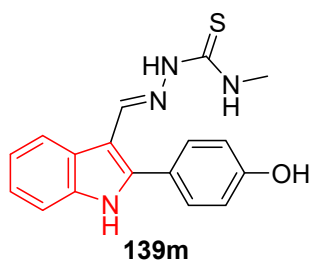
$IC_{50} = >100, >100, >100 \mu M$ against MCF-7, A-549 and HepG-2, respectively



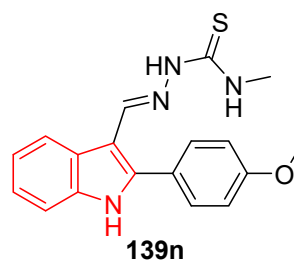
$IC_{50} = >100, >100, >100 \mu M$ against MCF-7, A-549 and HepG-2, respectively



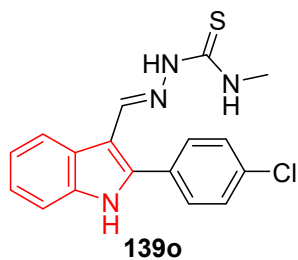
$IC_{50} = >100, >100, >100 \mu M$ against MCF-7, A-549 and HepG-2, respectively



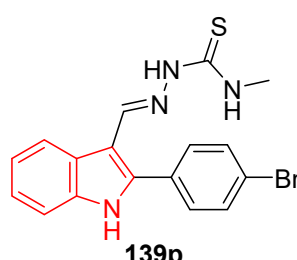
$IC_{50} = >100, 24.20 \pm 1.70, 51.70 \pm 4.10 \mu M$ against MCF-7, A-549 and HepG-2, respectively



$IC_{50} = >100, 12.50 \pm 1.00, 56.00 \pm 6.30 \mu M$ against MCF-7, A-549 and HepG-2, respectively

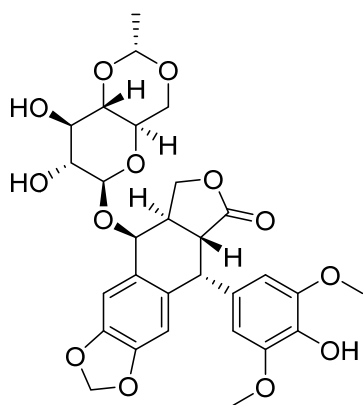


$IC_{50} = >100, 22.95 \pm 1.63, 48.94 \pm 3.91 \mu M$ against MCF-7, A-549 and HepG-2, respectively



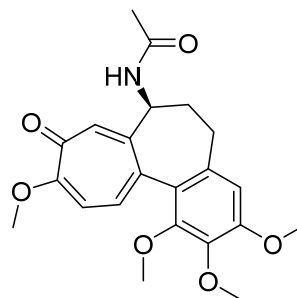
$IC_{50} = >100, 92.11 \pm 6.33, 49.97 \pm 5.52 \mu M$ against MCF-7, A-549 and HepG-2, respectively

Fig. S19 (continued). Antiproliferation properties ($\mu M \pm SD$) of the synthesized indolylthiosemicarbazones **139** and standards (Etoposide and Colchicine).



Etoposide

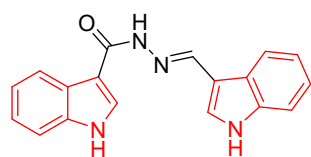
$IC_{50} = 34.25 \pm 3.12, 38.23 \pm 1.89,$
 $33.17 \pm 3.19 \mu M$ against
MCF-7, A-549 and HepG-2, respectively



Colchicine

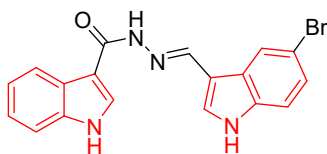
$IC_{50} = 7.10 \pm 0.61, 1.9 \pm 0.23,$
 $6.0 \pm 0.49 \mu M$ against
MCF-7, A-549 and HepG-2, respectively

Fig. S19 (continued). Antiproliferation properties ($\mu M \pm SD$) of the synthesized indolylthiosemicarbazones **139** and standards (Etoposide and Colchicine).



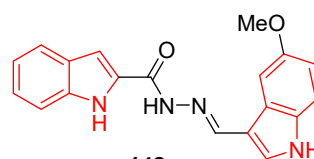
142a

IC_{50} = 18 μ M against A549 cell line; % inhibition of microtubule polymerization = 10 at 10 μ M of the respective ligand



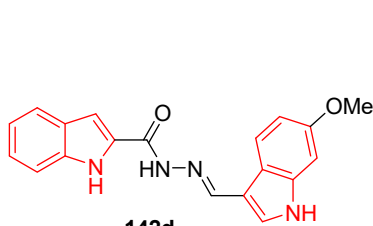
142b

IC_{50} = 7.5 μ M against A549 cell line; % inhibition of microtubule polymerization = 44 at 10 μ M of the respective ligand



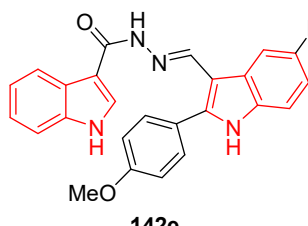
142c

IC_{50} = 2 μ M against A549 cell line; % inhibition of microtubule polymerization = 62 at 10 μ M of the respective ligand



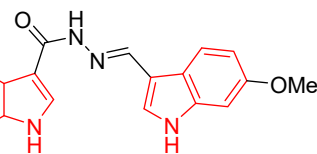
142d

IC_{50} = 6 μ M against A549 cell line; % inhibition of microtubule polymerization = 53 at 10 μ M of the respective ligand



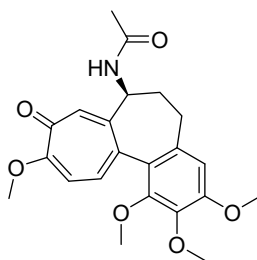
142e

IC_{50} = 21 μ M against A549 cell line



142f

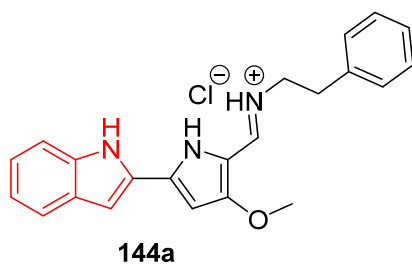
IC_{50} = 16.5 μ M against A549 cell line; % inhibition of microtubule polymerization = 11 at 10 μ M of the respective ligand



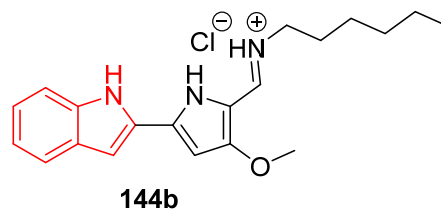
Colchicine

IC_{50} = 0.02 μ M against A549 cell line; % inhibition of microtubule polymerization = 11 at 79 μ M of the respective ligand

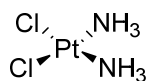
Fig. S20. Antiproliferation properties (μ M) and % inhibition of microtubule polymerization at 10 μ M of the respective ligand of the synthesized bis(indolyl)hydrazide-hydrazones **142** and Colchicine.



IC₅₀ = 10.66 ± 0.68, 8.04 ± 0.45,
8.67 ± 0.06, 8.37 ± 0.24, 4.04 ±
1.29, 4.34 ± 0.25 against A549,
DMS53, SW900, H460, PC#8
and PC#13, respectively



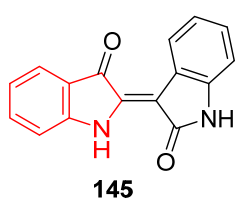
IC₅₀ = 7.61 ± 0.23, 6.46 ± 0.52,
7.55 ± 0.89, 7.29 ± 0.29, 3.34
± 0.86, 4.03 ± 0.19 against A549,
DMS53, SW900, H460, PC#8
and PC#13, respectively



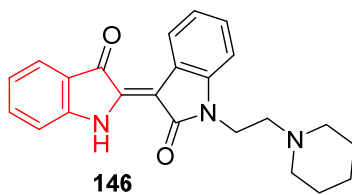
Cisplatin

IC₅₀ = >200, 107.9 ± 31.16,
49.4 ± 10.56, 74.2 ± 6.72, 49.28
± 9.88, 79.57 ± 9.37 against A549,
DMS53, SW900, H460, PC#8
and PC#13, respectively

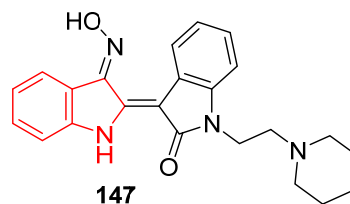
Fig. S21. Antiproliferation properties of indole-based tambjamine analogs **144** and Cisplatin.



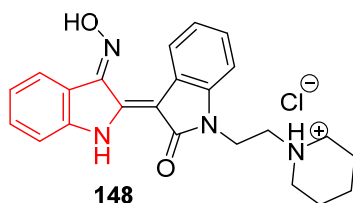
$IC_{50} = >25, >25, >25,$
 $>25 \mu\text{M}$ against SW480,
 A549, HepG2 and B16F10
 cell lines, respectively



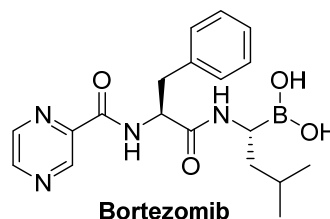
$IC_{50} = >25, >25, >25,$
 $>25 \mu\text{M}$ against SW480,
 A549, HepG2 and B16F10
 cell lines, respectively



$IC_{50} = 1.53 \pm 0.01, 0.57 \pm 0.07,$
 $1.64 \pm 0.11, 1.64 \pm 0.03 \mu\text{M}$
 against SW480, A549, HepG2
 and B16F10 cell lines, respectively

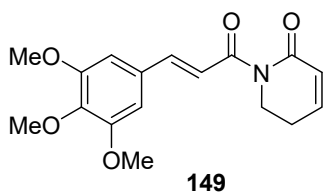


$IC_{50} = 0.53 \pm 0.06, 0.38 \pm 0.01,$
 $0.37 \pm 0.01, 0.53 \pm 0.01 \mu\text{M}$
 against SW480, A549, HepG2
 and B16F10 cell lines, respectively

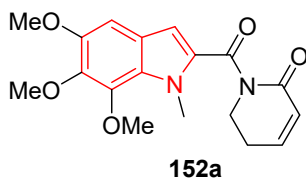


$IC_{50} = >25, >25, 18.17 \pm 1.42,$
 $13.470 \pm 1.73 \mu\text{M}$ against
 SW480, A549, HepG2 and
 B16F10 cell lines, respectively

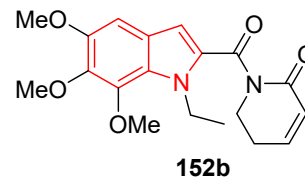
Fig. S22. Antiproliferation properties ($\mu\text{M} \pm \text{SD}$) of indirubin **145**, indirubin-piperidine conjugates **146–148** and Bortezomib.



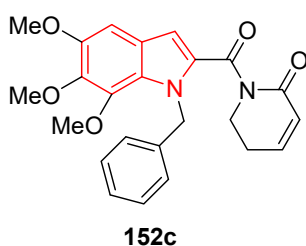
IC₅₀ = 47.80, 50.13, 15.16, 21.74, >100 μM against A54, HCT116, ZR-75-30, MDAMB-231 and MRC-5, respectively



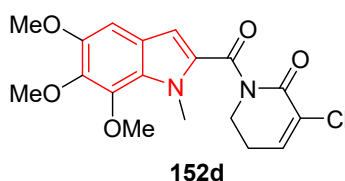
IC₅₀ = 36.09, 93.51, 15.83, 41.67, 51.14 μM against A54, HCT116, ZR-75-30, MDAMB-231 and MRC-5, respectively



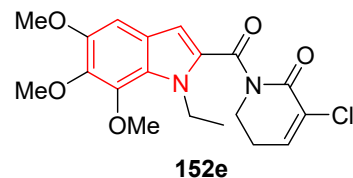
IC₅₀ = 44.56, 85.16, 3.16, 19.52, 64.75 μM against A54, HCT116, ZR-75-30, MDAMB-231 and MRC-5, respectively



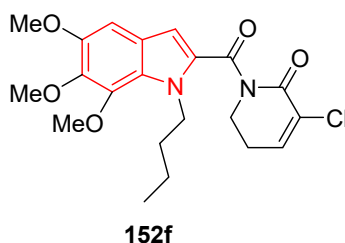
IC₅₀ = 27.45, 78.68, 24.09, 50.04, 90.07 μM against A54, HCT116, ZR-75-30, MDAMB-231 and MRC-5, respectively



IC₅₀ = 12.67, 4.73, 2.24, 10.30, 45.70 μM against A54, HCT116, ZR-75-30, MDAMB-231 and MRC-5, respectively



IC₅₀ = 19.17, 7.99, 2.88, 12.30, 57.96 μM against A54, HCT116, ZR-75-30, MDAMB-231 and MRC-5, respectively



IC₅₀ = 23.54, 8.40, 3.57, 8.59, 44.56 μM against A54, HCT116, ZR-75-30, MDAMB-231 and MRC-5, respectively

Fig. S23. Antiproliferation properties (μM) of the synthesized piperlongumine pharmacophore conjugated with indolyl scaffold **152**, and its precursor piperlongumine **149**.

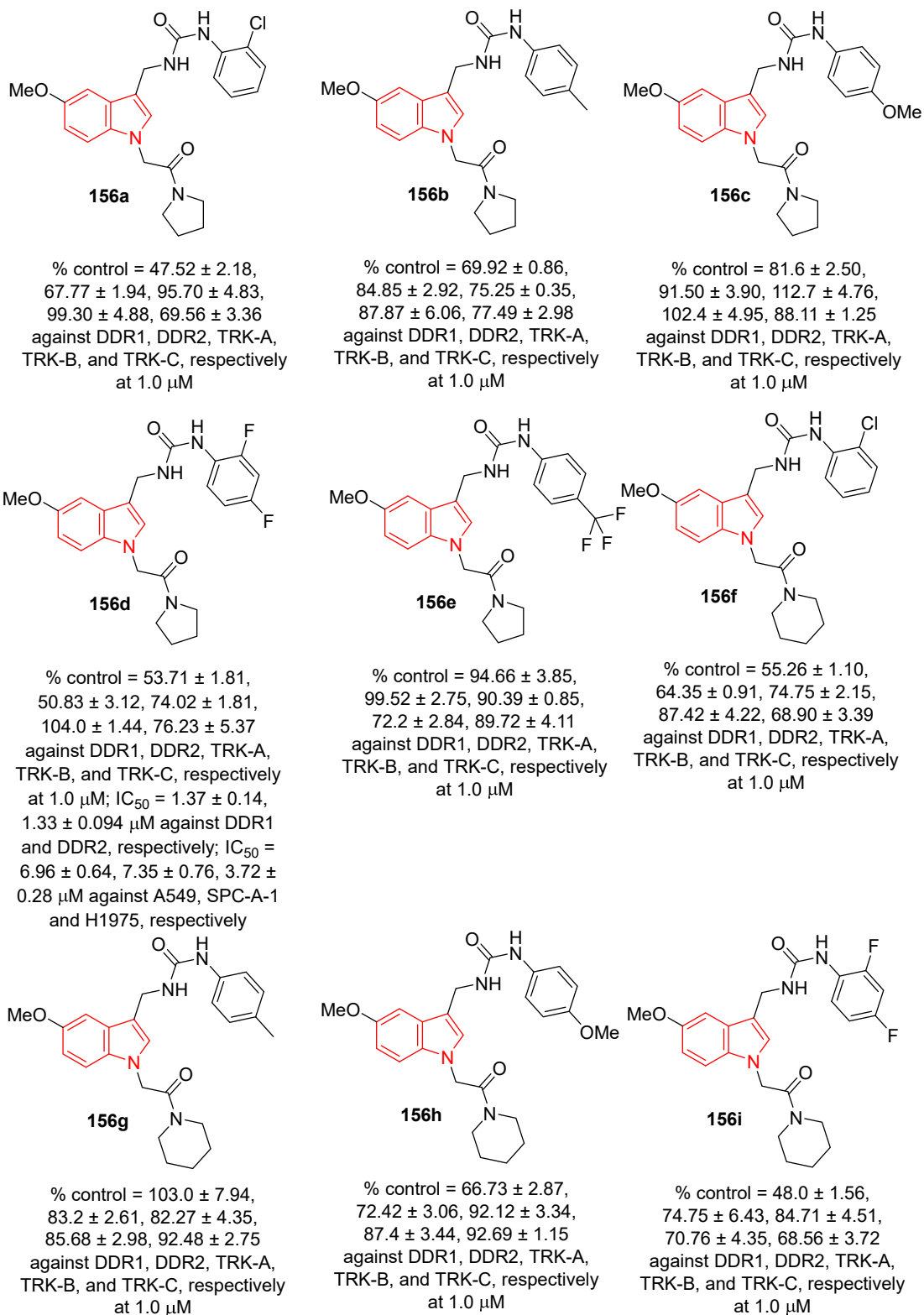


Fig. S24. Kinase inhibitory (% control at 1.0 μM) and antiproliferation (μM ± SD) properties of the synthesized indole-containing compounds linked to urea function **156** and Dasatinib (reference standard).

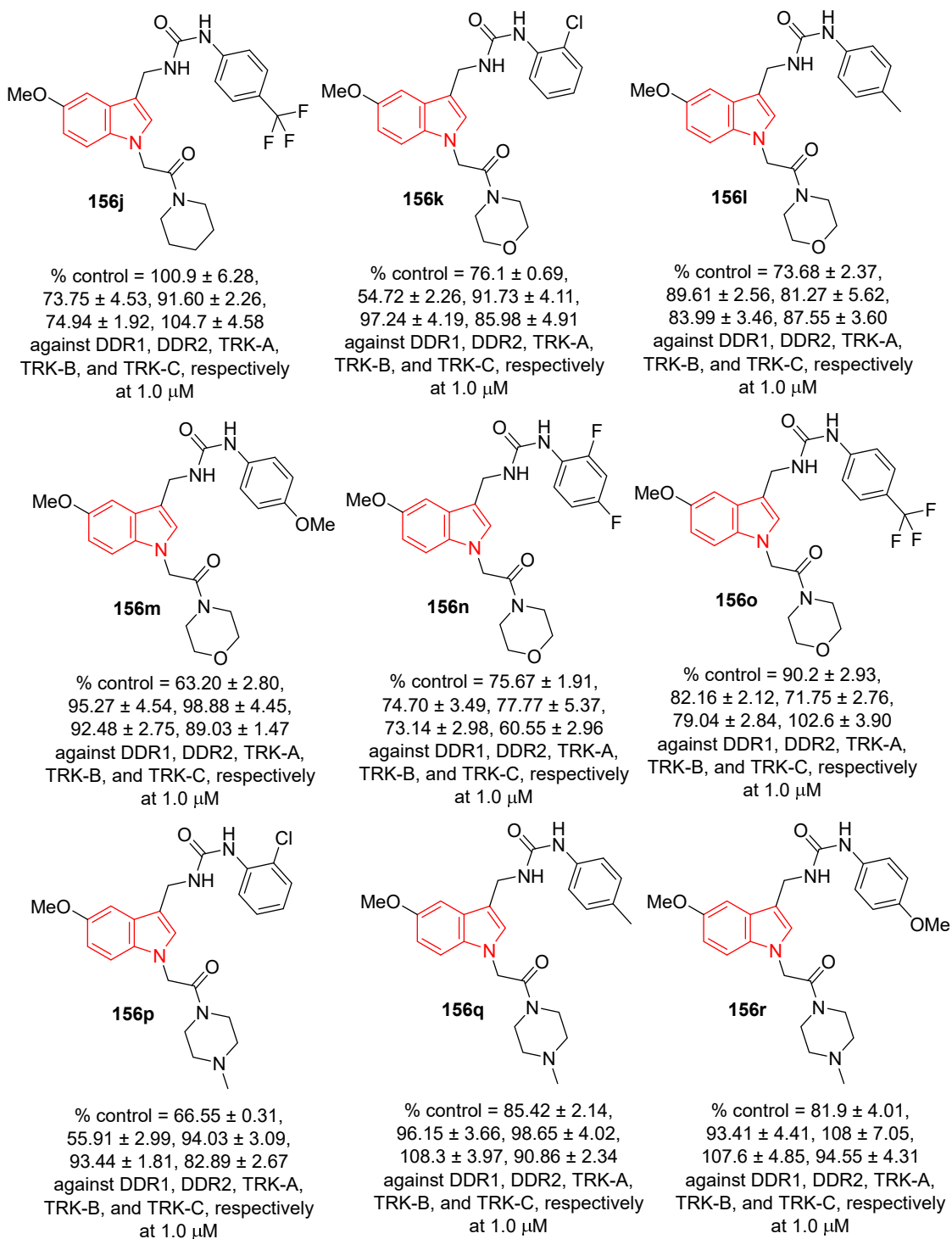


Fig. S24 (continued). Kinase inhibitory (% control at 1.0 μM) and antiproliferation (μM ± SD) properties of the synthesized indole-containing compounds linked to urea function **156** and Dasatinib (reference standard).

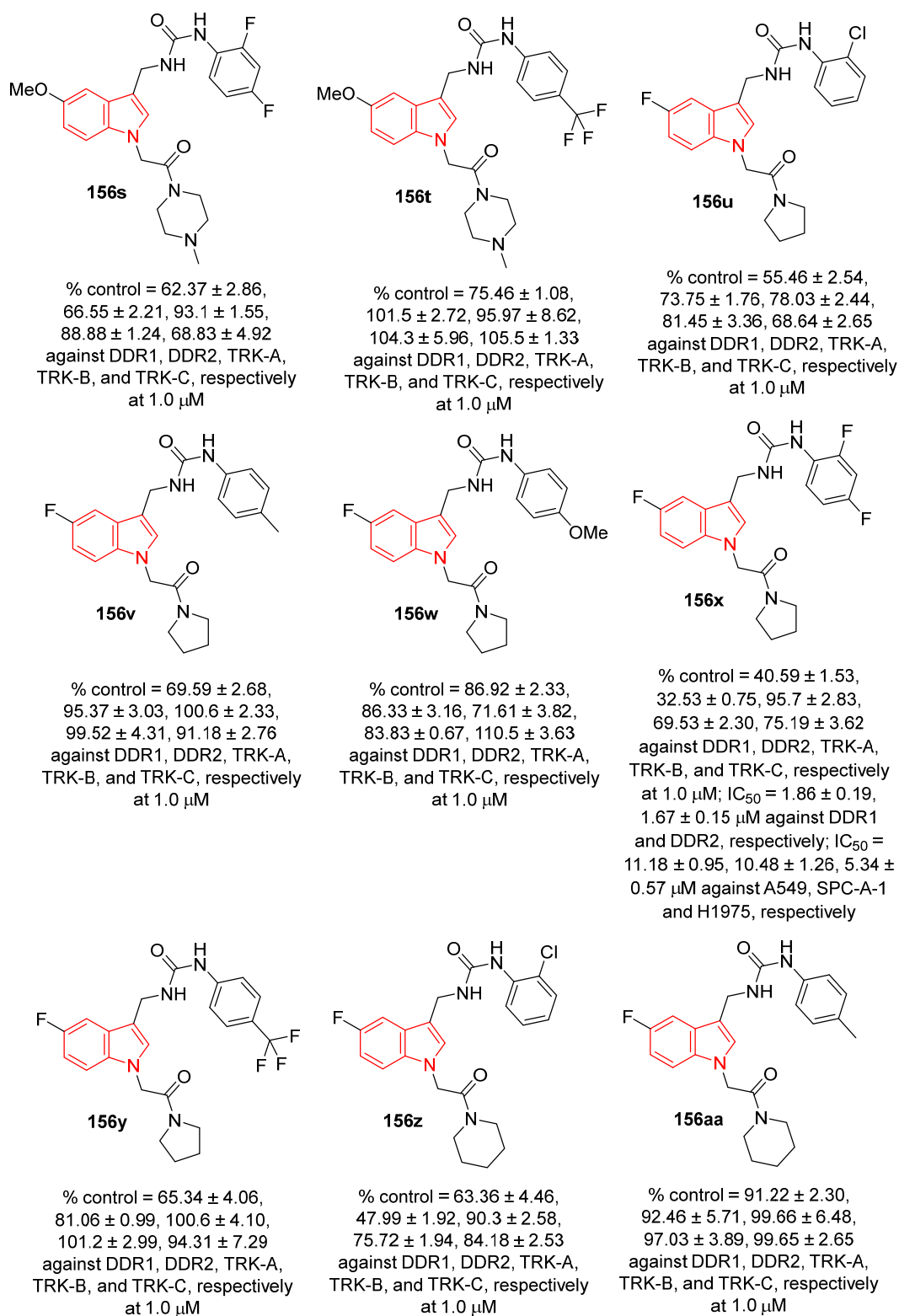


Fig. S24 (continued). Kinase inhibitory (% control at 1.0 μM) and antiproliferation (μM ± SD) properties of the synthesized indole-containing compounds linked to urea function **156** and Dasatinib (reference standard).

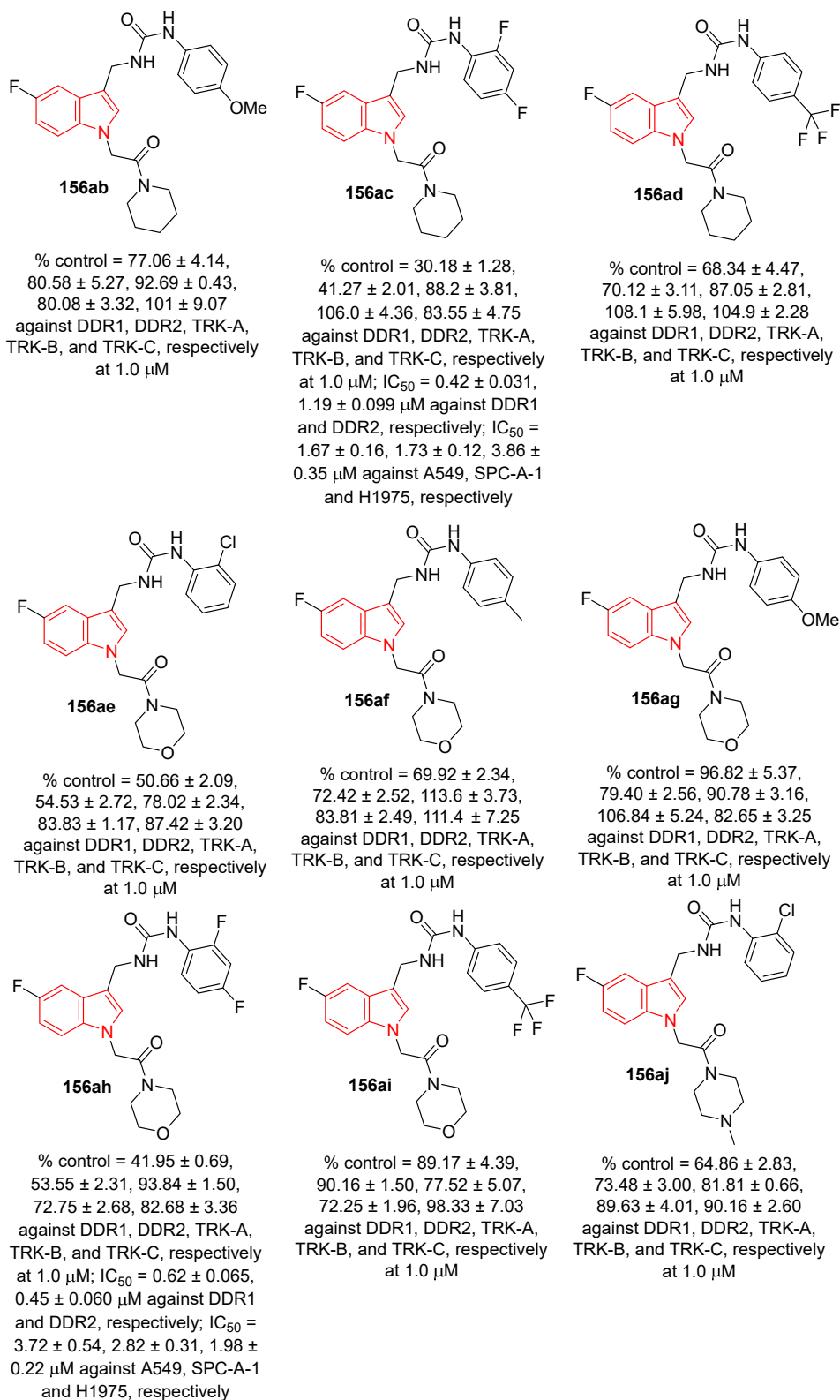


Fig. S24 (continued). Kinase inhibitory (% control at 1.0 μM) and antiproliferation (μM ± SD) properties of the synthesized indole-containing compounds linked to urea function **156** and Dasatinib (reference standard).

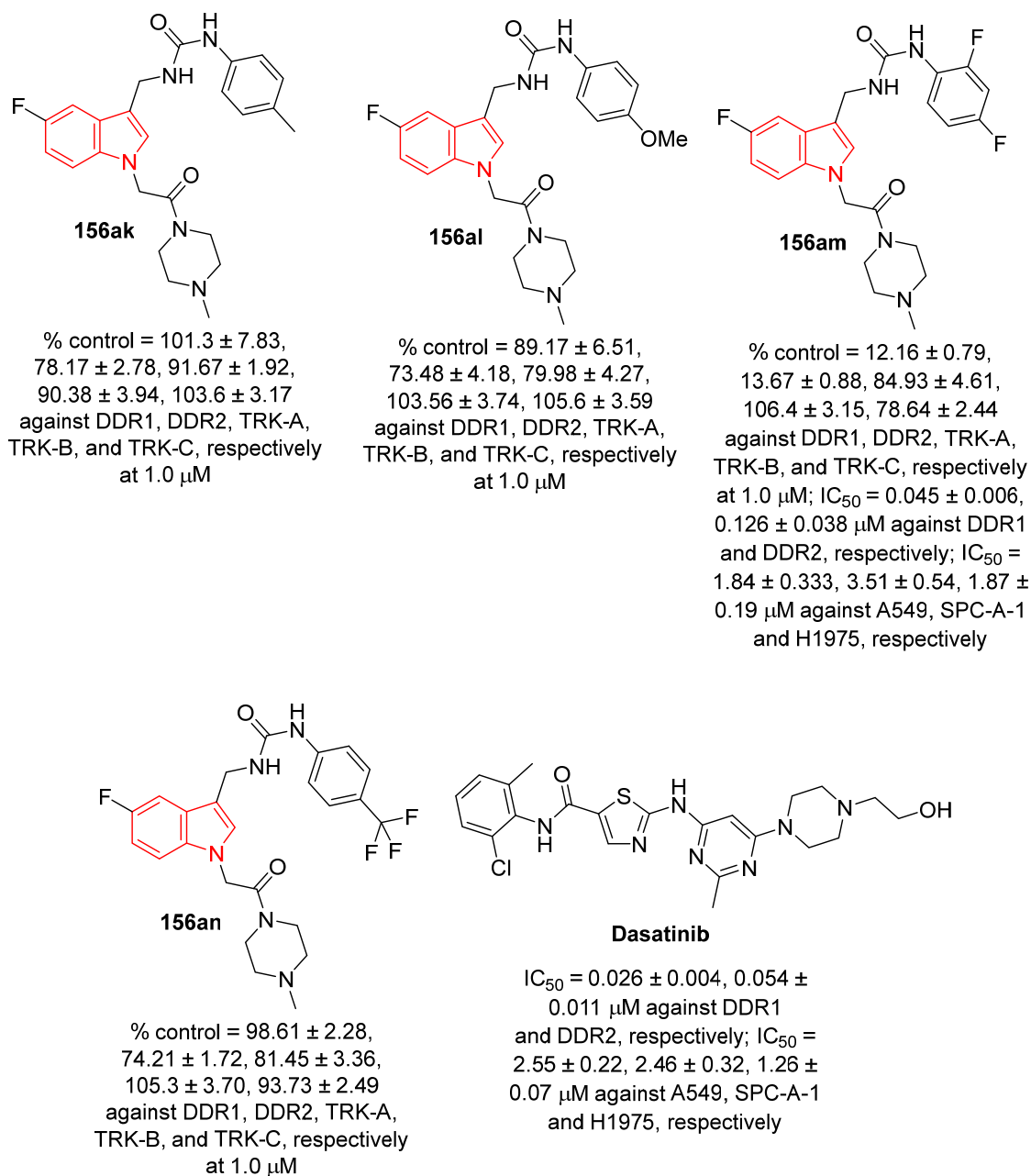


Fig. S24 (continued). Kinase inhibitory (% control at 1.0 μM) and antiproliferation (μM ± SD) properties of the synthesized indole-containing compounds linked to urea function **156** and Dasatinib (reference standard).

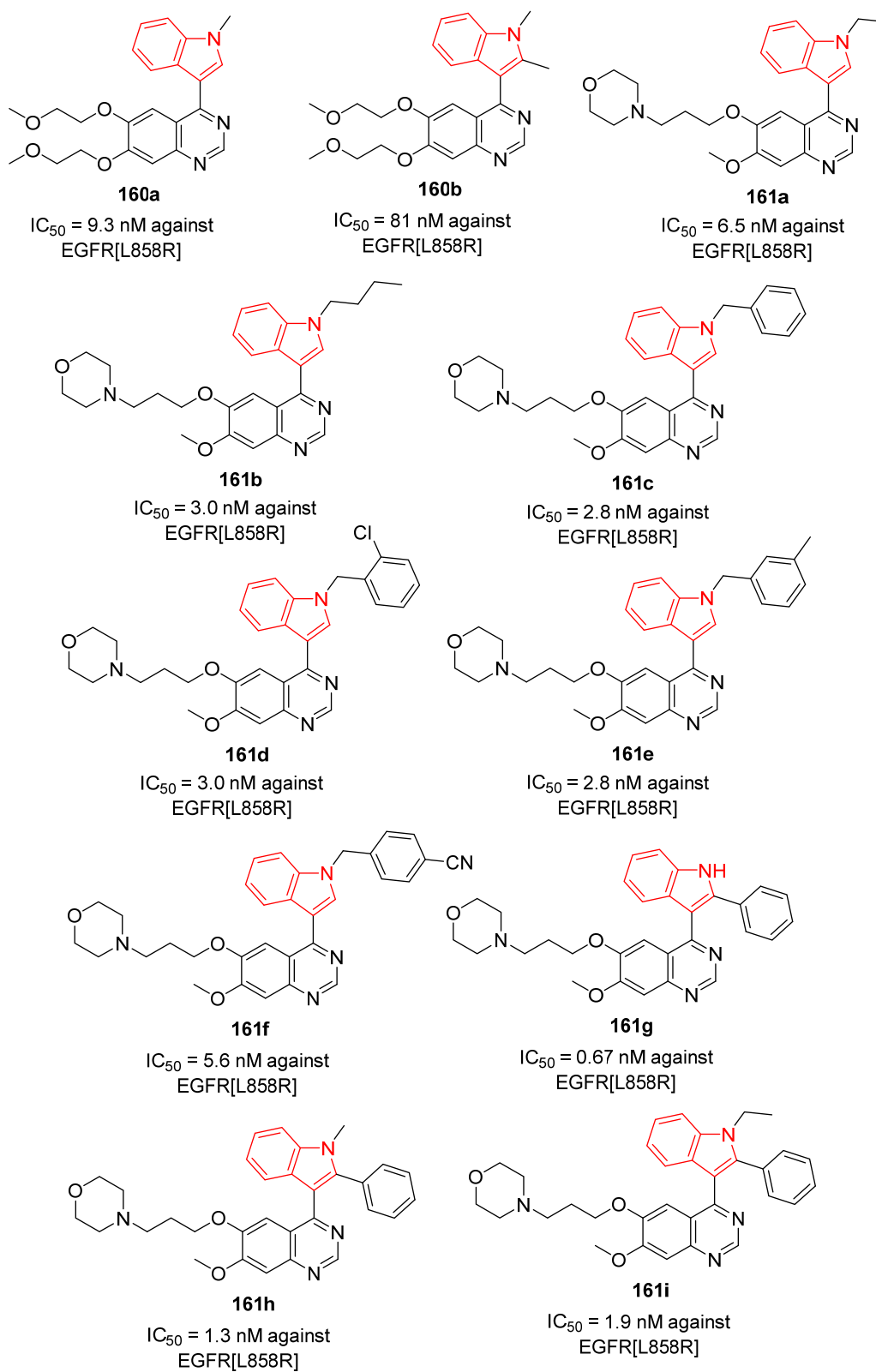


Fig. S25. enzymatic inhibitory properties of synthesized agents **160**, **161** and Gefitinib against EGFR[L858R].

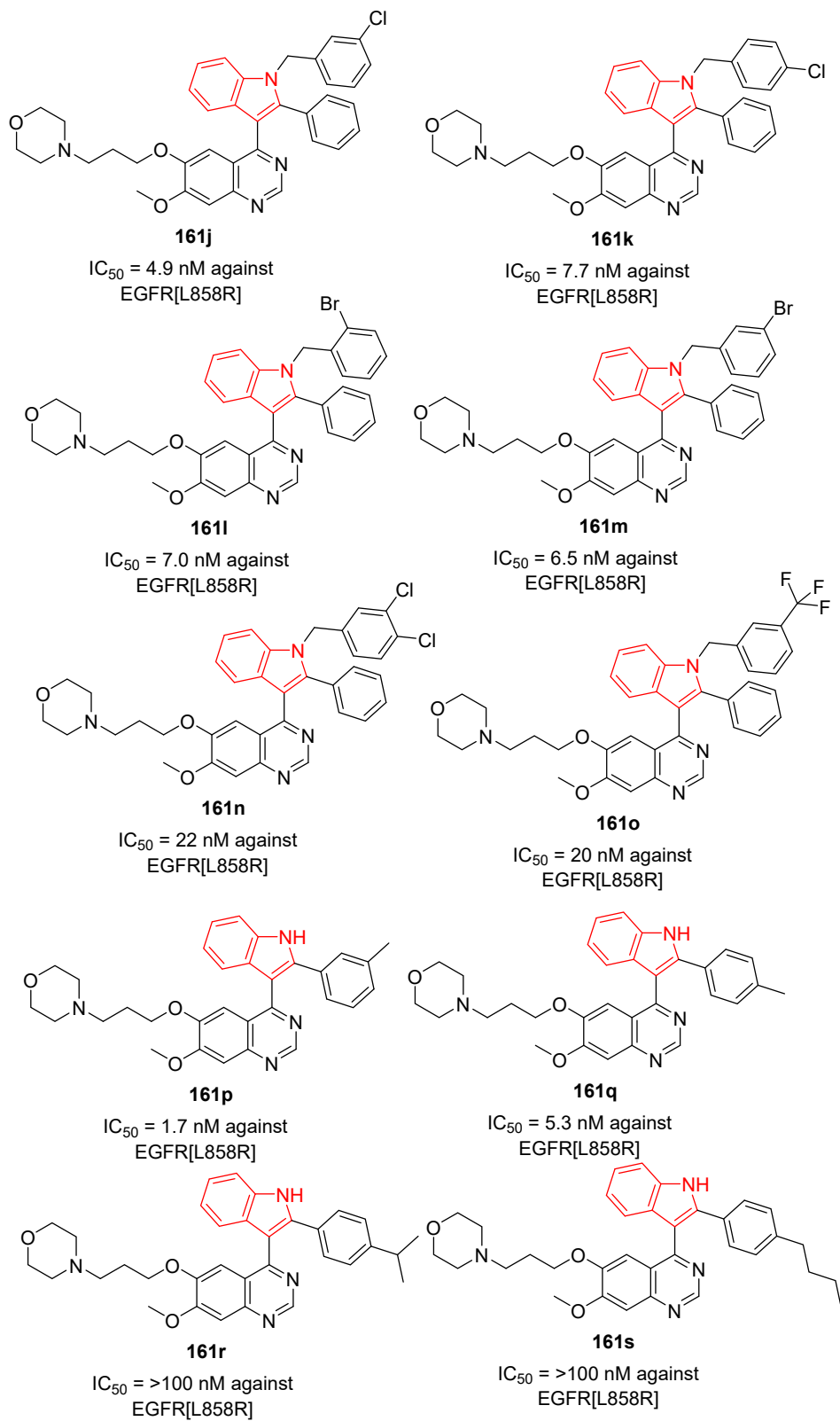


Fig. S25 (continued). enzymatic inhibitory properties of synthesized **160**, **161** and Gefitinib against EGFR[L858R].

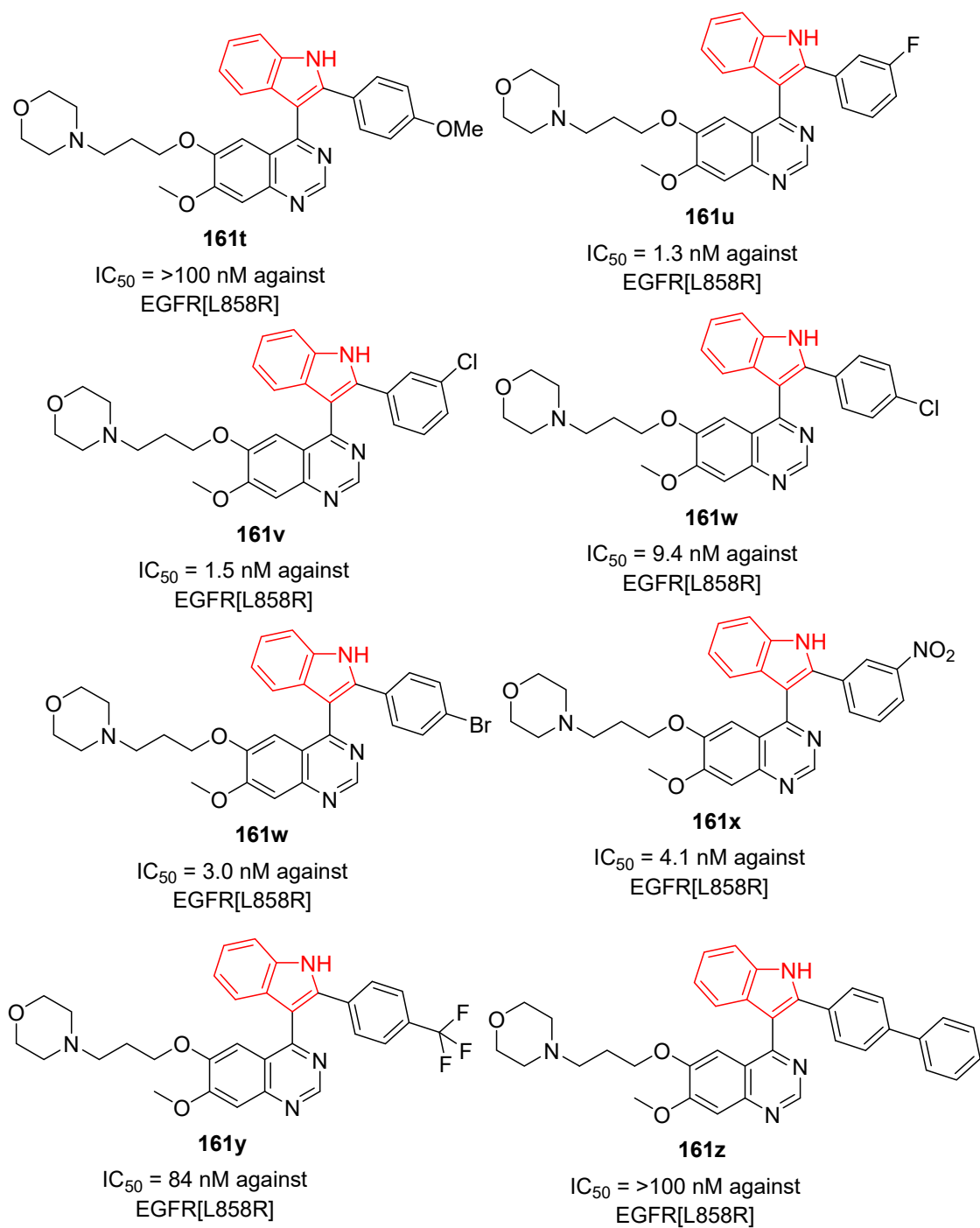


Fig. S25 (continued). enzymatic inhibitory properties of synthesized **160**, **161** and Gefitinib against EGFR[L858R].

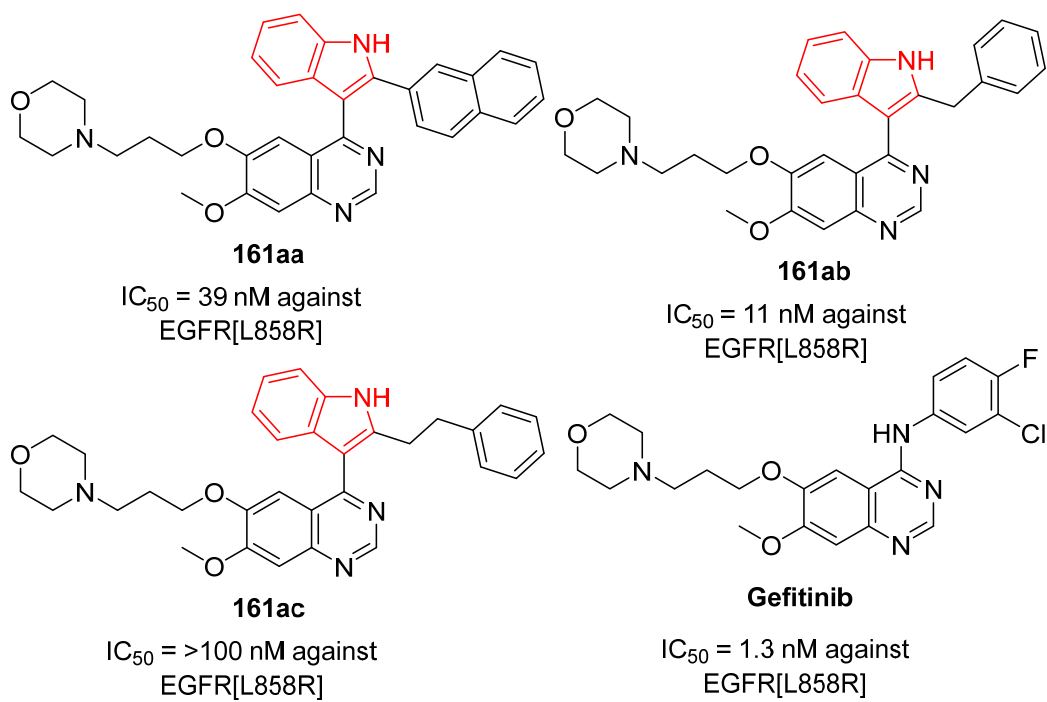


Fig. S25 (continued). enzymatic inhibitory properties of synthesized **160**, **161** and Gefitinib against EGFR[L858R].

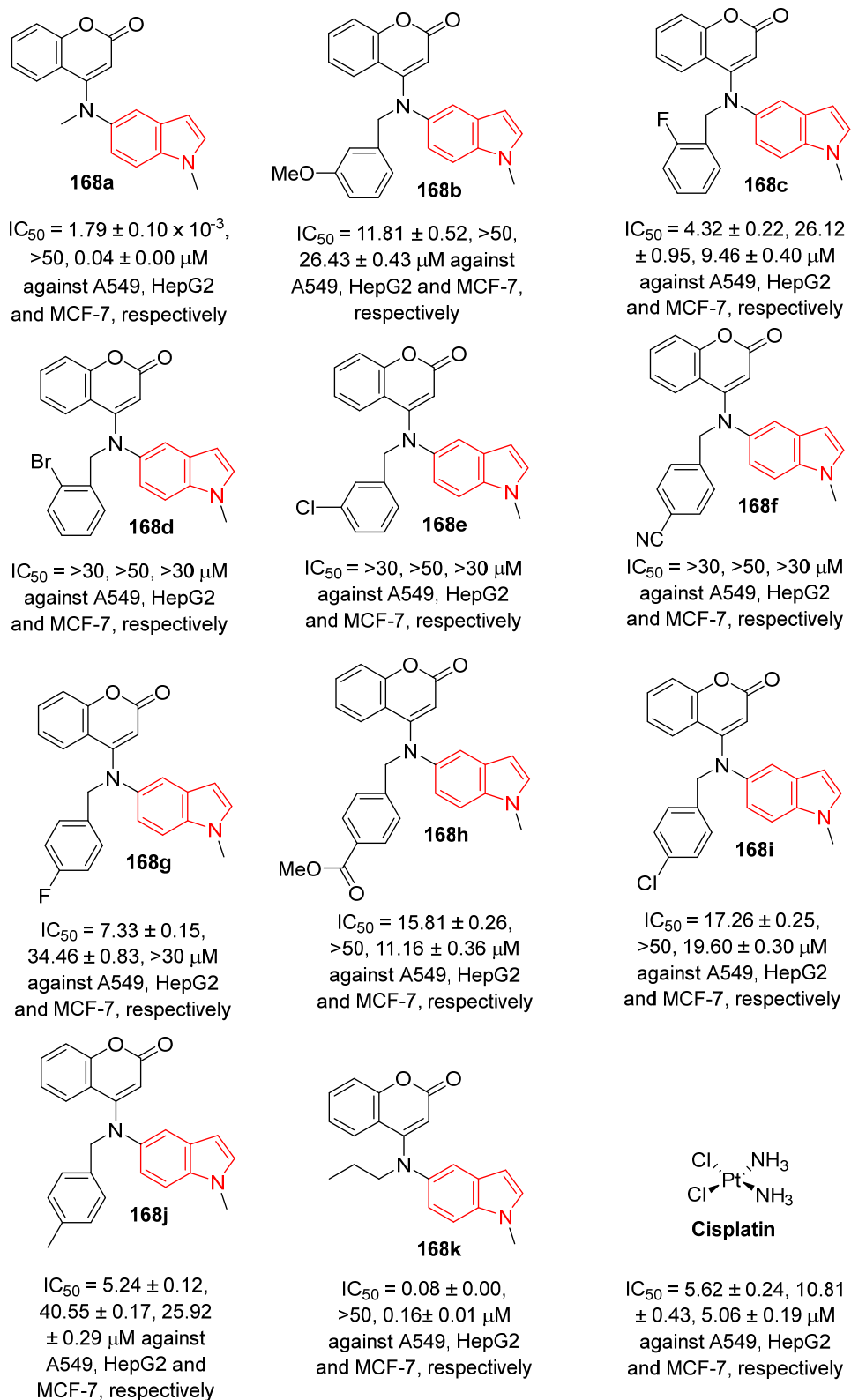
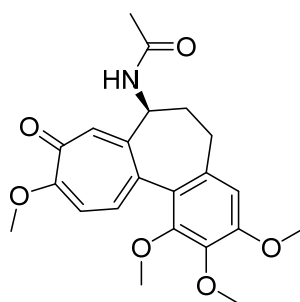


Fig. S26. Antiproliferation properties ($\mu\text{M} \pm \text{SD}$) of the synthesized coumarin-indole conjugates **168**, Cisplatin and Colchicine.



Colchicine

IC₅₀ = 0.01 ± 0.00, 8.36
 ± 0.28, 0.04 ± 0.00 μM
 against A549, HepG2
 and MCF-7, respectively

Fig. S26 (continued). Antiproliferation properties (μM ± SD) of the synthesized coumarin-indole conjugates **168**, Cisplatin and Colchicine.

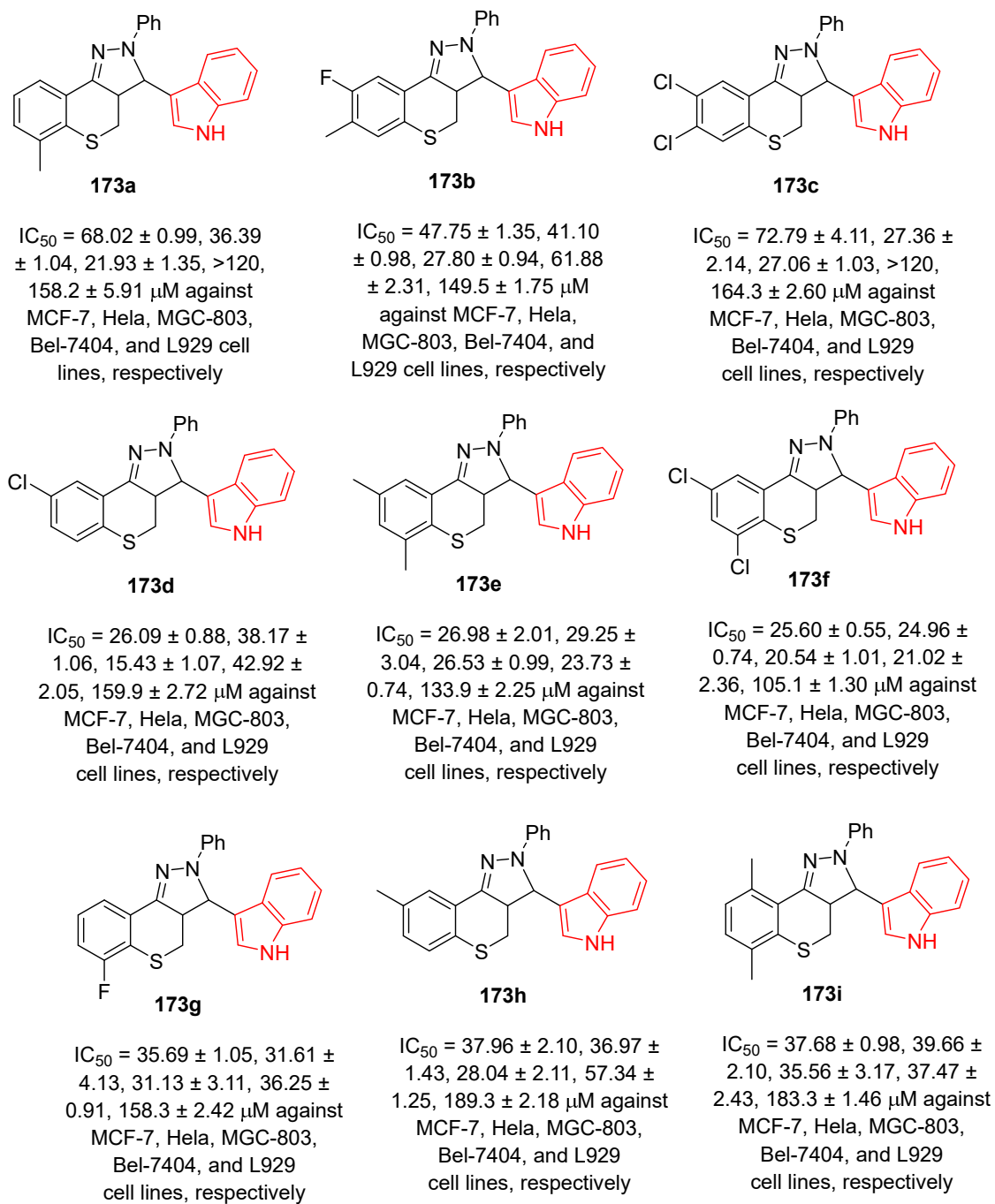
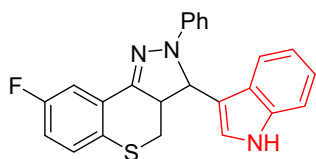
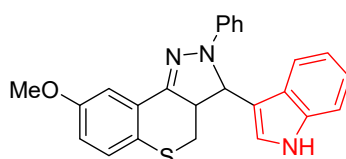


Fig. S27. Antiroliferation properties (μM ± SD) of thiochromeno[4,3-c]pyrazole-indole conjugates **173**, Etoposide and Cisplatin (standard references).



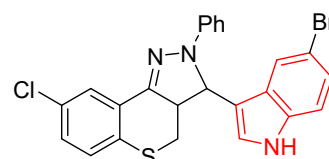
173j

$IC_{50} = 37.84 \pm 1.05, 50.04 \pm 5.32, 39.27 \pm 4.06, 50.24 \pm 1.46, 174.7 \pm 2.41 \mu\text{M}$ against MCF-7, Hela, MGC-803, Bel-7404, and L929 cell lines, respectively



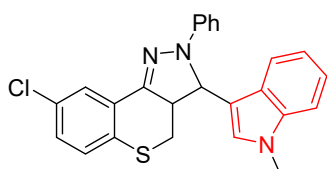
173k

$IC_{50} = >120, >120, 36.38 \pm 1.68, >120, 120.5 \pm 2.13 \mu\text{M}$ against MCF-7, Hela, MGC-803, Bel-7404, and L929 cell lines, respectively



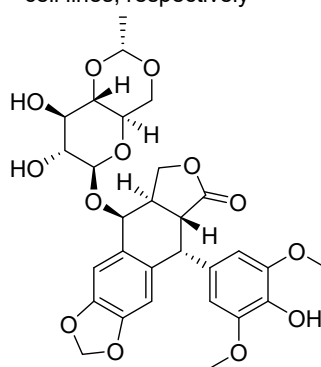
173l

$IC_{50} = 37.14 \pm 1.21, 35.08 \pm 2.06, 29.26 \pm 3.15, 32.14 \pm 0.45, 153.5 \pm 2.59 \mu\text{M}$ against MCF-7, Hela, MGC-803, Bel-7404, and L929 cell lines, respectively



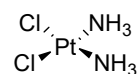
173m

$IC_{50} = 51.12 \pm 2.38, 48.67 \pm 1.48, 33.13 \pm 2.02, 36.17 \pm 1.33, 261.8 \pm 4.2 \mu\text{M}$ against MCF-7, Hela, MGC-803, Bel-7404, and L929 cell lines, respectively



Etoposide

$IC_{50} = 1.45 \pm 0.65, 5.35 \pm 0.47, 11.18 \pm 0.33, 7.76 \pm 0.46, 80.36 \pm 1.91 \mu\text{M}$ against MCF-7, Hela, MGC-803, Bel-7404, and L929 cell lines, respectively



Cisplatin

$IC_{50} = 0.86 \pm 0.75, 3.153 \pm 0.89, 11.38 \pm 0.91, 37.47 \pm 1.05, 31.69 \pm 1.50 \mu\text{M}$ against MCF-7, Hela, MGC-803, Bel-7404, and L929 cell lines, respectively

Fig. S27 (continued). Antioliferation properties ($\mu\text{M} \pm \text{SD}$) of thiochromeno[4,3-c]pyrazole-indole conjugates **173**, Etoposide and Cisplatin (standard references).

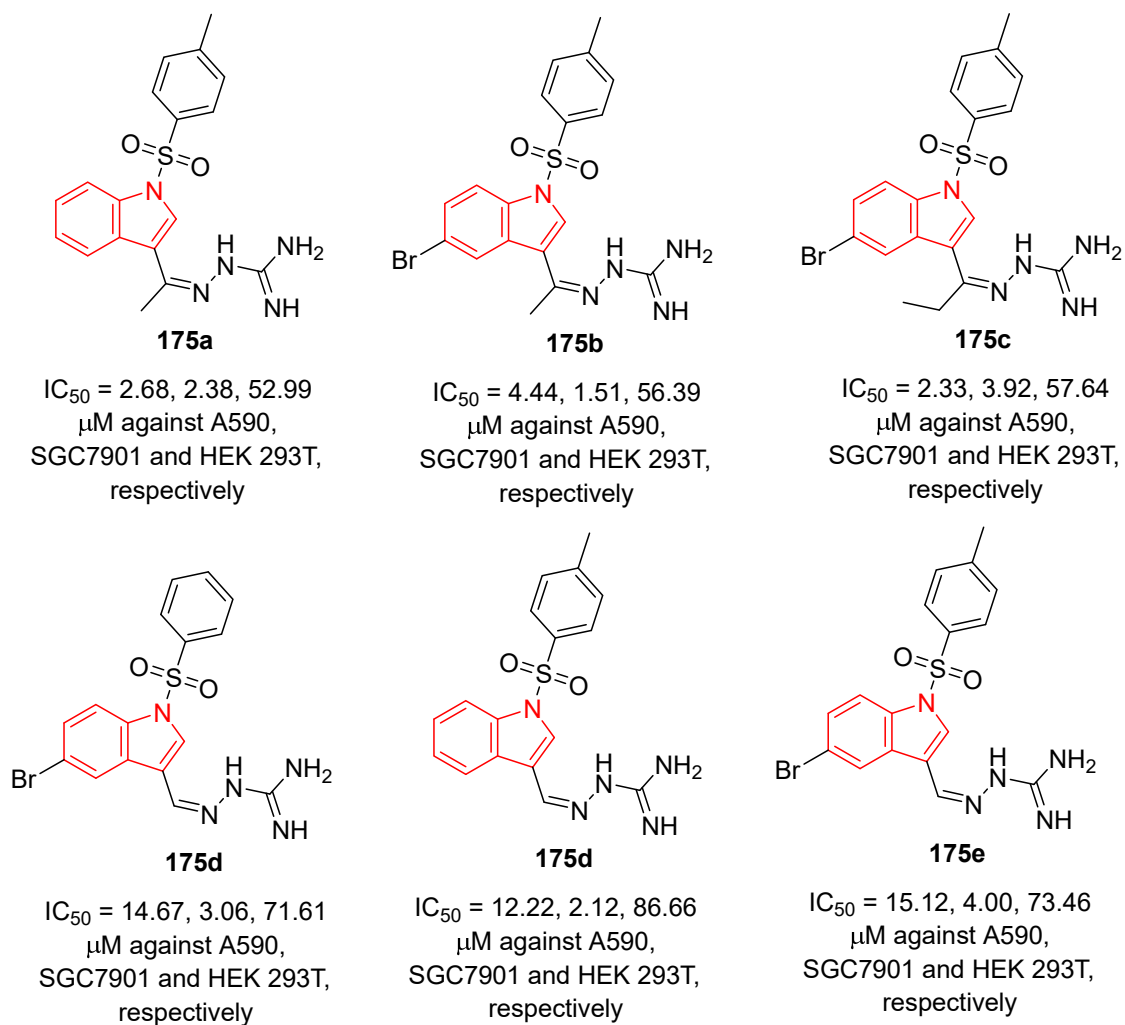


Fig. S28. Antiproliferation properties of the synthesized indolyldiazine-1-carboximidamide **175**.

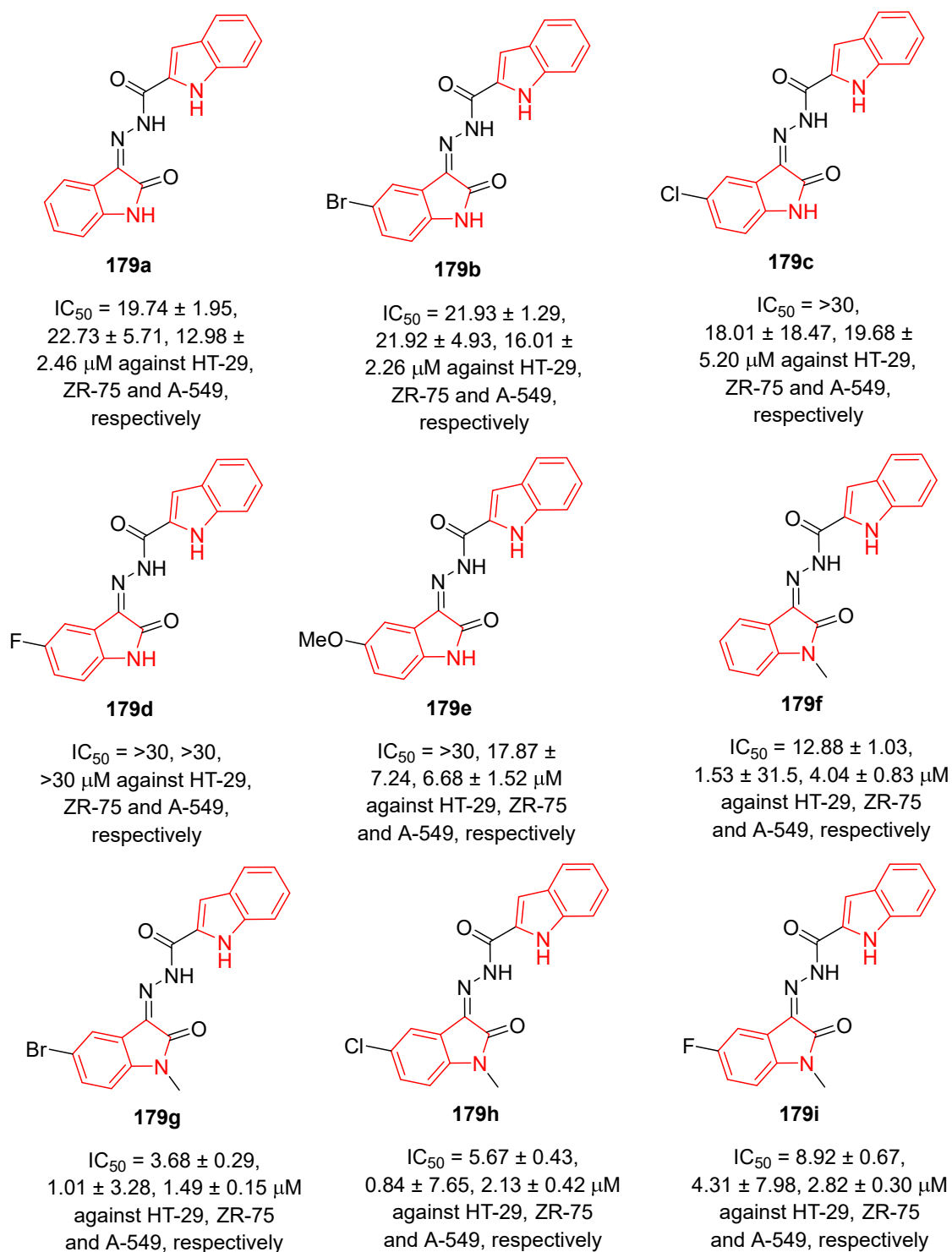
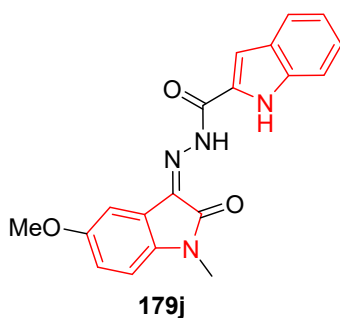
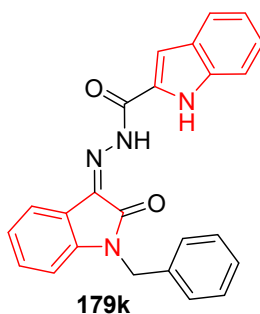


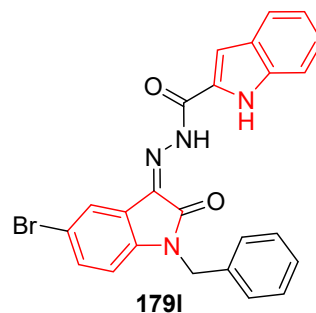
Fig. S29. Antiproliferation properties of the synthesized 2-oxo-3-indolylidene-2-indolecarbohydrazones **179** and Sunitinib.



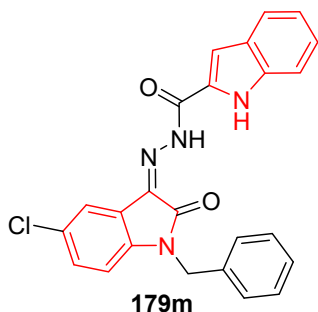
$IC_{50} = 5.73 \pm 0.67$,
 1.48 ± 7.06 , $1.93 \pm 0.27 \mu\text{M}$
 against HT-29, ZR-75
 and A-549, respectively



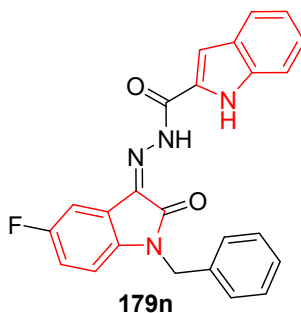
$IC_{50} = 6.19 \pm 1.58$,
 1.12 ± 3.05 , $1.06 \pm 0.37 \mu\text{M}$
 against HT-29, ZR-75
 and A-549, respectively



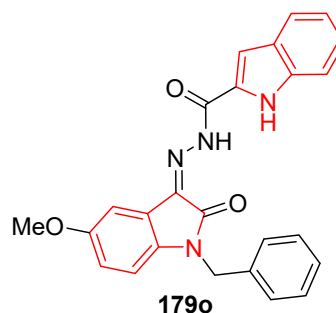
$IC_{50} = 2.26 \pm 0.33$,
 0.70 ± 12.04 , $0.65 \pm 0.12 \mu\text{M}$
 against HT-29, ZR-75
 and A-549, respectively



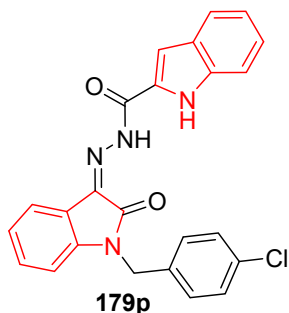
$IC_{50} = 2.02 \pm 0.36$,
 0.74 ± 0.88 , $0.76 \pm 0.12 \mu\text{M}$
 against HT-29, ZR-75
 and A-549, respectively



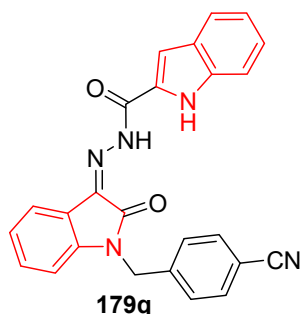
$IC_{50} = 3.50 \pm 0.49$,
 2.10 ± 3.15 , $1.41 \pm 0.21 \mu\text{M}$
 against HT-29, ZR-75
 and A-549, respectively



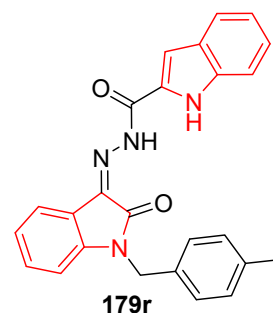
$IC_{50} = 2.28 \pm 0.22$,
 0.86 ± 0.76 , $0.64 \pm 0.24 \mu\text{M}$
 against HT-29, ZR-75
 and A-549, respectively



$IC_{50} = 2.64 \pm 0.27$,
 1.30 ± 0.58 , $1.05 \pm 0.15 \mu\text{M}$
 against HT-29, ZR-75
 and A-549, respectively

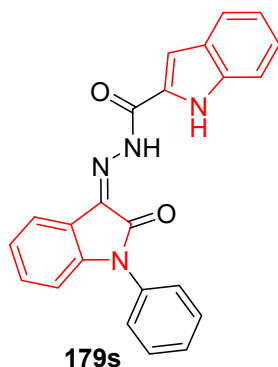


$IC_{50} = 8.11 \pm 1.27$,
 1.51 ± 5.03 , $2.13 \pm 0.49 \mu\text{M}$
 against HT-29, ZR-75
 and A-549, respectively

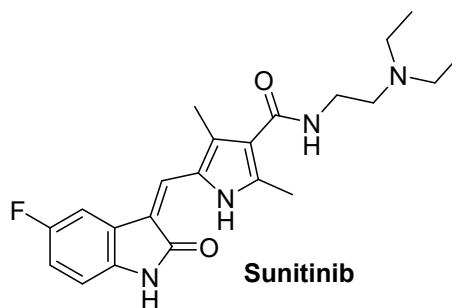


$IC_{50} = 2.45 \pm 0.32$,
 1.28 ± 12.44 , $0.64 \pm 0.61 \mu\text{M}$
 against HT-29, ZR-75
 and A-549, respectively

Fig. S29 (continued). Antiproliferation properties of the synthesized 2-oxo-3-indolylidene-2-indolecarbohydrazones **179** and Sunitinib.

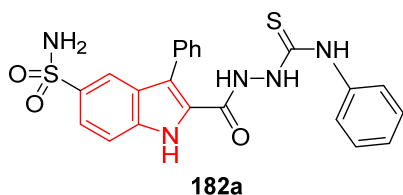


$IC_{50} = 6.34 \pm 0.76$,
 1.32 ± 2.89 , $2.41 \pm 0.29 \mu M$
 against HT-29, ZR-75
 and A-549, respectively

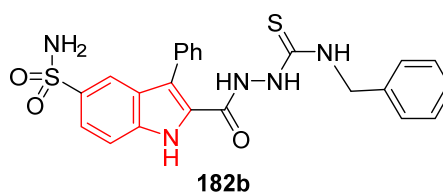


$IC_{50} = 10.14 \pm 0.8$,
 8.31 ± 2.4 , $5.87 \pm 0.3 \mu M$
 against HT-29, ZR-75
 and A-549, respectively

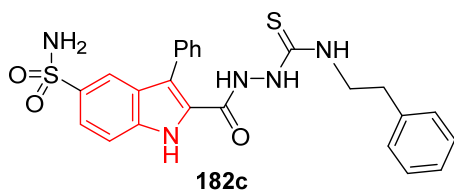
Fig. S29 (cintinued). Antiproliferation properties of the synthesized 2-oxo-3-indolylidene-2-indolecarbohydrazones **179** and Sunitinib.



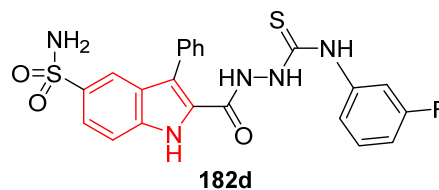
$IC_{50} = 132.28 \pm 26.06, 80.04 \pm 18.01$
 μM against HT-29, and CCD-986Sk,
 respectively; $K_i = 946.1, 375.3, 28.6,$
 54.2 nM against hCA I, hCA II, hCA XI,
 and hCA XII, respectively



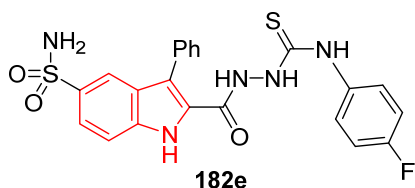
$IC_{50} = 153.55 \pm 32.95, 102.73 \pm 13.86$
 μM against HT-29, and CCD-986Sk,
 respectively; $K_i = 1809.5, 525.2, 112.5,$
 88.5 nM against hCA I, hCA II, hCA IX,
 and hCA XII, respectively



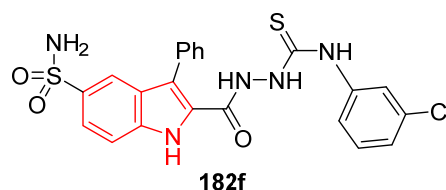
$IC_{50} = 454.04 \pm 122.22, 62.73 \pm 9.25$
 μM against HT-29, and CCD-986Sk,
 respectively; $K_i = 5566.3, 778.5, 250.5,$
 306.2 nM against hCA I, hCA II, hCA IX,
 and hCA XII, respectively



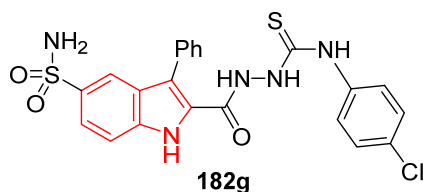
$IC_{50} = 111.81 \pm 13.22, 82.98 \pm 16.20$
 μM against HT-29, and CCD-986Sk,
 respectively; $K_i = 6239.3, 284.4, 45.6,$
 130.3 nM against hCA I, hCA II, hCA IX,
 and hCA XII, respectively



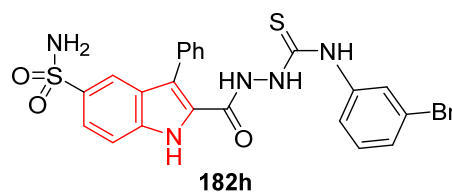
$IC_{50} = 53.32 \pm 7.74, 74.64 \pm 14.15$
 μM against HT-29, and CCD-986Sk,
 respectively; $K_i = 4162.4, 211.5, 31.0,$
 87.0 nM against hCA I, hCA II, hCA IX,
 and hCA XII, respectively



$IC_{50} = 115.69 \pm 30.88, 57.69 \pm 6.05$
 μM against HT-29, and CCD-986Sk,
 respectively; $K_i = 4789.8, 194.6, 34.8,$
 61.4 nM against hCA I, hCA II, hCA IX,
 and hCA XII, respectively

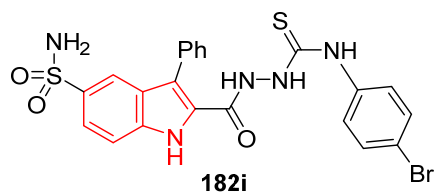


$IC_{50} = 76.69 \pm 19.31, 55.55 \pm 11.71$
 μM against HT-29, and CCD-986Sk,
 respectively; $K_i = 3627.0, 159.5, 25.7,$
 56.1 nM against hCA I, hCA II, hCA IX,
 and hCA XII, respectively

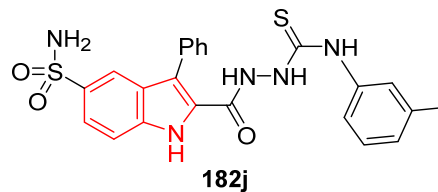


$IC_{50} = 192.77 \pm 69.81, 60.67 \pm 5.52$
 μM against HT-29, and CCD-986Sk,
 respectively; $K_i = 3977.2, 539.4, 11.7,$
 46.2 nM against hCA I, hCA II, hCA IX,
 and hCA XII, respectively

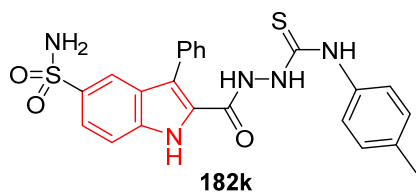
Fig. S30. Antiproliferation and carbonic anhydrase inhibitory properties of 1-(indole-2-carbonyl)thiosemicarbazides incorporating sulfonamide group **182** and standard references (Doxorubicin and Acetazolamide "AAZ").



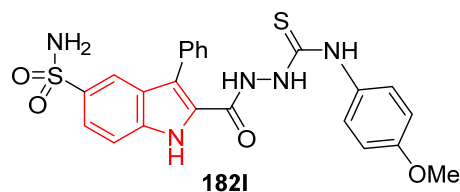
$IC_{50} = 71.70 \pm 15.97, 68.25 \pm 15.13$
 μM against HT-29, and CCD-986Sk,
 respectively; $K_i = 2651.5, 421.4, 9.1,$
 31.3 nM against hCA I, hCA II, hCA IX,
 and hCA XII, respectively



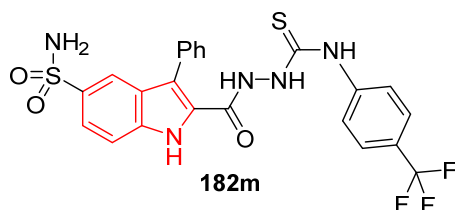
$IC_{50} = 200.12 \pm 59.51, 68.28 \pm 12.24$
 μM against HT-29, and CCD-986Sk,
 respectively; $K_i = 2833.3, 849.9, 94.6,$
 80.0 nM against hCA I, hCA II, hCA IX,
 and hCA XII, respectively



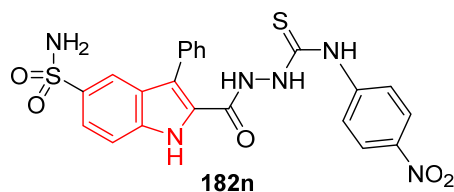
$IC_{50} = 94.06 \pm 18.52, 74.95 \pm 15.13$
 μM against HT-29, and CCD-986Sk,
 respectively; $K_i = 2137.0, 744.4, 63.4,$
 87.1 nM against hCA I, hCA II, hCA IX,
 and hCA XII, respectively



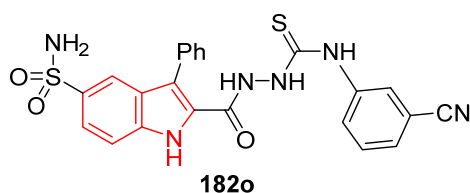
$IC_{50} = < 1000, 88.49 \pm 10.34$
 μM against HT-29, and CCD-986Sk,
 respectively; $K_i = 3448.8, 532.9, 131.9,$
 93.9 nM against hCA I, hCA II, hCA IX,
 and hCA XII, respectively



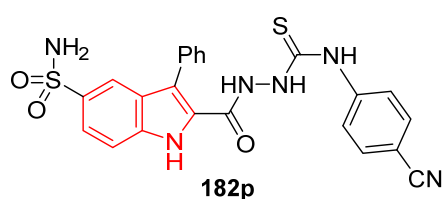
$IC_{50} = 145.58 \pm 40.85, 96.67 \pm 19.95$
 μM against HT-29, and CCD-986Sk,
 respectively; $K_i = 4071.5, 500.4, 30.8,$
 75.2 nM against hCA I, hCA II, hCA IX,
 and hCA XII, respectively



$IC_{50} = 183.17 \pm 53.37, 134.14 \pm 38.10$
 μM against HT-29, and CCD-986Sk,
 respectively; $K_i = 614.6, 63.2, 12.7,$
 21.8 nM against hCA I, hCA II, hCA IX,
 and hCA XII, respectively

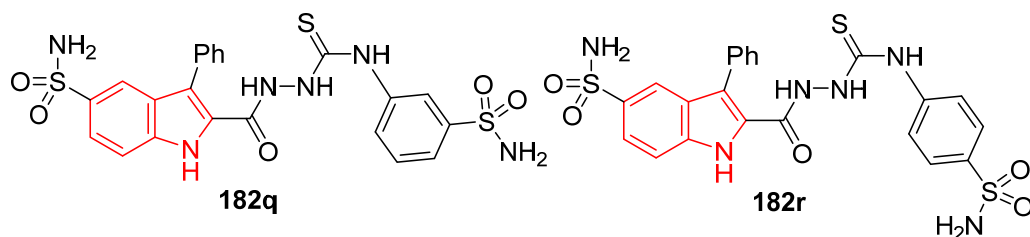


$IC_{50} = 215.68 \pm 46.15, 119.12 \pm 12.58$
 μM against HT-29, and CCD-986Sk,
 respectively; $K_i = 475.0, 73.5, 79.2,$
 19.3 nM against hCA I, hCA II, hCA IX,
 and hCA XII, respectively



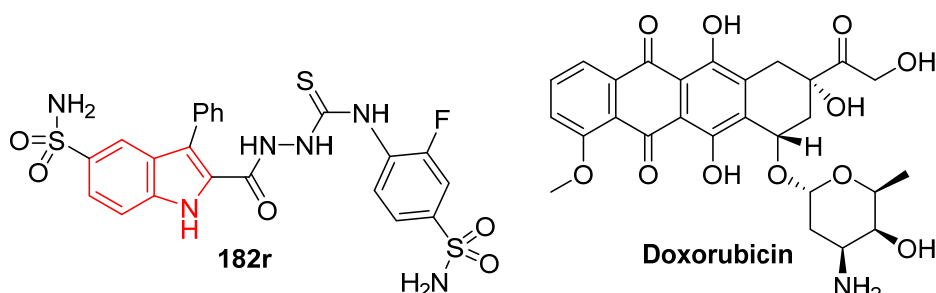
$IC_{50} = 364.95 \pm 84.84, 111.81 \pm 33.02$
 μM against HT-29, and CCD-986Sk,
 respectively; $K_i = 5719.5, 284.4, 191.3,$
 42.4 nM against hCA I, hCA II, hCA IX,
 and hCA XII, respectively

Fig. S30 (continued). Antiproliferation and carbonic anhydrase inhibitory properties of 1-(indole-2-carbonyl)thiosemicarbazides incorporating sulfonamide group **182** and standard references (Doxorubicin and Acetazolamide "AAZ").



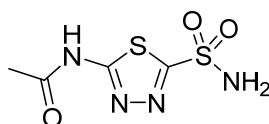
IC_{50} = 508.05 ± 130.77 , 155.63 ± 16.97 μ M against HT-29, and CCD-986Sk, respectively; K_i = 78.7, 38.0, 2.1, 0.69 nM against hCA I, hCA II, hCA IX, and hCA XII, respectively

IC_{50} = 407.14 ± 103.07 , 322.15 ± 43.69 μ M against HT-29, and CCD-986Sk, respectively; K_i = 75.9, 19.5, 1.4, 0.87 nM against hCA I, hCA II, hCA IX, and hCA XII, respectively



IC_{50} = 335.46 ± 75.93 , 132.50 ± 13.52 μ M against HT-29, and CCD-986Sk, respectively; K_i = 101.9, 58.4, 12.7, 5.3 nM against hCA I, hCA II, hCA IX, and hCA XII, respectively

IC_{50} = 17.20 ± 3.80 , 0.17 ± 0.05 μ M against HT-29, and CCD-986Sk, respectively



Acetazolamide (AAZ)

K_i = 250.0, 12.5, 25.0, 5.7 nM against hCA I, hCA II, hCA IX, and hCA XII, respectively

Fig. S30 (continued). Antiproliferation and carbonic anhydrase inhibitory properties of 1-(indole-2-carbonyl)thiosemicarbazides incorporating sulfonamide group **182** and standard references (Doxorubicin and Acetazolamide "AAZ").

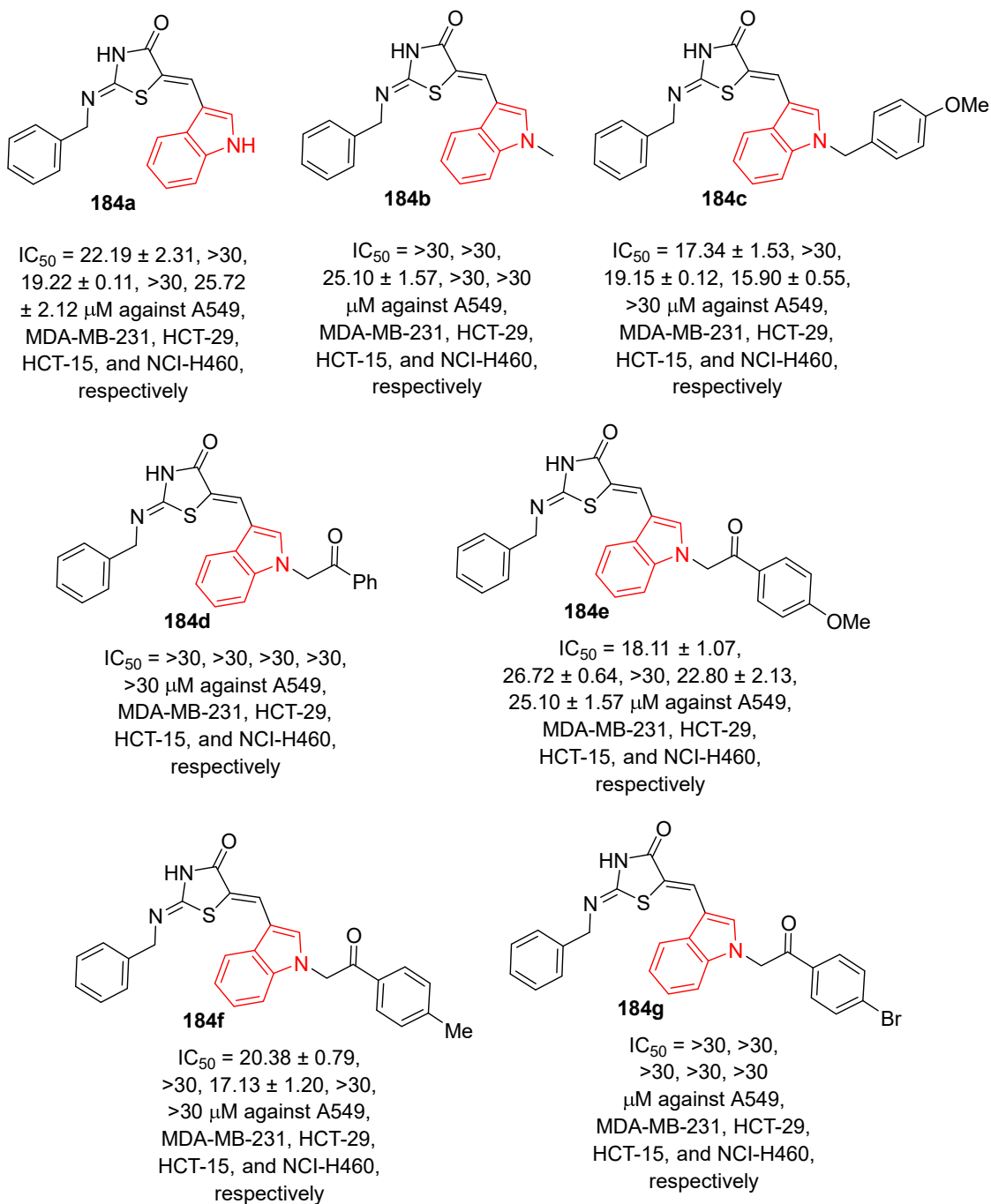


Fig. S31. Antiproliferation properties of thiazolidinone-indoles **184** and Podophyllotoxin.

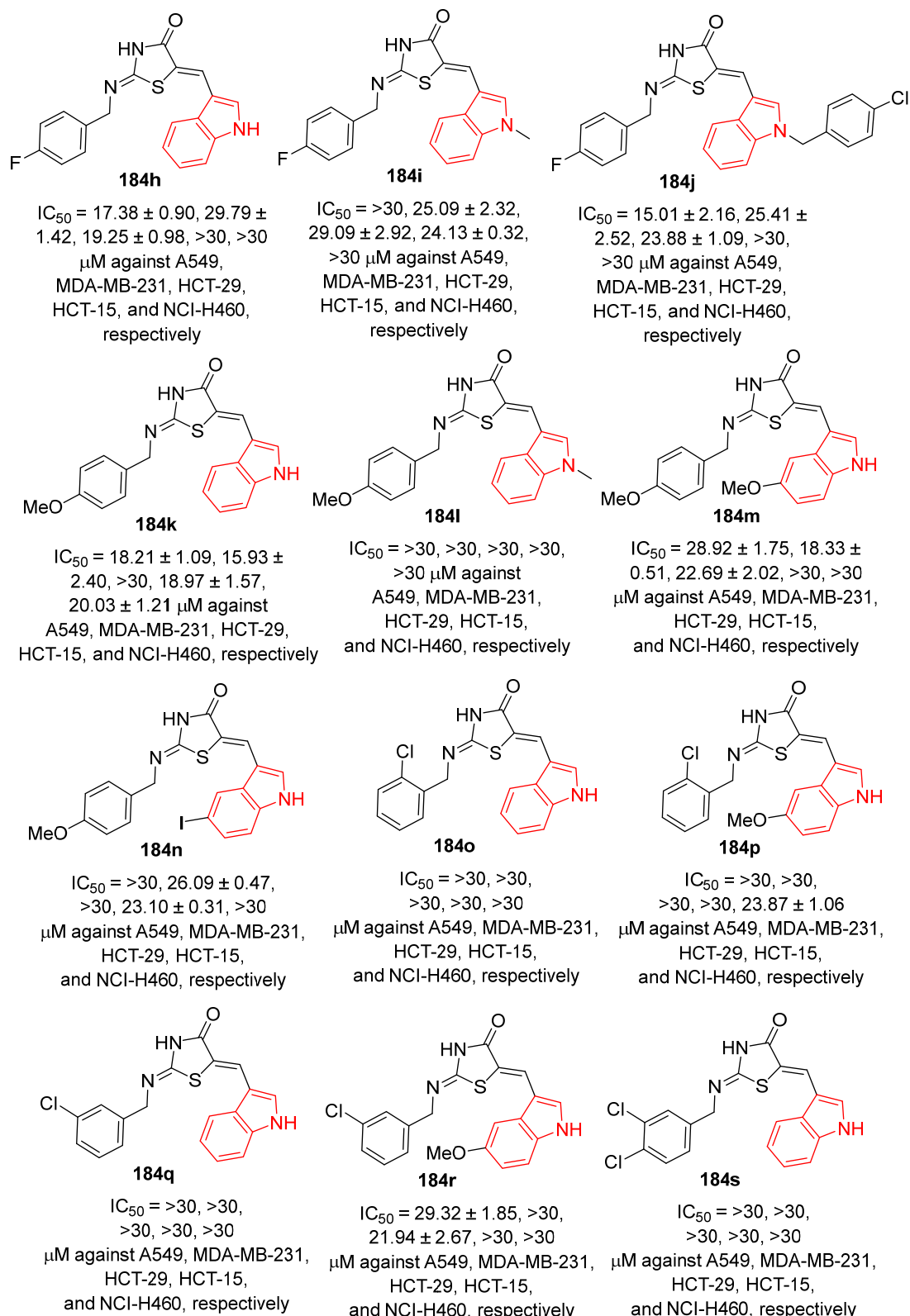


Fig. S31 (continued). Antiproliferation properties of thiazolidinone-indoles **184** and Podophyllotoxin.

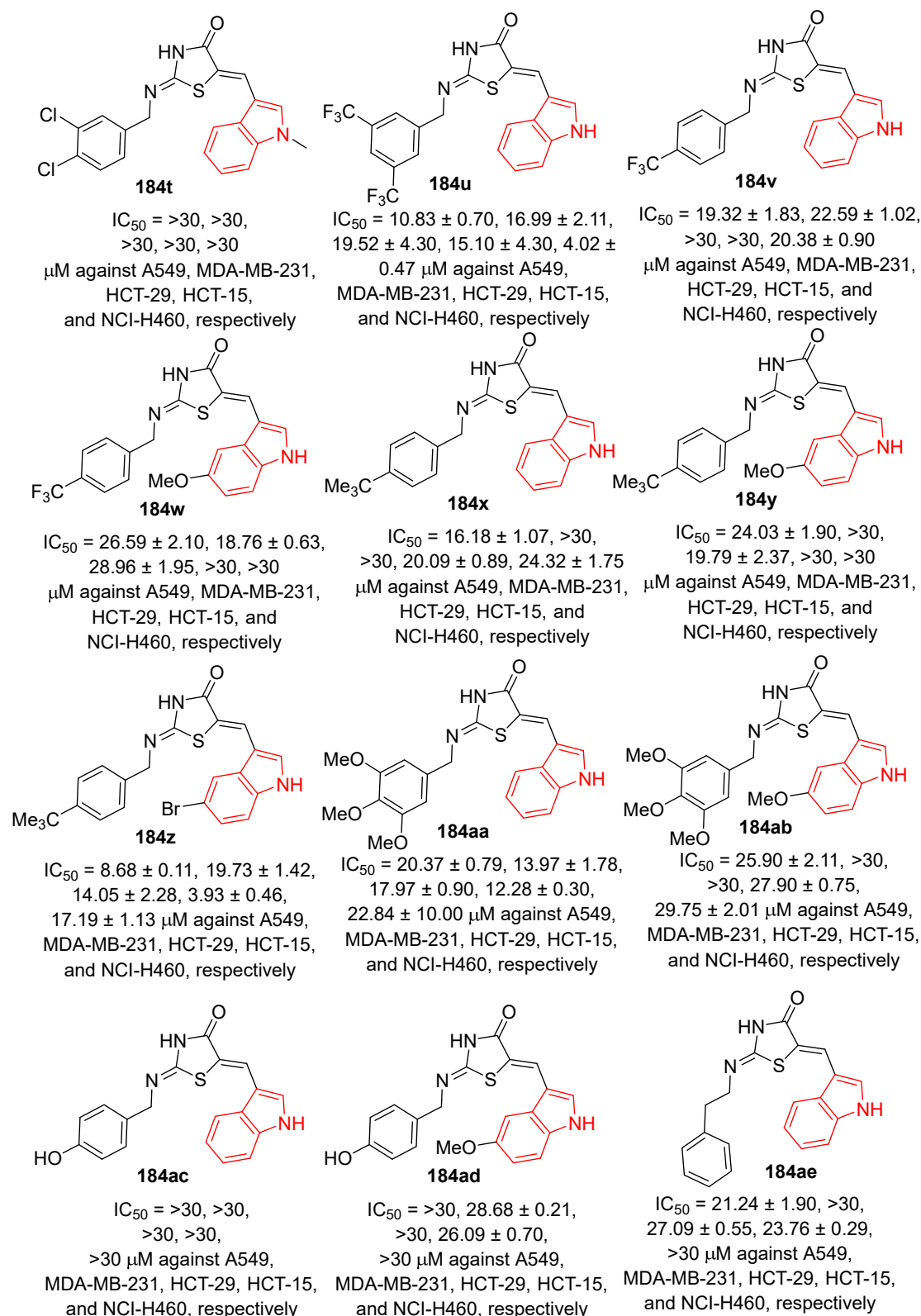


Fig. S31 (continued). Antiproliferation properties of thiazolidinone-indoles **184** and Podophyllotoxin.

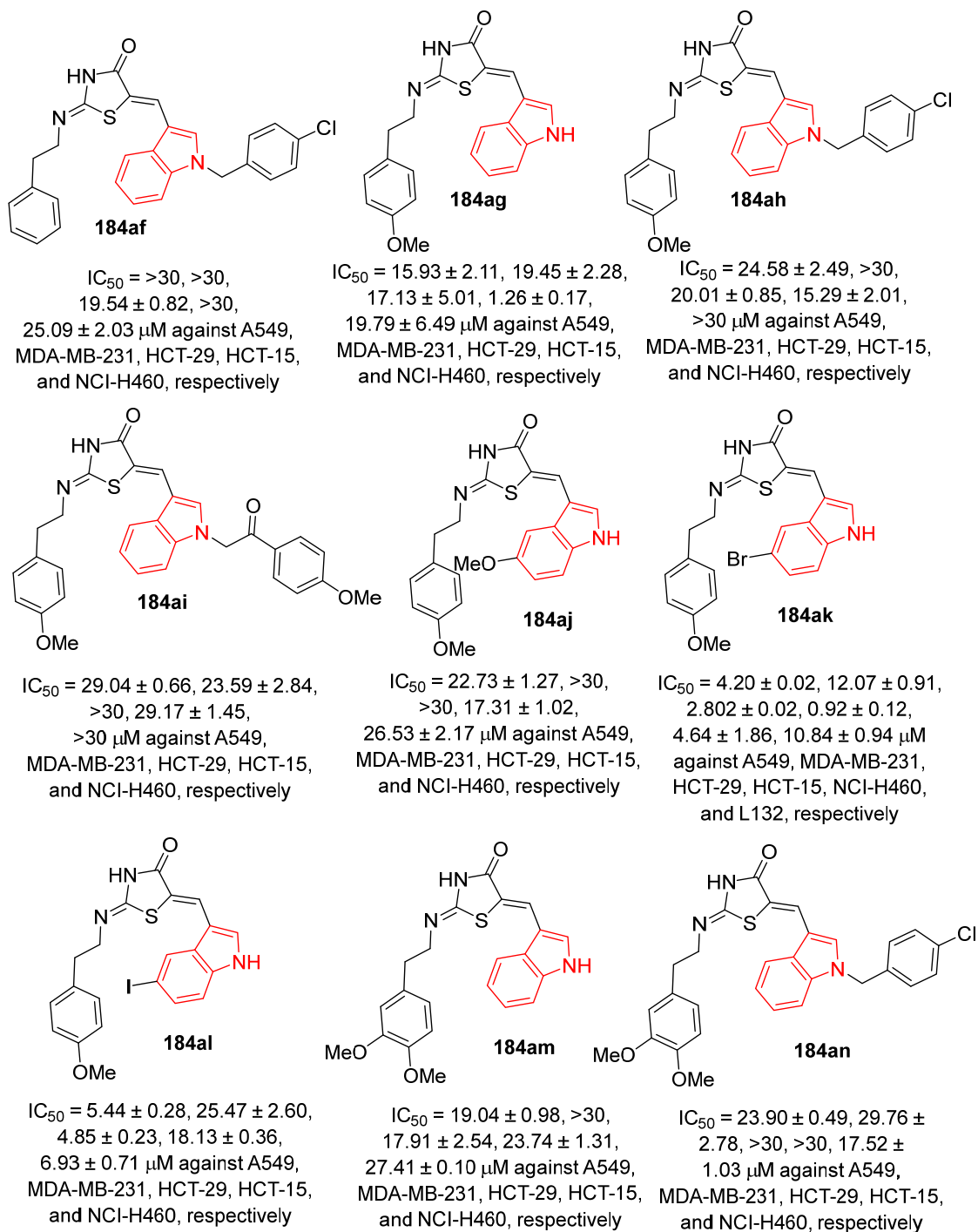
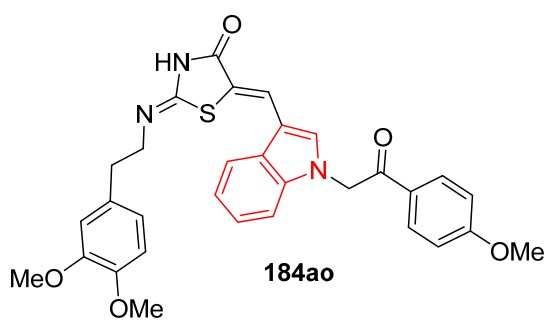
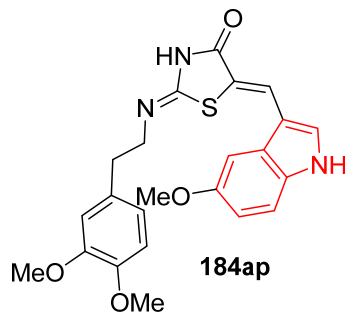


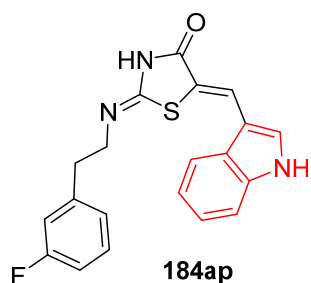
Fig. S31 (continued). Antiproliferation properties of thiazolidinone-indoles **184** and Podophyllotoxin.



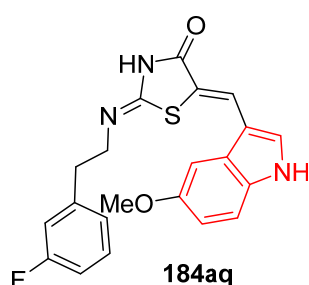
$IC_{50} = 29.05 \pm 0.11, >30,$
 $24.85 \pm 1.38, >30, 16.52 \pm$
 $0.94 \mu\text{M}$ against A549,
 MDA-MB-231, HCT-29, HCT-15,
 and NCI-H460, respectively



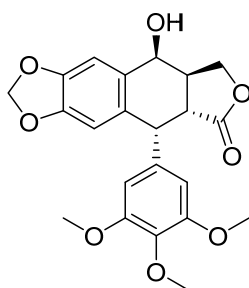
$IC_{50} = 15.09 \pm 2.74, >30,$
 $21.03 \pm 2.31, >30, 23.18 \pm$
 $0.51 \mu\text{M}$ against A549,
 MDA-MB-231, HCT-29, HCT-15,
 and NCI-H460, respectively



$IC_{50} = >30, 27.83 \pm 2.61,$
 $>30, 26.40 \pm 2.80, >30$
 μM against A549, MDA-MB-231,
 HCT-29, HCT-15, and
 NCI-H460, respectively

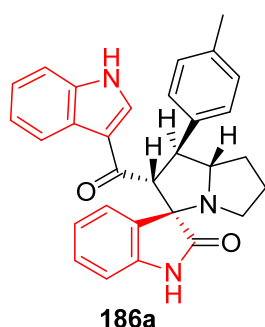


$IC_{50} = 29.01 \pm 2.13, >30,$
 $25.94 \pm 1.37, 17.13 \pm 2.50, 20.09$
 $\pm 0.57 \mu\text{M}$ against A549,
 MDA-MB-231, HCT-29,
 HCT-15, and NCI-H460,
 respectively

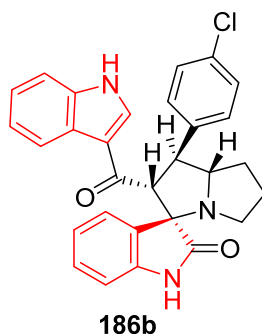


$IC_{50} = 0.027 \pm 0.25, 0.014 \pm 1.21,$
 $0.08 \pm 0.24, 0.029 \pm 0.98,$
 $0.037 \pm 2.54, 0.021 \pm 1.78 \text{ mM}$
 against A549, MDA-MB-231,
 HCT-29, HCT-15, NCI-H460,
 and L132, respectively

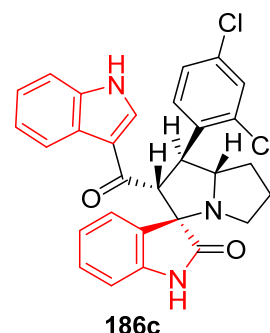
Fig. S31 (continued). Antiproliferation properties of thiazolidinone-indoles **184** and Podophyllotoxin.



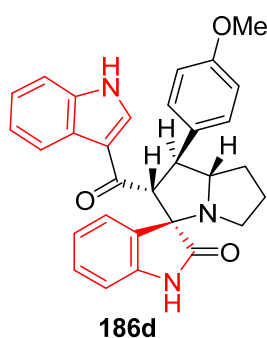
$IC_{50} = 21 \pm 2, 11.8 \pm 2, 16.3 \pm 2, 26 \mu\text{M}$ against HCT-116, HepG2, PC-3 and VERO-B, respectively



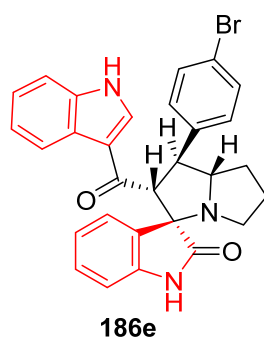
$IC_{50} = 20 \pm 1.5, 8 \pm 0.5, 11.8 \pm 1.3, 22 \mu\text{M}$ against HCT-116, HepG2, PC-3 and VERO-B, respectively



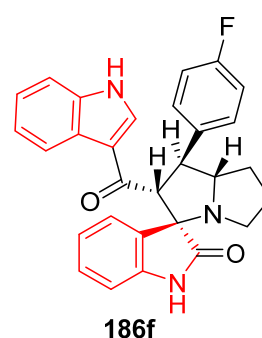
$IC_{50} = 9 \pm 0.6, 2 \pm 0.1, 2 \pm 0.125, 9 \mu\text{M}$ against HCT-116, HepG2, PC-3 and VERO-B, respectively



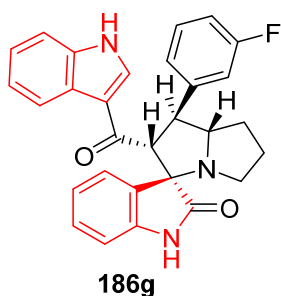
$IC_{50} = 26 \pm 2, 17.3 \pm 3, 15.5 \pm 2, 26 \mu\text{M}$ against HCT-116, HepG2, PC-3 and VERO-B, respectively



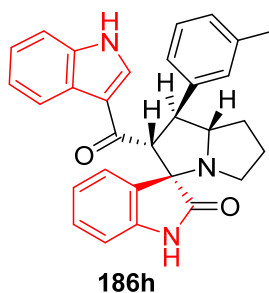
$IC_{50} = 21 \pm 1.3, 12 \pm 1.5, 16.3 \pm 2.5, 30 \mu\text{M}$ against HCT-116, HepG2, PC-3 and VERO-B, respectively



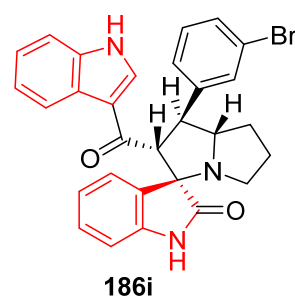
$IC_{50} = 16 \pm 1, 20 \pm 2, 16.3 \pm 30, 40 \mu\text{M}$ against HCT-116, HepG2, PC-3 and VERO-B, respectively



$IC_{50} = 15 \pm 1.4, 14 \pm 0.22, 11.5 \pm 11.5, 18 \mu\text{M}$ against HCT-116, HepG2, PC-3 and VERO-B, respectively

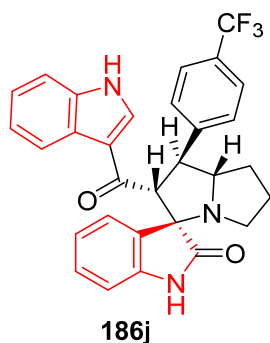


$IC_{50} = 7 \pm 0.2, 7 \pm 0.40, 7 \pm 0.6, 15 \mu\text{M}$ against HCT-116, HepG2, PC-3 and VERO-B, respectively

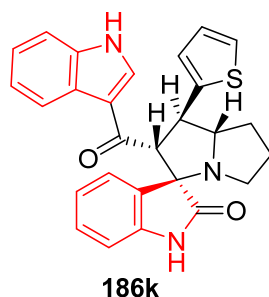


$IC_{50} = 9 \pm 0.5, 8 \pm 1, 7 \pm 0.2, 20 \mu\text{M}$ against HCT-116, HepG2, PC-3 and VERO-B, respectively

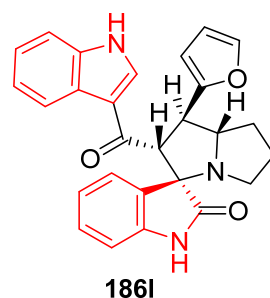
Fig. S32. Antiproliferation properties of spiro[indoline-3,3'-pyrrolizin]-2-ones **186** and cisplatin against HCT-116, HepG2, PC-3 (cancer) and VERO-B (normal) cell lines.



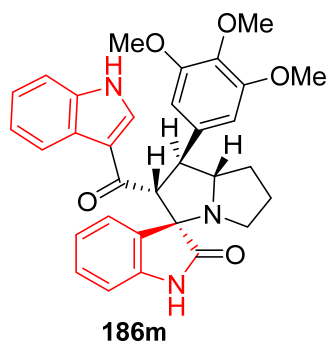
$IC_{50} = 9 \pm 0.5, 10 \pm 1.25, 9 \pm 0.2, 22 \mu\text{M}$ against HCT-116, HepG2, PC-3 and VERO-B, respectively



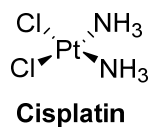
$IC_{50} = 50 \pm 3.5, 50 \pm 3, 29 \pm 3, 60 \mu\text{M}$ against HCT-116, HepG2, PC-3 and VERO-B, respectively



$IC_{50} = 29 \pm 2, 40 \pm 5, 26 \pm 1.7, 50 \mu\text{M}$ against HCT-116, HepG2, PC-3 and VERO-B, respectively



$IC_{50} = 20 \pm 1.25, 28 \pm 2, 17 \pm 2, 40 \mu\text{M}$ against HCT-116, HepG2, PC-3 and VERO-B, respectively



$IC_{50} = 12.6 \pm 0.40, 5.5 \pm 1.5, 5 \pm 0.45, 5 \mu\text{M}$ against HCT-116, HepG2, PC-3 and VERO-B, respectively

Fig. S32 (continued). Antiproliferation properties of spiro[indoline-3,3'-pyrrolizin]-2-ones **186** and cisplatin against HCT-116, HepG2, PC-3 (cancer) and VERO-B (normal) cell lines.

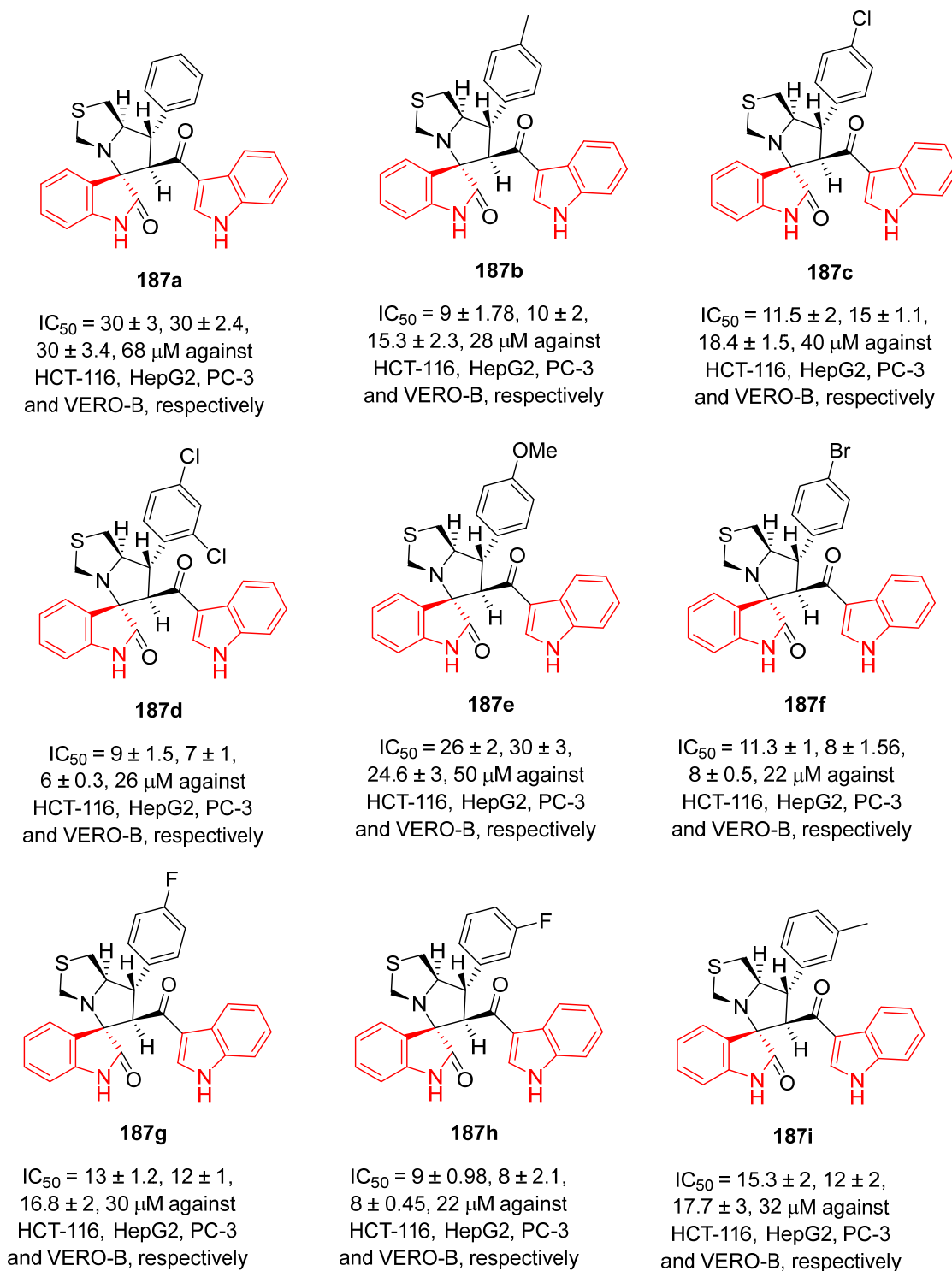
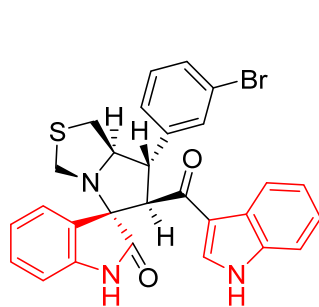
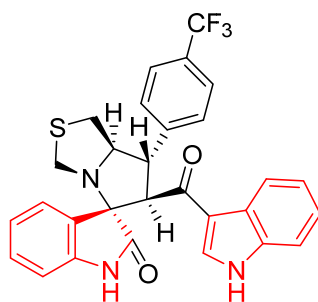


Fig. S33. Antiproliferation properties of spiroindoles **187** and Cisplatin against HCT-116, HepG2, PC-3 (cancer) and VERO-B (normal) cell lines.



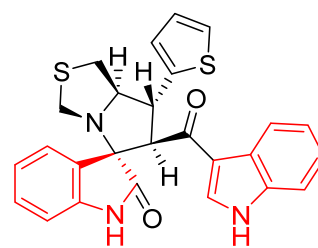
187j

$IC_{50} = 9 \pm 1, 7 \pm 1.5, 7 \pm 0.15, 20 \mu M$ against HCT-116, HepG2, PC-3 and VERO-B, respectively



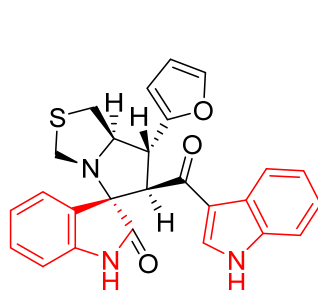
187k

$IC_{50} = 7 \pm 0.27, 5.5 \pm 0.2, 6 \pm 0.23, 26 \mu M$ against HCT-116, HepG2, PC-3 and VERO-B, respectively



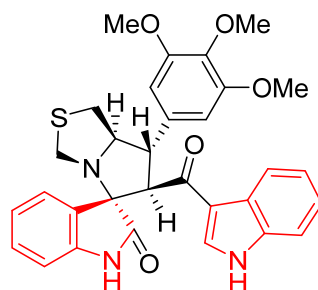
187l

$IC_{50} = 90 \pm 8, 35 \pm 4, 25 \pm 2.9, 40 \mu M$ against HCT-116, HepG2, PC-3 and VERO-B, respectively



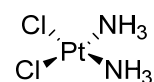
187m

$IC_{50} = 40 \pm 5, 30 \pm 2, 18.5 \pm 1.86, 33 \mu M$ against HCT-116, HepG2, PC-3 and VERO-B, respectively



187n

$IC_{50} = >40 \pm 3, 35 \pm 3, 18.5 \pm 2, 42 \mu M$ against HCT-116, HepG2, PC-3 and VERO-B, respectively



Cisplatin

$IC_{50} = 12.6 \pm 0.5, 5.5 \pm 0.3, 5 \pm 0.56, 5 \mu M$ against HCT-116, HepG2, PC-3 and VERO-B, respectively

Fig. S33 (continued). Antiproliferation properties of spiroindoles **187** and Cisplatin against HCT-116, HepG2, PC-3 (cancer) and VERO-B (normal) cell lines.

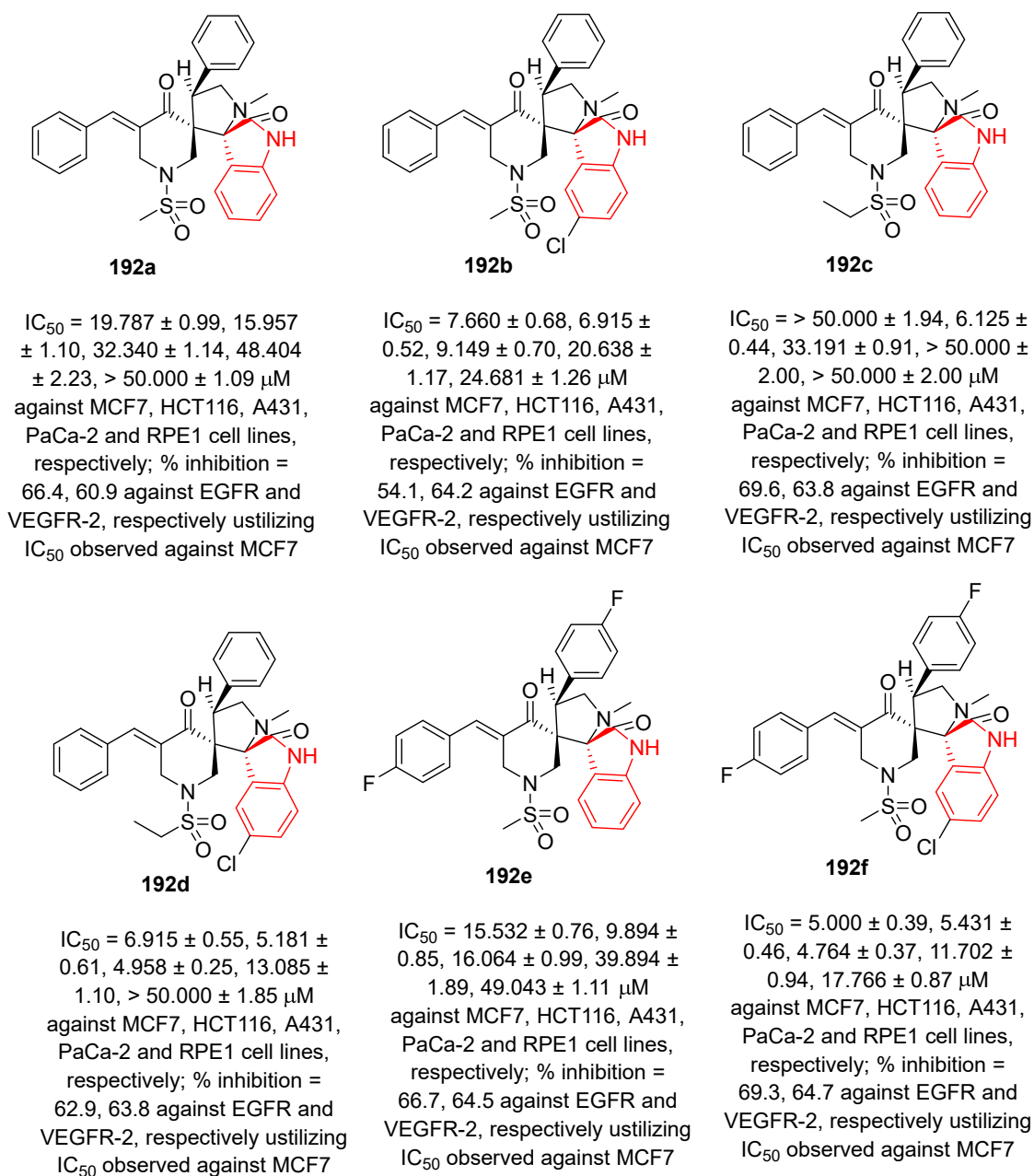
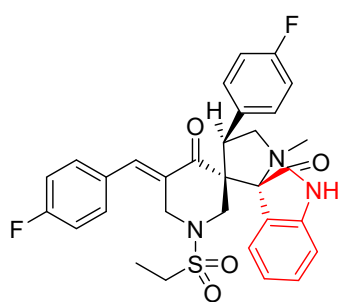
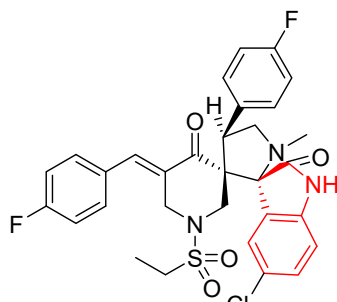


Fig. S34. Antiproliferation (IC₅₀, μM ± SEM against the tested cell lines), and % inhibitory properties against EGFR and VEGFR-2 utilizing IC₅₀ observed against MCF7 for the tested spiroindoles **192** and standard drugs (5-Fluorouracil and Sunitinib).



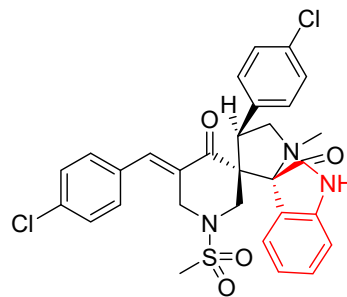
192g

$IC_{50} = 10.319 \pm 0.86, 4.944 \pm 0.25, 6.167 \pm 0.44, 28.404 \pm 0.85, 33.404 \pm 1.22 \mu M$
against MCF7, HCT116, A431, PaCa-2 and RPE1 cell lines, respectively; % inhibition = 62.8, 63.7 against EGFR and VEGFR-2, respectively utilizing IC_{50} observed against MCF7



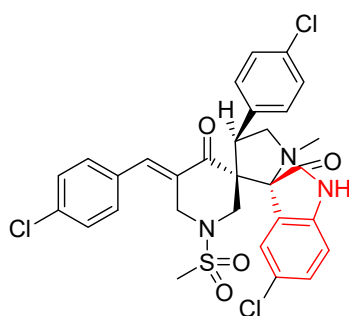
192h

$IC_{50} = 4.694 \pm 0.44, 4.597 \pm 0.18, 6.042 \pm 0.26, 14.043 \pm 0.73, > 50.000 \pm 2.38 \mu M$
against MCF7, HCT116, A431, PaCa-2 and RPE1 cell lines, respectively; % inhibition = 67.2, 66.2 against EGFR and VEGFR-2, respectively utilizing IC_{50} observed against MCF7



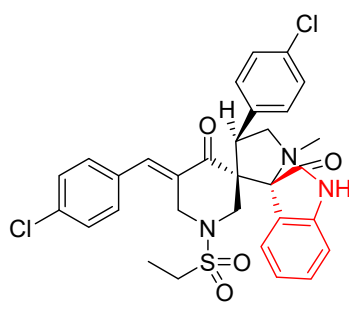
192i

$IC_{50} = 5.014 \pm 0.29, 5.472 \pm 0.32, 4.403 \pm 0.49, 9.043 \pm 0.62, 14.787 \pm 1.57 \mu M$
against MCF7, HCT116, A431, PaCa-2 and RPE1 cell lines, respectively; % inhibition = 68.7, 64.2 against EGFR and VEGFR-2, respectively utilizing IC_{50} observed against MCF7



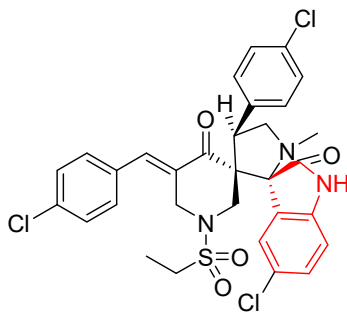
192j

$IC_{50} = 4.514 \pm 0.39, 4.722 \pm 0.25, 4.083 \pm 0.21, 8.830 \pm 0.51, 12.500 \pm 0.86 \mu M$
against MCF7, HCT116, A431, PaCa-2 and RPE1 cell lines, respectively; % inhibition = 63.3, 57.9 against EGFR and VEGFR-2, respectively utilizing IC_{50} observed against MCF7



192k

$IC_{50} = 4.375 \pm 0.26, 4.167 \pm 0.38, 2.966 \pm 0.29, 8.830 \pm 0.70, 14.792 \pm 0.99 \mu M$
against MCF7, HCT116, A431, PaCa-2 and RPE1 cell lines, respectively; % inhibition = 66.2, 66.2 against EGFR and VEGFR-2, respectively utilizing IC_{50} observed against MCF7



192l

$IC_{50} = 3.986 \pm 0.31, 4.111 \pm 0.41, 3.694 \pm 0.33, 11.915 \pm 0.83, > 50.000 \pm 2.32 \mu M$
against MCF7, HCT116, A431, PaCa-2 and RPE1 cell lines, respectively; % inhibition = 65.7, 60.2 against EGFR and VEGFR-2, respectively utilizing IC_{50} observed against MCF7

Fig. S34 (continued). Antiproliferation (IC_{50} , $\mu M \pm SEM$ against the tested cell lines), and % inhibitory properties against EGFR and VEGFR-2 utilizing IC_{50} observed against MCF7 for the tested spiroindoles **192** and standard drugs (5-Fluorouracil and Sunitinib).

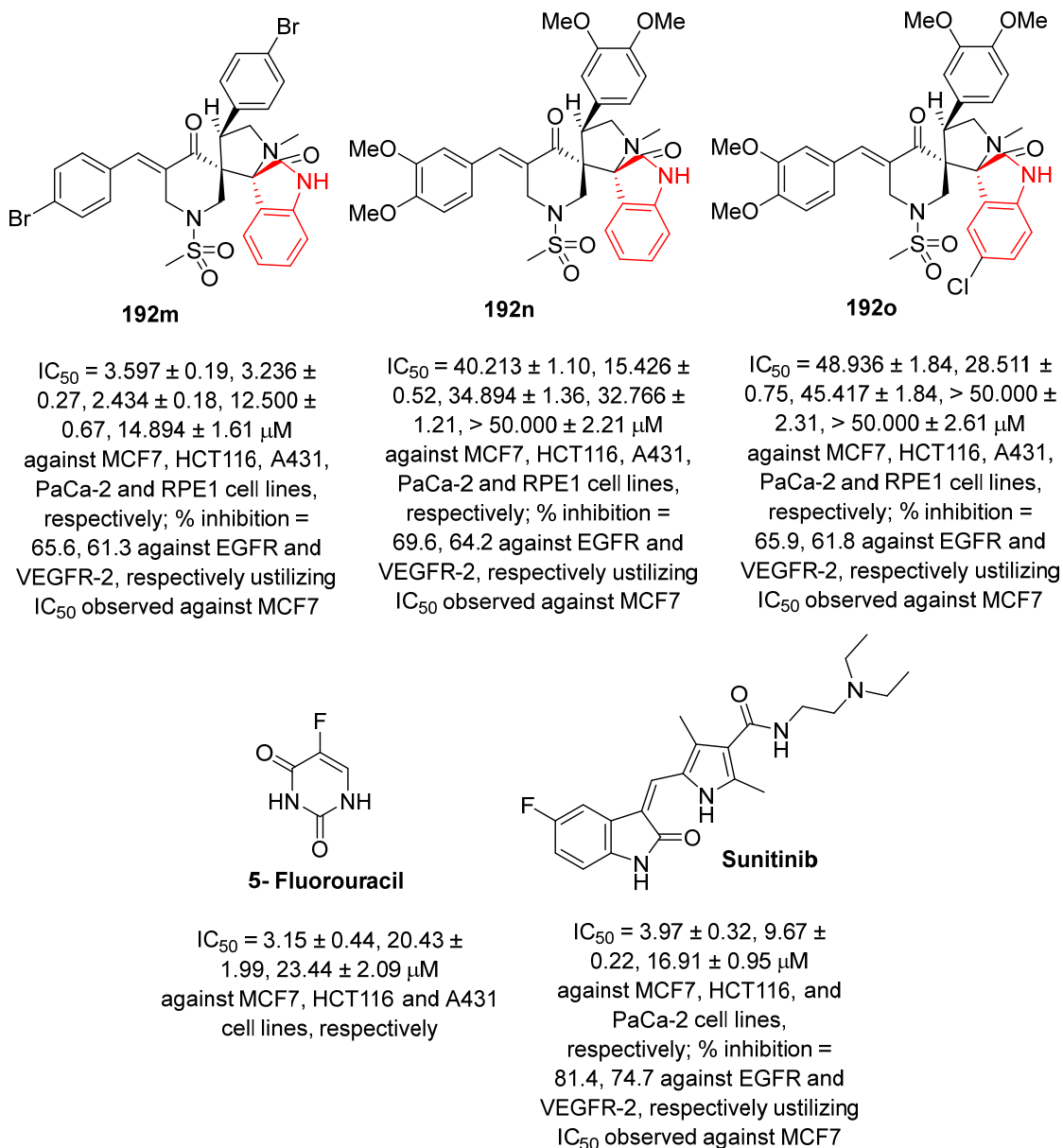
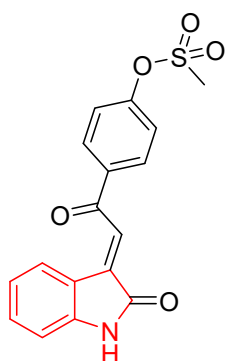
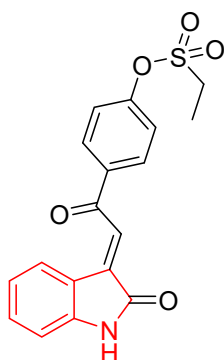


Fig. S34 (continued). Antiproliferation (IC₅₀, μM ± SEM against the tested cell lines), and % inhibitory properties against EGFR and VEGFR-2 utilizing IC₅₀ observed against MCF7 for the tested spiroindoles **192** and standard drugs (5-Fluorouracil and Sunitinib).



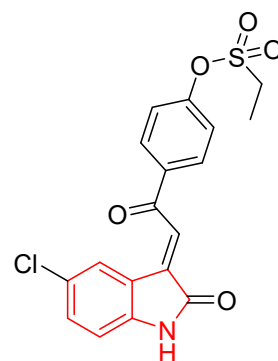
196a

$IC_{50} = 8.30 \pm 0.44$,
 6.85 ± 0.37 , 16.38
 $\pm 0.70 \mu M$ against
 PaCa-2, MCF7, and
 HCT116, respectively;
 $IC_{50} = 54.03 \pm 5.4$,
 119.8 ± 12.0 nM
 against VEGFR-2,
 and c-kit, respectively



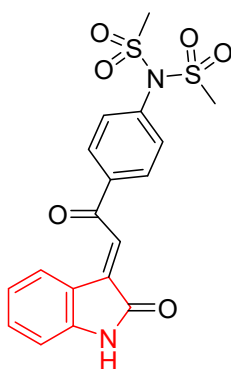
196b

$IC_{50} = 5.60 \pm 0.57$,
 4.25 ± 0.23 , 12.77
 $\pm 1.41 \mu M$ against
 PaCa-2, MCF7, and
 HCT116, respectively;
 $IC_{50} = 98.95 \pm 9.9$,
 247.7 ± 24.8 nM
 against VEGFR-2,
 and c-kit, respectively



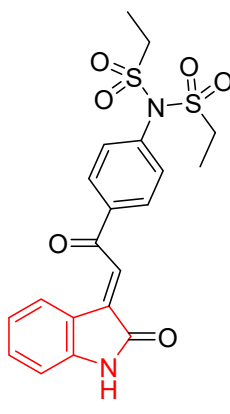
196c

$IC_{50} = 4.99 \pm 0.29$,
 4.28 ± 0.51 , 5.33
 $\pm 0.46 \mu M$ against
 PaCa-2, MCF7, and
 HCT116, respectively;
 $IC_{50} = 36.86 \pm 3.7$,
 72.35 ± 7.2 nM
 against VEGFR-2,
 and c-kit, respectively



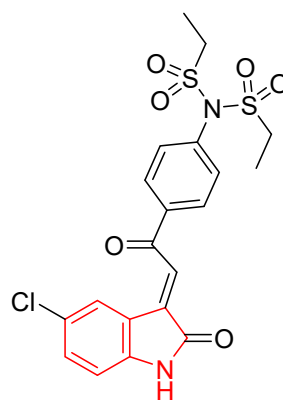
200a

$IC_{50} = 6.91 \pm 0.89$,
 6.07 ± 0.83 , 20.96
 $\pm 1.75 \mu M$ against
 PaCa-2, MCF7, and
 HCT116, respectively;
 $IC_{50} = 102.2 \pm 10.2$,
 103.3 ± 10.3 nM
 against VEGFR-2,
 and c-kit, respectively



200b

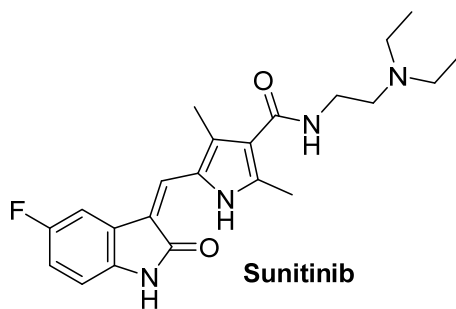
$IC_{50} = 5.08 \pm 0.57$,
 4.15 ± 0.78 , 13.83
 $\pm 1.06 \mu M$ against
 PaCa-2, MCF7, and
 HCT116, respectively;
 $IC_{50} = 74.06 \pm 7.4$,
 184.9 ± 18.5 nM
 against VEGFR-2,
 and c-kit, respectively



200c

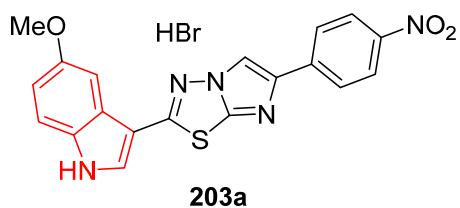
$IC_{50} = 6.18 \pm 0.32$,
 4.43 ± 0.47 , >50.00
 $\pm 0.84 \mu M$ against
 PaCa-2, MCF7, and
 HCT116, respectively;
 $IC_{50} = 53.36 \pm 5.3$,
 81.7 ± 8.2 nM
 against VEGFR-2,
 and c-kit, respectively

Fig. S35. Antiproliferation (IC_{50} , $\mu M \pm SE$ "standard error") and enzymatic inhibitory properties (IC_{50} , $\mu M \pm SD$) of 3-alkenyl-2-oxindoles **196**, **200** and Sunitinib.

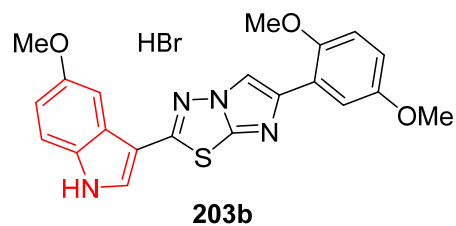


$IC_{50} = 16.91 \pm 0.95, 3.97$
 $\pm 0.14, 5.03 \pm 0.30 \mu M$
 against PaCa-2, MCF7,
 and HCT116, respectively;
 $IC_{50} = 47.54 \pm 4.8, 84.9 \pm 8.5$
 nM against VEGFR-2,
 and c-kit, respectively

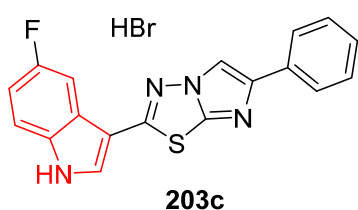
Fig. S35 (continued). Antiproliferation (IC_{50} , $\mu M \pm SE$ "standard error") and enzymatic inhibitory properties (IC_{50} , $\mu M \pm SD$) of 3-alkenyl-2-oxindoles **196**, **200** and Sunitinib.



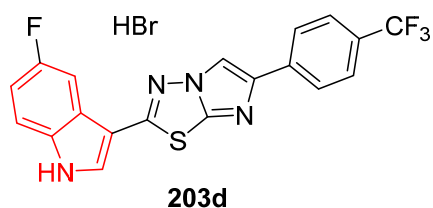
$IC_{50} = 5.5 \pm 0.19, 5.11 \pm 0.29,$
 $5.18 \pm 0.12 \mu\text{M}$ against SUI-2,
 Capan-1, and Panc-1, respectively



$IC_{50} = 10.26 \pm 0.20 \mu\text{M}$ against Panc-1



$IC_{50} = 10.4 \pm 0.07, 8.57 \pm 0.51,$
 $10.8 \pm 0.13 \mu\text{M}$ against SUI-2,
 Capan-1, and Panc-1, respectively



$IC_{50} = 11.8 \pm 0.54, 10.49 \pm 0.16$
 μM against SUI-2, and
 Capan-1, respectively

Fig. S36. Antiproliferation properties ($\mu\text{M} \pm \text{SEM}$) of indole linked to imidazo[2,1-*b*][1,3,4]thiadiazoles **203**.

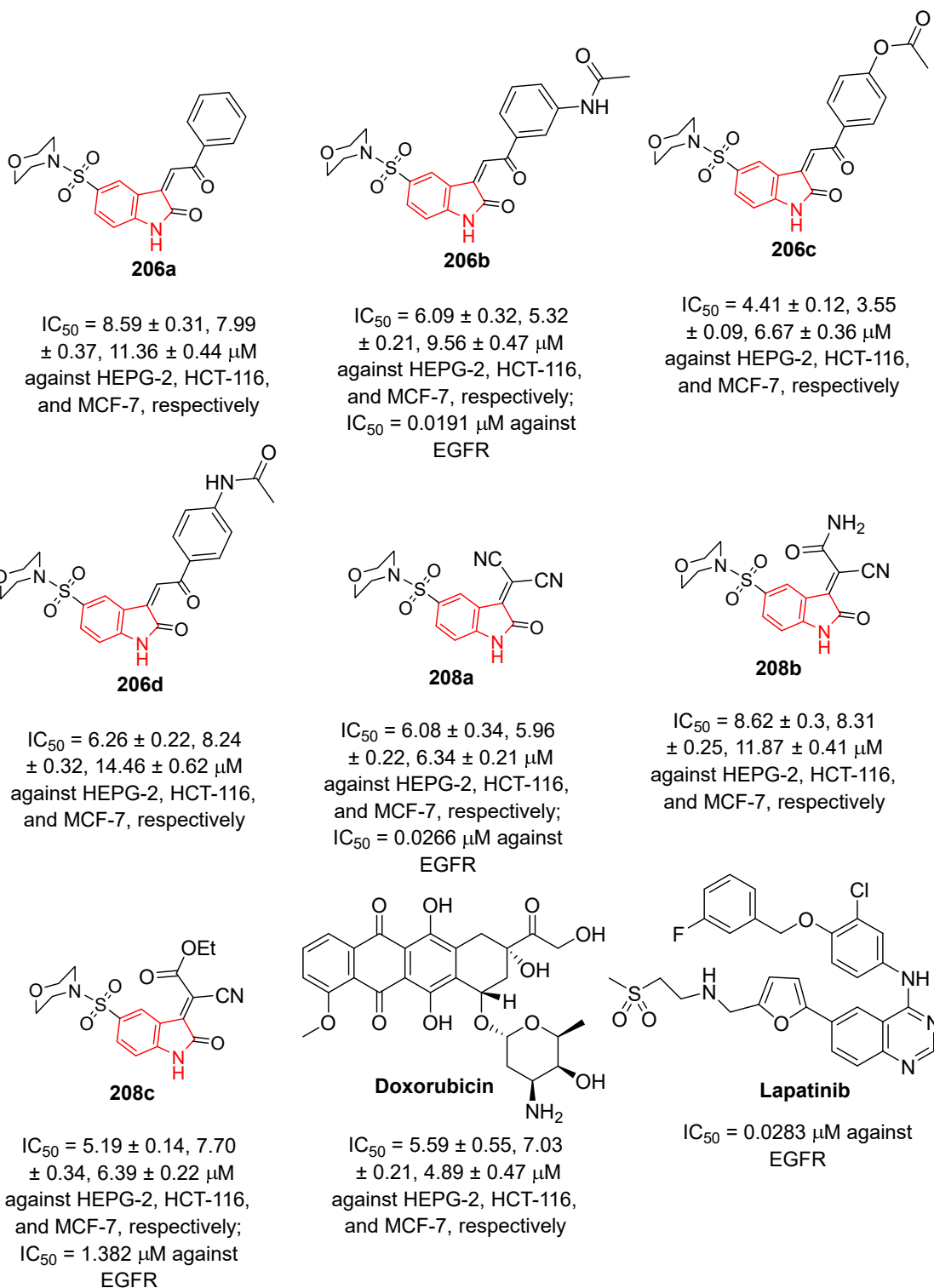


Fig. S37. Antiproliferation ($\mu M \pm SE$) and enzymatic inhibitory properties against EGFR of 5-(morpholinosulfonyl)-2-indolinones **206**, 3-ylidene-2-indolinones **208** and standard references (Doxorubicin and Lapatinib).

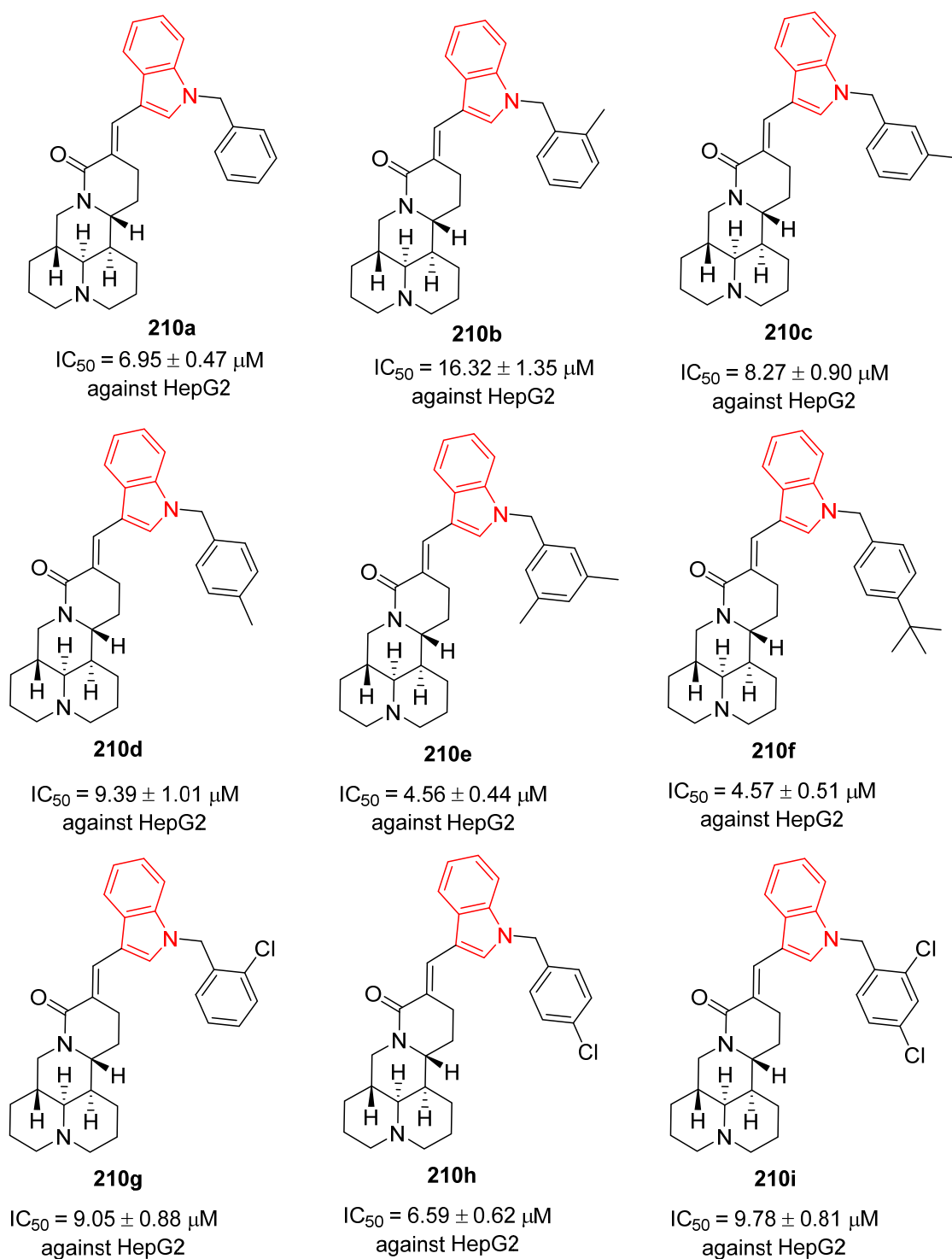


Fig. S38. Antiproliferation properties ($\mu M \pm SD$) of the synthesized sophoridine-indole conjugates **210**, Sophoridine **209** and Camptothecin (standard reference).

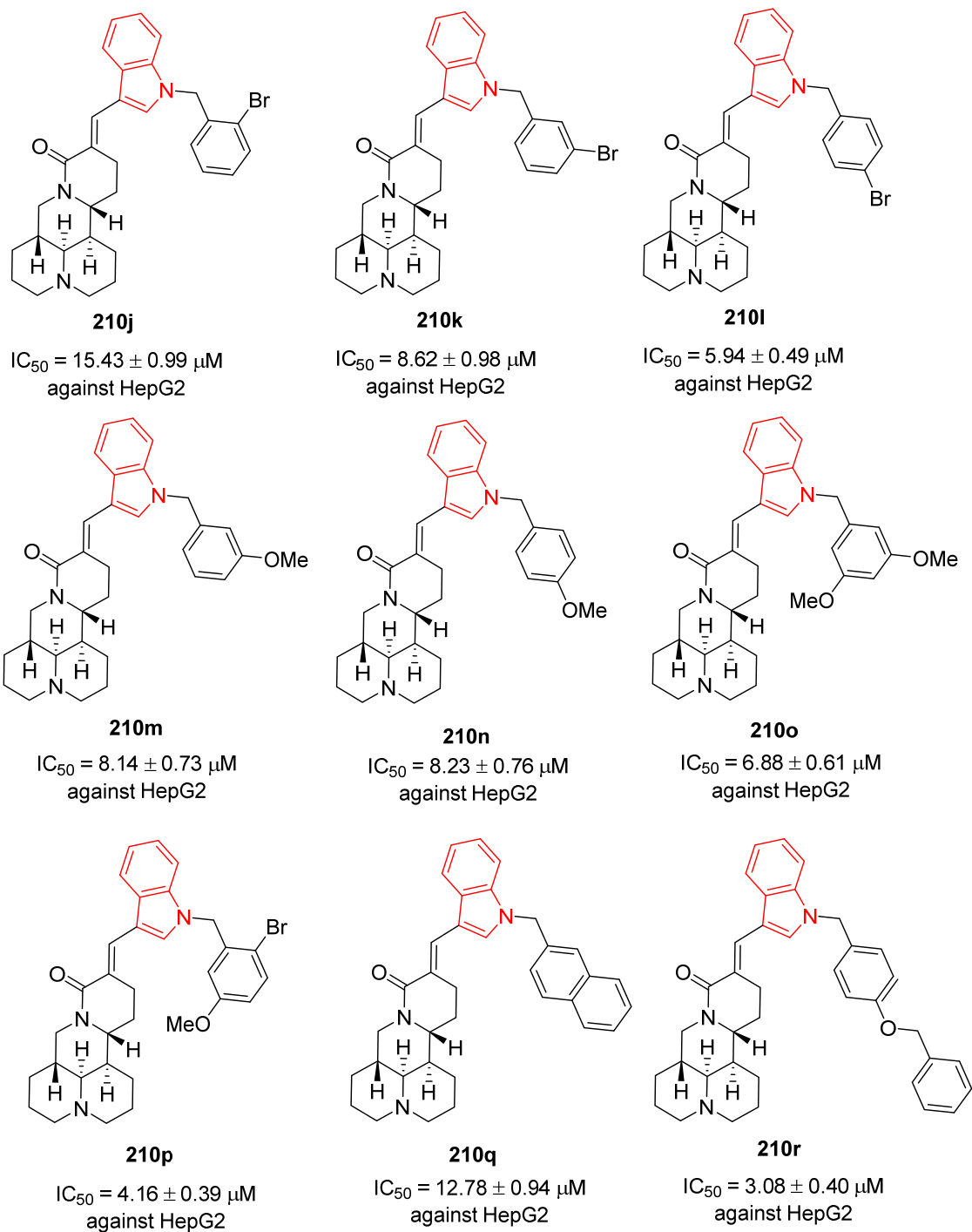


Fig. S38 (continued). Antiproliferation properties ($\mu M \pm SD$) of the synthesized sophoridine-indole conjugates **210**, Sophoridine **209** and Camptothecin (standard reference).

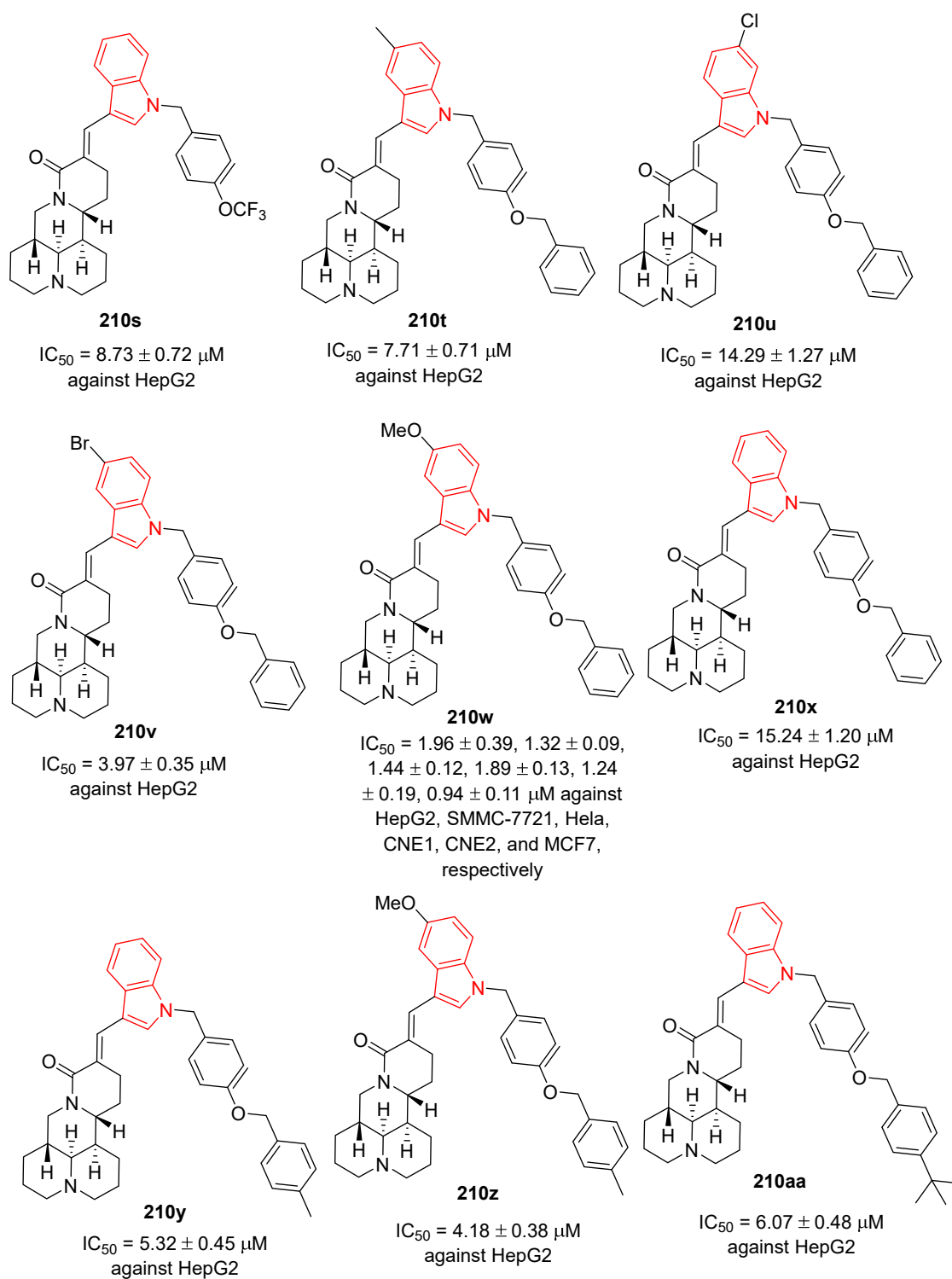


Fig. S38 (continued). Antiproliferation properties ($\mu M \pm SD$) of the synthesized sophoridine-indole conjugates **210**, Sophoridine **209** and Camptothecin (standard reference).

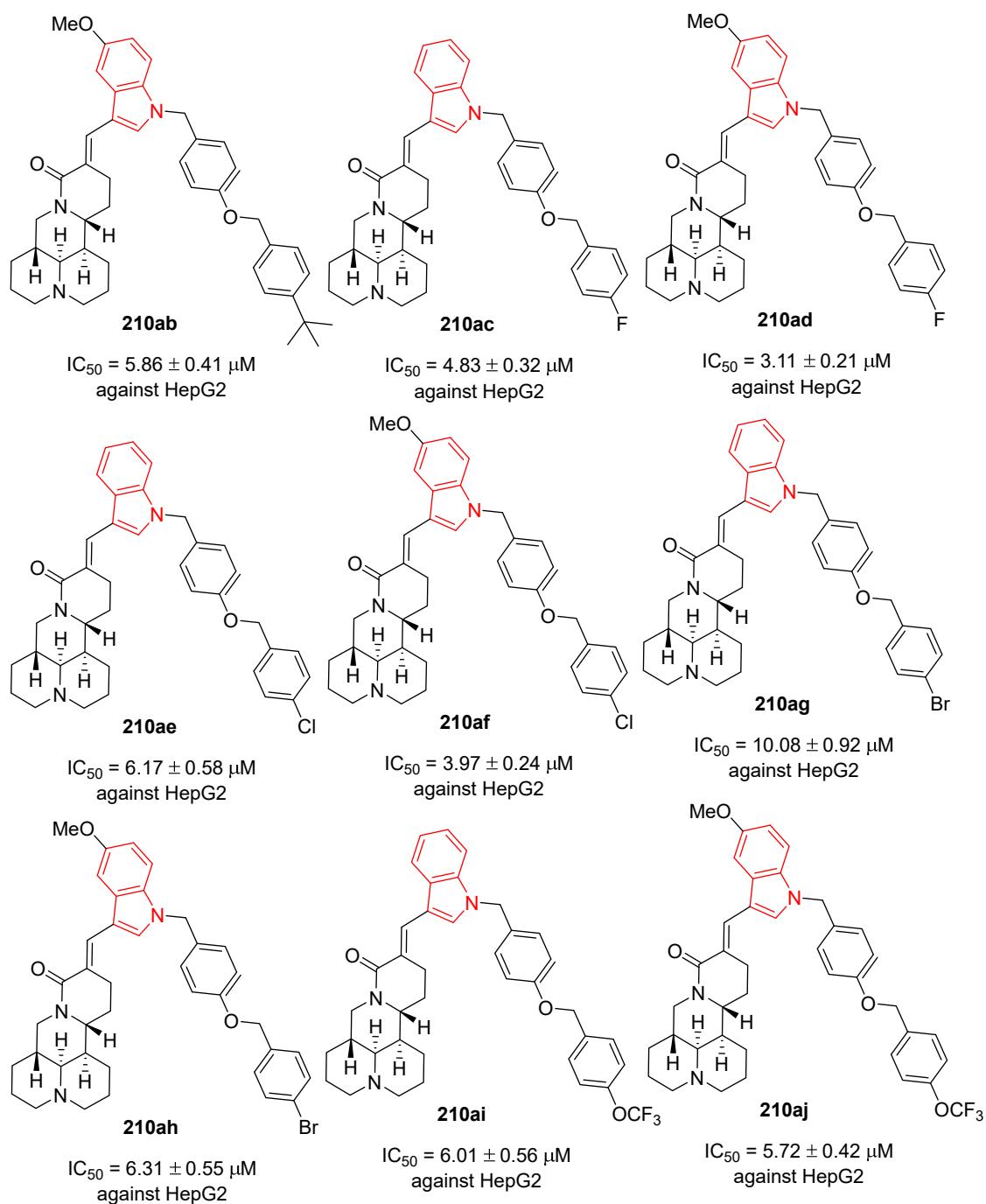
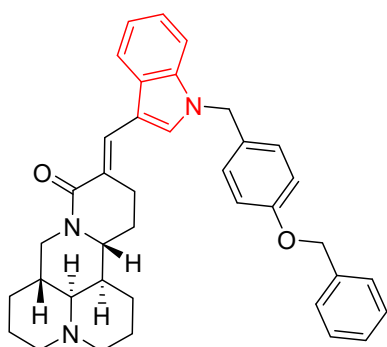
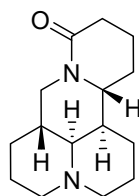


Fig. S38 (continued). Antiproliferation properties ($\mu\text{M} \pm \text{SD}$) of the synthesized sophoridine-indole conjugates **210**, Sophoridine **209** and Camptothecin (standard reference).



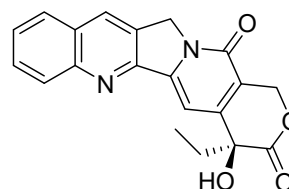
210k

$IC_{50} = 9.96 \pm 0.78 \mu M$
against HepG2



209 (Sophoridine)

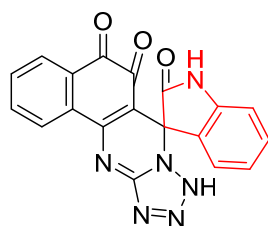
$IC_{50} = 4670 \pm 127 \mu M$
against HepG2



Camptothecin

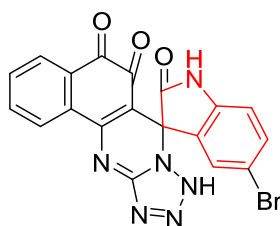
$IC_{50} = 1.36 \pm 0.17, 1.08 \pm 0.13,$
 $0.66 \pm 0.18, 0.34 \pm 0.07, 0.98$
 $\pm 0.11, 0.42 \pm 0.08 \mu M$ against
HepG2, SMMC-7721, Hela,
CNE1, CNE2, and MCF7,
respectively

Fig. S38 (continued). Antiproliferation properties ($\mu M \pm SD$) of the synthesized sophoridine-indole conjugates **210**, Sophoridine **209** and Camptothecin (standard reference).



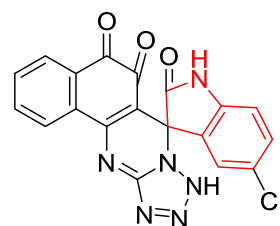
213a

IC_{50} = 23.63, 40.15 μ M
against HepG2 and
LO2, respectively



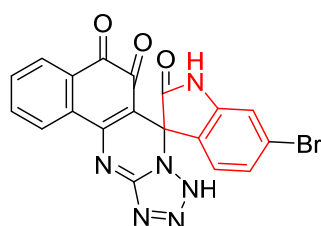
213b

IC_{50} = 23.41, 65.29 μ M
against HepG2 and
LO2, respectively



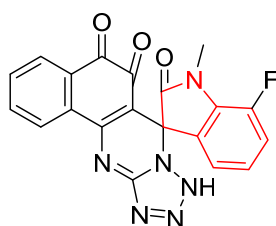
213c

IC_{50} = 21.93, 53.03 μ M
against HepG2 and
LO2, respectively



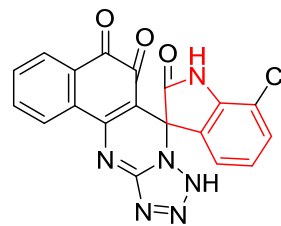
213d

IC_{50} = 36.34, 248.39 μ M
against HepG2 and
LO2, respectively



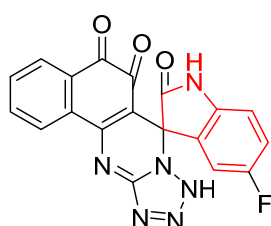
213e

IC_{50} = 31.83, 54 μ M
against HepG2 and
LO2, respectively



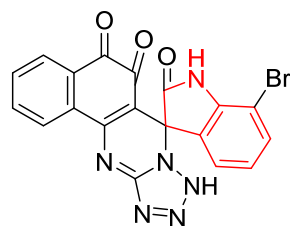
213f

IC_{50} = 3.03, 49.47 μ M
against HepG2 and
LO2, respectively



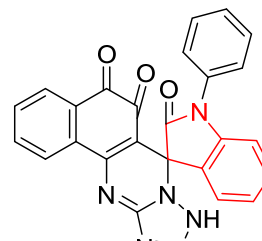
213g

IC_{50} = 2.86, 58.92 μ M
against HepG2 and
LO2, respectively



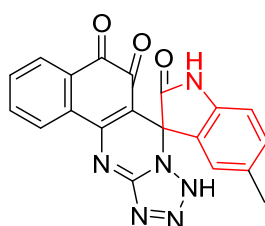
213h

IC_{50} = 20.74, 82.34 μ M
against HepG2 and
LO2, respectively



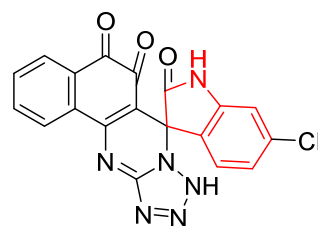
213i

IC_{50} = 27.87, 75.57 μ M
against HepG2 and
LO2, respectively



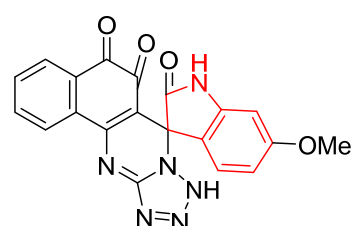
213j

IC_{50} = 12.58, 36.37 μ M
against HepG2 and
LO2, respectively



213k

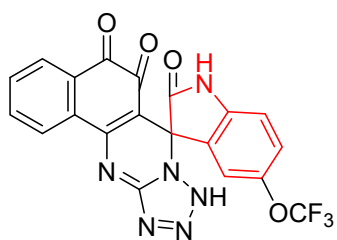
IC_{50} = 21.19, 51.99 μ M
against HepG2 and
LO2, respectively



213l

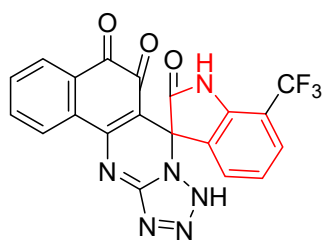
IC_{50} = 17.29, 78.6 μ M
against HepG2 and
LO2, respectively

Fig. S39. Antiproliferation properties of spirooxindoles **213** and Tanshinon IIA (TSA).



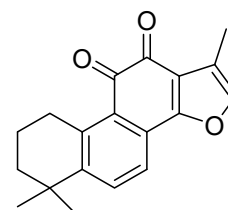
213m

IC₅₀ = 18.29, 48.42 μM
against HepG2 and
LO2, respectively



213n

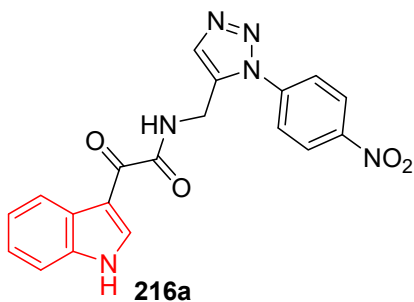
IC₅₀ = 7.9, 49.9 μM
against HepG2 and
LO2, respectively



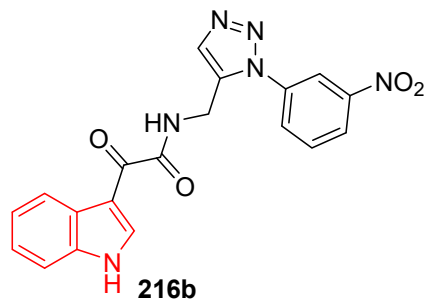
Tanshinon IIA (TSA)

IC₅₀ = 23.85, 65.29 μM
against HepG2 and
LO2, respectively

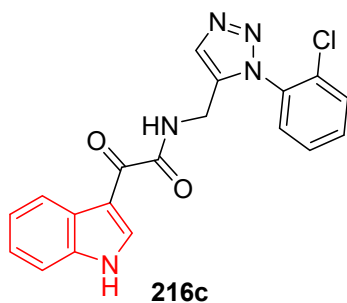
Fig. S39 (continued). Antiproliferation properties of spirooxindoles **213** and Tanshinon IIA (TSA).



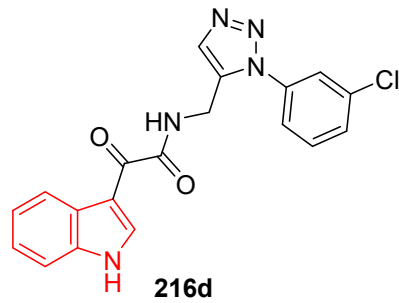
IC₅₀ = >100, >100, >100 μM against SKOV3, DU145, HELA, respectively;
IC₅₀ = 2.03, 0.85, 7.85 μM against COX-1, COX-2, 5-LOX, respectively



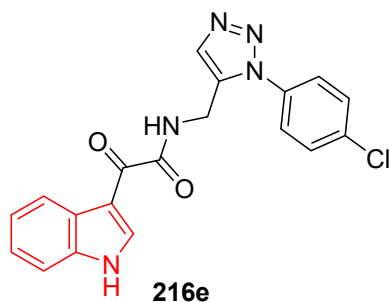
IC₅₀ = >100, >100, >100 μM against SKOV3, DU145, HELA, respectively;
IC₅₀ = 2.43, 0.65, 6.85 μM against COX-1, COX-2, 5-LOX, respectively



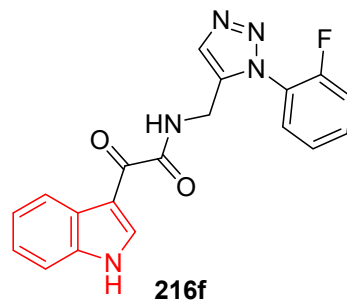
IC₅₀ = >100, >100, >100 μM against SKOV3, DU145, HELA, respectively;
IC₅₀ = 2.23, 0.35, 8.48 μM against COX-1, COX-2, 5-LOX, respectively



IC₅₀ = 22.8, >100, >100 μM against SKOV3, DU145, HELA, respectively;
IC₅₀ = 2.14, 0.18, 7.42 μM against COX-1, COX-2, 5-LOX, respectively

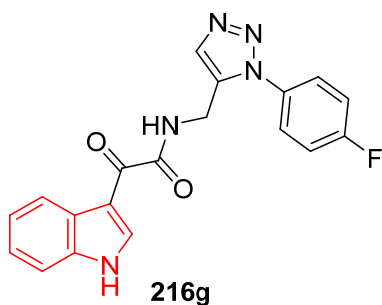


IC₅₀ = 12.70, >100, >100 μM against SKOV3, DU145, HELA, respectively;
IC₅₀ = 2.02, 0.99, 8.62 μM against COX-1, COX-2, 5-LOX, respectively

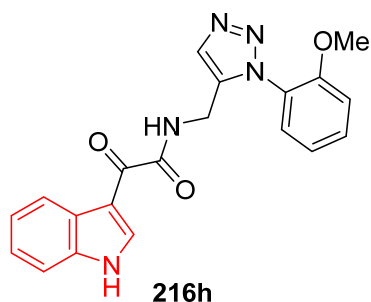


IC₅₀ = >100, >100, >100 μM against SKOV3, DU145, HELA, respectively;
IC₅₀ = 2.23, 0.35, 9.48 μM against COX-1, COX-2, 5-LOX, respectively

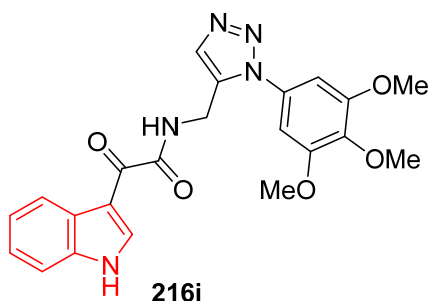
Fig. S40. Antiproliferation and enzymation inhibitory properties of indole-triazole conjugates **216**, Etoposide, Indomethacin, Celecoxib, and Norhiydroguaiaretic acid (ND = not done).



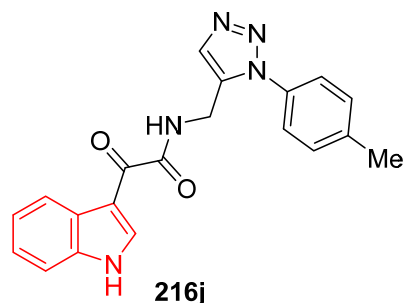
IC₅₀ = >100, 8.69, >100 μM against SKOV3, DU145, HELA, respectively;
 IC₅₀ = 2.14, 1.99, 8.62 μM against COX-1, COX-2, 5-LOX, respectively



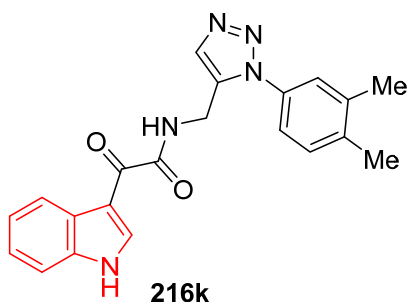
IC₅₀ = >100, 28.65, >100 μM against SKOV3, DU145, HELA, respectively;
 IC₅₀ = 3.01, 1.84, 9.54 μM against COX-1, COX-2, 5-LOX, respectively



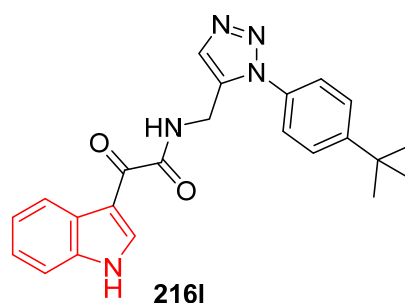
IC₅₀ = 11.91, 39.57, >100 μM against SKOV3, DU145, HELA, respectively;
 IC₅₀ = 2.44, 1.76, 7.83 μM against COX-1, COX-2, 5-LOX, respectively



IC₅₀ = >100, >100, >100 μM against SKOV3, DU145, HELA, respectively;
 IC₅₀ = 2.48, 0.33, 7.93 μM against COX-1, COX-2, 5-LOX, respectively

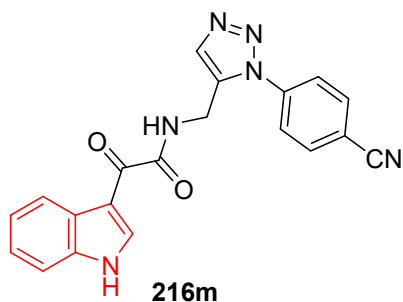


IC₅₀ = >100, >100, 6.29 μM against SKOV3, DU145, HELA, respectively;
 IC₅₀ = 3.02, 1.68, 8.59 μM against COX-1, COX-2, 5-LOX, respectively

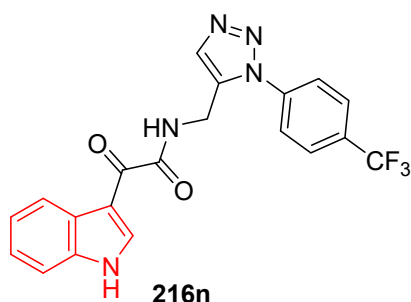


IC₅₀ = >100, >100, >100 μM against SKOV3, DU145, HELA, respectively;
 IC₅₀ = 2.24, 0.19, 7.51 μM against COX-1, COX-2, 5-LOX, respectively

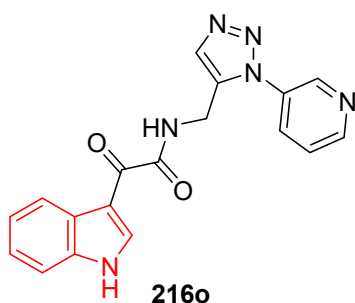
Fig. S40 (continued). Antiproliferation and enzymation inhibitory properties of indole-triazole conjugates **216**, Etoposide, Indomethacin, Celecoxib, and Norihydroguaiaretic acid (ND = not done).



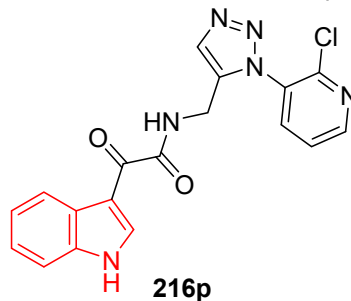
IC₅₀ = >100, >100, >100 μM against SKOV3, DU145, HELA, respectively;
IC₅₀ = 2.03, 0.159, 7.73 μM against COX-1, COX-2, 5-LOX, respectively



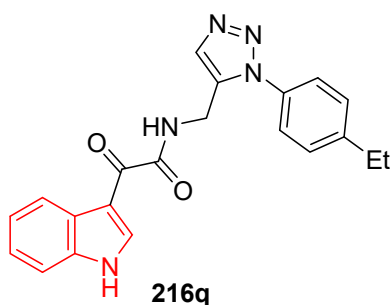
IC₅₀ = >100, 24.45, >100 μM against SKOV3, DU145, HELA, respectively;
IC₅₀ = 3.06, 2.95, 12.65 μM against COX-1, COX-2, 5-LOX, respectively



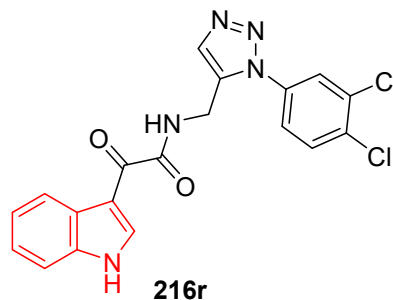
IC₅₀ = >100, 17.15, >100 μM against SKOV3, DU145, HELA, respectively;
IC₅₀ = 2.03, 0.48, 7.93 μM against COX-1, COX-2, 5-LOX, respectively



IC₅₀ = >100, >100, >300 μM against SKOV3, DU145, HELA, respectively;
IC₅₀ = 2.15, 0.85, 7.85 μM against COX-1, COX-2, 5-LOX, respectively

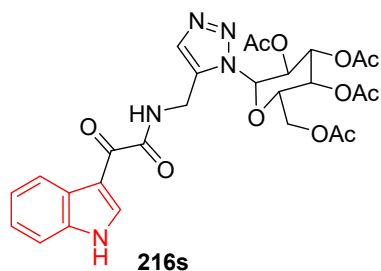


IC₅₀ = >100, 8.17, >100 μM against SKOV3, DU145, HELA, respectively;
IC₅₀ = 2.06, 0.12, 7.73 μM against COX-1, COX-2, 5-LOX, respectively

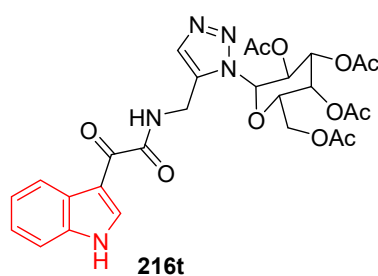


IC₅₀ = 12.63, 15.96, >100 μM against SKOV3, DU145, HELA, respectively;
IC₅₀ = 2.24, 0.16, 7.51 μM against COX-1, COX-2, 5-LOX, respectively

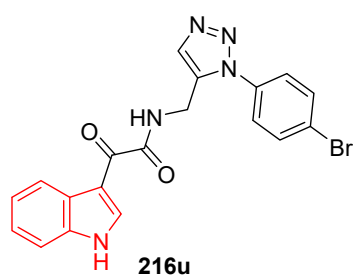
Fig. S40 (continued). Antiproliferation and enzymation inhibitory properties of indole-triazole conjugates **216**, Etoposide, Indomethacin, Celecoxib, and Norihydroguaiaretic acid (ND =not done).



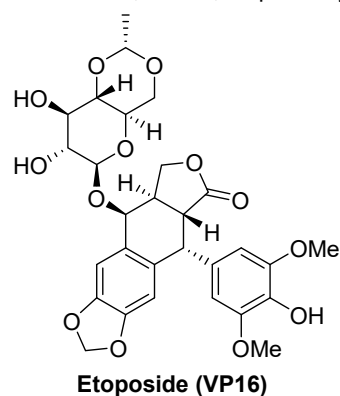
IC₅₀ = >100, >100, >100 μ M against SKOV3, DU145, HELA, respectively;
IC₅₀ = 2.15, 0.90, 8.62 μ M against COX-1, COX-2, 5-LOX, respectively



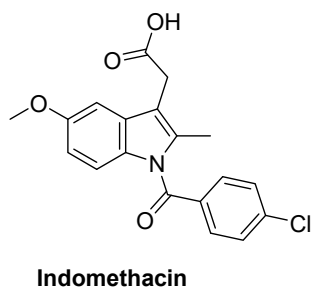
IC₅₀ = ND, ND, ND μ M against SKOV3, DU145, HELA, respectively;
IC₅₀ = 2.14, 1.88, 11.58 μ M against COX-1, COX-2, 5-LOX, respectively



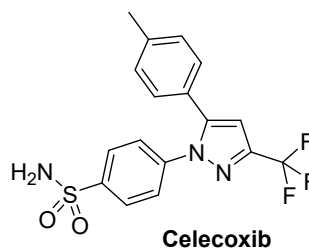
IC₅₀ = 63.42, >100, >100 μ M against SKOV3, DU145, HELA, respectively;
IC₅₀ = 2.13, 0.489, 11.36 μ M against COX-1, COX-2, 5-LOX, respectively



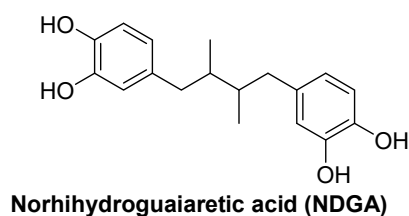
IC₅₀ = 2.39, 9.8, 7.43 μ M against SKOV3, DU145, HELA, respectively



IC₅₀ = 0.0068, 0.049 μ M against COX-1, COX-2, respectively

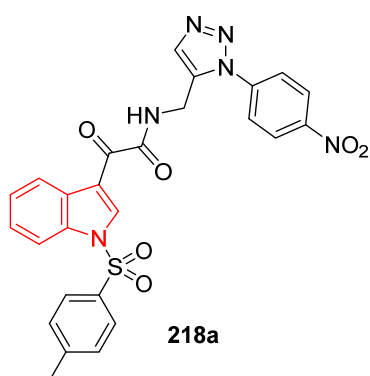


IC₅₀ = 14.8, 0.041 μ M against COX-1, COX-2, respectively

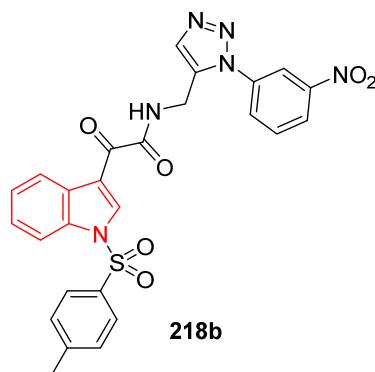


IC₅₀ = 7.31 μ M against 5-LOX

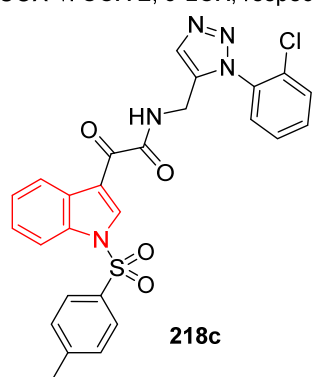
Fig. S40 (continued). Antiproliferation and enzymation inhibitory properties of indole-triazole conjugates **216**, Etoposide, Indomethacin, Celecoxib, and Norhihydroguaiaretic acid (ND = not done).



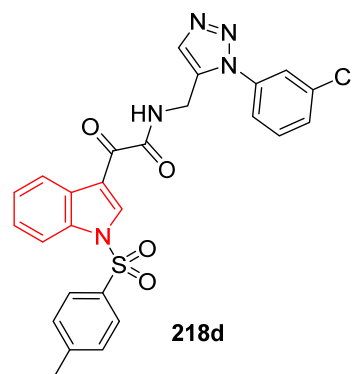
IC₅₀ = ND, ND, ND μ M against SKOV3, DU145, HELA, respectively;
IC₅₀ = 3.12, 0.66, 9.75 μ M against COX-1, COX-2, 5-LOX, respectively



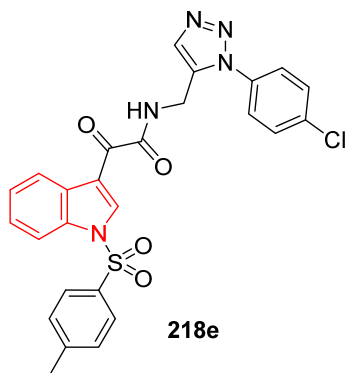
IC₅₀ = >100, 16.73, >100 μ M against SKOV3, DU145, HELA, respectively;
IC₅₀ = 2.28, 0.75, 11.43 μ M against COX-1, COX-2, 5-LOX, respectively



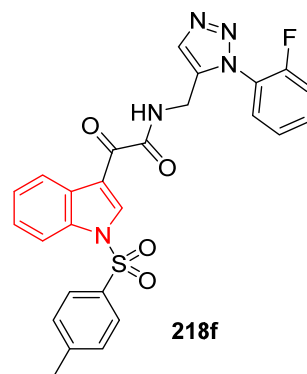
IC₅₀ = ND, ND, ND μ M against SKOV3, DU145, HELA, respectively;
IC₅₀ = 4.15, 1.85, 10.85 μ M against COX-1, COX-2, 5-LOX, respectively



IC₅₀ = >100, >100, >100 μ M against SKOV3, DU145, HELA, respectively;
IC₅₀ = 3.03, 0.85, 9.48 μ M against COX-1, COX-2, 5-LOX, respectively

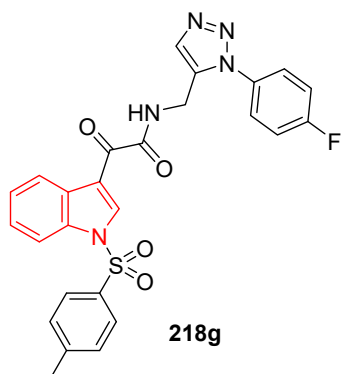


IC₅₀ = >100, >100, >100 μ M against SKOV3, DU145, HELA, respectively;
IC₅₀ = 2.14, 1.86, 10.62 μ M against COX-1, COX-2, 5-LOX, respectively

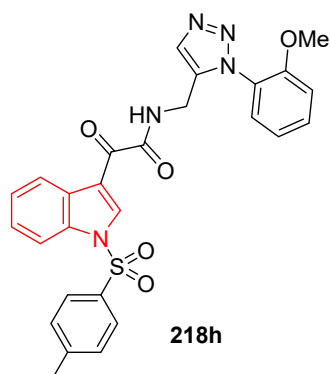


IC₅₀ = ND, ND, ND μ M against SKOV3, DU145, HELA, respectively;
IC₅₀ = 2.38, 0.97, 8.62 μ M against COX-1, COX-2, 5-LOX, respectively

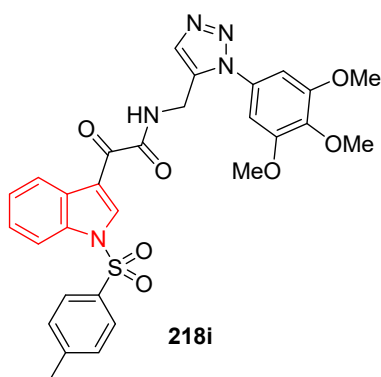
Fig. S41. Antiproliferation and enzymation inhibitory properties of indole-triazole conjugates **218**, Etoposide, Indomethacin, Celecoxib, and Norhiydroguaiaretic acid (ND = not done).



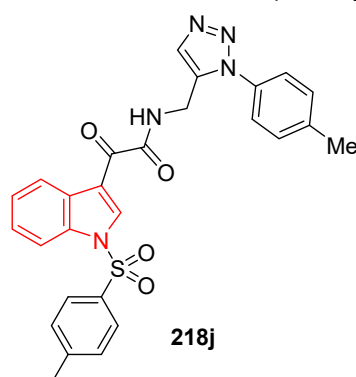
$IC_{50} = >100, >100, >100 \mu M$ against SKOV3, DU145, HELA, respectively;
 $IC_{50} = 2.14, 1.88, 11.58 \mu M$ against COX-1, COX-2, 5-LOX, respectively



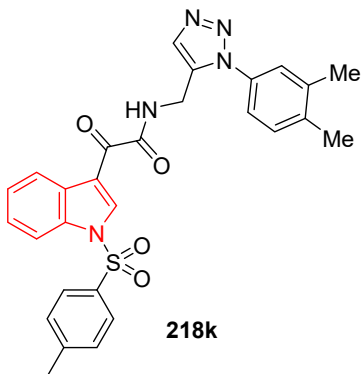
$IC_{50} = >100, >100, >100 \mu M$ against SKOV3, DU145, HELA, respectively;
 $IC_{50} = 2.25, 0.44, 7.93 \mu M$ against COX-1, COX-2, 5-LOX, respectively



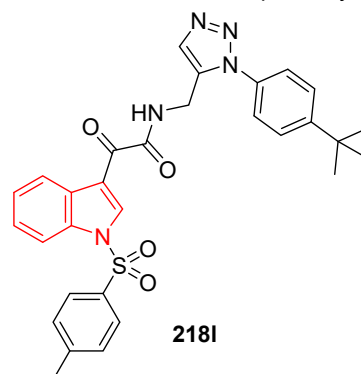
$IC_{50} = >100, >100, >100 \mu M$ against SKOV3, DU145, HELA, respectively;
 $IC_{50} = 2.15, 0.85, 7.85 \mu M$ against COX-1, COX-2, 5-LOX, respectively



$IC_{50} = >100, >100, >100 \mu M$ against SKOV3, DU145, HELA, respectively;
 $IC_{50} = 3.12, 1.43, 9.59 \mu M$ against COX-1, COX-2, 5-LOX, respectively

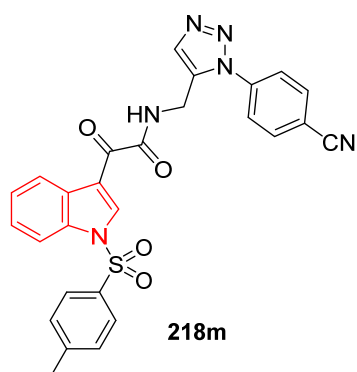


$IC_{50} = 20.71, >100, >100 \mu M$ against SKOV3, DU145, HELA, respectively;
 $IC_{50} = 3.52, 1.66, 9.74 \mu M$ against COX-1, COX-2, 5-LOX, respectively

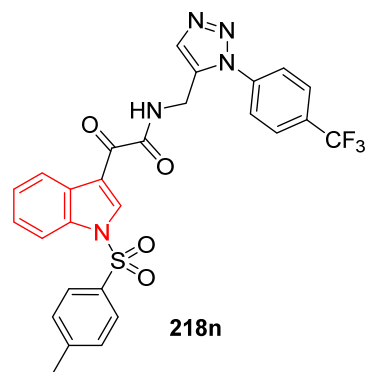


$IC_{50} = >100, 17.10, 50.24 \mu M$ against SKOV3, DU145, HELA, respectively;
 $IC_{50} = 2.26, 1.25, 9.83 \mu M$ against COX-1, COX-2, 5-LOX, respectively

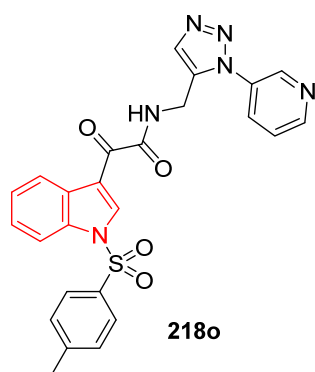
Fig. S41 (continued). Antiproliferation and enzymation inhibitory properties of indole-triazole conjugates **218**, Etoposide, Indomethacin, Celecoxib, and Norhiydroguaiaretic acid (ND = not done).



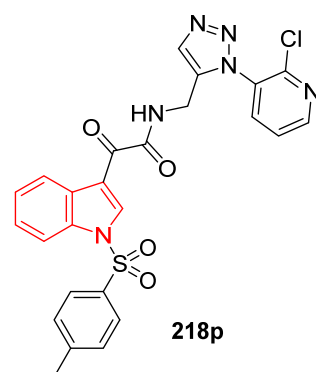
IC₅₀ = >100, 49.77, >100 μ M against SKOV3, DU145, HELA, respectively;
IC₅₀ = 2.13, 0.48, 11.36 μ M against COX-1, COX-2, 5-LOX, respectively



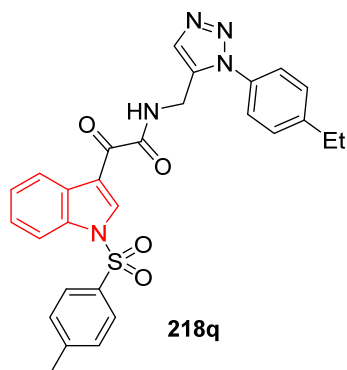
IC₅₀ = >100, >100, >100 μ M against SKOV3, DU145, HELA, respectively;
IC₅₀ = 2.86, 1.21, 9.54 μ M against COX-1, COX-2, 5-LOX, respectively



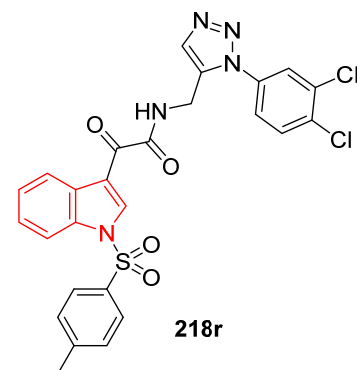
IC₅₀ = >100, >100, >100 μ M against SKOV3, DU145, HELA, respectively;
IC₅₀ = 2.23, 0.35, 9.48 μ M against COX-1, COX-2, 5-LOX, respectively



IC₅₀ = 29.32, >100, 21.64 μ M against SKOV3, DU145, HELA, respectively;
IC₅₀ = 2.14, 1.99, 11.62 μ M against COX-1, COX-2, 5-LOX, respectively

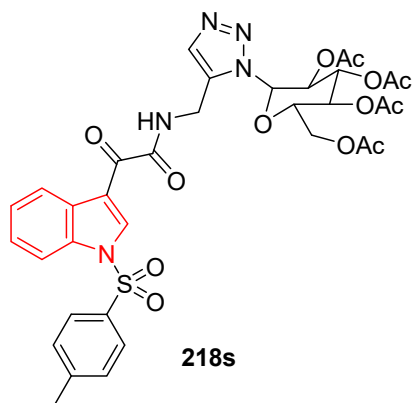


IC₅₀ = >100, >100, >100 μ M against SKOV3, DU145, HELA, respectively;
IC₅₀ = 2.65, 0.22, 7.46 μ M against COX-1, COX-2, 5-LOX, respectively

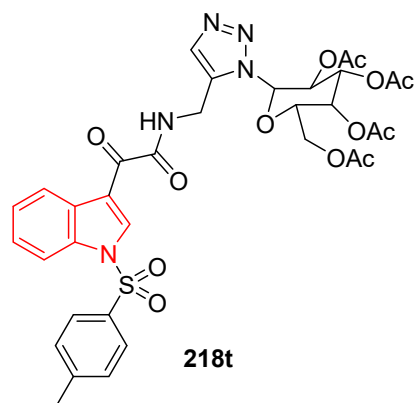


IC₅₀ = >100, 11.88, >100 μ M against SKOV3, DU145, HELA, respectively;
IC₅₀ = 2.44, 0.32, 8.51 μ M against COX-1, COX-2, 5-LOX, respectively

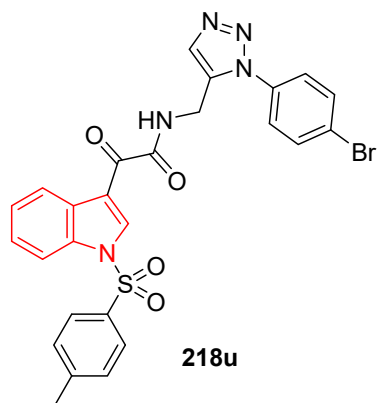
Fig. S41 (continued). Antiproliferation and enzymation inhibitory properties of indole-triazole conjugates **218**, Etoposide, Indomethacin, Celecoxib, and Norihydroguaiaretic acid (ND = not done).



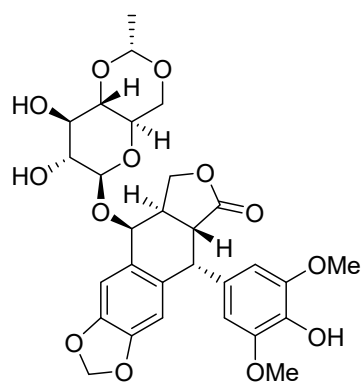
IC_{50} = >100, 18.53, >100 μ M against SKOV3, DU145, HELA, respectively;
 IC_{50} = 2.57, 0.12, 7.43 μ M against COX-1, COX-2, 5-LOX, respectively



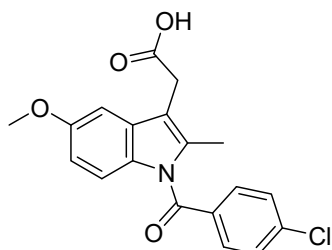
IC_{50} = ND, ND, ND μ M against SKOV3, DU145, HELA, respectively;
 IC_{50} = 3.06, 2.95, 12.65 μ M against COX-1, COX-2, 5-LOX, respectively



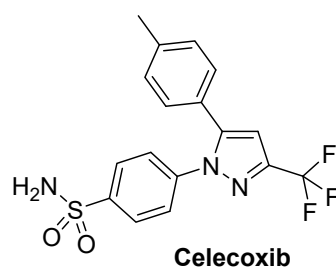
IC_{50} = >100, >100, 7.79 μ M against SKOV3, DU145, HELA, respectively;
 IC_{50} = 2.25, 1.75, 9.82 μ M against COX-1, COX-2, 5-LOX, respectively



IC_{50} = 2.39, 9.8, 7.43 μ M against SKOV3, DU145, HELA, respectively

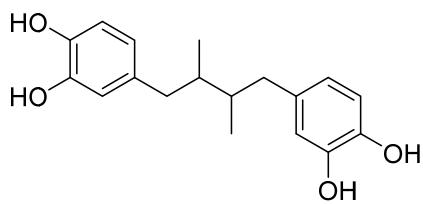


IC_{50} = 0.0068, 0.049 μ M against COX-1, COX-2, respectively



IC_{50} = 14.8, 0.041 μ M against COX-1, COX-2, respectively

Fig. S41 (continued). Antiproliferation and enzymation inhibitory properties of indole-triazole conjugates **218**, Etoposide, Indomethacin, Celecoxib, and Norhiydroguaiaretic acid (ND = not done).



Norhydroguaiaretic acid (NDGA)

$IC_{50} = 7.31 \mu\text{M}$ against 5-LOX

Fig. S41 (continued). Antiproliferation and enzymation inhibitory properties of indole-triazole conjugates **218**, Etoposide, Indomethacin, Celecoxib, and Norhydroguaiaretic acid (ND = not done).

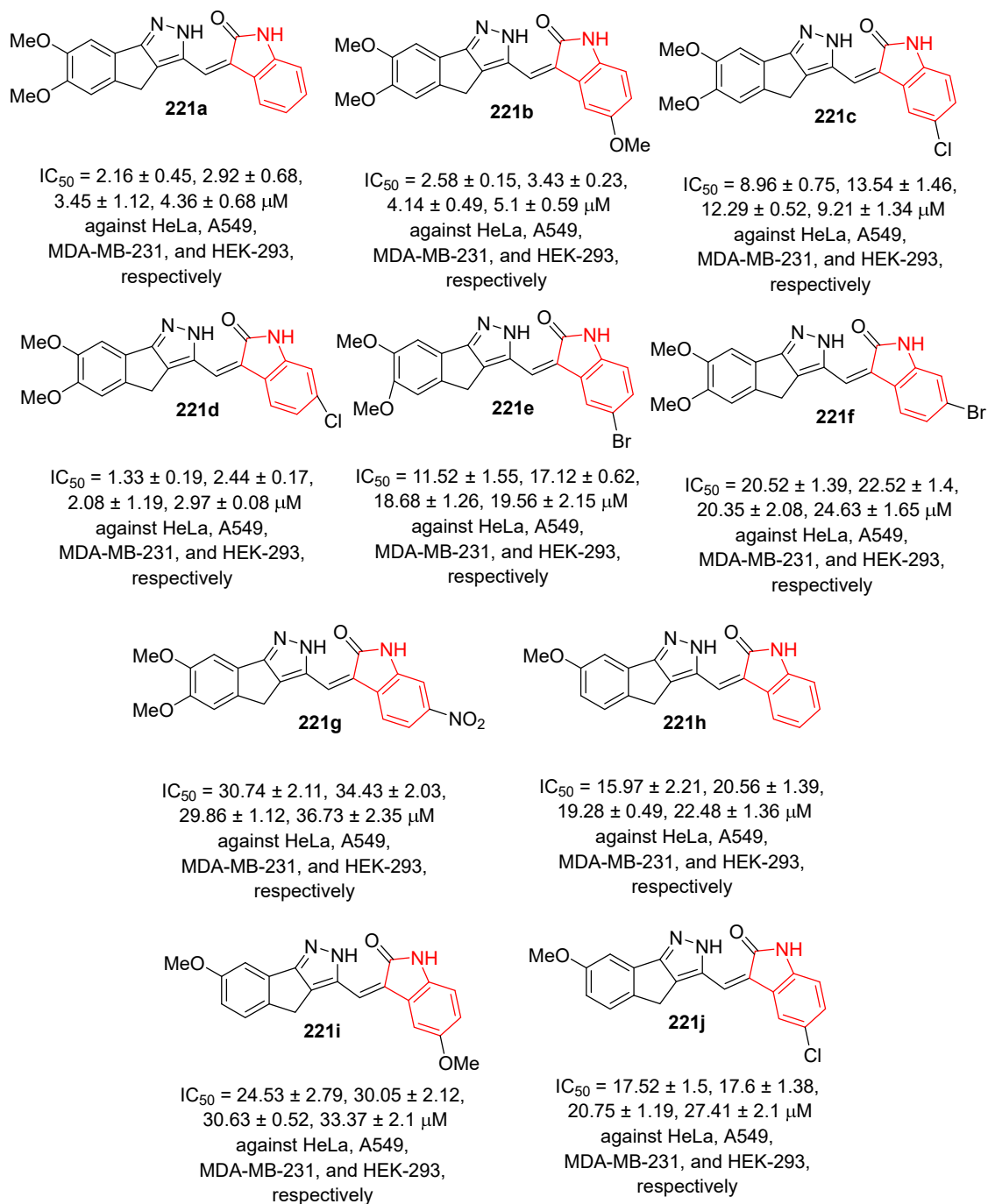
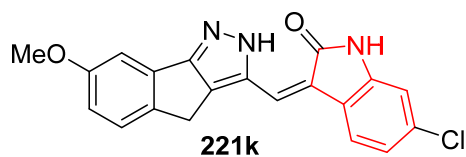
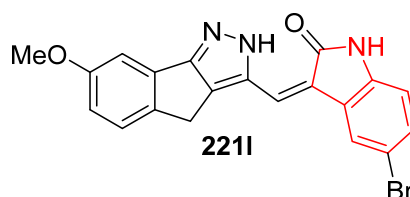


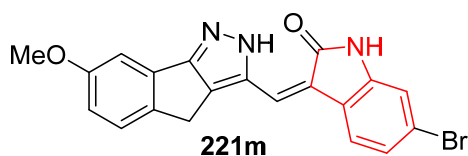
Fig. S42. Antiproliferation properties ($\mu\text{M} \pm \text{SD}$) of 3-[(indeno[1,2-c]-pyrazole-3-yl)methylene]indolin-2-ones **221** and Combretastatin A-4 (CA-4).



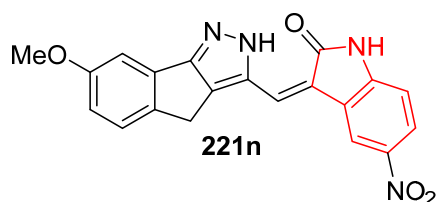
$IC_{50} = 16.99 \pm 0.59, 20.95 \pm 0.77, 19.04 \pm 1.26, 21.87 \pm 2.05 \mu\text{M}$ against HeLa, A549, MDA-MB-231, and HEK-293, respectively



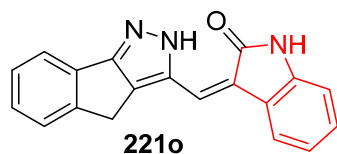
$IC_{50} = 30.94 \pm 2.12, 29.79 \pm 2.23, 34.15 \pm 2.08, 35.75 \pm 1.98 \mu\text{M}$ against HeLa, A549, MDA-MB-231, and HEK-293, respectively



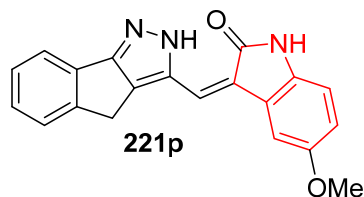
$IC_{50} = 25.38 \pm 1.49, 26.14 \pm 1.21, 23.4 \pm 1.12, 28.57 \pm 1.61 \mu\text{M}$ against HeLa, A549, MDA-MB-231, and HEK-293, respectively



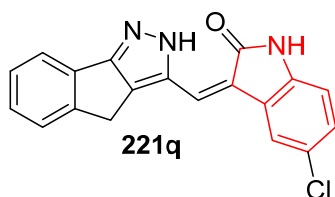
$IC_{50} = 22.09 \pm 0.78, 26 \pm 0.62, 29.17 \pm 0.49, 30.79 \pm 0.59 \mu\text{M}$ against HeLa, A549, MDA-MB-231, and HEK-293, respectively



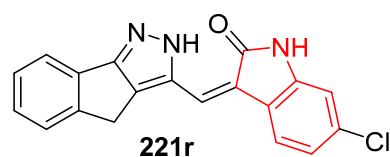
$IC_{50} = 11.65 \pm 0.84, 16.57 \pm 1.81, 18.96 \pm 1.12, 24.26 \pm 0.42 \mu\text{M}$ against HeLa, A549, MDA-MB-231, and HEK-293, respectively



$IC_{50} = 30.11 \pm 2.78, 29.55 \pm 3.4, 26.73 \pm 0.49, 33.86 \pm 1.84 \mu\text{M}$ against HeLa, A549, MDA-MB-231, and HEK-293, respectively

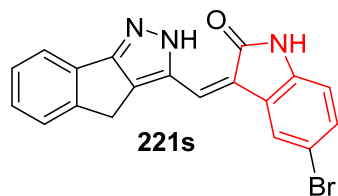


$IC_{50} = 15.16 \pm 1.95, 20.48 \pm 1.34, 16.81 \pm 0.52, 24.29 \pm 1.22 \mu\text{M}$ against HeLa, A549, MDA-MB-231, and HEK-293, respectively

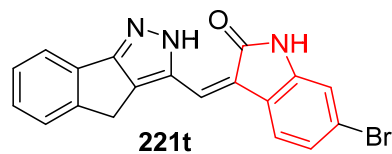


$IC_{50} = 14.6 \pm 1.36, 20.53 \pm 1.45, 24.34 \pm 1.19, 19.37 \pm 1.17 \mu\text{M}$ against HeLa, A549, MDA-MB-231, and HEK-293, respectively

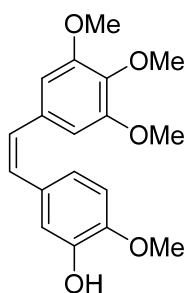
Fig. S42 (continued). Antiproliferation properties ($\mu\text{M} \pm \text{SD}$) of 3-[(indeno[1,2-c]pyrazole-3-yl)methylene]indolin-2-ones **221** and Combretastatin A-4 (CA-4).



$IC_{50} = 16.85 \pm 0.69, 21.09 \pm 1.54, 20.34 \pm 1.26, 22.48 \pm 1.32 \mu M$
against HeLa, A549,
MDA-MB-231, and HEK-293,
respectively



$IC_{50} = 30.69 \pm 1.33, 35.55 \pm 1.37, 29.65 \pm 2.08, 34.23 \pm 2.74 \mu M$
against HeLa, A549,
MDA-MB-231, and HEK-293,
respectively



Combretastatin A-4 (CA-4)

$IC_{50} = 1.43 \pm 0.25, 1.15 \pm 0.18, 0.92 \pm 0.007, 1.73 \pm 0.41 \mu M$
against HeLa, A549,
MDA-MB-231, and HEK-293,
respectively

Fig. S42 (continued). Antiproliferation properties ($\mu M \pm SD$) of 3-[(indeno[1,2-c]-pyrazole-3-yl)methylene]indolin-2-ones **221** and Combretastatin A-4 (CA-4).

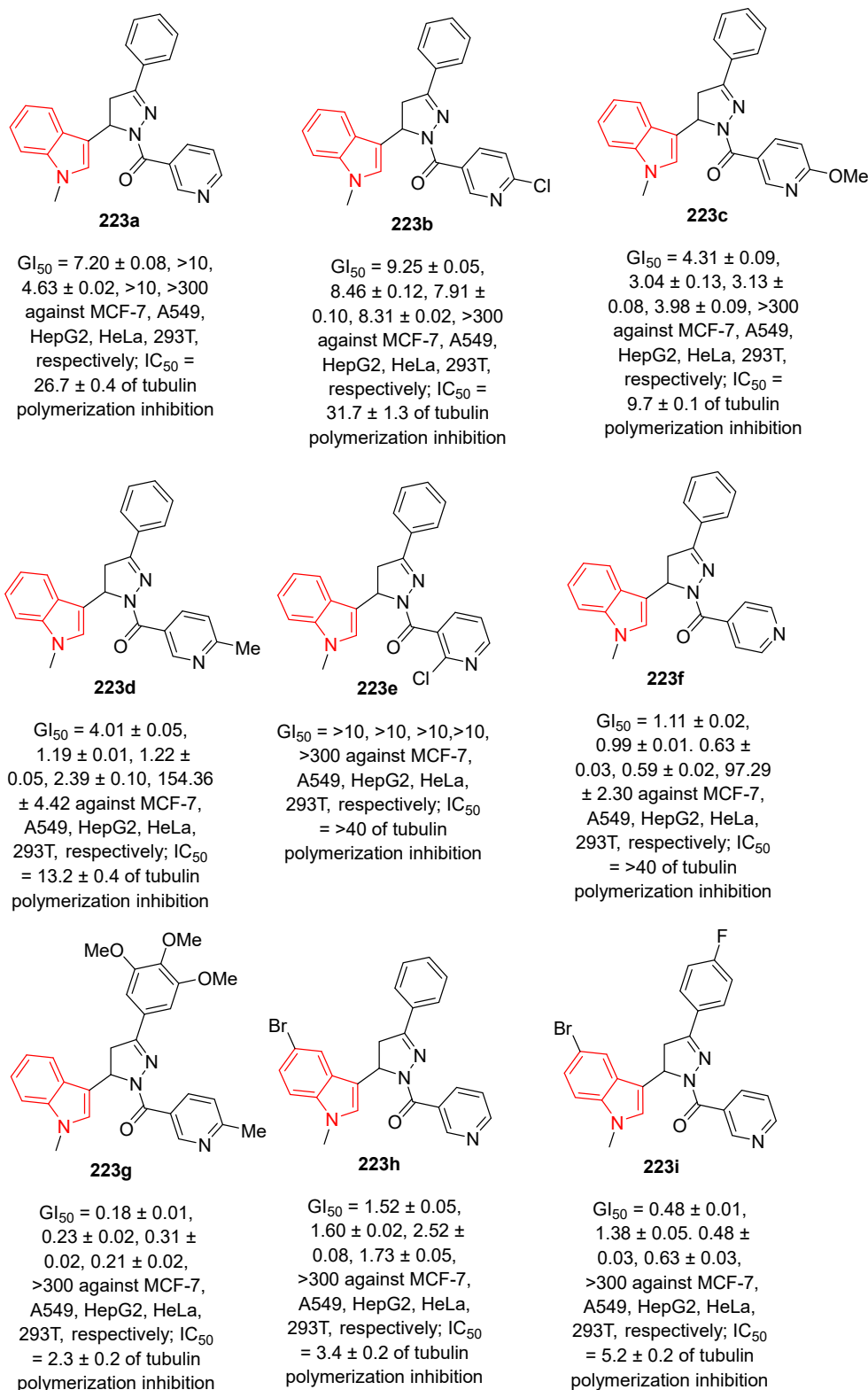


Fig. S43. Antiproliferation and tubulin polymerization inhibitory properties of the synthesized nicotinoyl/isonicotinyl pyrazolines featuring indolyl heterocycle **223** and Combretastatin A-4 (CA-4).

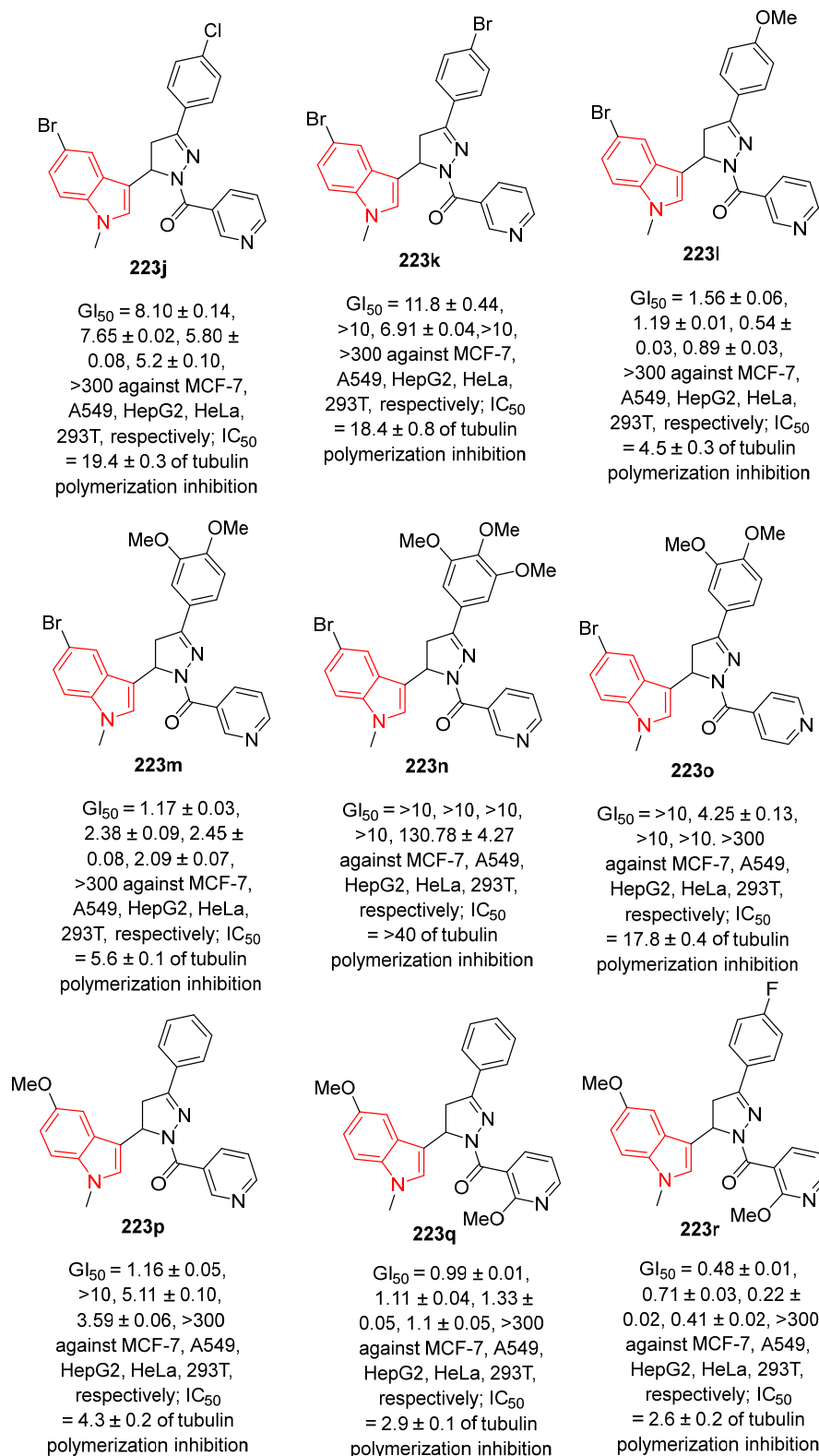


Fig. S43 (continued). Antiproliferation and tubulin polymerization inhibitory properties of the synthesized nicotinoyl/isonicotinyl pyrazolines featuring indolyl heterocycle **223** and Combretastatin A-4 (CA-4).

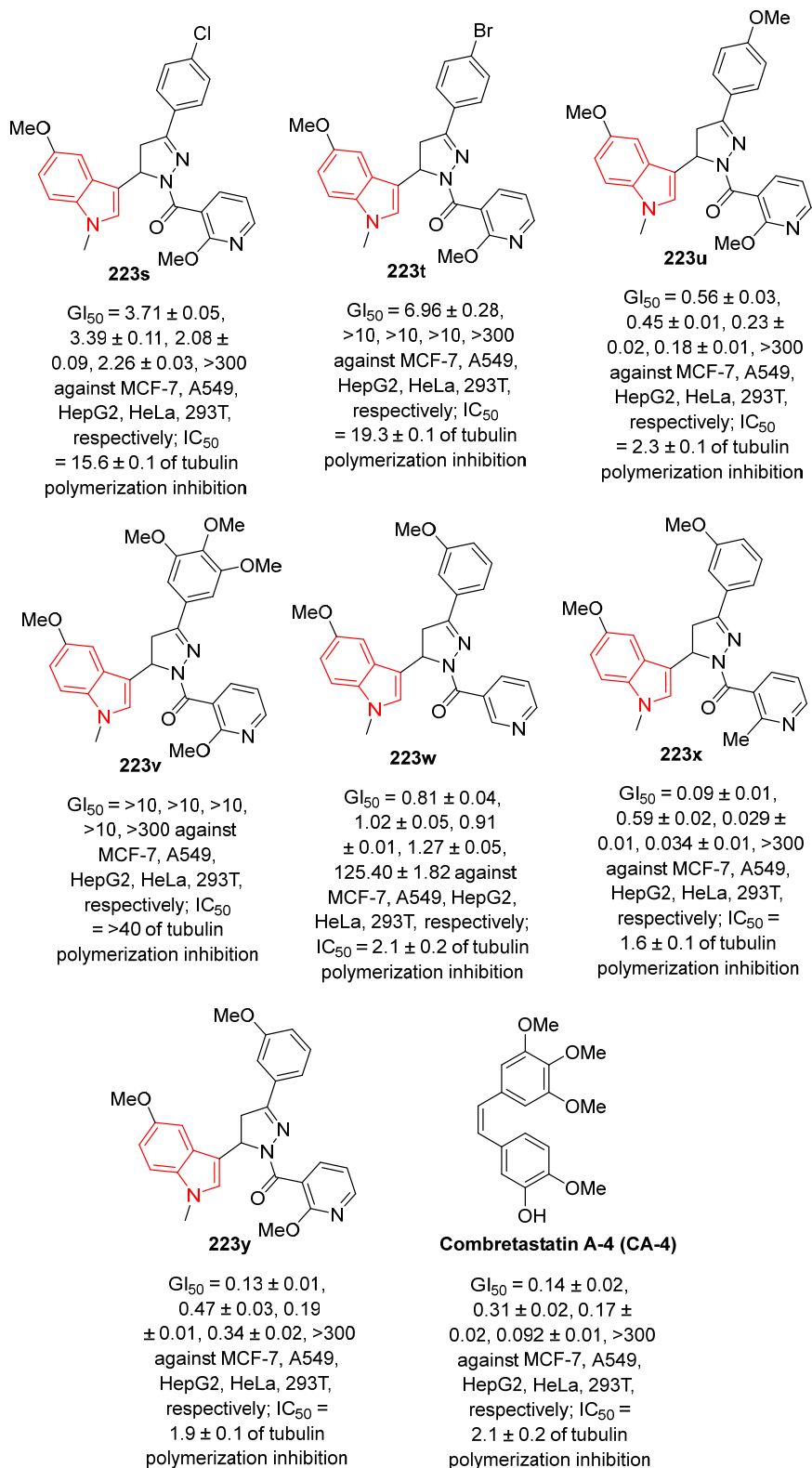
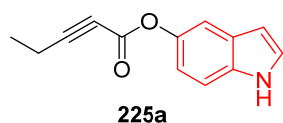
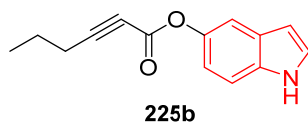


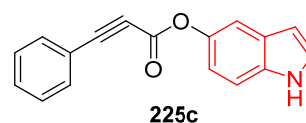
Fig. S43 (continued). Antiproliferation and tubulin polymerization inhibitory properties of the synthesized nicotinoyl/isonicotinoyl pyrazolines featuring indolyl heterocycle **223** and Combretastatin A-4 (CA-4).



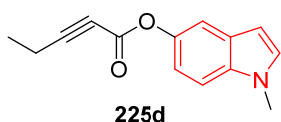
$IC_{50} = 13.1 \pm 0.3, 10.7 \pm 0.2, 9.8 \pm 0.3, 12.1 \pm 0.6, >200, >200, >200 \mu\text{M}$ against MCF-7, MDA-MB-231, HeLa, Ishikawa, MCF-10A, Hek-293, and 3T3-L1, respectively



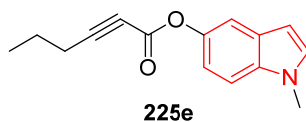
$IC_{50} = 30.2 \pm 0.2, 15.9 \pm 0.5, 14.5 \pm 0.6, 30.5 \pm 0.5, >200, >200 \mu\text{M}$ against MCF-7, MDA-MB-231, HeLa, Ishikawa, MCF-10A, Hek-293, and 3T3-L1, respectively



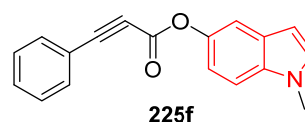
$IC_{50} = 3.8 \pm 0.7, 9.9 \pm 0.3, 3.6 \pm 0.5, 10.1 \pm 0.7, >200, >200 \mu\text{M}$ against MCF-7, MDA-MB-231, HeLa, Ishikawa, MCF-10A, Hek-293, and 3T3-L1, respectively



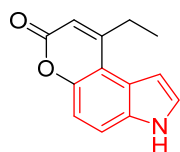
$IC_{50} = 23.0 \pm 0.4, 23.5 \pm 0.4, 14.0 \pm 0.7, 13.1 \pm 0.3, >200, >200 \mu\text{M}$ against MCF-7, MDA-MB-231, HeLa, Ishikawa, MCF-10A, Hek-293, and 3T3-L1, respectively



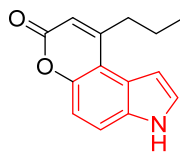
$IC_{50} = >200, >200, >200, >200, >200, >200 \mu\text{M}$ against MCF-7, MDA-MB-231, HeLa, Ishikawa, MCF-10A, Hek-293, and 3T3-L1, respectively



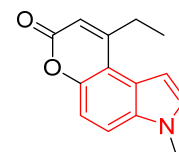
$IC_{50} = 37.6 \pm 0.5, 40.7 \pm 0.8, 49.5 \pm 0.9, 77.7 \pm 0.4, >200, >200 \mu\text{M}$ against MCF-7, MDA-MB-231, HeLa, Ishikawa, MCF-10A, Hek-293, and 3T3-L1, respectively



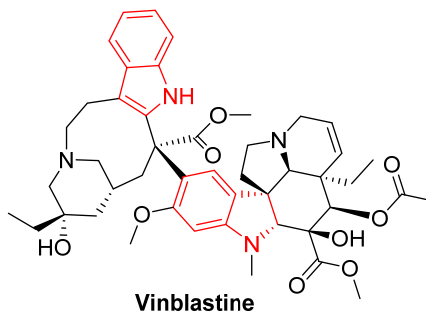
$IC_{50} = 86.0 \pm 0.3, 44.4 \pm 0.3, 21.1 \pm 0.7, 84.0 \pm 0.5, >200, >200 \mu\text{M}$ against MCF-7, MDA-MB-231, HeLa, Ishikawa, MCF-10A, Hek-293, and 3T3-L1, respectively



$IC_{50} = >200, 172.4 \pm 0.6, 141.4 \pm 0.7, >200, >200, >200 \mu\text{M}$ against MCF-7, MDA-MB-231, HeLa, Ishikawa, MCF-10A, Hek-293, and 3T3-L1, respectively

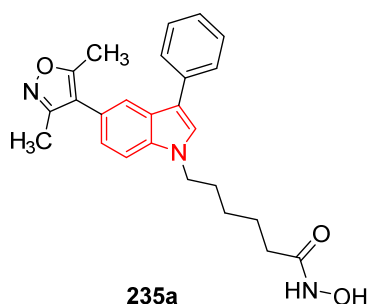


$IC_{50} = 131.5 \pm 0.3, 80.2 \pm 0.5, >200, >200, >200, >200 \mu\text{M}$ against MCF-7, MDA-MB-231, HeLa, Ishikawa, MCF-10A, Hek-293, and 3T3-L1, respectively

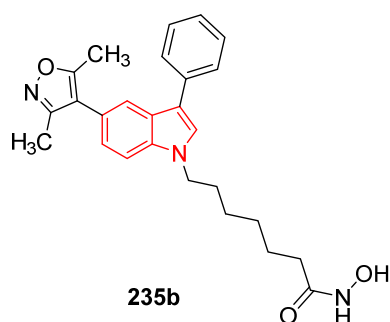


$IC_{50} = 4.5 \times 10^{-2} \pm 0.6, 1.6 \times 10^{-1} \pm 0.3, 6.7 \times 10^{-2} \pm 0.5, 2.5 \times 10^{-2} \pm 0.7, 2.3 \times 10^{-2} \pm 0.6, 80.8 \pm 0.4, 1.9 \times 10^{-4} \pm 0.8 \mu\text{M}$ against MCF-7, MDA-MB-231, HeLa, Ishikawa, MCF-10A, Hek-293, and 3T3-L1, respectively

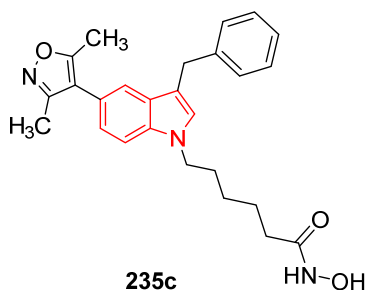
Fig. S44. Antiproliferation properties ($\mu\text{M} \pm \text{SD}$) of the synthesized indoles **225**, pyranoindole **226** and Vinblastine.



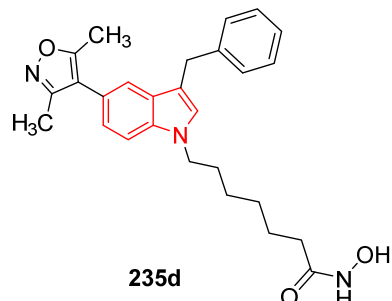
$GI_{50} = 11.29 \pm 1.22 \mu\text{M}$ against THP-1;
 $IC_{50} = 0.223 \pm 0.031, 0.260 \pm 0.022,$
 $0.154 \pm 0.023, 0.120 \pm 0.010, >1$ against
 HDACs, HDAC1, HDAC2, HDAC3, HDAC6,
 respectively; % inhibition rate = 86, 66, 21
 at 100, 10 and $1 \mu\text{M}$



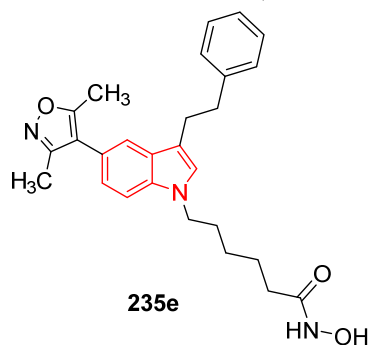
$GI_{50} = 12.43 \pm 1.63 \mu\text{M}$ against THP-1;
 $IC_{50} = 0.183 \pm 0.013, 0.287 \pm 0.016,$
 $0.180 \pm 0.009, 0.202 \pm 0.012, >1$ against
 HDACs, HDAC1, HDAC2, HDAC3, HDAC6,
 respectively; % inhibition rate = 91, 76, 34
 at 100, 10 and $1 \mu\text{M}$



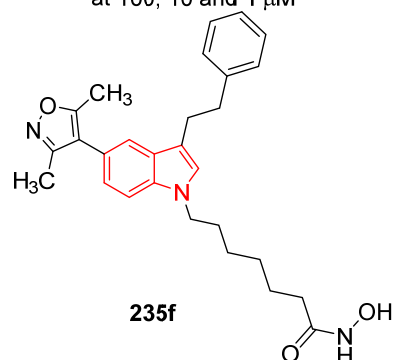
$GI_{50} = 12.45 \pm 2.01 \mu\text{M}$ against THP-1;
 $IC_{50} = 0.160 \pm 0.021, 0.189 \pm 0.011,$
 $0.110 \pm 0.012, 0.089 \pm 0.007, >1$ against
 HDACs, HDAC1, HDAC2, HDAC3, HDAC6,
 respectively; % inhibition rate = 96, 64, 16
 at 100, 10 and $1 \mu\text{M}$



$GI_{50} = 12.13 \pm 1.39 \mu\text{M}$ against THP-1;
 $IC_{50} = 0.122 \pm 0.013, 0.179 \pm 0.011,$
 $0.118 \pm 0.019, 0.023 \pm 0.009, >1$ against
 HDACs, HDAC1, HDAC2, HDAC3, HDAC6,
 respectively; % inhibition rate = 96, 65, 31
 at 100, 10 and $1 \mu\text{M}$

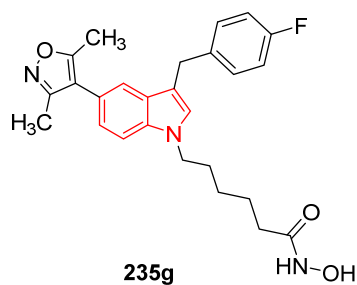


$GI_{50} = 10.06 \pm 0.97 \mu\text{M}$ against THP-1;
 $IC_{50} = 0.307 \pm 0.019, 0.247 \pm 0.021,$
 $0.538 \pm 0.064, 0.076 \pm 0.010, >1$ against
 HDACs, HDAC1, HDAC2, HDAC3, HDAC6,
 respectively; % inhibition rate = 98, 49, 39
 at 100, 10 and $1 \mu\text{M}$

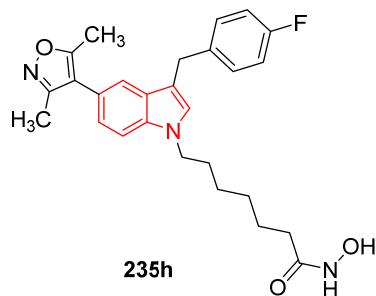


$GI_{50} = 8.79 \pm 0.65 \mu\text{M}$ against THP-1;
 $IC_{50} = 0.172 \pm 0.021, 0.240 \pm 0.017,$
 $0.139 \pm 0.016, 0.028 \pm 0.005, >1$ against
 HDACs, HDAC1, HDAC2, HDAC3, HDAC6,
 respectively; % inhibition rate = 94, 64, 24
 at 100, 10 and $1 \mu\text{M}$

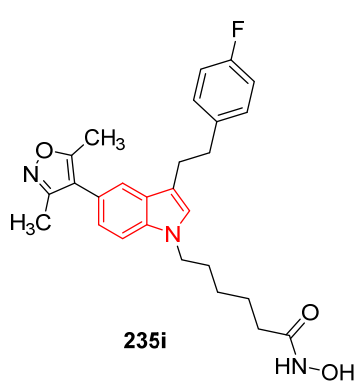
Fig. S45. Antiproliferation and inhibitory properties of HDAC and BRD4 of the synthesized indole-isoxazole conjugates **235**, Vorinostat and JQ1.



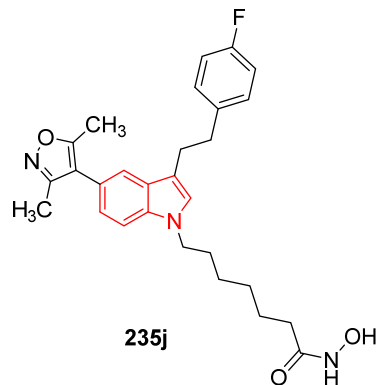
$GI_{50} = 21.26 \pm 2.54 \mu\text{M}$ against THP-1;
 $IC_{50} = 0.286 \pm 0.034, 0.341 \pm 0.023,$
 $0.517 \pm 0.073, 0.039 \pm 0.007, >1$ against
 HDACs, HDAC1, HDAC2, HDAC3, HDAC6,
 respectively; % inhibition rate = 96, 76, 19
 at 100, 10 and $1 \mu\text{M}$



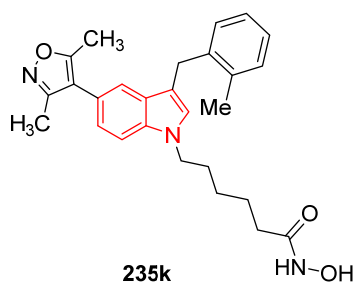
$GI_{50} = 15.5 \pm 1.23 \mu\text{M}$ against THP-1;
 $IC_{50} = 0.291 \pm 0.016, 0.181 \pm 0.011,$
 $0.298 \pm 0.033, 0.005 \pm 0.002, >1$ against
 HDACs, HDAC1, HDAC2, HDAC3, HDAC6,
 respectively; % inhibition rate = 95, 88, 28
 at 100, 10 and $1 \mu\text{M}$



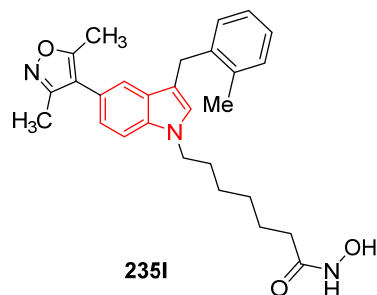
$GI_{50} = 12.98 \pm 1.35 \mu\text{M}$ against THP-1;
 $IC_{50} = 0.207 \pm 0.018, 0.259 \pm 0.031,$
 $0.946 \pm 0.086, 0.017 \pm 0.004, >1$ against
 HDACs, HDAC1, HDAC2, HDAC3, HDAC6,
 respectively; % inhibition rate = 97, 52, 9
 at 100, 10 and $1 \mu\text{M}$



$GI_{50} = 14.11 \pm 2.23 \mu\text{M}$ against THP-1;
 $IC_{50} = 0.030 \pm 0.008, 0.079 \pm 0.007,$
 $0.487 \pm 0.034, 0.064 \pm 0.007, >1$ against
 HDACs, HDAC1, HDAC2, HDAC3, HDAC6,
 respectively; % inhibition rate = 95, 50, 16
 at 100, 10 and $1 \mu\text{M}$

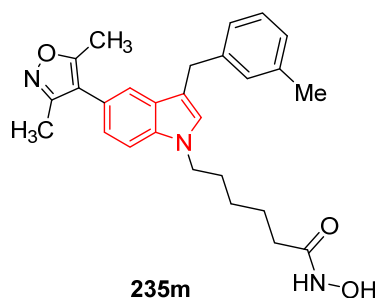


$GI_{50} = 14.82 \pm 0.78 \mu\text{M}$ against THP-1;
 $IC_{50} = 0.369 \pm 0.032, 0.314 \pm 0.046,$
 $>1, 0.062 \pm 0.012, >1$ against
 HDACs, HDAC1, HDAC2, HDAC3, HDAC6,
 respectively; % inhibition rate = 95, 59, 18
 at 100, 10 and $1 \mu\text{M}$

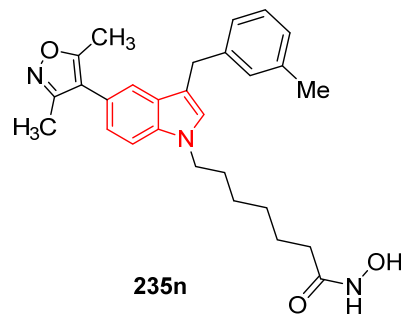


$GI_{50} = 13.93 \pm 1.23 \mu\text{M}$ against THP-1;
 $IC_{50} = 0.149 \pm 0.009, 0.220 \pm 0.031,$
 $>1, 0.050 \pm 0.009, >1$ against
 HDACs, HDAC1, HDAC2, HDAC3, HDAC6,
 respectively; % inhibition rate = 97, 55, 14
 at 100, 10 and $1 \mu\text{M}$

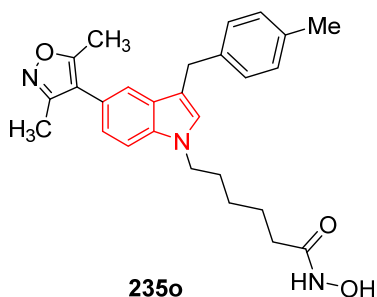
Fig. S45 (continued). Antiproliferation and inhibitory properties of HDAC and BRD4 of the synthesized indole-isoxazole conjugates **235**, Vorinostat and JQ1.



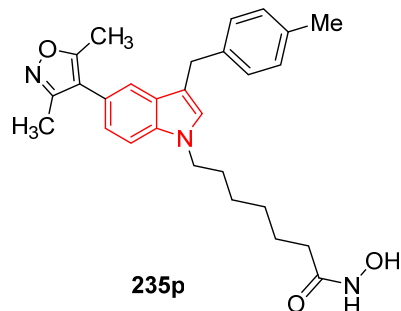
$GI_{50} = 24.21 \pm 2.35 \mu\text{M}$ against THP-1;
 $IC_{50} = 0.244 \pm 0.033, 0.222 \pm 0.019,$
 $0.568 \pm 0.067, 0.062 \pm 0.013, >1$ against
 HDACs, HDAC1, HDAC2, HDAC3, HDAC6,
 respectively; % inhibition rate = 94, 71, 15
 at 100, 10 and $1 \mu\text{M}$



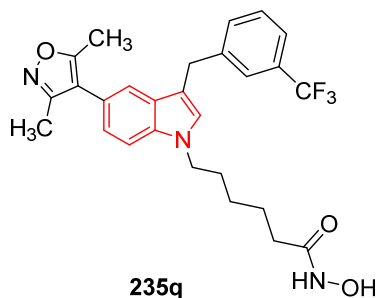
$GI_{50} = 23.34 \pm 1.87 \mu\text{M}$ against THP-1;
 $IC_{50} = 0.094 \pm 0.006, 0.253 \pm 0.012,$
 $0.127 \pm 0.013, 0.024 \pm 0.006, >1$ against
 HDACs, HDAC1, HDAC2, HDAC3, HDAC6,
 respectively; % inhibition rate = 96, 69, 14
 at 100, 10 and $1 \mu\text{M}$



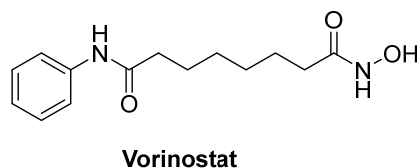
$GI_{50} = 16.00 \pm 2.01 \mu\text{M}$ against THP-1;
 $IC_{50} = 0.332 \pm 0.041, 0.650 \pm 0.053,$
 $0.956 \pm 0.071, 0.072 \pm 0.011, >1$ against
 HDACs, HDAC1, HDAC2, HDAC3, HDAC6,
 respectively; % inhibition rate = 97, 63, 18
 at 100, 10 and $1 \mu\text{M}$



$GI_{50} = 12.96 \pm 1.42 \mu\text{M}$ against THP-1;
 $IC_{50} = 0.186 \pm 0.023, 0.431 \pm 0.033,$
 $0.438 \pm 0.038, 0.018 \pm 0.007, >1$ against
 HDACs, HDAC1, HDAC2, HDAC3, HDAC6,
 respectively; % inhibition rate = 95, 76, 13
 at 100, 10 and $1 \mu\text{M}$

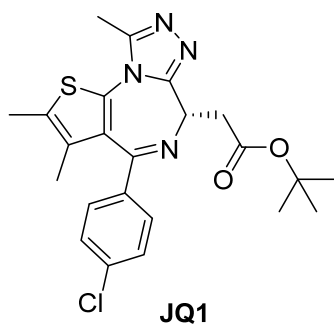


$GI_{50} = 7.82 \pm 0.54 \mu\text{M}$ against THP-1;
 $IC_{50} = 0.083 \pm 0.011, 0.031 \pm 0.005,$
 $0.079 \pm 0.010, 0.013 \pm 0.003, >1$ against
 HDACs, HDAC1, HDAC2, HDAC3, HDAC6,
 respectively; % inhibition rate = 92, 41, 12
 at 100, 10 and $1 \mu\text{M}$



$GI_{50} = 0.51 \pm 0.04 \mu\text{M}$ against THP-1;
 $IC_{50} = 0.076 \pm 0.002, 0.103 \pm 0.008,$
 $0.055 \pm 0.007, 0.027 \pm 0.006, 0.039 \pm$
 0.002 against HDACs, HDAC1, HDAC2,
 HDAC3, HDAC6, respectively

Fig. S45 (continued). Antiproliferation and inhibitory properties of HDAC and BRD4 of the synthesized indole-isoxazole conjugates **235**, Vorinostat and JQ1.



$GI_{50} = 0.13 \pm 0.02 \mu\text{M}$ against THP-1;
 % inhibition rate = 97, 96, 95
 at 100, 10 and 1 μM

Fig. S45 (continued). Antiproliferation and inhibitory properties of HDAC and BRD4 of the synthesized indole-isoxazole conjugates **235**, Vorinostat and JQ1.

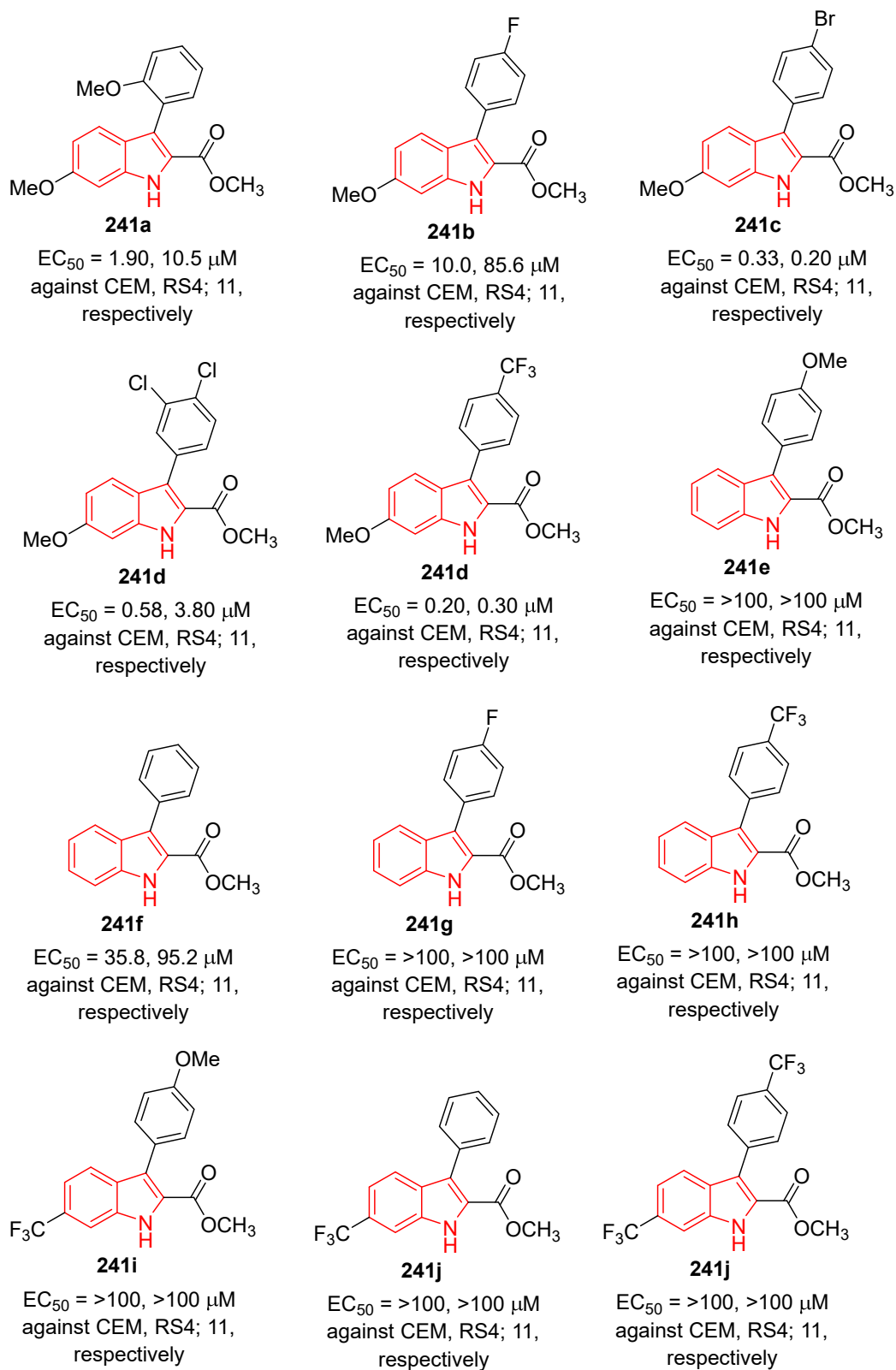


Fig. S46. Antiproliferation properties of 3,6-disubstituted-2-carboxyindoles **241**.